Benign Design for Dental Restorations

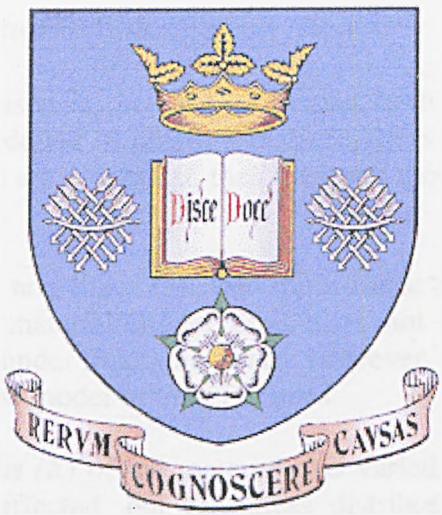

PhD Thesis

Charlotte Jane Richardson

18th November 1999

ORIGINAL COPY TIGHTLY BOUND

Abstract

This work investigates how the behaviour of a tooth containing a restored cervical lesion differs from that of a natural tooth. A hierarchy of 2-D Finite Element Analysis (FEA) models have been constructed, each examining a different aspect of the loads experienced by a human canine tooth in functional behaviour. Thus, the geometry and material property variables of a Class V restoration that adversely influence the performance of restored teeth can be evaluated. A philosophy of design to be employed when restoring cervical lesions can then be conceived.

The main conclusions drawn from this study are as follows:

The boundary constraints used in the FEA of human teeth are significant; the Periodontal Ligament (PDL) must be modelled to obtain a realistic stress distribution within the tooth. If the displacements of the tooth are of interest, then the bone should also be incorporated into the FEA model.

Various linear elastic (LE), non-linear (NL and multi-linear elastic (MLE) models were used to represent the PDL. The material model used does not appear to influence the stress distributions within the tooth under functional loads. However, the stress distribution within the bone is affected by the material model of the PDL used.

When the Young's Modulus *(E)* of the material was varied, the magnitudes of the stresses induced in the tooth were affected, but the stress distribution within the tooth remained unaffected.

The effect of varying the *E* of the restorative materials used to restore a rounded and a v-shaped cervical lesion were investigated. The materials used could be divided into 3 groups; a low-modulus group, a mid-range group, and a high modulus group. The results predicted by the mid-range group corresponded most closely with those predicted by the natural tooth, and are therefore most benign. The low-modulus group materials reduce stress in the restoration but increase stress in the tooth when compared to the natural tooth model. The high-modulus group materials increase stress in the restoration, but reduce stress within the tooth compared to the natural tooth model.

A v-shaped restoration causes a stress concentration in the tooth, behind the vertex of the restoration. Filleting the vertex reduces this stress concentration. The stress along the enamel-restoration interface is significantly increased for the rounded restoration, probably due to the angle at which the interface intersects the enamel.

Stresses induced due to thermal loading are smaller than those induced by bite loads; however, they are thought to be significant when considering the fatigue loading of teeth.

List of Abbreviations:

2-D	two-dimensional
3-D	three dimensional
Å	Angstrom
A-D converter	Analogue to Digital Converter
°C	degrees Celcius
CEJ	Cemento-Enamel Junction
Class V	A lesion in the cervical region of the tooth
cm	centimetres
cN	centi-Newton
DYNA	LS-DYNA3D
E	Young's Modulus
EDJ	Enamel Dentine Junction
FE	Finite Element
FEA	Finite Element Analysis
Fig.	Figure
g	grams
GIC	Glass Ionomer Cement
GPa	Giga Pascal
H_20	water
Hz	Hertz (frequency)
k	thermal conductivity
kg	kilogram
kHz	kilo Hertz
LE	Linear Elastic
LVDT	Linear Variable Differential Transformers
MLE	Multi-Linear Elastic
mm	millimetres
MOD	Mesio-Occlusal-Distal (cavity)
MPa	Mega Pascal = $1x10^6$ Pa
MRI	Magnetic Resonance Imaging
N	Newton
ν, ν_{xy}	Poisson's ratio
NL	Non-Linear
PDL	Periodontal Ligament
pg.	page
pH	percentage hydrogen
θ	angle between 2 edges of a right-angled triangle
ρ	density (kg/mm^3)
σ	stress; interfacial stress (Chapter 7)
SEDF	Strain Energy Density Function
SPATE	Stress Pattern by Analysis of the Thermoelastic Effect
SX	stress in the global x-direction
SY	stress in the global y-direction
τ	shear stress
UTS	Ultimate Tensile Strength
UX	displacement in the global x-direction
UY	displacement in the global y-direction
ω	frequency
x-stress	stress in the x-direction
y-stress	stress in the y-direction

Table of Contents

List of Figures

List of Tables

Acknowledgements

The author is extremely grateful to everyone who has helped her during the course of this work, and wishes to express her thanks to the following people:

My supervisors, Prof. Ric van Noort and Dr. Ian Howard for their continuous support and guidance throughout this project.

Prof. Eann Patterson and the members of the Experimental Stress Analysis Lab, particularly Elizabeth Olden, Richard Kay and Dick Cummins for their assistance with the SPATE work.

My colleagues, Alaster Yoxall, Miles Thornton, and Guan Chew for their guidance in using the FEA packages ANSYS, LS-DYNA3D and DYNASYS, and for Guan's curve fitting programme.

Chris Carmody for his help with FORTRAN routines and macros in ANSYS.

The staff of Corporate Information and Computing Services at the University of Sheffield, especially Alan Cartledge, Ian O'Sullivan, Dave Woollen and Ramen Sen for all their good advice.

Everyone at the University of Michigan who helped me during my time there.

CHAPTER 1

The Structure of the Tooth

1.0 Introduction

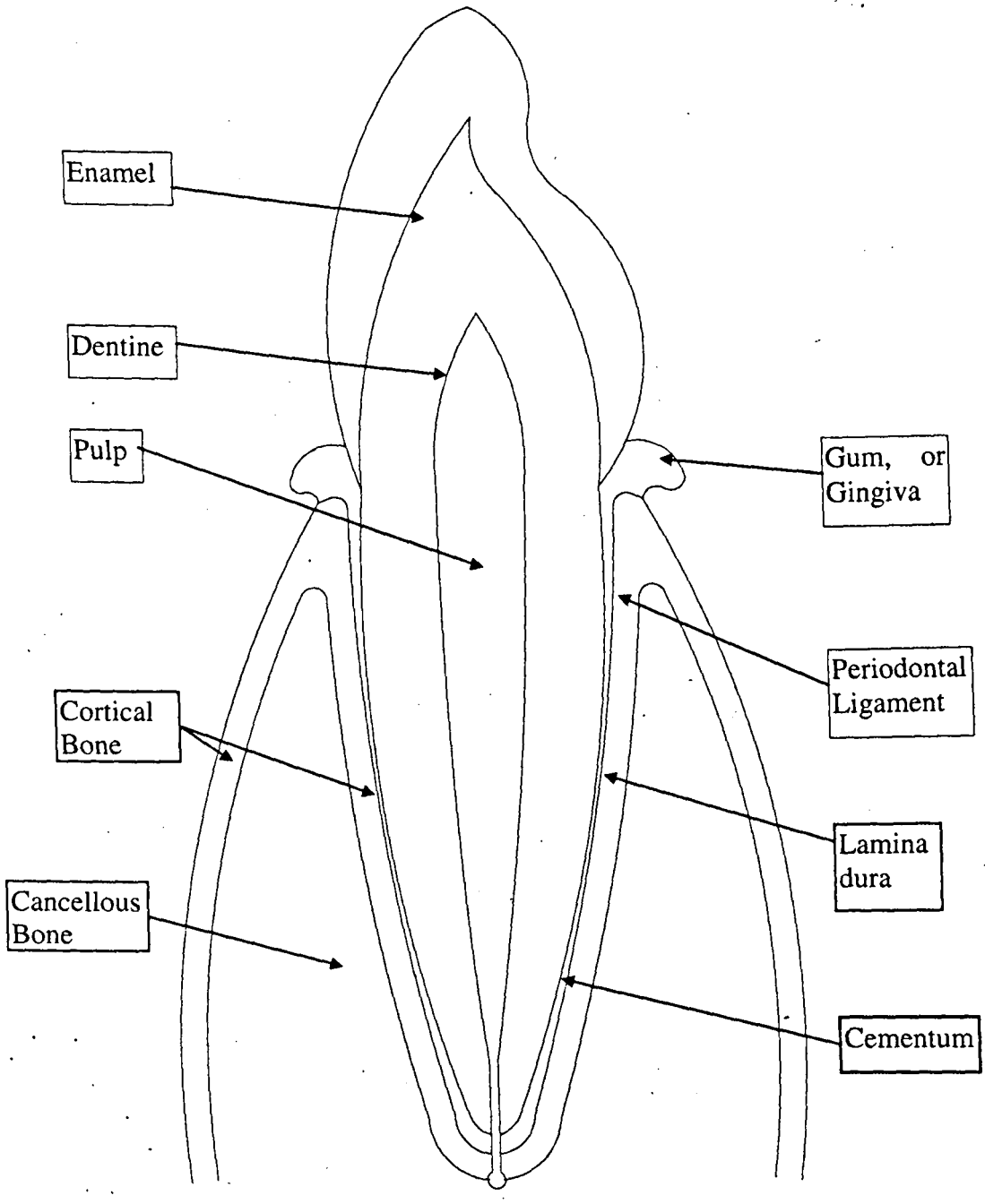

Fig. 1.0.1: The Structure of a Canine Tooth.

The anatomy of the tooth and the supporting structures are presented in this chapter. An understanding of the form, structure and behaviour of these tissues is

necessary in order that these materials can be correctly represented in the stress analysis techniques used.

Human teeth are composed of enamel, dentine and the pulp chamber, as shown in Fig. 1.0.1. Cementum around the root of the tooth attaches the dentine to the socket in the jaw bone, via the periodontal ligament. Gingival tissue, which makes up the gum, covers this over, protecting the root of the tooth from the harsh environment of the mouth.

Fig. 1.0.1 shows the form of a mandibular canine, as this will be studied in greater depth in the later chapters of this report. Teeth have a crown and a root. When referring to teeth such as canines, the crown is often divided into thirds; the incisal third, the middle third, and the gingival or cervical third. The incisal third refers to the part of the tooth that is specialised for biting, and the gingival third is naturally the part forming the neck of the tooth, nearest to the gum. Furthermore, to specify exactly which face of a tooth one is referring to, there are terms such as buccal, mesial, lingual, *etc.* Fig. 1.0.2 defines all of the terms that will be used in this text.

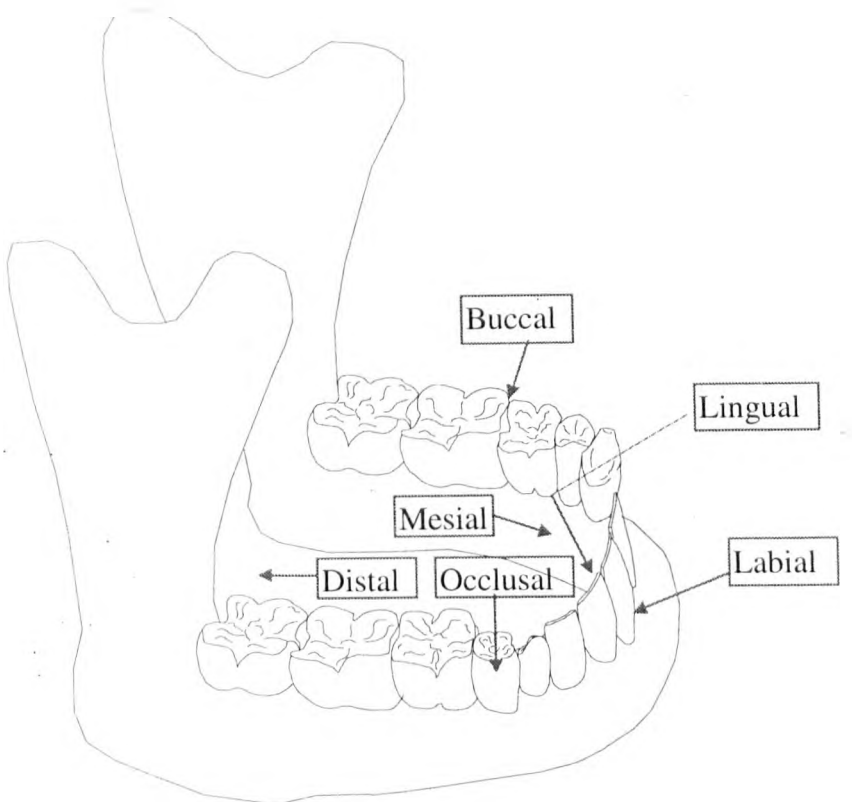

Fig. 1.0.2: Defining the dental terms used in this text.

Sections 1.1 to 1.4 discuss the materials that comprise a tooth in greater detail as the structure of these substances can greatly influence their properties and behaviour. This can be very significant when designing a Finite Element model, and when analysing the results, as will be demonstrated in later chapters.

1.1 Enamel

Enamel is a highly specialised tissue. Epithelial in origin, it is the hardest and most dense tissue in the human body, which makes it ideally suited to its function and resistant to wear. Enamel has a non-collagenous organic matrix, and is deposited in childhood until it is thick enough for the rest of the tooth to develop. A unique tissue, once it is formed and in situation, enamel is cut off from the cellular elements and hence cannot react to injury.

Enamel is composed of many tiny crystallites, as shown in Fig. 1.1.1. These crystallites group together to form hexagonal enamel prisms or rods, all oriented the same way. The crystallites are mainly arranged so that their long axis is parallel to that of the enamel prism, but this changes somewhat in the cervical region of the tooth. (Scott and Symons, 1982).

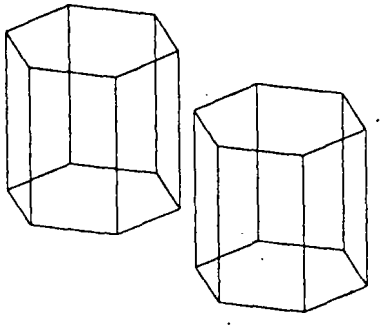

Fig. 1.1.1: The form of the enamel crystals

According to Scott and Symons (1982), the enamel prisms are arranged so that their long axis is generally perpendicular to the dentine-enamel surface. However, since enamel is laid down from the outside inwards, it may be that the long axis of each prism is perpendicular to the outer surface of the enamel. Scott and Symons state that "25% of premolars show a rootward inclination of the prisms as they pass outwards". This demonstrates the uncertainty upon this topic. This issue will be returned to in Chapter 4.

A study by Swancar, Scott and Njemirovskij (1970), attempted to further elucidate the precise form of the enamel prisms, since they are variously described as being: hexagonal, horse-shoe, key-hole, arcade and scale shaped. It is often stated

that the prisms have a head and a tail, but, although the head of the prism is generally accepted, belief in the existence of the tail is less wide-spread. The material of the tail of the prism does not differ from that of the head, although the morphology of the tail is less clearly defined.

Swancar, Scott and Njemirovskij (1970) illustrated that, for any concentration of acid, etching of enamel increased with depth, and this was shown by a white band bounding each prism in a horse-shoe or an arch shape. Occasionally, a black band was also observed, running within the white band, and parallel to it. The precise form of the white band showed considerable variation, commonly appearing as a Gothic arch, a horse-shoe, a square arch, a shield, and a rounded arch. The white band corresponded to the prism outline; the centres of the prisms were more likely to be completely removed from the structure than either the periphery region or the inter-prismatic material. The appearance of the black bands was thought to be technique dependent.

The conclusion of the study was that the enamel prisms consisted of a solid prism sheath, most commonly of arcade section, containing a confluent core of material similar to the inter-prismatic material. The tail of the prism appeared to be related equally to the surrounding prisms as to its head, hence the authors propose that it might more correctly be referred to as inter-prismatic enamel. Another finding of this study was that the fully enclosed, keyhole-shaped prism was significantly less common than the open, arcade form. The final conclusion from this piece of work was that the prism direction varied with increasing enamel depth. Possibly, this finding again reflects the debate concerning the enamel growing inwardly.

Gray (1958), describes the composition of enamel as, " A congeries[1] of minute hexagonal rods; they lie parallel with each other... vertically directed on the summit of the crown, and horizontally at the sides...and pursue a more or less wavy course, which gives the cut surface of the enamel the appearance of a series of concentric lines".

[1] Congeries = *a disorderly collection, from the Latin "to heap together". (Pocket Oxford Dictionary, 1982).*

This waviness is more pronounced in the cuspal regions of the grinding teeth; the molars and premolars. Here, the prisms become markedly twisted, causing this region of the enamel to become known as gnarled enamel.

Spears *et al.* (1993) reviewed the material properties of enamel, and found that reported values for the Young's modulus *(E)* could reasonably be divided into two groups; one with a value of E that was 8 times greater than the other. They proposed that this was because enamel is an anisotropic material, and that the high *E* value corresponded to the material properties measured parallel to the long axis of the prisms, whereas the low *E* represented the perpendicular to the prism axis. This would permit the enamel prisms to transfer load down into the dentine of the enamel, into the root, and away into the supporting tissues. Spears (1997) reconsiders this theory and proposes that a ratio of 5:1 is more appropriate.

If the gnarled enamel is considered, this illustrates the suitability of enamel for its function; the cusps are often used for crushing food, which means that the forces exerted upon them can be very large, and can come from many different directions. Since enamel is believed to be very strong along the length of its prisms, and quite weak across their width, the gnarled enamel ensures that a strong surface will always be presented to the food. (Gray, 1958).

This is a very different situation from the incisal tips of the biting teeth (incisors and canines) which are generally loaded from one direction only. Consequently, the prisms at the tips of these teeth are more or less vertically orientated, as Gray stated.

The preceding discussion implies that enamel does not have uniform properties either along the length of its prisms, or within the structure as a whole. It is a slightly soluble material, and ions in saliva can pass into the enamel, and *vice versa.* Fluoride toothpastes work on a similar principle to protect the teeth; the fluoride ions can be substituted for some of the hydroxy groups of the hydroxyapatite (of which enamel is mainly composed) close to the surface. This forms fluorapatite, which is more dense and less soluble in acids than enamel, and hence more resistant to decay. This layer of enamel, known as surface enamel, contains 5 to 10 times more fluoride and a higher proportion of carbohydrate than other enamel. (Combe, 1992; Scott and Symons, 1982).

The above brief description on the form and function of enamel, of its suitability for purpose, *etc.* is intended to show the extremely anisotropic nature that enamel is believed to exhibit, and the importance of bearing this in mind when trying to emulate the behaviour of teeth in laboratory or computer studies. It is also important to consider that biological materials are not uniform structures; their material properties, microstructure, and composition varies throughout the structure, and material interfaces are often more of a gradation from one material to another than a definite interface, as seen in engineering materials. This may be a cause of differences between the predicted and observed behaviour of biological structures.

1.2 Dentine

Dentine and cementum are both calcified, collagenous tissues, mesodermal in origin (as are cartilage, muscle, and bone). Cementum is very similar to bone, whereas dentine is much harder since it contains more inorganic matter, or more "earthy matter", according to Gray. (In fact, dentine contains approximately 75% by weight inorganic matter, most of which is hydroxyapatite). However, dentine is less hard than enamel, but is much tougher (*i.e.*, much less brittle), and has a higher degree of elasticity, which may imply that it is a better medium for dissipating stress.

Dentine is a composite structure, containing crystals, although the crystals are much smaller in dentine. They are of the order of 200-1000Å x 30Å; similar to the size of the crystals in bone or cementum. Dentine is anisotropic in nature, although the anisotropy does not appear to cause a significant difference between the strength properties in the three directions (Spears *et al.*, 1993). Contrary to this, a study by Poolthong *et al.* (1998) found that the values of E and hardness of dentine were significantly higher when the forces were applied parallel to the tubules. However, the findings of this study do go against popular belief at this time, and Rees and Jacobsen (1997) reported that they could not detect anisotropy in their determination of the static and dynamic moduli of dentine.

The most striking feature of the dentine layer is that it is permeated everywhere by dentinal tubules containing fluid. These allow the odontoblast processes (odontoblasts are cells that form dentine) to run from the pulp cavity to the outer

surface of the dentine, where they form a surface layer. In between these tubules, collagen fibres (bundles of collagen fibrils) are arranged in a gently curved lattice, becoming coarser towards the Enamel-Dentine Junction (EDJ).

Dentine can be laid down throughout life on its inner surface. This often occurs in response to some trauma of the tooth, for example after the fracture of an incisal edge, extra dentine may be laid down behind the site of this injury. (Scott and Symons, 1982; Combe, 1992).

1.3 The Periodontal Ligament

The periodontal ligament (PDL), sometimes referred to as the periodontal membrane, comprises bundles of slightly wavy collagen fibres surrounded by a ground substance. The fibres are rooted in the cementum of the tooth and pass to the *lamina dura* of the tooth socket, to the surrounding gingival tissue or to adjacent teeth. There are approximately 9 per mm^2 (Parfitt, 1965). The spaces between the fibres are occupied by a ground substance, tissue fluid, and many blood vessels.

Many theories about the behaviour of the PDL exist. The most common of these, proposed originally by Synge (1933), and Gabel (1956) (Moxham, Berkovitz and Newman, 1995), is that the collagen fibres provide a tensile support for the tooth. It has been supposed that displacement of the tooth is permitted by the straightening of the collagen fibres, and that once the waves have been removed, the tooth can move no further without distorting the alveolus.

However, Parfitt (1965), in his analysis of the tooth-supporting structures, states that he observed an elastic reaction in the supporting structures as soon as a load was applied to the tooth. This appears to contradict the theory that the collagen fibres initially straighten, providing a small, non-linear, initial region.

Also, Tanne *et al.* (1993) reported that functional loads on teeth cause distortion of the jaw bone.

Referring to heart valves, Thubrikar (1991) states that the flexibility of collagen tissue of a similar type to that of the PDL is dependent upon the degree of waviness of the collagen fibrils.

Trowbridge *et al.* (1985) provide a thorough review of different aspects pertaining to the behaviour of collagenous tissue (specifically bovine pericardial tissue). They confirm some of the observations of Parfitt (1965). These were that under a load maintained for a period of time, stress gradually relaxed, and that tissue exhibited a highly non-linear relationship between stress and time. Trowbridge *et al.* (1985) also note that hysterisis is observed in the behaviour of natural tissue.

To investigate whether or not the PDL behaved purely as a suspensory ligament, Picton and Davies (1967), removed a $9mm^2$ section of *labial mucosa* (mucous membrane) from four adult cynomologous monkeys, and drilled a hole through the bone and PDL, down to the roots of their teeth. By this process, Picton and Davies were then able to place a transducer for their Periodontometer on to both the root and the bone. This enabled simultaneous recordings of root movement and socket distortion to be taken. These readings showed that the PDL experienced both tension and compression during the experiment. Experimental details and the function of the Periodontometer are described in Chapter 4.

Parfitt (1965), observed the behaviour of the supporting structure when the tooth was subjected to an intermittent load and a maintained load. He states that there is a semi-logarithmic relationship between the load and the elastic reaction, and also that an "after-elastic" effect can be observed. Furthermore, the tooth continues to displace under the influence of a constant, maintained load. This would tend to confirm the generally accepted view that the behaviour of the PDL is visco-elastic. A further discussion of the behaviour of the PDL under applied loads is to be found in Chapter 5.

The initial region of a strain energy density function to describe natural tissue has been regarded by Huang *et al.* (1990), and Chew, Howard and Patterson (1994), as being non-linear due to the uncrimping of the wavy collagen fibres. All of the controversy surrounding this issue serves to illustrate the importance of the assumptions made in Finite Element modelling.

1.4 Bone

Bone is a living tissue that is constantly being resorbed and reformed. It is a composite connective tissue, consisting of a type I collagen matrix (about 36% by weight) and hydroxyapatite crystals (about 43% by weight). It also contains about 14% water, and some ground substance (mainly mucopolysaccharides). The mechanical properties of bone are determined mainly by the porosity of the material. There are two types of bone; cortical and cancellous bone. Cortical bone is more mineralised; it consists of about 90% solid bone tissue, whereas cancellous bone, or spongy bone, is 80 to 90% cavities filled with marrow. Compact bone surrounds the cancellous bone, and is itself covered by the periostium. The marrow cavity is at the heart of the bone, and the marrow spaces tend to be larger in children and adolescents than in adults. (Ganong, 1995; Berger, Goldsmith and Lewis, 1996).

The bony layers which surround each tooth are known as the alveolar process. The *lamina dura*, or alveolar bone is composed of thin, compact bone, and forms the wall of the socket. Beneath this layer is the supporting bone. This layer varies in thickness around a tooth. The walls of the middle and marginal regions of the socket are usually quite dense, with few marrow spaces (Lavelle, 1988). In the apical region, on the lingual and palatal aspect, the bone is cancellous bone, or trabecular bone, and may incorporate large marrow spaces. The bone on the mesial and distal aspects tends to be thinner and less dense than that on the labial and lingual sides; hence, tooth movement tends to occur preferentially on these sides.

The failure strain of bone is about 1.5%, and it has viscoelastic properties.

Consideration of the anatomy and material properties of the tissues discussed in this chapter is necessary to enable the construction and analysis of a model that represents the behaviour of these tissues in harmony the most faithfully. The findings of this analysis are presented in the subsequent chapters of this document.

CHAPTER 2

Dental Literature Review

2.0 Introduction

This chapter outlines the problems associated with the formation and treatment of Class V lesions that this research seeks to address. Section 2.1 outlines the classical theories of the formation of non-carious cervical lesions, and the evidence supporting the theory of stress-induced cervical lesions is discussed in section 2.2. The treatment of these cavities is then discussed in section 2.3, and the problems associated with the various restorative techniques and materials used are outlined in section 2.4.

2.1 The Formation of Cervical Lesions

A Class V lesion is one that is located in the cervical third of the tooth, and can be carious or non-carious. Some examples are shown in Fig.'s 2.1.1a-c below.

Fig. 2.1.1a: A carious cervical lesion.

Fig. 2.1.1b: Cervical lesions caused by tooth-brush abrasion.

Fig. 2.1.1c: Cervical lesions caused by tooth-brush abrasion.

(©University of Sheffield - DERWeb Project).

Non-carious lesions are known to be caused by the processes of abrasion, erosion and attrition. Some researchers have also hypothesised that non-carious lesions may be caused by occlusal stress on teeth, although opinion among clinicians on this

matter remains divided. Grippo (1992) has proposed that all of these factors can be encompassed by the general term **abfraction**.

2.1.1 Abrasion

The term **abrasion** refers to the removal of tooth substance by mechanical means, such as by a tooth-brush (Grippo, 1992), or by an object other than another tooth (Mair, 1992).

In tribology, abrasion describes the cutting away of a surface by rough particles or asperities. It can be sub-divided into either two-body or three-body abrasion. Two-body abrasion occurs when the asperities are fixed to one or both surfaces of the contacting bodies, and three-body abrasion results from the presence of a slurry of loose particles between the two surfaces. Two-body abrasion imposes the shape of the harder body upon the softer one. Three-body abrasion can produce hollowed out areas in the softer surface (Mair, 1992).

Dental materials scientists also use the term abrasion to describe the wear of restorations at non-contacting sites. The terminology frequently occurs in literature concerned with the wear of early types of posterior composite restorations, where loss of substance across the whole restoration surface occurred.

2.1.2 Attrition

Attrition describes the loss of tooth substance as a result of tooth to tooth contact occurring in either functional or para-functional behaviour (Tyas, 1995). Mair (1992), defines attrition as, "The wear of teeth at sites of direct contact between the teeth." Biting, chewing or swallowing (which can occur about 500 times per day, resulting in tooth contact every time, according to Grippo, 1991) are regarded as functional behaviour. Para-functional behaviour can include bruxism (clenching and grinding of teeth, often nocturnally), nail biting, clenching a pipe stem, hair grips or pins between the teeth, chewing biros, and other potentially damaging habits that we have developed since we grew too big for our parents to tell us not to put things in our mouths. Attrition results in flattened cusp tips, or the incisal edges of the teeth. However, attrition affects mainly the occlusal or incisal surfaces of the teeth, and hence it is not a major cause of Class V restorations.

2.1.3 *Erosion*

Erosion is the chemical or idiopathic loss of tooth substance by fluid, non-bacterial in origin (Tyas, 1995; Mair, 1992), either with or without abrasive particle content, and can be dietary or environmental in cause (Lee and Eakle, 1984). However, Mair sub-divides erosion into dietary, regurgitative, or environmental in origin, and Zero (1995), further proposes that erosion can be classified as dietary, environmental, lifestyle, or medication related. To save confusion, an alternative classification of the origination of the erosive fluids is to describe them as either intrinsic (originating from within the body), or extrinsic (from outside the body). (Mair, 1992.)

Erosion may be observed in patients who consume many cans of carbonated drinks, in babies who have had sugary drinks in their bottles, for example, or in bulimic, anorexic or hiatus hernia patients, or pregnant women. Chronic alcoholics also frequently exhibit erosive lesions in their teeth. This is believed to be due to gastric regurgitation. Examples of incidences of industrial erosion have also been found in patients who work in acidic environments, such as industrial chemical plants (Grippo, 1991), or manufacturers of batteries (Mair, 1992).

Of all of these categories, research into dietary erosion has been by far the most prevalent in studies, although the general conclusion is that, whilst acidic drinks and fruits are likely to cause erosion of enamel and dentine, and are indeed shown to erode tooth substance in *in vitro* studies, it is very difficult to link clinical incidences of erosion positively to a particular dietary factor.

This is also found to be the case with abrasion; the effects of toothbrush abrasion on a tooth are worsened considerably if an erosive substance has just been consumed first, *e.g.* if teeth are cleaned immediately after eating a piece of citrus fruit.

In animal and clinical studies, grapefruit and cranberry juice have been shown to have particularly high erosive potentials (Zero, 1995) followed by carbonated colas, sports drinks and squashes.

Other studies considering dietary erosion have focused on para-functional or unusual dietary habits; for example, a study by Linkosalo and Markkanen (1985)

compared erosion in a group of lacto-vegetarians to that of a gender and age matched control group. Over 75% of the lacto-vegetarians had dental erosion, compared to a zero incidence within the control group. This finding was attributed to the higher consumption rate of vinegar, vinegar-containing conserves, acidic beverages, and citrus fruits within the lacto-vegetarian group.

High (1977) reported a case where a patient would hold cola in his mouth until the carbonation had gone before swallowing, leading to an unusual erosion pattern. Some authors have advocated drinking carbonated drinks through a straw, permitting the beverage to pass the anterior teeth before entering the mouth. However, High cites incidences of unusual wear patterns on the surfaces of anterior teeth as a result of this practice, due to children placing the straws adjacent to the labial surfaces of their maxillary, anterior teeth.

Comparison of the results of studies by different researchers is not easy, since the National Survey of Child Dental Health, carried out in the UK in 1993, indicated that dentists have difficulty in agreeing upon determining the presence of erosion within enamel. Concurrence improves when the damage extends into the dentine or pulp chambers.

Clinical studies attempting to relate erosion to a particular dietary factor generally suffer from the difficulties of trying to isolate one factor independently.

2.1.4 Corrosion

Grippo, in his 1992 paper on non-carious cervical lesions, defines a fourth mechanism whereby tooth substance can be removed; that of **corrosion**. He defines corrosion as "the physical deterioration of a material by chemical, electro-chemical, or physio-chemical attack". Corrosive wear is defined by Mair (1992) as the interaction between chemical degradation, which weakens the surface, and the removal of substance by friction from another body.

Building upon this idea, Grippo further hypothesises that such lesions are enlarged by **stress-corrosion**; the tooth is weakened by removal of material, and the lesion develops due to a combination of occlusal loading causing flexure of the tooth, and the action of acidic solutions which are present during chewing. In chewing, stress is

concentrated at the cemento-enamel junction, where most lesions of this type are observed. A notch missing from the tooth material in this region would significantly increase the magnitudes of the stresses occurring there. An example of this may be drinking red wine, containing a great deal of acid with a meal; the chewing inducing stress in the corrosive environment caused by the red wine.

In 1991, Grippo proposed that the general term **abfraction** should be used in place of the terms: abrasion, erosion, attrition and corrosion, when referring to the formation of lesions of this type. This was because such lesions are often produced by a combination of these effects, and to eliminate the confusion created by the terminology used in earlier work. For example, Black, in 1908, (Grippo, 1991) stated that the effects of brushing, and the very abrasive tooth powders that existed at that time, produced erosion of non-carious tooth substance. Miller, in 1907, (Grippo, 1991) performed some research into the effects of brushing on the wear of teeth, and concluded that no degradation occurred from brushing without the presence of a toothpaste. Since the tooth powders consisted of coarsely ground oyster shell, and sometimes cigar ash, it seems likely that these effects would be termed abrasive under the current definitions of the terms. Miller's findings have been supported by an *in vitro* study by Saxton and Cowell (Mair, 1992) using a brushing machine. Mair (1992) states that in the process of toothbrush abrasion, it is the abrasivity of the toothpaste that controls the wear process; the action of the bristles on the teeth is very small.

The effect of thermal degradation due to abrasion is believed to be significant; protein polysaccharides and collagen tissues are very susceptible to thermal damage (Grippo, 1992).

2.2 Stress Induced Cervical Lesions

It has also been proposed by several authors that Class V non-carious cavities could be caused by bending stresses exerted upon the teeth. This could be due to malocclusion, causing eccentric loading (Lee and Eakle, 1984), or due to lateral forces during normal function (Braem, 1995). Grippo (1991) proposes that abfraction should encompass the process of wear due to biomechanical loads

resulting from static loads due to swallowing or clenching, or cyclic loads from chewing.

The theory proposed by Lee and Eakle (1984) is that eccentric loading produces bending in the tooth, causing the enamel in the cervical region to be in tension. Enamel is believed to be anisotropic (Spears *et al.*, 1993) and tensile stress in the cervical third would induce stresses in the inter-prismatic enamel, pulling apart the stiffer prisms. Similarly, if the loading was applied axially, "barrelling" of the tooth would occur, causing alternate tensile and compressive stresses in this region (Tyas, 1995). This type of deformation permits water and other substances to enter the gaps that open up between the prisms, disrupting the re-establishment of the inter-prismatic bonds when the stress is relaxed. Ultimately, these micro-cracks propagate and the enamel prisms break away; hence the name "abfraction" (from the Latin *"ab"* - away, and *"fractio"* - to break).

Grippo (1992) provides evidence that there are greater instances of Class V lesions in elderly patients, and that these lesions do not appear to have been caused by the normal erosion or abrasion mechanisms. Lee and Eakle (1984) also find it difficult to explain the aetiology of lesions which affect one tooth, but not its neighbours by these conventional theories. Researchers such as Grippo (1992), Lambrechts, Braem and Vanherle (1987), Lee and Eakle (1984), and de Lange *et al.*, (1996) have surmised that these teeth must be subjected to cyclic bending stresses and hence the formation of such Class V lesions is due to fatigue failure of the teeth.

The recession of the gum in elderly patients is an accepted affliction (hence the expression "long in the tooth"), suggesting that this process might potentially lower the centre of rotation of the tooth, thus inducing more bending stress in the tooth. This in turn increases the cyclic load on the teeth, and could cause any existing cracks to propagate.

Interestingly, Grippo (1992) also reports that the Koreans suffer a significantly increased incidence of sub-gingival Class V lesions due to their dietary preference for dried squid. Since this is rubbery in texture, it requires a great deal of chewing, and so the cyclic loads on their teeth are increased. Similarly, it is also interesting that in one of the three case studies presented by Lee and Eakle (1984), the patient

exhibits signs of bruxism, and these authors reference other studies which quote a high incidence of bruxists among patients exhibiting cervical lesions of this type.

Lee and Eakle characterise the form of a lesion created by tensile stress as being a wedge-shaped defect occurring at, or close to, the fulcrum of the tooth. The size of this lesion would be determined by the magnitude and frequency of application of the tensile force, and the location of the lesion would be influenced by the direction of the lateral force. The defect is most likely to be wedge-shaped because the volume of the tooth experiencing the tensile stress concentration will have this form.

Using research performed by Brunski (1988), the number of cycles experienced by a human tooth by the age of 60 can be calculated:

The total time of contact between teeth in a 24 hour period is between 10 and 17.5 minutes.

The duration of tooth contact in one chewing cycle is 0.2 to 0.3 seconds.

$\Rightarrow$ The number of cycles that a tooth experiences in a 24 hour period is between:

$$\frac{10 \text{ minutes} \times 60 \text{ seconds}}{0.3 \text{ seconds}} \qquad \frac{17.5 \text{ minutes} \times 60 \text{ seconds}}{0.2 \text{ seconds}}$$

$$= \frac{600}{0.3} \qquad = \frac{1050}{0.2}$$

$$= 2000 \text{ cycles} \qquad = 5250 \text{ cycles}$$

$\Rightarrow$ The number of cycles experienced in one year by a tooth is between:

$$2000 \text{ cycles} \times 365.25 \text{ days} \qquad 5250 \text{ cycles} \times 365.25 \text{ days}$$

$$= 73.05 \times 10^4 \text{ cycles/year} \qquad = 19.18 \times 10^5 \text{ cycles/year}$$

Therefore, by 60 years of age, if the assumption is made that second teeth did not develop until the age of 10, a tooth will have experienced:

50 years x 7.31×10^5 cycles/year = 3.653×10^7 cycles

50 years x 1.92×10^6 cycles/year = 9.588×10^7 cycles

Grippo (1991) states that the average duration of tooth contact in one day is 9.0 minutes for contact during chewing, and 17.5 minutes for contact due to swallowing. This would give a total contact time of 26.5 minutes in a 24 hour period.

This is interesting, since many engineering components are designed for a life of 10^7 cycles; that is, they are expected to suffer high cycle fatigue failure after they have experienced cyclic load of low magnitude (below the yield strength of the material) 10^7 times (Gere and Timoshenko, 1991). A patient who suffered bruxism (para-functional clenching and nocturnal grinding of the teeth) would experience many more cycles on their teeth than this average. Thus, if cervical lesions can be induced by cyclic stress, then it would be expected that they would occur at a younger age in a bruxist, or that the lesions would be worse.

2.3 Treatment of Non-Carious Cervical Lesions

A great deal of controversy surrounds the diagnosis and treatment of cervical lesions. The treatment of non-carious cervical lesions may involve many techniques, depending on what is the most likely cause. Restoration may be necessary, but if the causal factors are not also treated, the destruction of the tissues in the affected area will not be prevented (Braem, 1992).

2.3.1 Treatment of the condition

If abrasion is the diagnosis of the cause of the lesion, it may be necessary to advise the patient on tooth brushing technique. If erosion or corrosion are thought to have contributed to the aetiology, causal factors need to be determined. Dietary

adjustment may be advocated, or the environment in which the patient works may have to be examined, if the source of the erosion is believed to be extrinsic. If the lesions originate from attrition, the patient may have to make an effort to cease a particular habit, such as clenching a pipe stem, or biting their nails. It may also be necessary to adjust the patient's occlusion in order to reduce the likelihood of further damage, if the lesions are thought to be induced by stress (Tyas, 1995). Similarly, if the lesions are believed to result from a medical condition such as bulimia nervosa or anorexia nervosa, it is advisable to refer the patient for treatment of this condition too.

Lee and Eakle (1984) propose that micro-cracks, potentially caused by malocclusion and hence eccentricity of loading, "could be expanded by water, and further weakened by chemical means...". Braem, in his 1995 paper on stress induced cervical lesions, also proposes that Class V lesions could be induced by lateral forces exerted on teeth, causing them to bend. Certainly, it appears, from all of the literature reviewed on this subject, that, once these lesions appear in teeth, they invariably grow. Grippo (1991) discusses at some length whether to ignore or restore a non-carious cervical lesion, but ultimately recommends the restoration of the cavity.

From an engineering perspective, this makes sense, since such a lesion can be regarded as a crack, or part of an unplugged hole, and hence will already have a high stress concentration factor associated with it. Thus, the engineer's solution is the same as the dentist's; the hole should be filled, preferably with a material with a similar value of E to that of the natural tooth.

2.3.2 *Restoration of the Lesion*

Class V lesions in anterior teeth are restored currently with materials commonly described as aesthetic restorative materials; materials that can closely match the original tooth colour. These are composite resin restorative materials and glass ionomer cements; these now also include resin modified GICs and polyacid modified resin composites, or compomers. Sometimes, a mixture of the two types of materials are used.

Composite Resins

Composite resin restoratives have been developed since the 1960s, and are the most widely used material in the filling of cavities in anterior teeth. The advantages of composite resin restoratives over amalgam are:

they permit more conservative cavities to be cut, preserving the sound natural tooth tissue,

they have material properties close to that of the natural tooth,

they can closely match the shade of the original tooth.

Composite resin restoratives incorporate particles of a filler in a resin in order to increase resistance to wear, and improve the compressive strength and the E of the material. The resin is initially in a matrix phase, and has to be set by some means. This is usually either a chemically activated, or light activated reaction, causing polymerisation and hence cross-linking of the polymer chains.

Chemically activated polymerisation

Chemically activated setting is usually achieved by mixing two (or more) reactants together and applying the restoration. This has advantages over light-curing in that curing should occur equally throughout the restorative, and that no special equipment is necessary to catalyse the polymerisation reaction. However, the quality and properties of the resulting material is dependent on the thorough mixing of the components, and air can be introduced into the restoration during mixing. Another disadvantage of chemical curing is that the material may begin to set during treatment, and that changes in the workability of the material are likely to occur as a result of this.

Light activated polymerisation

Light activated polymerisation gets around these disadvantages, but concern has been expressed in many quarters about the limitations of the depth of cure able to be reached by a light source, and it is recommended that light cured composite resins are placed incrementally to reduce the effect of incomplete curing. Incomplete curing would leave the restoration set hard on the outside, but still fluid towards the base of the restoration. This could cause sensitivity to the patient, and would result in poor mechanical properties of the material. Incremental curing may lengthen the treatment time, and much debate exists about the best way to place the increments.

One of the biggest problems with anterior teeth and composite resin restorations is that the resin matrix tends to shrink on setting. The inclusion of filler particles will also reduce polymerisation shrinkage and the thermal expansion of the restorative (Versluis, 1994). The type of filler particles used characterises the restorative. These are categorised by Versluis (1994) as: conventional, microfine, and hybrid resins.

Conventional Fillers

Conventional fillers are particles of glass, based on barium, boron or strontium, and containing alumino-silicate glasses. These materials tend to have high resistance to erosion, and high hardness characteristics, but this high hardness can also result in abrasion of the opposing teeth. Other disadvantages of conventional filler materials are the high wear rates and staining of the material that can occur. This is because the distances between the particles are relatively large; typically 10 - 40μm, so the particles can chip out during function.

Microfine Fillers

These are very small particles, typically 0.05 to 0.10μm, of colloidal silica, producing excellent cosmetic properties. However, they increase viscosity of the resin greatly, meaning that a high % weight fraction is not possible, thus microfine

composites tend to have poor strength characteristics and are prone to chipping. (Chipping is probably more of a problem in posterior teeth).

Hybrid Composites

Hybrid composite resins combine conventional and microfine filler particles. This improves the wear resistance of the materials, and makes them more suitable for use in highly stressed environments.

Glass Ionomers

In the late 1960s, the first adhesive dental cement was developed. This cement contained poly(acrylic acid) and zinc oxide, but later cements using alumino-silicates were developed. These have become known as glass ionomer cements (GICs), or glass polyalkenoate cements, and are widely used today. Fluoride is an important constituent of a GIC; it assists in the manufacture of the glass by lowering the fusion temperature, it enhances the mechanical properties and working characteristics of the glass, and can improve the translucency of the material (Combe, 1992). After placement of a restoration, fluoride is released into the surrounding tissues, giving the material good anti-cariogenic properties.

GICs have been shown to be highly cytotoxic in mice, and it has been suggested that they should not be used adjacent to the pulp, and that a liner of calcium hydroxide should always be placed between the pulpal aspect of the cavity and the restoration (van Noort *et al.*, 1990).

GICs have also been shown to erode at low pH, causing concern (van Noort et al., 1990), although Combe (1992) states that a fully hardened GIC is more durable than other cements in resistance to oral fluids. Combe also advocates protecting a freshly placed cement from moisture; GICs absorb water after placement, reducing volumetric shrinkage. GICs have a low coefficient of thermal diffusivity, and are able to bond to both enamel and dentine reliably; more reliably than can dentine bonding agents (van Noort, 1990). However, they are brittle materials with low tensile strength (Combe, 1992), and so cannot be used in highly stressed situations.

Hood (1991) observed that premolars restored with amalgam or glass ionomer were no stronger than those with prepared but unrestored cavities.

Tyas (1995) compares the results of restoring Class V lesions with 3 different techniques;

a type IIa restorative aesthetic glass ionomer cement,

a type III liner / base glass ionomer cement with a composite resin overlay,

a composite resin used in conjunction with a dentine bonding agent.

Type IIa glass ionomer cements are referred to as resin-modified glass ionomers, and are set by an acid-base reaction and by polymerisation of the resin, whether chemical or photo-initiated. The advantages of using resin-modified glass ionomers are that the restoration technique is simple, a large reservoir of fluoride is provided, and that other self-curing materials have showed very good long-term performance records.

Photo-cured materials have the added benefits above self-cured ones of achieving a higher bond strength, better polish, shade matching and translucency, improved physical properties, and immediate finishing. However, the shade matching and polish is still not as good as that obtained by a micro-fine composite.

Type III glass ionomers with composite resin overlay use a glass ionomer to line the inside of the cavity (Bitter, 1986). The use of a glass ionomer liner provides high fluoride release to fight caries, and permits improved bonding because the glass ionomer does not undergo the same degree of polymerisation shrinkage as the composite resin. Polymerisation shrinkage will be discussed in greater detail in Chapter 9. The use of the composite resin as the overlay is to improve the aesthetics; the polish and shade match of the final restoration.

The disadvantages of using this technique are that photo-cured composite resins may have to be placed incrementally to allow the total depth of the resin to polymerise, and that the liner needs to be placed in the cavity. This increases the complexity of placing the restoration, and the time that it takes, especially if the composite resin has to be placed incrementally in several layers.

Composite resin restorations used with a dentine bonding agent provide excellent aesthetics, a highly polished surface, and simple placement techniques. However, if the cavity is more than 2mm deep, Tyas advocates incremental placement to ensure complete curing, and composite resin restorations suffer from shrinkage of the resin upon curing.

Tyas recommends the techniques in the order 1, 2, 3 based upon the results of a study by Powell *et al.* (1995).

Modern micro-filled composite resins fulfil this specification very well; they have similar elasticity properties to dentine, and can be bonded to enamel and dentine to a high strength. Polymer-based materials are also relatively resistant to the acidity levels experienced in the oral environment, making them a good choice when erosion is believed to be the cause of the lesion (Mair, 1992; Grippo, 1992).

Grippo (1992) recommends using microfilled composite resin restorations with a low value of E, since this would permit the restoration to flex with the tooth rather than to distort under occlusal load. This issue will be addressed in greater detail in Chapter 7.

However, it is believed that the dentine-resin bond is not as strong as the enamel-resin bond, and so a great deal of effort has been expended on trying to increase the strength of the dentine-resin bond (often known simply as the dentine bond).

Another problem associated with composite resin restorations is that polymerisation shrinkage occurs; that is, the resin contracts as it solidifies. This obviously causes the restoration to pull away from the edges of the cavity, leaving cracks. These cracks can then become ideal sites for decay to develop. As already stated, it has been proposed that these cracks could be expanded by water, acidic food and drink, or propagated by the uncorrected dietary anomaly or malocclusion that caused the lesion in the first place. This can lead to marginal discoloration of the restoration, sensitivity of the tooth, the onset of secondary caries, and sometimes to the loss of the restoration itself.

This is clearly something that dentists and patients alike would wish to avoid, and so a great deal of research into testing dentine bonds, and increasing the strengths of the adhesives used in dentine-resin bonds has been carried out. However, grave doubts have been expressed as to the validity of experiments to test the strength of

dentine bonds (van Noort *et al.*, 1989, 1991) since there is little consistency between the techniques of different groups of researchers, and the scope for the introduction of experimental errors is large.

In subsequent chapters of this thesis, the stresses induced upon a finite element model of a lower canine tooth due to various load types are considered. The tooth is analysed as a natural, intact tooth, an unrestored tooth containing a Class V lesion, and as a restored tooth using various different material properties.

2.4 Dentine Bonding

Traditional dental restorative materials play no structural role; they merely fill a cavity. Bio-compatible composite resin restorative materials have been developed (see section 2.3), along with adhesives able to bond them to the tooth structure. However, these adhesive agents bond to enamel far better than to dentine. The bond to enamel is strengthened by etching the prepared surface of the enamel with a strong acid such as phosphoric acid.

The difficulties associated with bonding to dentine are believed to be caused, to a large extent, by the composition and histology of dentine (Swift, Perdigao and Heymann, 1995). Dentinal hydroxyapatite is arranged much more randomly than that of enamel, inside an organic matrix; mainly collageneous (see Chapter 1, Section 1.1). Dentine is also interspersed with tubules containing pressurised fluid. Normal pulpal pressure is 14cm H_2O; however, this can increase under anaesthetic up to 33cm H_2O (Pashley *et al.*, 1995).

Also, when a cavity is prepared in dentine, a smear layer of the debris from the cutting or grinding process results. Swift, Perdigao and Heymann (1995) describe the smear layer as varying in thickness from 0.5 to 5.0μm. The smear layer acts to reduce the permeability of dentine at the surface, but much has been written about the necessity of removing the smear layer in order to permit the formation of "resin tags" deep inside the tubules, forming cohesive bonds. Pashley *et al.* (1995) states that most of the early failures of dentine bonds were adhesive, due to bonding to the smear layer.

Swift, Perdigao and Heymann (1995) also explain that the smear layer needs to be removed because bacteria can become entrapped beneath it, breeding and causing secondary caries. This layer is usually removed by application of acid, similar to the acid etching of enamel.

In the 1950s, a resin was developed that could be bonded to dentine etched with hydrochloric acid (Swift, Perdigao and Heymann, 1995). Unfortunately, the strength of the bond was reduced when immersed in water. To combat this, a compound was developed, enabling water resistant bonding to dental calcium. This compound did not perform well clinically when used to restore Class V lesions without mechanical retention.

In the 1980s, a second generation of dentine bonding agents was developed, most of which are no longer available. The bonding mechanism used by these materials involved surface wetting of the dentine as well as ionic bonding between the calcium in the dentine and the phosphate groups of the resins. However, these compounds only achieve bond strengths of 1 to 10 MPa (Swift, Perdigao and Heymann, 1995), but bond strengths of between 17 and 20 MPa (Swift, Perdigao and Heymann, 1995) or 20 and 30 MPa (Pashley *et al.,* 1995) have been advocated in order to ensure that the margins do not de-bond during the contraction due to polymerisation of the resin. It is important to bear in mind the problems associated with extrapolating bond strength data from laboratory experiments to clinical situations (van Noort *et al.,* 1989; 1991).

It has also been suggested that these bonds are hydrolysed when immersed in water, causing the resin to separate from the dentine. This forms gaps at the margins which leads to micro-leakage. This in turn can lead to secondary caries, sensitivity and loss of the restoration. Clinical studies showed high loss rates of cervical lesions restored with these resins over 1-3 years. One of the major reasons for this loss is that the resins tended to be bonded to the smear layer, limiting the strength of the bond to the cohesive strength of the smear layer, or by the adhesion of the smear layer to the underlying dentine (Swift, Perdigao and Heymann (1995), Pashley *et al.* (1995)).

Third generation dentine bonding agents have been developed more recently. The bonding mechanism used here is mechanical also; resin penetrates the dentine tubules, helping to "lock" the restoration in place, as shown in Fig. 2.4.1.

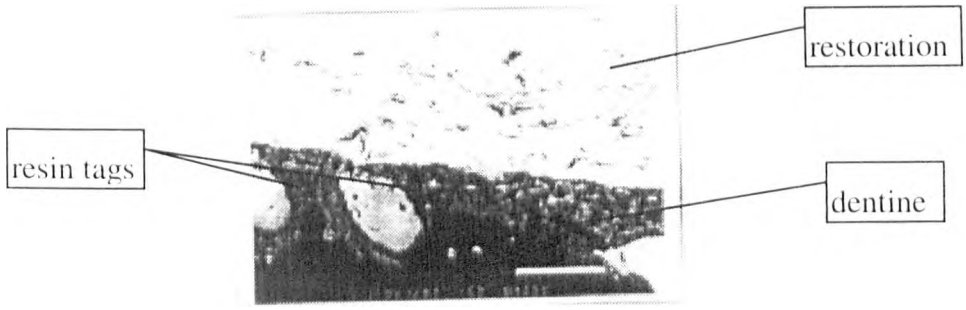

Fig. 2.4.1: Transmission Electron micrograph of the resin-dentine interface (Swift, Perdigao and Heymann, 1995).

This mechanism, described by Swift, Perdigao and Heymann (1995), works as follows:

Acid is applied; currently, one acid is commonly used both to etch the enamel and to remove the smear layer from the dentine. Removal of the smear layer opens the tubules, increasing the permeability of the dentine and decalcifying the inter- and peri-tubular dentine. This leaves a collagenous network that can collapse and shrink without inorganic support. So, after rinsing to remove the acid, a primer is applied to the dentine, generally containing both hydrophilic and hydrophobic functional groups. The hydrophilic group has an affinity for the dentine surface, and the hydrophobic group has an affinity for the resin. The primer wets and penetrates the collagen structure, taking it back to close to its original level of mineralisation, and increasing the surface energy of the dentine. The unfilled resin is then applied, copolymerising with the primer and extending into the opened dentinal tubules, forming a mixed layer of collagen and resin; the resin-infiltrated or hybrid layer.

The strength of these bonds typically approaches that of etched enamel to resin bonds; Pashley *et al.* (1995) say that the strengths are often higher. Marginal integrity is better preserved with third generation bonding systems, although marginal leakage is not totally eliminated. However, the stress distribution that has

been developed in laboratory studies has been shown to be very non-uniform, making the performance of the bond very unpredictable.

Doubt has been cast upon the validity of commonly used *in vitro* testing methods, and the propriety of extrapolating data from these shear bond tests to clinical situations (van Noort *et al.*, 1989, 1991). Microleakage studies and the relevance of thermocycling has also been questioned (Swift, Perdigao and Heymann, 1995; Barclay, 1998).

It has also been suggested that this situation is worsened by using stiff or highly filled composite resins (Swift, Perdigao and Heymann, 1995).

2.4.1 Summary

Generally, there are many problems associated with the bonding of composite resin restorative materials to dentine. It is more difficult to achieve a uniform, high strength bond to dentine than to enamel due to non-uniformity of the dentine and its composition. Composite resin restorations shrink with polymerisation, creating high stresses at this interface, sometimes leading to debonding of this interface. Application of a dental anaesthetic increases the pulpal pressure, which could potentially affect the stresses induced during the polymerisation contraction and dentine bonding stages of treatment.

Class V restorations are believed to experience flexural stresses during function, particularly at the cervical margins, which are often compromised during polymerisation. The combination of these effects means that there are significant problems associated with the retention of cervical restorations. A greater understanding of the combined effects of these mechanisms would facilitate research into the improvement of Class V restorations. The following chapters of this thesis seek to address these issues.

CHAPTER 3

A Review of Related Finite Element Studies

3.0 Introduction

Finite Element Analysis is a numerical stress analysis technique. In modern FEA systems, a computer model of the structure to be analysed is constructed, usually using a pre-processor. This model will then be sub-divided, or discretised, into a number of smaller parts, or elements. These elements are usually generated by an automatic mesh generator, with varying degrees of intervention by the analyst. The model must be sub-divided in such a way that the geometric features of the original structure can still be adequately represented. Ideally, elements should be square, and the change in size between one element and the next should be very gradual. This makes it impractical to model very small details, such as fillets in engineering, or precise, anatomical detail in bio-engineering.

The points where the elements join one another are called nodes. The model must be continuous; *i.e.* all of the elements must be connected to their neighbours at the nodes. Fig. 3.0.1a shows an example of a continuous model and Fig. 3.0.1b depicts a discontinuous model.

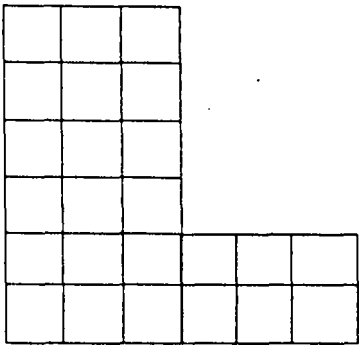

Fig. 3.0.1a: Continuous mesh.

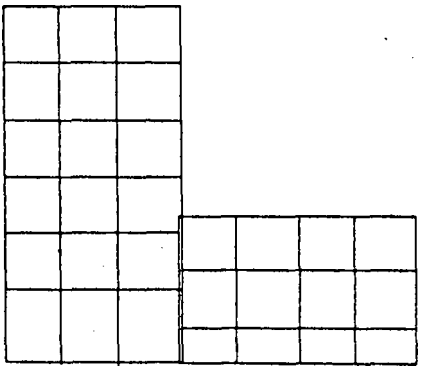

Fig.3.0.1b: Discontinuous mesh.

The analyst makes assumptions about how the loads (temperatures, forces, pressures, vibrations, *etc.*) can best be represented on the model, and how the model can be constrained; made to resist these loads. From this information, the structure can be analysed to determine the stresses acting within each element. More details of this process are given in Chapter 5.

In engineering, the utility of FEA is that it enables the suitability of the design of a component for withstanding the loads that it is likely to experience in its working life to be investigated before a model or a prototype is ever built. If the size and shape of the component are dictated by matters beyond the control of the designer, and the component has been empirically designed for many years, there is little point in performing FEA of the component. In this case, previous experience will have shown the suitability of the structure for the purpose (Baguely and Hose, 1995).

This is true of many of the Victorian engineering structures still in use today. However, in modern engineering, components are generally designed to be strong enough for their purpose, whilst using as few materials as possible. In this case, there is a definite need for more detailed stress analysis techniques to be used. Standard formulae listed in engineering handbooks should be used as part of any design process, but it is rare that the component to be designed will have identical loads and constraints to these formulae. The more simplifications that have to be made to a complex model, the less accurate will be the prediction of the stresses and strains within the structure. With FEA, designs can be analysed in terms of their structural or thermal performance, and the effect of a modification to a feature can quickly and cheaply be evaluated.

In dentistry, cavities have been cut, and restorations placed according to tradition for many years. Now, however, technology that is widely used in other industries can be applied to dentistry, enabling the effect of varying small details in the design of restorations to be evaluated in a scientific manner. Laboratory tests *(in vitro)* do not always give meaningful data (see Chapter 4), and often, the results cannot be extrapolated to predict *in vivo* behaviour. Even when they can, clinical studies take a long time to yield results. The intention of the studies undertaken in the subsequent chapters of this thesis is merely to advise upon the potential effects of certain criteria upon the stress distribution within a restored tooth, as compared to that of a natural tooth.

3.1 Classification Of Finite Element Models

Many different types of finite element models exist in this field. These represent the different assumptions that have been made, whether consciously or unwittingly, by various researchers. For example, a common assumption has been that enamel can be represented by an isotropic material for the purposes of FEA. However, Spears *et al.* (1993) demonstrated that the anisotropy of enamel cannot be ignored.

Some researchers have modelled only the crown of a tooth, whereas others have modelled the entire tooth, PDL and jawbone system. Between these two extremes are many variations, *e.g.* modelling the tooth and the jaw, but excluding the PDL, or modelling the tooth and the root, but no supporting structures.

The aim of this chapter is to examine the assumptions made by different researchers, and to consider what effects such assumptions will have on the results of their analyses. The function of the materials and the principles of engineering design will be used in this evaluation. In order to simplify this task, a number of models have been classified into four basic types; A, B, C and D.

Type A models are those which consist of the crown alone, or the crown and a small amount of the root.

Type B models include the whole tooth with no supporting structures.

Type C models consist of the tooth and the PDL, but no bone.

Type D models encompass the tooth, the PDL and the jaw bone.

3.2 Discussion

Throughout this thesis, Young's Modulus will be referred to as E. Generally, in engineering texts, Young's Modulus in the direction of the 3 global co-ordinate axes is denoted as E_x, E_y, and E_z respectively. However, for an isotropic material, $E_x = E_y = E_z$. All of the materials used throughout this study are regarded as being isotropic, except for the enamel, as documented in Chapter 4. Thus, the Young's Modulus is denoted by the letter E here, unless anisotropic enamel is being discussed.

Initially, the Type A model produced by Rees and Jacobsen for their 1995 anisotropic study will be considered. This model has been devised to incorporate the

enamel and dentine, with or without a Class I restoration. Unfortunately, permitting this facility appears to have been a problem, causing the incorporation of many kite-shaped elements with a poor aspect ratio, and producing quite large changes in size between neighbouring elements.

Anisotropic characteristics have been ascribed to the enamel, by rotating the axes of the material properties so that the direction of the x-axis is approximately parallel to the Enamel-Dentine Junction (EDJ). This is a very unusual approach to the problem.

A further problem associated with this model is that it is a Type A model, cut off just below the crown. Type A models do not permit the load to be reacted anywhere other than in the crown, which is unlikely to happen in practice. It has been known since 1965 that the deformation of the tooth is related to the rigidity of its anchorage (Korbar and Korbar, 1965). Therefore, if the root is assumed to be rigid, and thus represented by constraints, the deformation and the stresses within the crown will be affected by this assumption.

The study by Rees and Jacobsen (1995) was designed to reproduce the results of an *in-vitro* study by Hood (1991). Whilst close comparisons may exist between this paper and that of Hood, it does not necessarily follow that the results of these studies can be extrapolated to predict the biological reality of the situation. It is also possible that the displacement of the loading system may have been reproduced

O'Grady, Sheriff, and Likeman (1996) have produced a detailed Type D labio-lingual model of a mandibular canine incorporating the enamel, dentine, cortical and cancellous bone and the pulp, but neglecting the PDL. Whilst the authors have been at pains to reproduce the geometry of the tooth and bone precisely, the FEA mesh that they have used is comprised entirely of triangles. Although triangles facilitate the meshing of complex geometries, they are much stiffer than quadrilateral elements, and this affects the stresses predicted.

Furthermore, although the authors cite the small section of the PDL as one of the reasons for its omission in their model, the mesh that they have used includes large changes in size of adjacent elements, and elements with a very poor aspect ratio are situated next to elements with a good aspect ratio. This is considered very bad practice in engineering applications of FEA.

Another criticism of this model is that a number of elements meet at one node in several locations in this model. This again will affect the stiffness of this node, and hence the stresses and strains predicted. These authors too have neglected to model the enamel as an anisotropic material.

O'Grady, Sheriff, and Likeman (1996) have made the assumption that the PDL can be omitted from a 2-D FEA simulation, given that the precise nature of the behaviour of this tissue is still not yet understood, and that its small cross-section makes inclusion in an FEA model very difficult. However, since the stresses induced in the alveolar bone due to loading of the tooth as a denture abutment were the subject of this paper, the absence of the PDL from this model may be significant.

Another example of the differing assumptions made in FEA models can be found in the orthodontic analysis of a mandibular canine tooth carried out by Cobo *et al.* (1993). This research group was interested in the stresses induced in the PDL with an increasing degree of bone loss. A Type D model (with a good mesh) was used for this investigation. In this case, although the supporting structures of the tooth have been modelled, the assumption has been made that the tooth can be represented by a single substance with isotropic, uniform Young's Modulus *(E)*. The value used for *E* here of 1.96 $x10^6 N/mm^2$ ($200x10^3 kg/mm^2$) is an average of the values for enamel and for dentine.

The assumption of isotropy was probably made because Orthodontists were not interested in the behaviour of the constituent parts of the tooth; only in the performance of the PDL, the tooth as an entity, and the mandible. However, the work of Spears *et al.* (1993) has demonstrated that failure to incorporate the anisotropy of the enamel into a finite element model severely alters the resulting stress distribution. Work presented in Chapter 5 of this project also shows that this will alter the stress magnitudes and distributions in the supporting structures.

Cobo *et al.* (1993) make the point that the PDL is not a membrane of uniform thickness, but is hourglass-shaped, thinnest in the mid-root region. In their model, the PDL is represented as a uniform layer 0.25mm thick. They believe that this assumption may cause significant differences between the behaviour of their model and the real situation. This project also uses the assumption of a uniform thickness

PDL on the sides of the tooth (it is thicker at the bottom). This highlights another area of possible future work.

McGuinness *et al.* (1991), and Wilson *et al.* (1994) have produced one of the best FE models seen in this field; a 3-D, Type D model. However, they too have not ascribed anisotropic properties to the enamel. This is again probably due to the fact that they are interested in the stresses within the PDL. Consequently, they have been at pains to ensure that this region had the best aspect ratios possible in the elements, and that everything is as correct as possible in this region.

A different application of the FEA technique can be observed in the work of Hojjatie and Anusavice (1990). This paper describes the three-dimensional analysis of glass-ceramic crowns. Hojjatie and Anusavice have used a Type A model in 3-D for their work, constraining the base *xy*-plane of their model against translation in all directions 3mm below the crown. They have assumed that the influences of the cement layer and the PDL are negligible.

One of the important results from the work of Hojjatie and Anusavice (1990) is that the orientation of the load has a very marked effect upon the development of the large tensile stresses that tend to break prosthetic crowns. However, the results described in Chapter 5 suggest that the tensile stresses developed in crowns of teeth are much greater when using a Type A model constrained in this manner than if the supporting structures had been included. Since the incorporation of anisotropy has been shown to significantly affect the load transfer paths in natural teeth (Spears *et al.*, 1993), it is possible that the effects can be extrapolated to the behaviour of glass-ceramic prosthetic crowns. (Hojjatie and Anusavice have regarded glass-ceramic prosthetic crowns as having isotropic properties.)

Thresher and Saito (1973) used a type C model of the tooth, comprising dentine, enamel and the PDL, to investigate the importance of modelling the tooth as an inhomogenous body. They conclude that this is very important, and also recommend that the supporting bone should be modelled in the future. However, the model is meshed quite coarsely with triangular elements; possibly due to the limitations of both software and computing hardware at the time. If it is possible to mesh a 2-D model with quadratic elements instead of triangular ones, this is preferable because

triangular elements are degenerated quadrilaterals; 2 of the nodes are joined together to form the shape. This makes it difficult for the solver to calculate the modes of deformation that will occur in these elements. A possible solution would be to incorporate a central node in triangular elements, but convergence then becomes a problem (Zienkiewicz, 1977).

However, the paper was written in 1973, when FEA was in its infancy, and the development of pre-processing software has greatly facilitated the production of higher quality meshes.

Darendeliler, Darendeliler and Kinoglu, in their 1992 analysis of a central maxillary incisor have produced a Type B, 3-D model. Again isotropic, linear elastic material properties are assigned to it. Although this means that the model will suffer the same limitations as those discussed above in terms of anisotropy, this paper was published one year before the work of Spears *et al.*, (1993).

Neglecting to include fundamental material properties in an FEA model, and the use of unverified assumptions concerning the constraint of a model may significantly affect the load transfer patterns, and the distributions and magnitudes of the stresses predicted.

3.3 Software Evaluation

In this study, various different FEA codes were used. All of them have different merits, and with the increasing availability of translation software, the initial choice of software is less important. Pre-processors assist in the construction of meshes of higher quality, but have penalties in that they require increasing amounts of processing power to use.

The aim of this section is neither to provide an exhaustive review of all of the different commercially available FEA codes, nor to say which software is "the best" but merely to discuss the different merits of several codes with which the author has worked in an academic and an industrial environment. It is hoped that this might be useful for a novice user of FEA software.

The FEA codes used during the course of this research included:

ANSYS (versions 5.0a, 5.3 and 5.4)

ABAQUS5.6

LS-DYNA3D

HYPERMESH2.0

TOMECH

FEMGV

The author also has experience of NISA386 from previous work in industry.

LS-DYNA3D is fundamentally different from all of the other software codes used in that its formulation and solution algorithms were designed for the study of large deformation, dynamic events. It should not therefore be compared directly to the other software codes discussed here.

In the field of bio-engineering, LS-DYNA3D has been used for such applications as the modelling of heart valve prostheses and studying the effect of impact upon skulls. For such applications, LS-DYNA3D is highly suitable, since the models undergo large deformations, and the events under simulation are dynamic. However, an understanding of the concepts of dynamics is a necessity when using LS-DYNA3D.

FEA codes generally comprise three major parts;

the **Pre-Processor**, where models are constructed, meshed, and material properties are defined,

the **Solver**, in which loads and constraints are defined, and the stresses, strains and displacements resulting from these boundary conditions are calculated.

the **Post-Processor**, which displays the resulting stresses, strains and displacements graphically, and permits interrogation of this data.

However, the other software codes are all based upon the same fundamentals. The general trend in the development of FEA software currently is in improving the pre-

processing facilities and mesh generators, and to incorporate more specialised element types, *e.g.* hyperelastic elements, work-hardening, *etc.*

Improved mesh generators are a great advantage to new users in FEA, as the need for prior knowledge about what constitutes a good mesh is reduced. Since this knowledge takes time to learn and skill to apply, better meshing algorithms reduce the time of the learning curve considerably.

Improvements to the Pre-Processors generally make construction, selection and visualisation of the different parts on an FEA model much simpler. Examples of common features included in recent pre-processors are dynamic viewers, and the ability to define more levels of "selection logic".

Pre-Processors also enable more complex geometry to be constructed easily; later versions of ANSYS for example include more Boolean Algebra, enabling shapes to be constructed from combinations of standard "primitives"; regular geometric shapes. This is an extremely useful feature, reducing modelling time greatly.

3.4 Discussion

Most of the FEA models used in dental applications use tetrahedral elements in 3-D, or triangular elements in 2-D analyses. The use of tetrahedral elements as compared to quadratic elements is a contentious issue among FE analysts. Tetrahedral elements have become increasingly popular, largely because automatic mesh generators can quickly mesh complex geometries with them. This permits initial analyses to be performed, providing insight into what the orders of magnitude of the final solution might be. However, automatic mesh generators only work within the constraints specified by their programmers, and intervention by the analyst is still necessary to ensure that the resulting mesh is accurate enough to fulfil the purpose required.

In most cases, the mesh produced by the automatic mesh generator will be sufficient to indicate a rough solution to the problem. However, meshing will need to be edited to include more, smaller elements in the areas of interest, or around fine geometry features. The size of the elements approaching these regions will need to be adapted so that the element size reduces gradually. An adequate number of

elements through the thickness of the structure under analysis must be specified, and singularities (a number of elements meeting at one single point) need to be avoided.

Comparison of models meshed with tetrahedra to identical models meshed with bricks suggest that, to obtain information about the peak stresses in a model meshed with tetrahedra equivalent to that obtained from a model meshed with bricks, a much higher density of elements is required (Baguely and Hose, 1994, Ramsay, 1994). Similar information can be obtained from tetrahedral models if local refinement is used. This is easier to perform with tetrahedral elements, but the resulting meshes often have far worse aspect ratios than models meshed with hexagons. However, the mesh density required seems to be far finer than is commonly believed (Baguely and Hose, 1994).

3.5 Summary

In this chapter, the assumptions made by various other researchers using the Finite Element method have been examined. Only a small selection of the papers reviewed have been presented here. (Others have included Kelly *et al.*, 1995, Aydin and Tekkaya, 1992, Katona, 1994, Katona and Moore, 1994.)

The most important conclusion to be drawn from the literature reviewed in this chapter is that there is a lack of consistency in the assumptions made by various researchers when constructing Finite Element models. This suggests a need for critical analysis of these assumptions to identify those which were reasonable, and those which could lead to potentially erroneous results.

CHAPTER 4

The Influence of Boundary Constraints On Numerical Simulations of Teeth

4.0 Introduction

Increasingly, the Finite Element Method is being used in dentistry to assess the effects of occlusal loading on the movement of teeth and the resulting stress distribution. The literature review presented in the previous chapter identified a marked lack of consistency concerning the assumptions made by other researchers who have previously used FEA techniques to study the behaviour of human teeth.

In this chapter, the effect of different boundary conditions on the stresses, displacements and stress distributions in a mandibular canine tooth were investigated. Variations resulting from the use of anisotropic and isotropic enamel were also evaluated, following from the work of Spears *et al.* (1993). FEA requires certain assumptions to be made when constructing the model, applying loads and constraints, or assigning material properties. It is imperative to ensure that the assumptions made are appropriate to the topic under investigation and of relevance to the area of study. Assumptions must not affect the results in the area of concern, and that the model is insensitive to the variation of non-essential attributes.

Many studies have been undertaken to analyse the behaviour of the tooth-adhesive-restoration system in an attempt to improve the performance of dental restorations. Finite Element Analysis (FEA) is an ideal tool for such analyses since clinical studies take years to reach fruition, and *in-vitro* testing can alter many of the environmental conditions, thus affecting the results. FEA permits the study of the mechanical behaviour of human dentition to be simulated more realistically, and for results to be obtained cheaply and quickly.

De Vree *et al.* (1984) used FEA techniques to study the influence of alternative cavity designs upon the overall distribution of forces in a molar restored with amalgam. This appears to have been the first study of this type to consider the entire tooth. De Vree *et al.* (1984) used an axisymmetric, 2-D, type A model of a molar, with isotropic material properties throughout.

Since this study, other researchers have analysed FEA models of teeth constrained in a variety of ways. For example, the crown alone of a molar tooth was considered in one analysis (Rees and Jacobsen, 1992). In a second study, a normal and a restored mandibular premolar were cut off approximately 3mm below the crown and

analysed (Yettram *et al.*, 1976). Peters and Poort (1983) state that the inclusion of the roots of a tooth in FEA simulations does not influence the resulting stress patterns in regions of the tooth relevant to this study. In these cases, the aim of the research has been to study the behaviour within the crown; in particular, in the incisal third of the crown.

A 3-D model of an entire canine, including the Periodontal Ligament (PDL) and jaw bone, has been assessed to study the PDL under orthodontic loading (Wilson, Middleton, *et al.*, 1994a and b). In another case, a model of the tooth set in the jaw bone has been analysed, but the tooth has been regarded as composed of a single, isotropic substance (Cobo *et al.*, 1993).

Peters and Poort (1983) summarise the information required to apply FEA techniques to dental systems. Information about the geometry of the structure, the load and support types, the physical properties and the interface characteristics of the materials are required. The importance of supplying the most relevant input data to an FEA model is stated clearly here, and this point cannot be impressed too strongly. If the initial assumptions made with a numerical analysis technique are flawed, the results of the analysis may not be relevant. Hence, assumptions should be made with extreme caution!

This numerical study examines the effect of applying boundary conditions to different parts of the model upon the stress distribution and the movement of a mandibular canine tooth. Teeth are attached to their sockets in the jaw, and to adjacent teeth via the PDL. This, as discussed in Chapter 1, consists of bundles of collagen fibres and blood vessels surrounded by a ground substance. The PDL plays an important part in the response of a tooth to loading, but often it is excluded from FE models because of its small size. This investigation explores the effect of different methods of constraint, and the rôle of the PDL and the jaw bone in the mechanical behaviour of restored and unrestored teeth.

4.1 Construction of the Model

Many researchers gather the necessary data for the construction of a FE model by selecting a tooth believed to be typical of its type, sectioning it in various planes and measuring, tracing or digitising the sections. This can create very detailed, precise

geometry of a particular tooth. However, it could be regarded as somewhat wasteful for every researcher wishing to create a FE model of a tooth to go through this process, especially when there already exists a wealth of data concerning the standard measurements and forms of different teeth.

Furthermore, the digitising of complex structures often creates as many problems as it solves; biological structures are usually far from ideal, and one of the first problems facing a researcher trying to use digitised data is how to reduce the quantity of information available to a manageable amount. In engineering, one of the first tasks facing an analyst is to decide what features of the component under scrutiny can reasonably be missed out. For example, can fillet radii be omitted, since the incorporation of such a feature would require the mesh to be very small in this region? This would significantly increase the computational expense of the model during the solution phase, and would require more time and skill from the analyst to produce an acceptable mesh. Failure to include gradual changes in the size of the elements could decrease the accuracy of the solution, as discussed in Chapter 3.

FEA software does not respond well to being asked to mesh the type of undulating surfaces that would typically result from a digital scan of a tooth. Surface characteristics of this type would cause unrealistic stress concentrations in the model under analysis, and would mean that the number of elements required to represent such geometry was extremely large. Thus, lines and surfaces of "best fit" have to be created.

In this study therefore, data collected by experienced clinicians over many years was used to construct the model of the tooth. Table 4.1.1 lists the standard dimensions reported for mandibular canine teeth.

Table 4.1.1: Dimensions for a sample of 316 mandibular canines (Woelfel, 1990).

Dimensions Measured	*Average*	*Range*
Crown Length	11.0	6.8-16.4
Root Length	15.9	9.5-22.2
Overall Length	25.9	16.1-34.5
Crown Width (M-D)	6.8	5.7-8.6
Root Width (cervix)	5.2	4.1-6.4
Facio-lingual Crown Size	7.7	6.4-9.5
Facio-lingual Root Size	7.5	5.8-9.4
Mesial Cervical Curve	2.4	0.2-4.8
Distal Cervical Curve	1.6	0.2-3.5

This information was used in the construction of the model shown in Fig. 4.1.2. However, some interpolation is required in order to produce an FEA model from this data, and hence the model may be compromised geometrically by this process. On the other hand, it may be of more use to produce a model typical of an "average" canine tooth than a detailed model of a specific tooth.

The PDL is quoted as varying in thickness between 0.1 and 0.33mm in many standard texts, being thinnest towards the middle of the root. The outline of the root of the tooth model was used as a template to create the PDL model.

Constructing the model of the bone presented more of a problem. Information concerning the precise form and thickness of cortical and cancellous bone is scant, and at the time of the creation of the model, none could be found. The author therefore used radiographs and Magnetic Resonance Imaging (MRI) scans to elucidate the form of the bone. Scans of adult mandibles published in the book Maxillofacial Imaging (1990) were measured and scaled. These figures are

incorporated in Appendix 3. Cortical bone was taken to be the dense bone material visible on these scans, and the less dense spaces were assumed to be cancellous bone. An average of the measurements was used to specify the approximate form and thickness of the mandibular bone. The resulting FEA model was then shown to an experienced oral pathologist (personal correspondance with G. Craig, 1996), and an experienced clinician (personal correspondance with S. Northeast, 1996), who declared it to be a realistic representation of a bucco-lingual section through a mandible.

For the purposes of this study, the models of other researchers were classified into four categories, A, B, C and D, as described in Chapter 3. These ranged from the crown alone (type A) through to a model encompassing the entire tooth, Periodontal Ligament (PDL) and supporting bone (type D). Each model was analysed with both isotropic and anisotropic enamel.

Four basic Finite Element models (models A, B, C, and D) of a canine tooth were constructed as shown in Fig.s 4.1.2a-d *(see Chapter 3).* Four noded, isoparametric, plane strain elements were used to construct the models. Models A, B, and C are reduced versions of model D, made by unselecting sets of nodes and elements to ensure the consistency of the mesh. All four models are constrained against translation in the global X and Y-directions. Model A examines the case where the tooth is cut off and constrained just below the crown (Fig. 4.1.2a). The tooth alone is considered in model B, constrained along the root (Fig. 4.1.2b). Model C comprises the tooth and the PDL, with constraints applied to the outer surface of the PDL. (Fig. 4.1.2c.) The entire tooth, set in the jaw bone, and incorporating the PDL is examined in Model D. Constraints have been applied, as shown, to the base of the jaw bone. (Fig. 4.1.2d.) All analyses were performed using the commercial *ANSYS5.0a* software. Fig. 4.1.2e shows the different materials modelled. The Young's Modulus (E) of the PDL was determined by a quasi-static analysis of model C using the software *LS-DYNA3D* and the proprietary software *DYNASYS* (Thornton *et al.*, 1997). Further details are given in section 4.3 of this chapter.

Both isotropic and anisotropic material properties were ascribed to the enamel, and analyses of the four models were undertaken with each, subject to an occlusal load of 100N, as shown in Fig. 4.1.3.

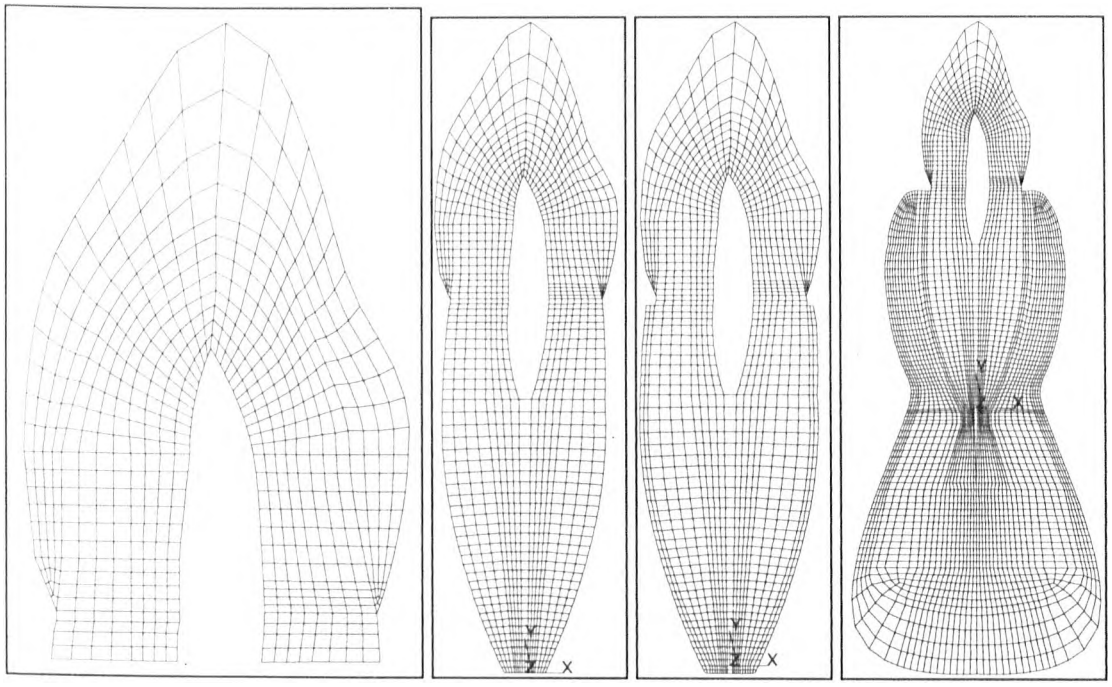

Fig. 4.1.2: Showing the mesh and the materials used in models A-D.

Fig. 4.1.2a *Fig. 4.1.2b* *Fig. 4.1.2c* *Fig. 4.1.2d*

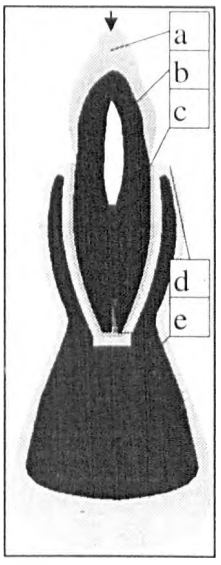

Materials Key:

a = Enamel

b = Dentine

c = PDL

d = Cortical Bone

e = Cancellous Bone

Fig. 4.1.3: The materials used in the model.

4.2 Loading

It is difficult to specify exactly how a particular tooth will be loaded *in vivo*, since the type, direction, and magnitude of the load applied will be a complex function of the situation under investigation. This includes factors such as the properties of the object inflicting the load, the physiological and emotional state of the patient, and the relationship with the surrounding teeth. In view of this complex problem, FEA analyses often use a point load as a reasonable approximation of a hard food substance being bitten by a patient. This has the advantage of simplifying the analysis process for the solver.

The magnitude of bite loads for anterior teeth is often quoted as being between 100N and 200N. For posterior teeth, loads are higher; of the order of 300N to 400N.

A point load on a mandibular canine tooth would generally tend be applied perpendicular to the buccal surface of the cusp. However, since the analyses presented here are basic simulations to investigate the effect of the boundary constraints upon the stress distribution in a tooth, a simple vertical load applied to the incisal tip is used, as shown in Fig. 4.1.2. An occlusal load of this type simplifies the analysis, particularly when anisotropic material properties are used. The magnitude of the load applied was 100N.

4.3 Materials

When this work was undertaken, there was very limited information available about the material properties of the PDL.

The non-linear, stress-strain behaviour of natural tissue can be represented by an exponential strain energy density function, as described by Huang *et al.*, 1990. The resulting curve has been defined as a material type in the *DYNA* package (Chew *et al.*, 1994), and is shown in Fig. 4.3.1. Furthermore, an interface, called *DYNASYS* (Thornton *et al.*, 1997) between the two software packages used, *ANSYS5.0a* and *DYNA*, has been created by the Heart Valve Research Group at the University of Sheffield.

The value of E for the PDL was determined by a quasi-static analysis using the commercial software *LS-DYNA3D (DYNA)*. Using *DYNASYS*, it was possible to transfer Model C from *ANSYS* to *DYNA*, using the material properties given in Table 4.3.1. The E of the PDL was assigned as Material 40 in *DYNA*; this uses the non-linear strain energy density function for natural tissue. A vertical load of 100N was applied.

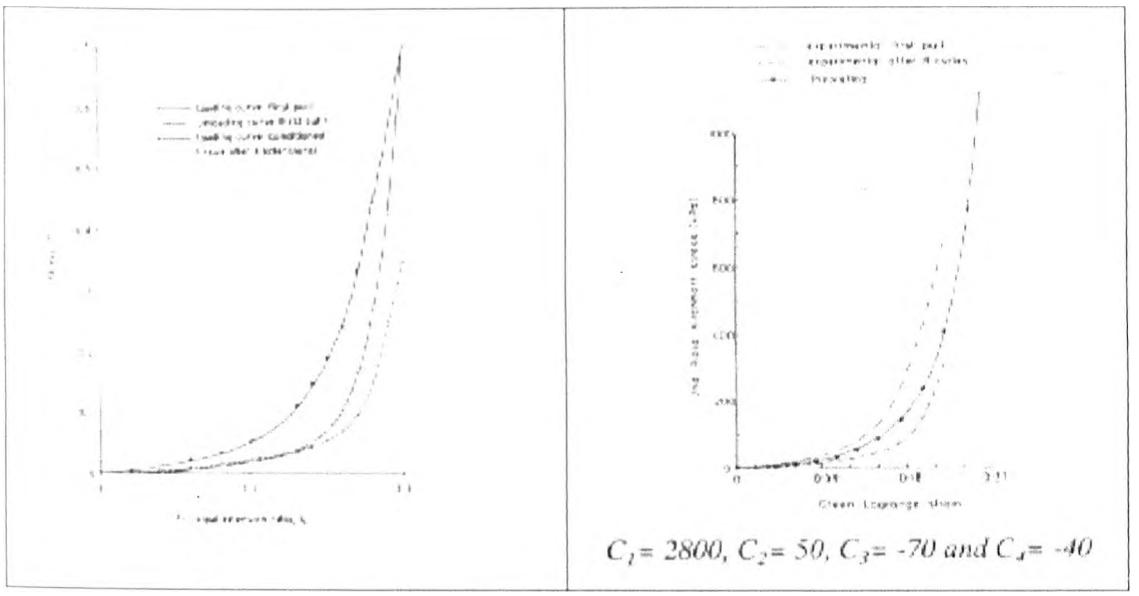

Fig. 4.3.1: Examples of the SEDF used to model bovine pericardium tissue, and the modified model used for human tissue (Stevens, 1998).

When the analysis was complete, the values of stress found at various points on the PDL were noted and a curve fitting program (Chew *et al.* (1994)) was used to determine E for the stresses predicted by *DYNA*. An average value of 30 MPa was then selected and used in subsequent analyses. An average value was used to avoid over-complication of a model to be used for preliminary analyses. Chapter 5 redresses the implications of the assumption that the PDL can reasonably be represented as a linear elastic tissue for analyses of this type, and explores the effect of varying the value of E used.

Table 4.3.1: The Material Properties Used.

MATERIAL	Ex (MPa)	Ey (MPa)	ν_{xy}	DENSITY kg/mm^3
Isotropic Enamel	80 000[c]	/	0.3[c]	2.8x10^{-6}[c]
Dentine	15 000[c]	/	0.3[c]	1.96x10^{-6}[c]
PDL	30	/	0.3	1000x10^{-6}
Restoration	15 000[b]	/	0.3[c]	/
Anisotropic Enamel	80 000[b]	10 000[b]	0.3[b]	2.8x10^{-6}[c]
Cancellous Bone	689[a]	/	0.3[a]	/
Cortical Bone	13 700[a]	/	0.3[a]	/

[a]Cook, S. D., Weinskin, A. M., Klawitter, J. J. *A 3-D Finite Element Analysis of a Porous-Rooted Co-Cr-Mo Alloy Implant,* J Dent Res, 61, (1), 1982, 25-29.

[b]Spirings, A. M., de Vree, J. H. P., Peters, M. C. R. B., Plasschaert, A. J. M. *The Influence of Restorative Dental Materials on Heat Transmission in Human Teeth,* J Dent Res, 63, (8), 1984, 1096-1100.

[c]Spears, I. R., Van Noort, R., Crompton, R. H., Cardew, G. E., Howard, I. C. *The Effects of Enamel Anisotropy on the Distribution of Stress in a Tooth,* J Dent Res, (72), 1993, 1526-1531.

4.4 Results

Fig. 4.4.1 shows an example of the stress distribution resulting from anisotropic analyses of model D subjected to an occlusal load of 100N. The PDL and bone have been blanked out in Fig. 4.4.1 so that only the stresses in the tooth are presented. This practice is continued for the subsequent figures in this chapter since the stress distribution within the tooth is the likely area of interest, and comparison of the models is facilitated. Also, the stresses in the global vertical direction (the y-stresses) only are presented because these are largest in magnitude, although, obviously, other stresses were analysed.

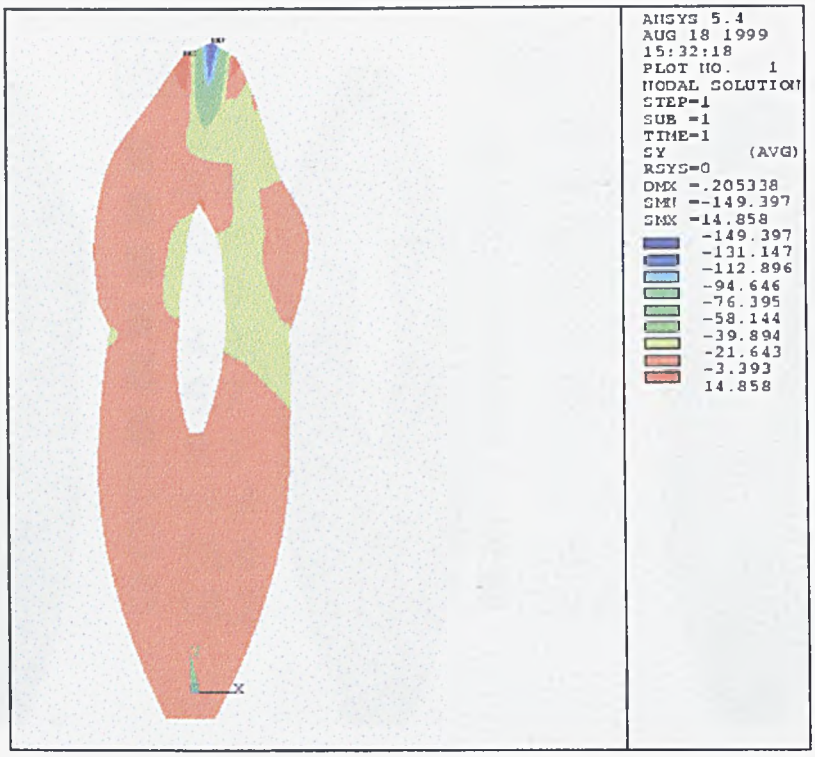

Fig. 4.4.1: The distribution of y-stresses in model D.

To further aid the comparison of models, plots of the differences in stress distributions have been produced. These are shown in Fig. 4.4.2a-c. From these, it can be seen that the most significant differences exist between models B and C (Fig. 4.4.2b). Since the only parameter to be altered between models B and C is the presence of the PDL, it can be seen that this has a profound effect upon the results.

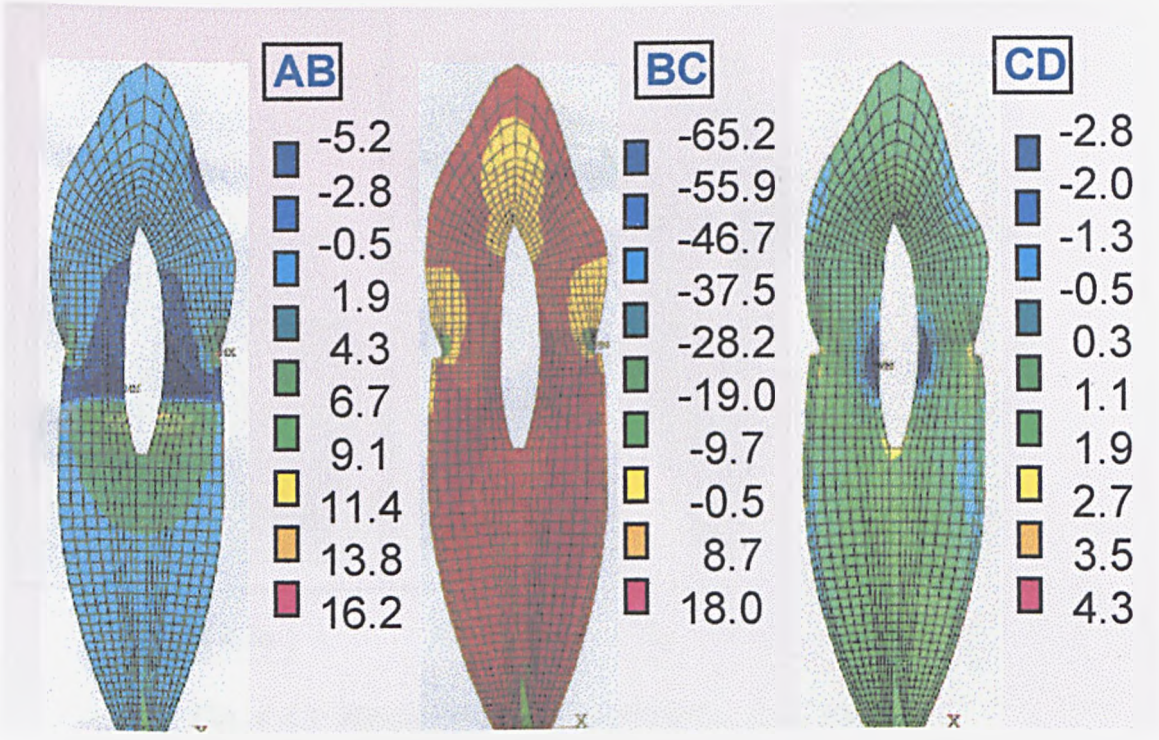

Fig. 4.4.2: The differences between y-stress between models A and B, B and C and C and D.

Differences in the stresses exist between models A and B, and between models C and D, but these are comparatively insignificant.

In light of this, it is interesting to observe the differences in displacements that result from these analyses, shown in Fig. 4.4.3a-c. The differences in displacements between models A and B are shown in Fig. 4.4.3a, between models B and C in Fig 4.4.3b, and between models C and D in Fig. 4.4.3c.

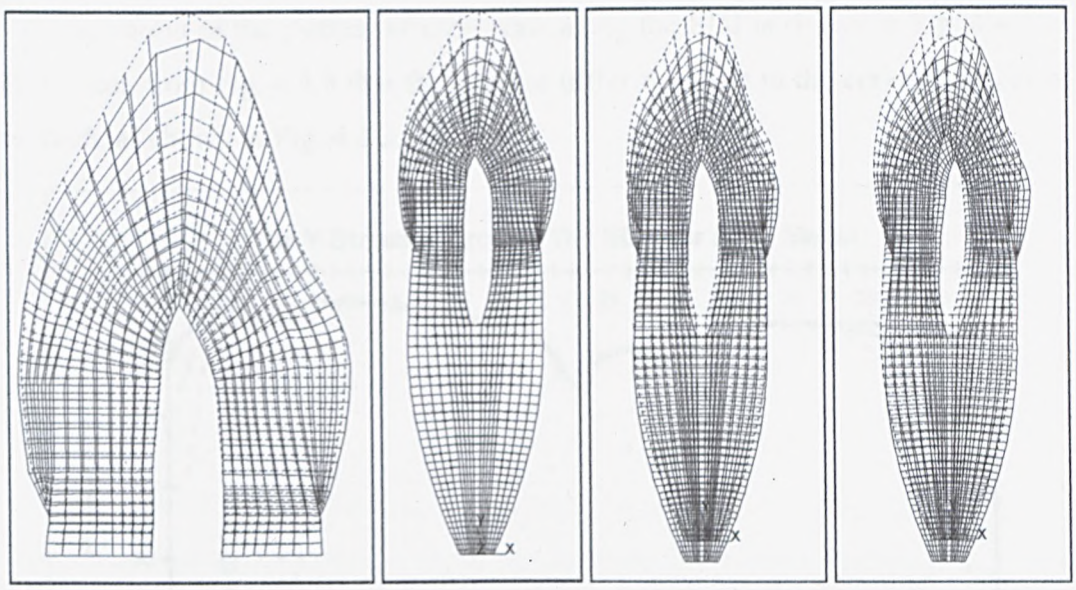

Fig. 4.4.3a | Fig. 4.4.3b | Fig. 4.4.3c | Fig. 4.4.3d

Fig. 4.4.3: The Deformations of Models A, B, C, and D.

Finally, a comparison of Fig. 4.4.4a and 4.4.4b shows the different stress distributions that result from using anisotropic and isotropic enamel. In this comparison, model D is once again considered. From Fig. 4.4.4, the load channelling effect of the anisotropic enamel prisms can clearly be seen. Hence, using isotropic material properties for enamel could evidently result in misleading results.

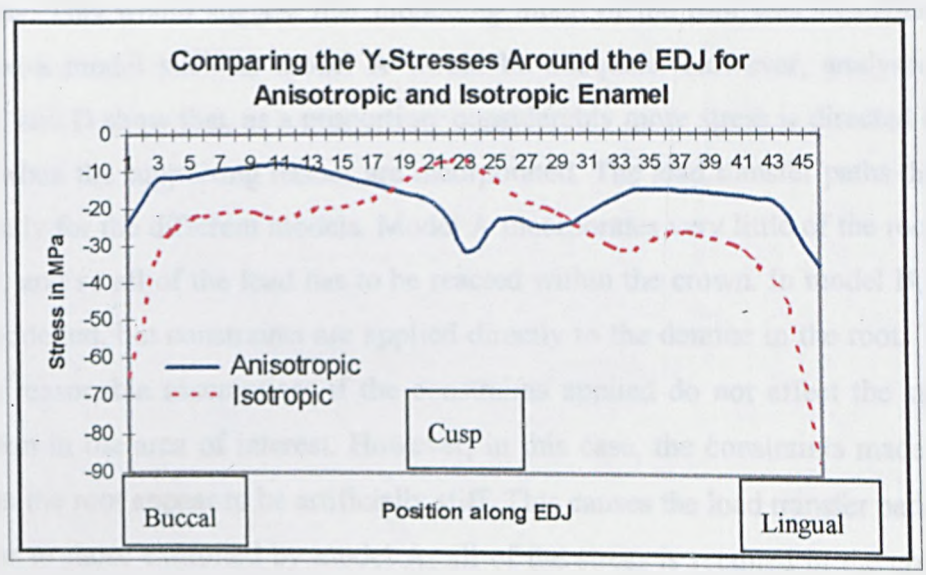

Fig. 4.4.4: The stresses predicted for analysis with isotropic and anisotropic enamel.

The variation of the y-stress at each node along the EDJ is shown in Fig. 4.4.5. It can be seen from Fig. 4.4.5 that the stresses differ the most in the cervical region of the tooth, as shown in Fig. 4.4.2.

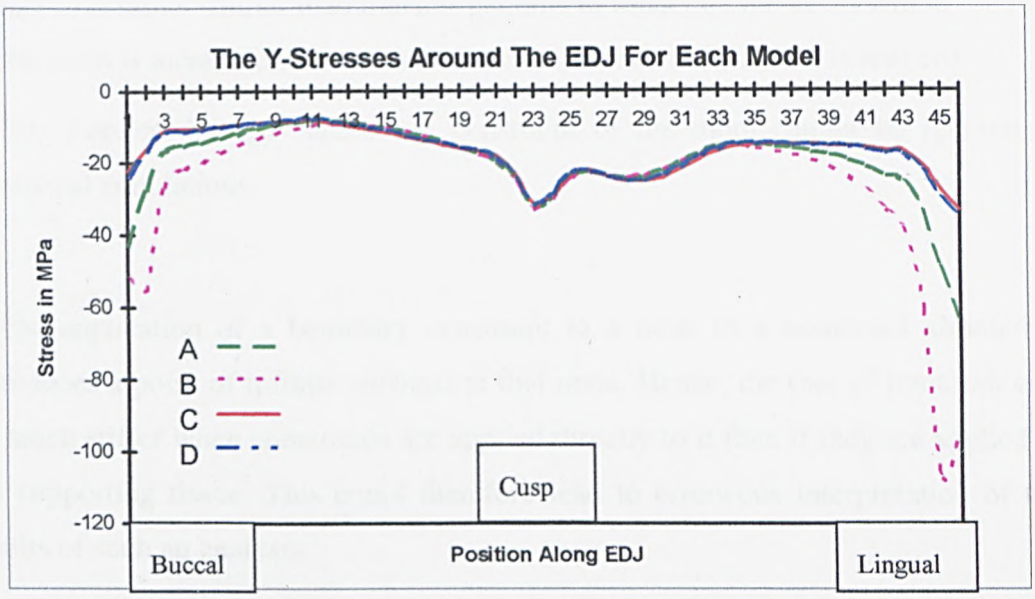

Fig. 4.4.5: A comparison of the y-stresses around the EDJ for each of the models.

4.5 Discussion

The most important finding of this work is that the boundary constraints imposed upon such models can significantly affect the results. If the softer, supporting structures of the PDL and the jaw bone are neglected, then the root experiences very little stress. This would suggest that modelling much of the root was superfluous, and hence a model such as model A would be adequate. However, analyses of models C and D show that, as a proportion, considerably more stress is directed into the root when the supporting tissues are incorporated. The load transfer paths differ significantly for the different models. Model A incorporates very little of the root of the tooth, and so all of the load has to be reacted within the crown. In model B, the root is modelled, but constraints are applied directly to the dentine in the root. This can be a reasonable assumption, if the constraints applied do not affect the stress distribution in the area of interest. However, in this case, the constraints made the dentine in the root appear to be artificially stiff. This causes the load transfer paths to be similar to those exhibited by model A; all of the stress is retained in the crown. This can be seen in Fig. 4.4.3b and c; most of the root cannot be displaced in model B (Fig. 4.4.3b), but is able to in model C (Fig. 4.4.3c). In model C, the constraints

are applied to the more flexible material of the PDL. This permits the load to be dissipated through the root of the tooth into the PDL, increasing the stress observed in the root, but reducing the stress magnitudes at the cemento-enamel junction. Model D exhibits similar load transfer patterns to model C; the stress within the root of the tooth is increased, but stress at the cemento-enamel junction is reduced.

This implies that the method of constraint of the tooth cannot be ignored in numerical simulations.

The application of a boundary constraint to a node in a numerical simulation introduces a point of infinite stiffness at that node. Hence, the root of the tooth will be much stiffer when constraints are applied directly to it than if they are applied to the supporting tissue. This could therefore lead to erroneous interpretation of the results of such an analysis.

It is standard engineering practice to ensure that the constraints are removed far enough from the area of interest not to influence the results. From this study, it can be seen that the way in which the constraints have been applied has affected the stiffness of models A, B, and C. In comparison with model D, the stresses and displacements of models A and B differ significantly, and the displacements are altered in model C. To ensure that the constraints imposed upon model D did not influence the stresses in the tooth, a fifth model was analysed. This comprised model D with the boundary constraints attached by beams. There were no changes in the stress or displacement plots for the tooth resulting from these two analyses. Thus it can be inferred that the constraints applied to model D do not affect the behaviour of the tooth.

The stresses in model C do not differ significantly from those obtained from analysis of the tooth in model D. However, the displacements do differ appreciably between these two models. Hence, if the stresses in the tooth only are of interest, then a model such as model C would be sufficient for this purpose. Conversely, if information about the displacements was required, then it would be necessary to incorporate the mandible into the model too.

It is also interesting to note that the largest stresses occur in models A and B.

Limitations of the models A-D used in this study are that they are only 2-D, and that the PDL is modelled as a uniform thickness ligament of 0.33mm. This latter assumption could introduce errors in the estimation of the magnitudes of the stresses and displacements.

Certain of the models produced by other researchers and considered in this study were 3-D. Since the geometry of the crown and the root can be thought of as roughly symmetrical, and the plane strain criterion is applied, it is believed that the concerns regarding the application of boundary constraints to FE studies of teeth can equally be applied to 2-D and 3-D simulations.

From the results of this study, it would appear that very few of the FEA models produced by other researchers are suitable for analysis of the stresses induced in the crowns of teeth due to functional loading.

4.6 Validation

The displacements of the models were compared to those predicted by Picton, 1965. The *LS-DYNA* model predicted that the displacement of the apex of the crown would be of the order of 0.21mm in response to a load of 1N applied horizontally to the labial surface of the tooth, about 1/3 of the way below the apex of the crown. This finding compared well with the upper bounds of the displacements measured by Picton. Validation of the FEA models is treated in greater detail in Chapter 6.

4.7 Conclusions

The following remarks state the conclusions that can be drawn from this study:

It is essential to model the root and the supporting structure of the tooth when investigating the behaviour of either a restored or an unrestored tooth, in accordance with good engineering practice.

To analyse the stresses in the vicinity of the restoration, it is sufficient to constrain the PDL only, but the mandible must be incorporated to produce displacements of the right order of magnitude.

An anisotropic model of the enamel should be used to produce a realistic load transfer mechanism in such analyses.

The results of this investigation can be extrapolated to a large extent to 3-D Finite Element models.

4.8 Recommendations for Further Work

Cobo et al. (1993) recommended that the PDL should be modelled as a tissue of variable thickness. This ought to be investigated in future studies.

The PDL ought to be modelled with at least 3 elements across the thickness, in line with standard FEA recommendations.

The model needs to be modified in order to permit investigation of the stresses around typical restoration geometries.

CHAPTER 5

Comparing the Behaviour of a non-linear, linear and multi-linear Elastic PDL in Different FE Codes

5.0 Introduction

The field of Bio-Mechanics is beset by the difficulty associated with obtaining reliable values of material properties to be used in stress analysis techniques.

A wide range of values suitable for the Young's modulus (E) of a linear elastic PDL have been suggested in experimental and FEA studies. Rees and Jacobsen (1997) have listed a table of the values used previously by other researchers in Dental FEA studies. The reported values of E range from 0.07 MPa to 1750 MPa. This is an extraordinary range of values for the E of a material.

Some of the deviation in the magnitudes of the values reported may be due to the physical state of the patient at the time of determination of E of the PDL. Bien (1966) reports that the material properties of the PDL of a rat were significantly altered when the animal was sacrificed. This could be attributed to the fluid component of the PDL; once the heart of the animal is stopped, the blood pressure within the vascular network cannot be maintained and hence the resistance of the tissue to an applied load is significantly reduced.

Another possible reason for the discrepancy in measured values of E of the PDL could be that the response of the PDL may be non-linear; *i.e.* load-dependent. Thus, if a large load was applied to the tissue, a high resistance to the load might be measured, whereas the lower values of E measured may correspond to applications of low loads, possibly because live subjects are used.

Other possible reasons for the differences between the values reported could be accounted for in consideration of the experimental set-up; *e.g.* was E measured by calculation from the displacement of the tissue, and if so, was the displacement measured independently from the surrounding materials? Or was E determined by applying standard engineering formulae to the measured modulus of rupture of the tissue? If this was the case, given that the PDL is so different to a standard engineering material, is this a reasonable assumption to make?

Evidently, this makes it difficult to select an appropriate value of E for use in FEA iterations.

5.0.1 *The Fluid components of the PDL*

Considering the fluid components of the PDL, Bien (1966) divides the material into 4 morphological components:

Cells

Vessels

Fibres

Interstitial fluid.

Each of these plays a separate role in the overall behaviour of the PDL.

The cells consist of protoplasmic gel, surrounded by a membrane, and the fibres of the PDL weave around the rich network of blood vessels, connecting to the tooth and the bone. The remaining spaces are filled with interstitial fluid, or ground substance, which is of changing viscosity (Heilbrunn, 1950; Johnson *et al.*, 1954) (Bien, 1966). It is also reported that the viscosity of the protoplasmic gel changes with pressure; hence protoplasmic gel is a **thixotropic** fluid (*i.e.* it is a jelly when not in motion, but flows easily under pressure (like toothpaste) (Champion and Davy, 1563; Frey-Wyssling, 1953) (Bien (1966). Protoplasmic gel also exhibits visco-elastic properties; it flows under application of a steady force, but will bounce if a load is briefly applied and removed. This describes the difference between a functional, mechanical load and an orthodontic, or applied load.

Bien (1966) states that the damping forces are either due to friction from viscous drag within the fluid, or a hydraulic damping effect , dissipating energy by forcing fluid through narrow oficices.

Mathematical analysis of the hydrodynamics of the PDL is very complex.

The roles of the PDL are described by Bien (1966) as being to provide a nutrition and gas exchange mechanism between the tooth and the alveolar bone, and to resist or to transmit forces applied to the tooth to the bone. Studies of the histology of the PDL after loading have been made by Castelli and Dempster (1965), Cohen (1965) (Bien, 1966) and Reitan (1960) . Living studies are rare, due to difficult access. Schwarz (1932) (Rygh, 1972) has indicated that the an optimum orthodontic force

would be one in which the blood capillary forces are not exceeded. However, this contradicts the clinical finding that bite forces of 1500g/cm^2 do not crush the PDL.

Sicher (1970) suggested that the tooth maintained its location in the socket via the PDL, and that the PDL protected the hard and soft tissues of the socket. Synge (1933) and Gabel (1956) (Moxham, Berkovitz and Newman, 1995) proposed mathematical evidence that the PDL could not function by the suspensory mechanisms of the collagen fibres alone, and this work was supported by an histological study by Main (1965) who showed in a study of proliferating pulpal cells that the PDL did not posses the characteristics to transmit tension to the alveolar bone. Hence, the theory is purported that the vascular structure of the PDL must play a part in resisting and transmitting load. (Speculations on this theory also put forward by Kindlova and Matena, 1959 and 1962).

Bien (1966) identifies three distinct and interacting fluid systems within the PDL are identified in the text; they are:

the vascular system of blood and lymph vessels

the cell and fibre system

the interstitial fluid continuum, permeating the spaces between the above systems, the tooth and the bone.

Parfitt found a multi-phasic response to the applied, intrusive load on human teeth, but a bi-phasic recovery upon removal of it; with repeated applications of 500g at 2-5 second intervals, the tooth became increasingly intruded. Parfitt surmised from this that two force systems played a part here; the vascular system resisting force up to 15g, and the interstitial fluid beyond this ceiling. Picton confirmed Parfitt's findings, but added the discovery of the behaviour of the PDL upon extended application of a load.

Bien and Ayers found that dead rats did not respond in the same way as live ones; a live rat can sustain an impulse load, whereas a dead one cannot, and that it was possible for the tooth to remain intruded in the skull for the sacrificed rats (Bien, 1966). However, thoracic massage of the sacrificed rats was able to extrude the

intruded teeth once again. Their data also showed instantaneous and delayed elasticity, during intrusion and restoration in live rats, whereas creep only provided the restoring mechanism in dead rats. They propose that this complex, visco-elastic behaviour can be modelled by Maxwell and Voigt spring-dashpot models. (A Maxwell model is a spring and a dashpot in series (Fig. 5.0.1a); a Voigt model comprises a spring and dashpot in parallel, as shown in Fig. 5.0.1b).

Fig. 5.0.1a: Maxwell model.

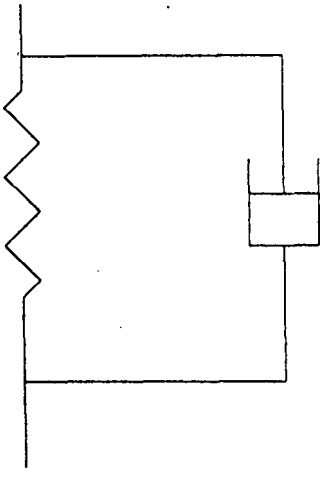

Fig. 5.0.1b: Voigt model.

Synge assumed a linear-elastic, homogeneous PDL, enabling him to develop equations to show that the PDL behaved in a rubber-like manner (Bien, 1966). If this was the case, then the PDL of both live and dead rats should have behaved like a Voigt model. Furthermore, it was shown that the PDL was not dynamically or anatomically homogeneous.

Picton also observed that the displacement of the alveolar bone (resulting from the fluid transmittal of load) could be observed, confirming that the dead animals would respond differently since the fluid was expelled from their veins during loading.

Reynold's Number was determined for the PDL (Bien, 1964, 1966) and was found to be very low, and not to greatly vary with applied load or increased average velocity. This implied a "squeeze film" type behaviour of the PDL. Hays (1961, 1963) (Bien, 1966) investigated squeeze films; very thin layers of fluid between two plates in non-rotating bearings, which enabled the bearings or plates to withstand

loads far in excess of those generated by mastication. The assumptions made in the bearing application, and in the PDL model are consistent, except that the PDL cannot be considered homogeneous.

The squeeze film model of the PDL was investigated under instantaneous and sustained loads. In the instantaneous case, the fluid tends to push the boundaries of the PDL upwards in the apical region, whilst still cushioning the load. If the load is removed, the film is replenished from the capillary network, and from re-circulation. Low sustained (orthodontic) loads permit the film equilibrium to be replenished, but high loads do not, and hence the load carrying capacity of the film decreased markedly as the thickness of the film was reduced.

Bien (1966) concluded that the squeeze film model seems to be fairly accurate for the case of the interstitial fluid.

Bien and Ayers (Bien, 1966) then went on to investigate the restoring force, K that would result if the PDL was regarded as a spring system. These varied between 4.2e-4 and 5.5e-4 for live rats, but were much smaller; 0.2e-4 to 1.3e-4 for dead rats.

However, none of the theories proposed so far can fully explain the damping behaviour of the PDL. Hence, Bien and Ayers went on to consider the possibility of the fibres of the PDL tightening as an intrusive load was applied, thus compressing and occluding the blood vessels between them. This, they proposed, would cause the vessels to balloon, due to the back pressure acting against the arteries which are partly embedded in bone. This is **stenosis**, causing the interstitial fluid to pass through the contracted spaces at an increased pressure, thus providing a damping mechanism. Histological sections through experimental teeth show a larger number of vacuoles than one would see in a normal periodontium, supporting their hypothesis. This behaviour is termed **exogeneous cirsoid aneurysm**, and accounts for the spring-like behaviour observed by Picton (Bien, 1966).

If this theory is correct, Rouse and Ince (1957) have shown that, at a vascular constriction, pressure is reduced, but is regained after the constriction. It has further been shown that it is possible for cavitation to occur within smaller blood vessels at the site of such a stenosis (Numanchi, 1936, and Malcolm, 1957) (Bien, 1966). However, during normal function, very few gas bubbles can form, since the force is applied for a short period only, and the force is damped by the squeeze film

mechanism. Nonetheless, the hypothesis is presented that, under sustained, orthodontic loads, oxygen cavitation can occur in the capillaries and small vessels caught between the constricting fibres of the PDL. If these bubbles lodge under bone, it has been proposed that they might create a climate favourable to local resorption of the bone, although, of course, many go back into solution (Bien, 1966).

Analysis has shown that the thinnest region of the PDL corresponds with the area associated with the centre of rotation of the tooth, where minimum periodontal pressure resulting from applied transverse forces occurs. The authors stress that it is of fundamental importance that the gases remain in the vessels of the PDL during decompression.

A network of loops and coils of blood vessels was found in the alveolar crest, following the form of the alveolar crest. These loops and coils did not appear to have a purpose, and Kindlova and Matena (1959, 1962, 1965) felt that nutritional needs alone could not account for this phenomenon (Bien, 1966). It is thereby proposed by Bien, that these loops assist in the resistance of the high pressure forces generated during function.

The authors propose that the fluids of the PDL (*i.e.* the interstitial fluid, the vascular fluid and the intracellular fluid) all play a part in the damping of small movements of teeth. All of the experimental observations recorded here have pointed to multi-phasic, non-linear characteristics of tooth movement, both during intrusive loading, and in restoration of the tooth to its equilibrium position. All of this points to a cessation in the belief that a tooth is simply suspended in its socket by a rubber-like material, of by collagen fibres.

A correlation is found to exist between the pulsations of teeth in their sockets, and the pulsation of the vascular system supplying them.

Bien (1966) proposes that observations of a non-linear response to applied loading implies the involvement of several mechanisms of tooth support. These are believed to include viscous damping forces due to the Reynold's number of the interstitial fluid, the squeeze film behaviour of the interstitial fluid, and the architecture of the PDL providing a spring constant type of response. Remodelling is believed to result from the damping mechanisms breaking down, causing local resorption of the tooth root.

The role played by the PDL in the support and the function of teeth is fundamental. From an anatomical and histological point of view, the PDL is well documented, but little is known about the exact mechanisms by which it functions. The PDL consists of bundles of collagen fibres embedded at one end into the cement on the tooth root, and at the other, variously in the *lamina dura* of the alveolar bone, in the gingiva, or in the cement of a neighbouring tooth. However, a study of silver-impregnated sections through a human tooth showed that no single fibre can be traced from bone to cementum or vice-versa. (Sicher, 1970). Instead, all seem to begin or end in the middle zone of the PDL. This implies that each fibre bundle in the PDL consists of shorter fibres that are spliced together in the middle. Hence, Sicher (1970) refers to the human PDL as consisting of alveolar fibres, dental fibres and an intermediate plexus.

Between these fibres is a rich network of blood vessels, surrounded by a ground substance. It varies in thickness between approximately 0.1 and 0.33mm. The collagen fibres of the PDL are crimped or wavy in their state of rest. It is often reported in dental literature that the initial, linear response of the PDL to loading of the tooth was due to the straightening, or uncrimping of these fibres, and that the non-linear response after this was due to the stretching of the fibres themselves (*e.g.* Scott and Symons, 1982; Gordon, 1991).

It has been generally reported that the collagen fibres of the PDL provide a tensile, or suspensory support system for the tooth. However, a great deal of debate exists as to how compressive forces are resisted. One theory is that the blood vessels and ground substance, having a comparatively high density, can be considered relatively incompressible, and so provide resistance to compressive forces. This idea portrays the PDL as a visco-elastic medium (the damping being provided by the fluids of the material). There is evidence to suggest that the ultra-structure of a connective tissue is dictated by the mechanical demands placed upon the tissue. However, the behaviour of the PDL is the subject of much discussion (Moxham, Berkhovitz and Newman, 1995).

Table 5.1, from page 232, summarises this debate:

Table 5.1: Is the PDL a tensile or a compressive medium?

Features of the PDL suggesting tension	Features of the PDL suggesting compression
Sharpey fibre structure	Small collagen fibril diameters
Large, flattened disc shape of fibroblasts	Unimodal collagen size/frequency distribution
Dermatan-sulphate rich composition of ground substance	Smooth surface of fibroblast membrane
	Large amounts of ground substance
	Masson rich trichrome staining

Table 5.1 refers to Masson's trichrome; Masson's trichrome stains collagen under tension red, and collagen in compression green. Moxham and Berkovitz (1995) state that Flint *et al.* (1975) reported that stretched connective tissue of skin changed colour from green to red, on application of tension (Moxham, Berkovitz and Newman, 1995). The collagen fibres of the PDL stained green with Masson's trichrome. The reader is referred to Moxham, Berkovitz and Newman (1995) for further explanation of the information summarised in Table 5.1.

There appears to be more observations suggesting compressive behaviour of the PDL, but opinion is likely to remain divided.

Many researchers have carried out clinical studies to determine material properties for the PDL. For example, Ralph (1982) carried out some tensile tests in an attempt to find the UTS of the ligament. Ralph also proposed that the fibres of the PDL are continuously in tension, and that the initial displacement of a tooth was associated with the straightening of the crimps in the fibre bundles, whilst the behaviour exhibited under a sustained load (Picton (1967); Parfitt (1967)) was due to time-dependent effects associated with the movement of fluid within the tissue. Picton (1972) also links these "secondary" displacement effects to the elastic deformation

of the bone structure. However, deformation of the bone at low loads is not anticipated.

Ralph created tensile testing samples of human mandibles, within 48 hours of death, by taking transverse sections through the mandible of 1mm thickness, including the root dentine and the surrounding PDL of the sectioned teeth. Each specimen was trimmed to have a diameter of 8mm, and all specimens were tested immediately. A displacement transducer was housed in a close-fitting brass cylinder and mounted vertically on the cross-head of a Universal Testing machine. A stainless steel wire (0.5mm in diameter) ran from the transducer, through the pulp cavity in the sectioned specimen, to a 5kg load cell. A brass button was located on the wire, immediately below the sectioned tooth, in order to apply a uniform load over the sectioned surface of the tooth. The average value of UTS obtained by this method was $2.4N/mm^2$, with the range of values between $1.87N/mm^2$ and $2.7N/mm^2$.

Ralph notes that the behaviour of the PDL is dependant on the different loading situations applied, referencing studies by Picton (1964, 1965), Parfitt (1965), and Korber (1971). This leads to speculation that the fluid content of the PDL plays a defining role in the behaviour of the tissue. However, Ralph also suggests that behaviour observed may be due in part to the curved surfaces of attachment of the PDL; an applied load would be initially absorbed by the straightening of the fibres, and subsequently transmitted to more of the attachment surface as more fibre bundles were recruited.

Kardos and Simpson (1980) propose the idea of thixotropy in relation to the PDL. A thixotropic fluid is one that thins with time, under a sustained, applied load. More specifically, thixotropy means that the viscosity of the PDL changes as a result of the pressure applied to it via the tooth alone, and will make a time-dependent recovery without any corresponding temperature change occurring. It will also exhibit a hysterisis loop on the shear rate *vs.* shear flow curve.

If the PDL was a thixotropic medium, this would permit its behaviour to be described by a single theory, rather than requiring a discontinuity to exist. This would account for the time-dependent behaviour of the PDL, and the response of this tissue to a sustained, low load.

Both Reitan (1960), and Kardos and Simpson (1980) describe the process of hyalinisation that occurs under a force adequate to bring about tipping of the tooth examined. Hyalinisation is the absence of the cells in the PDL which one would expect to see in the normal tissue architecture of this medium. Kardos and Simpson also propose that the super-crestal fibres of the PDL possess a greater degree of cross-linking (and hence are more polymerised) than the lower PDL fibres, since these are the slowest to adjust in orthodontic treatment.

In 1960, Parfitt (Moxham, Berkovitz and Newman, 1995) discovered that after an applied intrusive load on a tooth was removed, the tooth underwent a two phase recovery to its original position. The initial phase was a rapid extrusion, with the displacement against time graph being almost linear. The second phase was much slower recovery to the original position, and appeared to Parfitt to be logarithmic. The process took about 1-2 minutes if an intermittent load was applied, and longer if the load was maintained. Parfitt believed that this showed that the support provided by the PDL could not be uniquely suspensory; tension within the collagen fibres could not explain this behaviour. He proposed that the fluid components of the PDL must play a role in the support of the tooth, having also observed that the tooth moved in synchrony with the arterial pulse when subject to loads of less than 0.15N. The discontinuity in behaviour observed in this study may tend to support a two stage model of the PDL rather than the thixotropy theory.

Bien and Ayers (1965) and Bien (1966) conducted experiments on rat incisors using loads ranging between 0.35N and 15N (Moxham and Berkovitz, 1995, Bien, 1966). They measured the displacement of the loaded tooth relative to the adjacent, unloaded incisor using a Vernier micrometer fitted to a microscope. The tooth was loaded by the sudden application of a dead-weight to the test tooth. The load was sustained for several minutes and then removed, enabling the displacement *vs.* time behaviour of the tooth to be studied.

They also reported a bi-phasic response of the PDL to this type of loading, and Bien (1966) went on to propose that the PDL behaved as a visco-elastic gel. He examined various mechanical models of time-dependent behaviour of materials, including the idea of a squeeze-film mechanism of behaviour, and the Maxwell and Voigt models commonly seen in engineering.

Bien (1966) and Wills *et al.* (1972) have analysed the time-dependent behaviour of the PDL, and both groups are in agreement that the tissue appears to exhibit a visco-elastic response to loading over time, but none of the mechanical models discussed fully describes the recorded responses of the tissue. For example, Bien (1966) suggests that the tissue response could be modelled by a Maxwell element (a spring-damper model), whereas Wills *et al.* (1972) observed three to four phases in the recovery of the tooth, and suggested that these should best be represented as a series of Voigt elements. Moxham and Berkovitz (1995) discuss these results, and point out that it is difficult to differentiate between possible experimental errors and actual observations in the reported experiments. From this point of view, representing the recorded curve as a series of exponentials is a risky thing to do, and mathematically, it would generally be considered more appropriate to initially model the observed curve as a series of linear elements.

Jones *et al.* (1998) used laser technology to measure the displacements of human teeth *in vivo* teeth state that if the physical properties of the PDL are to be determined by back calculation, it is evident that further development of their apparatus is necessary in order to apply and sustain accurate loads of low magnitude. They also report that their experiments have confirmed the intial elastic response, and the basic visco-elastic response of the PDL.

Overall, it seems that there have been a number of attempts to study the response of anterior teeth to an applied load using various measuring techniques. Most of these techniques involve the measurement of the displacement of a loaded tooth relative to a neighbouring tooth. Since the collagen fibres of the PDL connect adjacent teeth, it would seem reasonable to assume that the behaviour of an adjacent tooth would also be affected by the load applied to the test tooth. Furthermore, the mandible is believed to flex during function *(see Chapter 4)*, which would also affect the magnitudes of the displacements observed.

In summary, the quality of the experimental observations to date is not sufficient to fully elucidate the response of the tooth-PDL system to an applied load, and therefore, it is very difficult to formulate a precise mathematical model of the PDL to be used in the FEA of dental systems.

Currently, FEA is used by many researchers in an attempt to understand the behaviour of the PDL under physiological loads. Most of this research focuses on the time-dependent response of a tooth subjected to an orthodontic load, as discussed in the previous paragraphs. However, it is rare to see the studies extrapolated to predict the response of a tooth-PDL system to a functional load. It is the aim of this study to investigate the extent to which the non-linear nature of the PDL influences the stresses and displacements within a tooth under bite loading conditions.

Because of the difficulties reported in measuring the response of the tooth-PDL system to an applied load, and in representing experimental observations accurately in an FEA model, it seemed appropriate to draw upon the experience of natural tissue models used in other biomechanics disciplines.

Since this research concentrates on the instantaneous response of the tooth-PDL-bone system to an applied load, the time-dependent response of the material is of lesser importance than the initial response. If it was the intention of the study to examine the response of such a dental system to a sustained load (for example, an orthodontic load), the time-dependent behaviour of the tissue would be significant. However, in this study, no attempt is made to incorporate time-dependent behaviour into the material models used.

The use of an hyper-elastic, strain energy density function to describe the behaviour of natural tissue in modelling heart valve prosthesis has been well described (*e.g.* Trowbridge *et al.* (1985), Thornton (1997), Chew, Patterson and Howard (1994), Huang *et al.* (1990)). Within Finite Element Software packages, various types of hyper-elastic models are available. These commonly include Mooney-Rivlin, polynomial and Ogden models. However, many of these models are more suited to describing the characteristic behaviour of engineering materials such as rubbers than to describe the behaviour of natural tissue. When a material model is proposed, it is common practice to test it, initially under uni-axial tension, and then by inflating a sample of the material, and employing multi-axial tests.

Sahay (1984) reviewed various models of hyper-elasticity with a view to modelling natural tissue, and reported that the models of Treloar, Mooney and Varga were unsuitable for this application purely from a uni-axial testing point of view. Furthermore, Sahay ruled out the use of the Blatz, Gou, Vito, and Veronda and

Westman models after inflation tests were carried out. Finally, Fung's model (1967) was eliminated on the multi-axial test cases. Sahay proposed that the Hart-Smith model was appropriate.

From the work of Trowbridge (1985), Huang *et al.* (1990) went on to develop a 2-dimensional, large deformation finite element model for bio-prosthetic heart valve tissue. This model was built into the Finite Element code LS-DYNA3D by Chew (1996) and Thornton (1997).

Since so little is known about the precise manner in which the PDL behaves under functional loading, in initial investigations, it was decided to use this natural tissue model to represent the behaviour of the PDL. The displacements of a 2-D model of a lower canine subjected to a 1N load compared favourably to the experimental observations of Picton (1965) and also, the more recent *in vivo* study by Jones *et al.* (1998). Hence, it was decided that, in the first instance, the tissue model used by the Heart Valve Research Group at the University of Sheffield would provide a suitable model for the PDL.

Some FEA studies have been used in conjunction with clinical trials. For example, Ishida, Haibara and Soma (1996) investigated the dynamic response of the PDL to both occlusal and orthodontic forces. They found that their model could be used to simulate either type of loading, but that the different types of loading have different effects on the PDL and the bone. They used a 3-D, type D model, representing the PDL as a combination of homogeneous, linear elastic elements, and homogeneous, isotropic viscous elements. The elements were arranged alternately in three dimensions, so that each elastic element was surrounded by viscous elements, and *vice versa*. A 0.5N load was applied, and the maximum displacement measured was 0.14mm for a static load, and -0.5×10^{-3}mm for an impact load. Overall, they found that the PDL responded differently to loads applied over time than to instantaneous loads.

In another case, Andersen, Pedersen and Melsen (1991) carried out a joint *in vitro* and FEA study to determine material parameters and stress profiles within the PDL, using strain gauges to measure the strain in 3 post-mortem specimens under various loading conditions. The loads applied to the autopsy specimens ranged in magnitude between 0.05N and 0.025N (5 and 250cN). They then varied the E of the PDL in

their FEA models until the results approximately equalled those measured experimentally, for loads of 0.5, 1 and 1.5N (50, 100, and 150cN).

By this method, they found that a value of $E = 0.07$ MPa, with a Poisson's ratio of 0.49 was most appropriate. They also found that a linear elastic model of the PDL was suitable.

It appears that the stress results and profiles presented in this paper correspond to loads of 1N (100cN), representing an orthodontic type load, and 50N (500cN), representing a chewing force. In Chapter 4 of this study, 100N load was used to represent the bite load on an anterior tooth.

If the behaviour of the PDL is non-linear, then the magnitude of the stiffness of the material would be dependent upon the load applied, hence the value of E of 0.07 MPa determined may not be valid for the larger, chewing force model.

Rees and Jacobsen (1997) carried out an investigation to use FEA to model 2 different *in vivo* tooth loading systems; that used by Tanne and Sakuda (1983), and that of Picton (1963). Tanne and Sakuda had applied a 2.45N (250g) force horizontally to the buccal cusp of a lower premolar, about halfway up the tooth. The resulting horizontal displacement of the lingual cusp was measured with a strain gauge.

Picton applied a vertical load of 19.65×10^{-3}N (2g) halfway along the slope of the buccal cusp, measuring the displacement by means of two strain gauge transducers soldered to the wings of a rubber dam clamp applied to the test tooth.

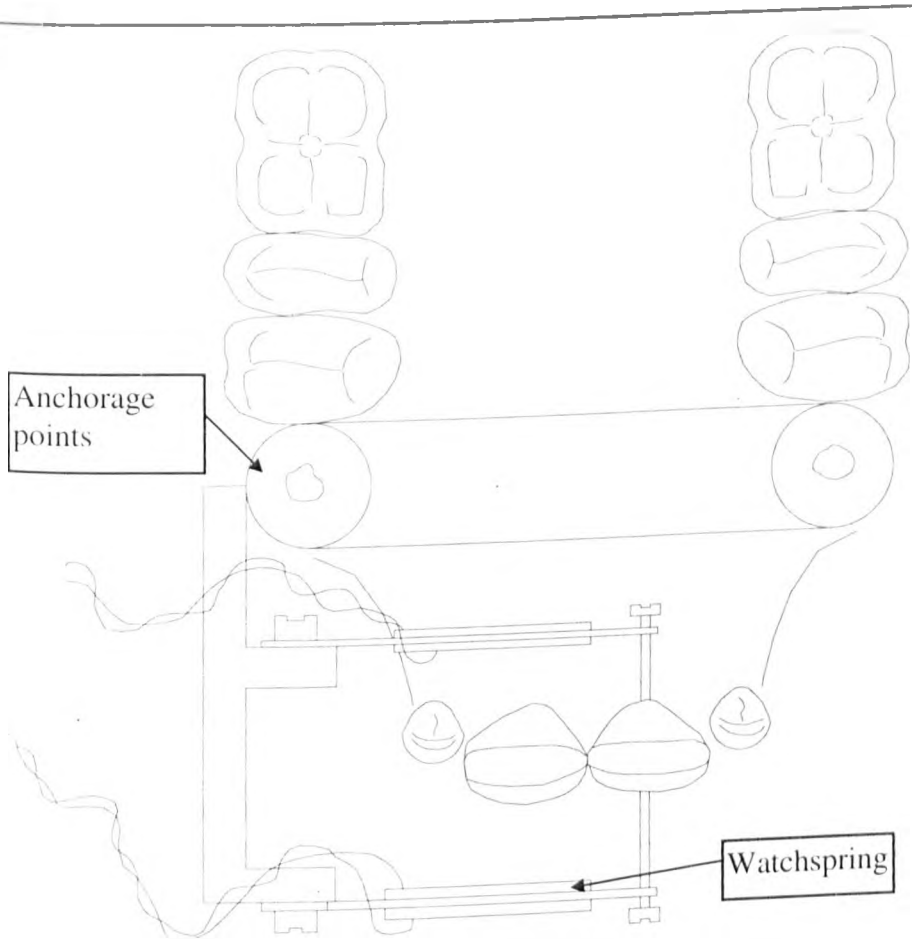

Fig. 5.0.1: The Periodontometer used by Picton.

By varying E of the linear elastic PDL model used in their FEA simulation until the predicted displacements were as close as possible to those measured experimentally, Rees and Jacobsen (1997) proposed that the optimum stiffness of the PDL was 50 MPa. Jones *et al.* (1998) carried out a dual FEA and *in vivo* study, using a non-invasive version of the Periodontometer. In this study, low loads were applied to the teeth of patients, and the displacements were measured. They also measured mean displacements of 0.012mm, with a range of 0.002mm to 0.021mm for loads of 0.39N, and their FEA study predicted that the E of the PDL should be less than 0.18 MPa; generally of the order of 1 MPa, to match this. However, it was reported that difficulties were associated with determining a suitable value of E for the tissue, and that there were significant variations between individuals.

In this study, they also confirmed the initial elastic response of the PDL to an applied load, and the visco-elastic behaviour of the tissue over time.

It is conceivable that the extent of this range of suitable values comes about because of the non-linear, and hence, load-dependent nature of the PDL. For example, a number of studies are concerned with the effect of orthodontic type loads on the PDL, and on tooth movement. In general, these seem to suggest low values of E for this tissue. However, studies more interested in loads of the "bite load" magnitude have tended to predict higher values of E. It is possible that the two types of study carried out may lead to two distinct groups in the prediction of values of E; the lower end of the range predicted by those studying physiological tooth movement, and the higher end of the range by those interested in the response of the tooth-PDL-bone system to larger, applied loads.

Since the aim of this study is to investigate normal (and, ultimately, restored) teeth under bite loading conditions, the hypothesis that the behaviour of the PDL could be accurately described by the properties of the collagen fibres under an impact-type load (*i.e.* one applied and removed instantaneously) was adopted. The behaviour of collagenous tissue in heart valves and skin tissue is believed to be hyper-elastic, and so this study aimed to investigate whether it was necessary to include the hyper-elastic effects of the PDL for loading conditions of this type, or whether a linear-elastic model of the PDL, assigned an appropriate value of E, could reasonably be used instead.

In a previous study, it was assumed that the non-linear, hyper-elastic behaviour of the generic natural tissue model described by a Strain Energy Density Function (Huang *et al.*, 1990) could accurately predict the displacements of the tooth-PDL-bone system. The displacements predicted by this tissue model compared closely to those found experimentally by Jones *et al.* (1998), and to those of Picton (1965).

5.1 Materials and Methods

The introduction to this chapter outlines the complexity of the behaviour of the PDL under various types of loading, and discusses some of the different theories about how best to model the behaviour under functional and orthodontic loads. It was thus important to investigate the effect of the material model of the PDL used for analysis of canine teeth under functional loads.

Hence, non-linear, linear elastic, and multiple step linear elastic models of the PDL were constructed in three different Finite Element Analysis (FEA) codes. The effects of the different models and FEA codes were studied, comparing the stress magnitudes, distributions, and displacements within the tooth and the surrounding tissues. The aims of this study were:

to investigate whether the PDL had to be modelled as a non-linear material, or whether a simple linear elastic model would suffice for the analysis of teeth subjected to funtional bite loads,

to investigate whether the FEA code used would significantly influence the results.

5.1.1 *The Simple Material Model*

Initially, a simple model was constructed to test the behaviour of the materials before they were applied to the tooth model. This consisted of a square (10mm x 10mm), comprising 100 elements, depicted in Fig. 5.1.1. One edge of the material was constrained in the x-direction, with the central node fully constrained, as shown in Fig. 5.1.1. Displacements were then applied to the opposite edge, as shown in Fig. 5.1.1, pulling the material horizontally. The range of displacements applied was between 0.1mm to 2.5mm, and the extension of the material was measured. Various material models were tested with this method before they were used to represent the PDL. The models tested were:

Mooney-Rivlin hyper-elastic model in ANSYS.

Multi-linear elastic model in ANSYS.

Various non-linear material models in ABAQUS.

The LS-DYNA3D non-linear material model was not tested here since its validity had already been established (Chew *et al.* (1994), Thornton (1997)).

In ANSYS, 2-D plane-strain elements *plane42* were used, as in the tooth model. However, it was not possible to use planar elements in LS-DYNA because the non-linear, hyper-elastic material used to model generic natural tissue cannot be used with 2-D plane elements. Therefore, shell elements were used in this study, constrained in the z-direction, since this was the closest approximation to the situation used in the other models.

For comparability, analysis using ABAQUS with both shell elements and planar elements was attempted. The shell elements used were S4R shell elements (4-noded shells with hourglass control factor), and the 2-D plane elements used were CPE4R elements. Three integration points were initially specified through the thickness of the shell elements.

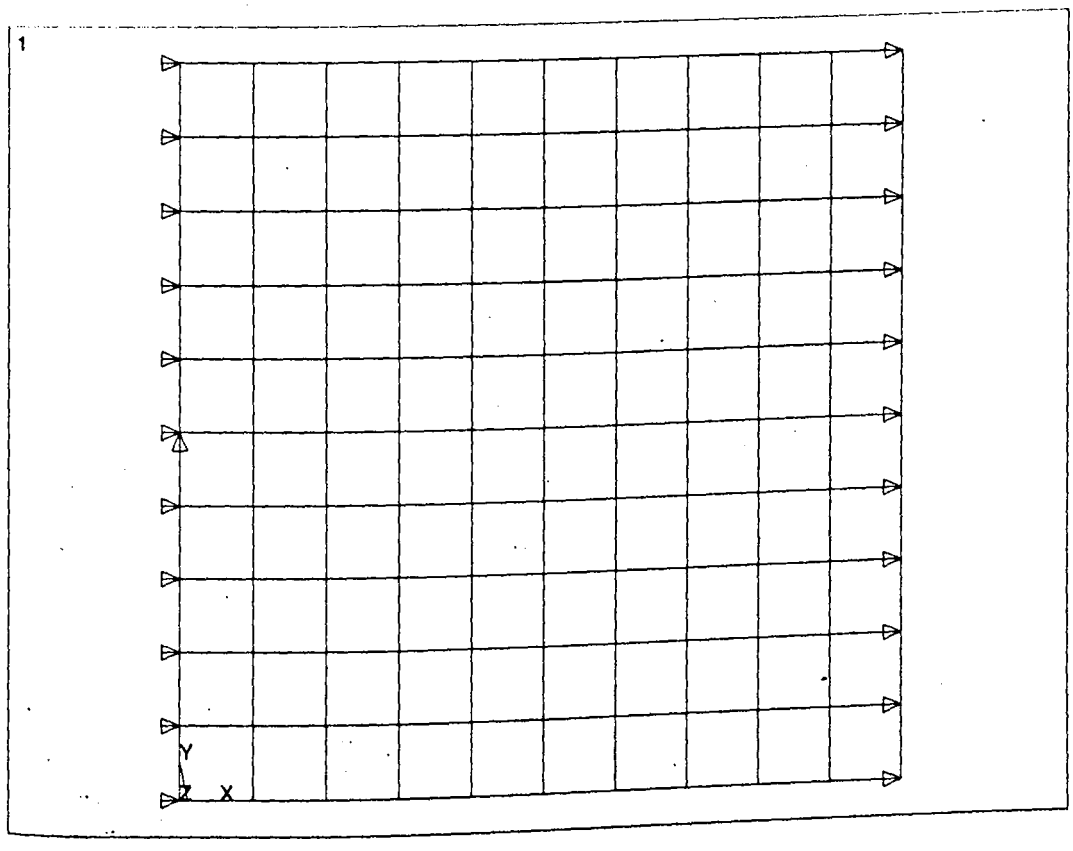

Fig. 5.1.1: The square model used to test the materials.

Tension was applied to all of the nodes on the opposite edge of the model in the form of a displacement in the x-direction. The stress and strain within the elements was evaluated, and compared to the values obtained by Thornton (1997).

Three different software codes were used in this evaluation; ANSYS, ABAQUS and LS-DYNA. Four material models were compared, as summarise in Fig. 5.1.2 below. The simplest of these was the linear elastic model, where a single value of E was specified. This was carried out in all of the codes evaluated. Using ANSYS, values of E of 3MPa, 30MPa, and 50MPa were specified in order to compare the effect that this had upon the stresses in the crown of the tooth. These are shown by lines *a*, *b*, and *c* in Fig. 5.1.3.

Linear Elastic models:	**Non-Linear models:**	**Multi-Linear model:**
Ansys	Abaqus	Ansys
Abaqus	Ls-Dyna	
LS-Dyna		

Fig. 5.1.2: The material models and codes used.

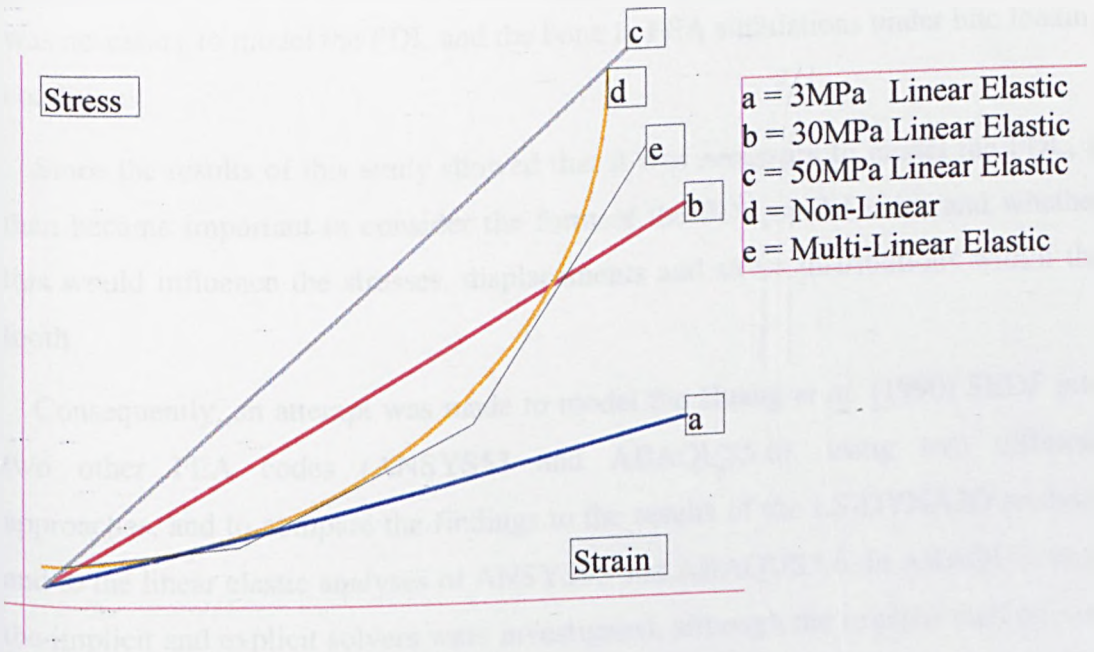

Fig. 5.1.3: Defining the material models used.

A non-linear (NL) model; *i.e.* a model which permitted the E of the material to vary with the load applied, was used in two of the software codes, ABAQUS and LS-DYNA. This material model is represented by line *d* in Fig. 5.1.3.

A non-linear (NL) model; *i.e.* a model which permitted the E of the material to vary with the load applied, was used in two of the software codes, ABAQUS and LS-DYNA. This material model is represented by line *d* in Fig. 5.1.3.

Finally, a material model which approximated this non-linear material by a series of straight line steps; a multi-linear elastic (MLE) model was used in ANSYS. This is shown by line *e* in Fig. 5.1.3.

In the MLE material model, magnitudes of the stresses at various strains are specified in a data table, and the solver interpolates between the two values closest to the required strain, assuming that a straight line connects them. The stress and displacement are then predicted accordingly. If enough data points are defined, a model which closely approximates the smooth curve of the hyper-elastic function can be obtained. An initial value of E is still required by the solver.

The Huang *et al.* (1990) Strain Energy Density Function (SEDF) was coded in LS-DYNA3D to produce a generic, natural tissue model suitable for the FEA of natural and bio-prosthetic heart valves, and had been shown to predict similar displacements to those observed experimentally. Chapter 4 investigated whether it was necessary to model the PDL and the bone in FEA simulations under bite loading conditions.

Since the results of this study showed that it was necessary to model the PDL, it then became important to consider the form of the PDL model used, and whether this would influence the stresses, displacements and stress distributions within the tooth.

Consequently, an attempt was made to model the Huang *et al.* (1990) SEDF into two other FEA codes (ANSYS53 and ABAQUS5.6), using two different approaches, and to compare the findings to the results of the LS-DYNA3D analysis and to the linear elastic analyses of ANSYS53 and ABAQUS5.6. In ABAQUS, both the implicit and explicit solvers were investigated, although the implicit method was deemed more appropriate. The equations used to define the hyper-elastic material model are included in Appendix 2.

Fig. 5.1.4. The E of the PDL was specified as 30MPa, as described in Chapter 4, but simulations were also carried out with E = 3MPa and 50MPa, to correspond to the lower bound of values reported in heart valve literature, and to the value proposed by Rees and Jacobsen respectively. A vertical load was applied to the node on the tip of the tooth.

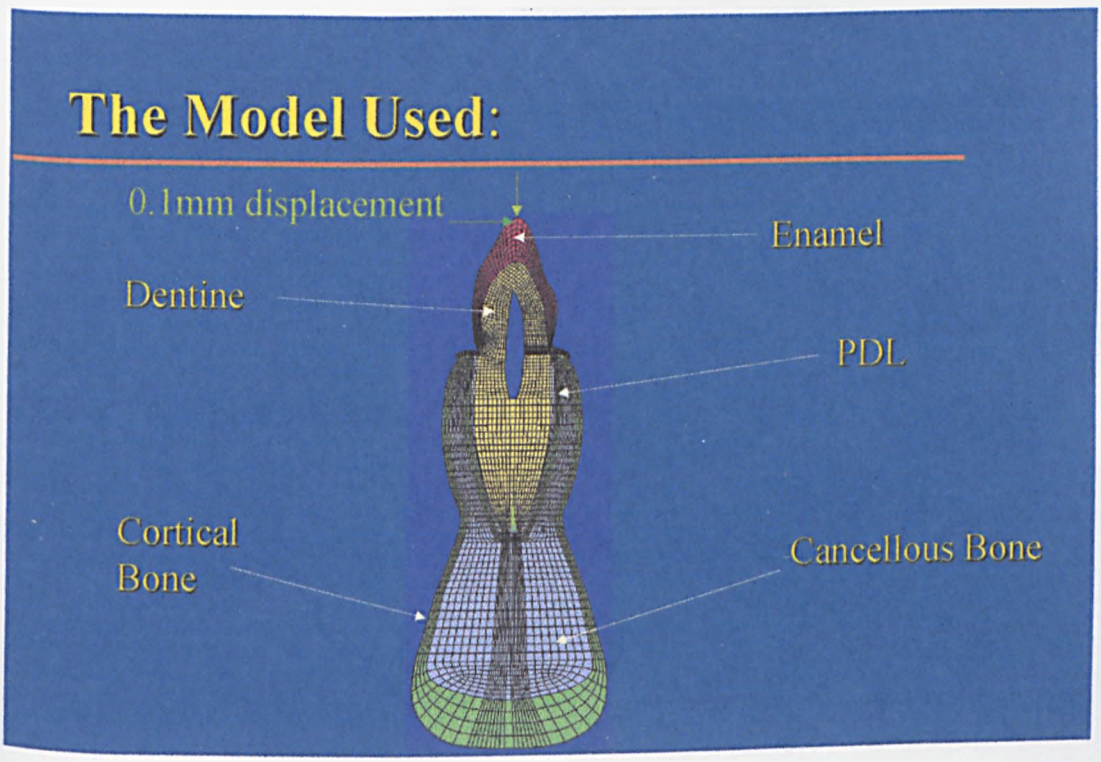

Fig.5.1.2.1: The tooth model used to investigate the behaviour of the material model of the PDL.

Fig. 5.1.2.1 shows the materials used in the model, the mesh of the model and the displacement loads applied to the model. Either a horizontal or a vertical load was applied; never both at once. Displacements were used as this meant that the analyses were more likely to solve.

ANSYS53 MLE model

Also in ANSYS53, attempts were made to model the material using the Mooney-Rivlin hyper-elastic material model, which is a feature of the code. Again, the stresses for various levels of strain are specified, but this time, the solver tries to fit the Mooney-Rivlin model to these data points. This method failed, because the Mooney-Rivlin model defines a curve in which the initial gradient is the steepest, and the final gradient is the least. However, the generic natural tissue, hyper-elastic material curve is the opposite to this; the initial gradients are the smallest, becoming steeper with increasing strain.

ABAQUS5.6 LE model

An older version of the ANSYS53 model (model D, as described in Chapter 4) was converted to ABAQUS5.6 using HYPERMESH at the University of Michigan. The material properties are identical to those listed in Table 4.2.1. *E* of the PDL was 30 MPa. This model primarily differs from the others used in that the PDL was modelled as a uniform thickness material of 0.33mm, and that fewer elements were used in the older model.

ABAQUS5.6 NL model

The mesh of the model was identical to the ABAQUS5.6 LE model.

The PDL material was modelled in ABAQUS5.6 using the user routine UHYPER, in which the constitutive equation of the Strain Energy Density Function (SEDF), and the first, second and third derivatives were specified. The implicit solution method was employed. *(See Appendix 2 for the subroutine used).*

LS-DYNA3D LE and NL models

The model of the tooth, PDL and supporting bone constructed in ANSYS53 was converted to LS-DYNA3D using the University of Sheffield's interface programme DYNASYS (1994). 30 MPa was again used for the *E* of the PDL in the LE analysis.

The solution method employed by LS-DYNA3D calculates the deformations and stresses at a node at the centre of each element, and extrapolates them to the corner nodes. This technique is efficient for dynamic solution. However, certain modes of deformation of an element can be predicted by this method which cannot occur in practice. These are "zero-energy" modes of deformation, known as "hourglassing". They manifest themselves as zigzag elements, and the stresses predicted within them are unreasonably large, and can swamp the results of an analysis (OASYS DYNA3D User manual, 1992). Dynamic relaxation analyses are particularly prone to hourglassing problems, especially when the displacement is small, as in this problem.

Hourglassing can generally be avoided by spreading the point of application of the load across several nodes and elements. However, in this case, this was not possible. Generally, in LS-DYNA3D analyses, hourglassing is resisted by an imposed viscosity term automatically calculated by the code. It is possible to change the value used here, but this is not usually desirable. A stiffness method of hourglass control can also be used instead of the viscous method, and is recommended if the solution converges partially, but not completely.

Initial analyses of the LS-DYNA3D NL model showed hourglassing in the smallest elements in the enamel. The stiffness method of hourglass control was therefore used in subsequent analyses, avoiding this problem.

5.2 Results

The results of testing material models using a square test case are presented first, in section 5.4.1. Section 5.4.2 presents the resulting stresses, displacements and stress distributions of the tooth models analysed in the different FEA codes, with the various material models of the PDL. These models are all subjected to a vertical load applied to the incisal tip of the tooth. Section 5.4.3 presents the results of the models subject to a horizontal load applied to the same point.

5.2.1 *The Tissue Models*

No difficulty was found running any of the LE models.

5.2.1.1 *ABAQUS*

Considerable difficulty was found in running the ABAQUS material model. The implicit solution routine was used in ABAQUS, and the tissue did not appear to be particularly stable.

Initially, an incompressible, non-linear, hyper-elastic material was defined using the UHYPER routine in ABAQUS Implicit. Reduced integration, 4-noded shell elements were used. Shell elements were chosen because these had to be used in LS-DYNA. Elements with 4 nodes only were used because 8 noded shells would have been much stiffer, and this would have caused solution problems in an analysis involving large deformation. Reduced integration was included because the deformation was very large. Originally, the analysis was run with the *RIKS algorithm, to try to maintain stability by reducing the chances of the elements "locking up" in the large deformation analysis *(see the ABAQUS manuals).* Shell elements were unsuitable however, and so 2-D plane elements were used instead, as in all of the other analyses.

Unfortunately, the size of the time-steps required to run this analysis were tiny, and solution could only be obtained with an extremely small load. Even within these constraints, the solution still predicted huge residual forces, and many other problems occurred in the analysis.

The constraints that were applied caused problems; if the nodes were constrained in 6 degrees of freedom (DOF), singularities occurred in the analysis. If some constraints were removed to alleviate this problem, pivots occurred. It is not appropriate to use shell elements for an analysis of this type, so analysis was attempted using plane elements instead of shells. It was thought that the thickness of the shell elements might cause further solver problems, and also that the extra degrees of freedom permitted by shell elements could interfere with the solution. Increasing the thickness of the shells did alleviate problems to an extent, but did not cure the problem.

The material model should ideally be slightly compressible. Initially, it was easier to specify the material as incompressible, and allowing the material to be slightly compressible lead to problems with the transverse extension ratio of the material. This was probably because the material had a negative tangential stiffness and hence the Drucker stability criterion would not be satisfied.

Singularities occurred in the analysis, and zero pivots. Furthermore, the tissue, when given the constants defined in the Huang *et al.* (1990) SEDF, behaved like a material with a Poisson's ratio that was closer to 0.5 than the value of 0.45 used in the other (it appeared to grow in the x-direction when stretched in y). However, since the value of Poisson's ratio is not a user specified constant, but is derived from the UHYPER routine, nothing could be done about this other than altering the constants of the SEDF. The constants had to be modified in order to solve, hence the SEDF is not identical to that used in LS-DYNA3D, but was regarded as being similar enough for comparative analysis to take place.

5.2.1.2 ANSYS53 (Multi-Linear Elastic model)

The stresses and strains predicted by ANSYS were compared to the specified values of stress and strain, and to the strains that would be expected for the displacements specified. It was noted that there were some differences between the specified and the predicted values. The difference between the specified and the predicted stresses differs markedly after 15% strain. To compare these discrepancies, the values were verified in EXCEL. However, some discrepancies resulted from comparing the direct stress in the x-direction resulting from this analysis to those stresses specified on the input curve. This is shown in Fig. 5.2.1.1.

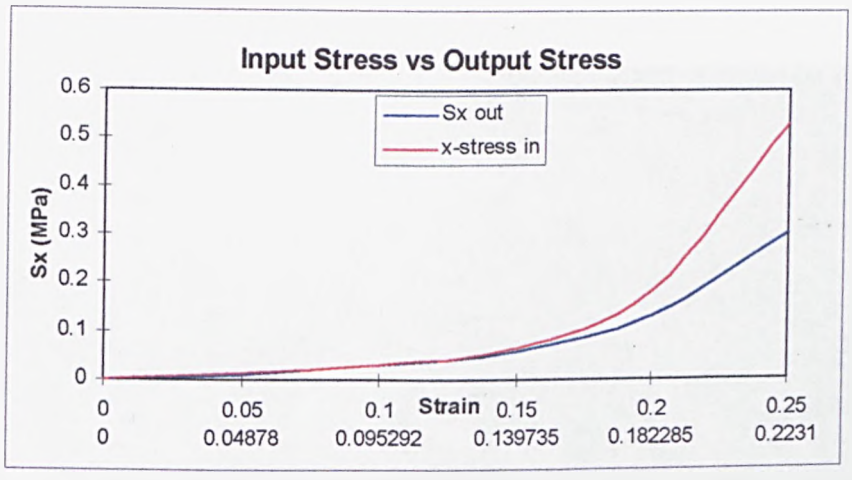

Fig. 5.2.1.1: The difference in predicted and actual stresses for the MLE model.

For ABAQUS5.6 and ANSYS53, the model was analysed using quadrilateral, plane elements with the plane strain option chosen.

From the above figure, it can be seen that the MLE model concurs with the NL model until approximately 15% strain is reached. After this, the MLE model predicts much lower strains, despite the fact that values of stress and strain were specified in the input data up to 25%. By 25% strain, there is approximately 43% difference between the input and output stress, and 11% between the input and output strains. It is likely that this difference could result from the way in which the stresses used by various FEA codes are calculated.

5.4.2 *The Tooth Models*

Fig. 5.4.2.1 compares the stress distributions within the tooth for the LE models. It can be seen from Fig. 5.4.2.1 that the stress distributions are very similar in each case; *i.e.* the regions of the tooth that experience the most tensile stress or compressive stress correspond in every model, regardless of FEA code used.

The magnitudes of the stresses predicted do vary with the different FEA codes used (Fig. 5.4.2.1). The range of stress predicted by the ABAQUS model is smaller than that predicted by either of the other codes.

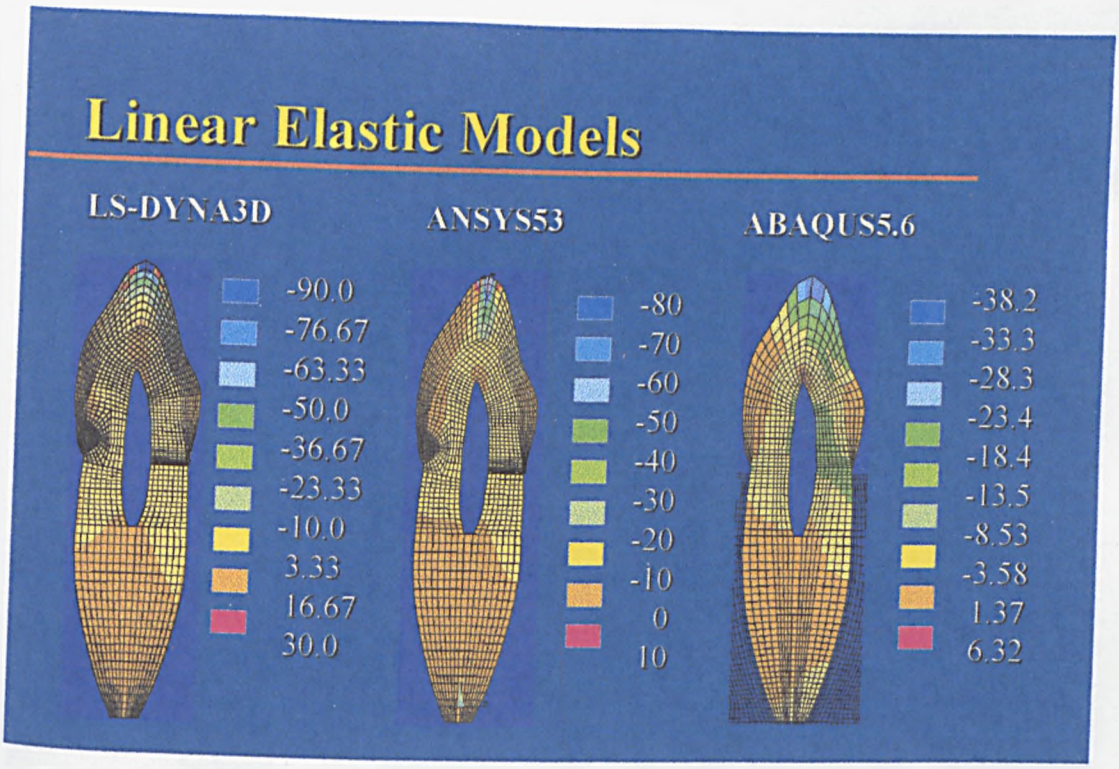

Fig. 5.2.2.1: Comparing the y-stresses predicted in the tooth for the different LE models.

The point of application of the displacement caused a stress concentration effect, or "hot-spot" to occur at the incisal tip of all of the models analysed. This makes the range of predicted stresses within the tooth seem very large. It is common engineering practice to unselect the nodes and elements affected by this hot-spot in order to compare the magnitudes of the stresses and the stress distributions more readily. This technique was employed when considering the stress distributions within the body of the tooth. There is less variation between the stresses predicted within the body of the tooth.

An alternative technique is to specify the range of stress to be used by the legend in the contour band plots can be specified, so that colours can be compared between the contour plots in the different codes.

Fig. 5.2.2.2 compares the stress distributions for the NL, MLE and an example of the LE models. The contour bands in Fig. 5.2.2.2 have been set so that the same colours are used in the NL and LE models, facilitating comparison of the stresses induced. However, it was not reasonable to do this for the MLE model since the stress distribution could not be seen at all with the chosen range of contours. Again,

it can be seen that the distributions of stresses in every case are similar, although the magnitudes vary.

The magnitudes of the stresses predicted by the MLE model were very similar to those found by the LE model with E = 3MPa, but were much lower than those found for the other models.

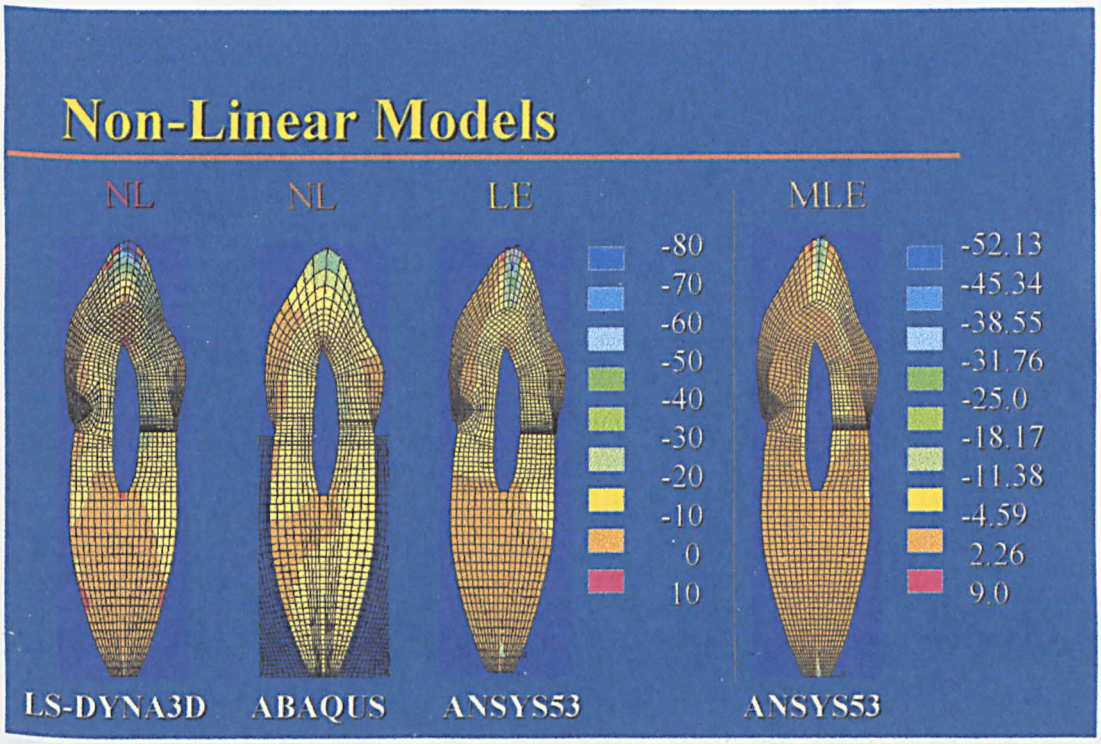

Fig. 5.2.2.2: Comparing the y-stresses induced in the tooth for the NL, MLE and one LE model (E=30MPa).

Fig. 5.2.2.3 shows the effect of varying the value of E of the LE PDL in ANSYS53 upon the whole model of the tooth and the bone. Fig. 5.2.2.4 shows the stress distribution within the tooth alone, as E is varied in ANSYS. In Fig. 5.2.2.3 once again, the contours have been left in default mode, but it is clear that the stress distributions do not significantly differ with variation of the stiffness of the PDL, although the magnitudes of the stresses predicted is affected by this process.

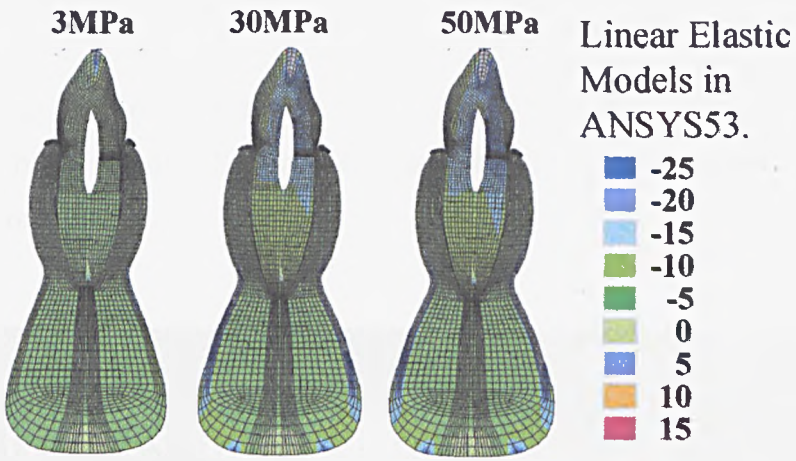

Fig. 5.2.2.3: The effect of varying E for the LE models in ANSYS.

The contour bands are shown in Fig. 5.2.2.4 to enable comparison of the stresses induced with variation of E. For the 30MPa and the 50MPa models, the magnitudes of the stresses predicted in the body of the tooth are very similar. However, less stress is predicted in the 3MPa model. Since the stress distributions are similar for each model, regardless of *E* used, if it is shown that the PDL can be represented by a LE material, then the stresses predicted in the tooth could simply be scaled.

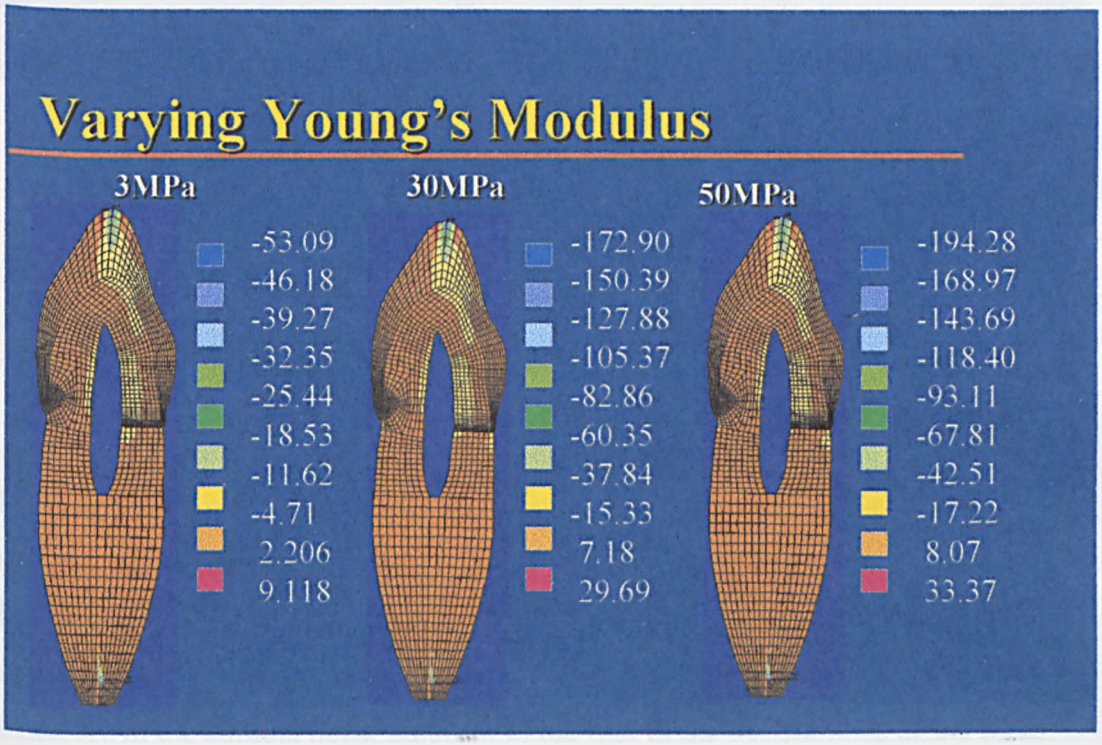

Fig. 5.2.2.4: The effect of varying E on the stress distributions within the tooth in ANSYS.

Comparing the stresses in the bone, for the vertical loading condition, in Fig. 5.2.2.4, it can be seen that the stress distributions differ markedly with FEA code used and material model of the PDL. There is also the possibility that the differences in geometry of the ABAQUS5.6 model affects the stress distribution and magnitudes within the bone.

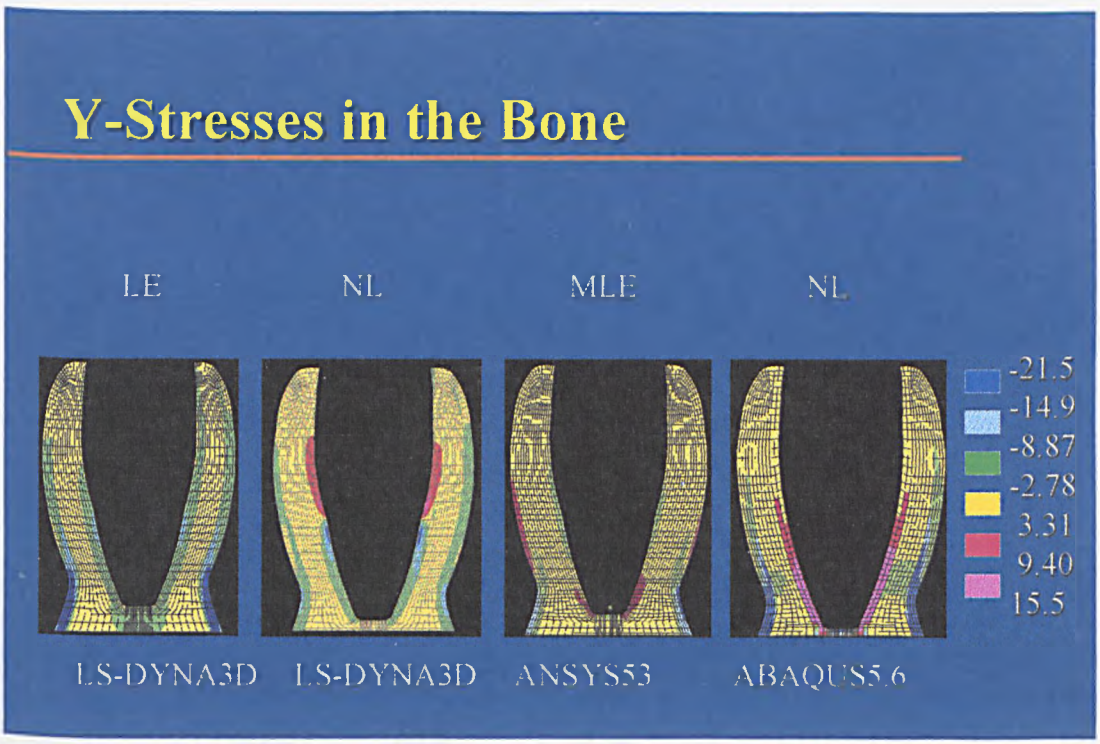

Fig. 5.2.2.5: Comparing the stress distributions in the mandible for various models.

5.2.2.1 ABAQUS Non-Linear model

This model behaved differently from all of the others analysed. In this case, the Poisson's ratio is not defined, but is calculated from the other properties specified, and the value calculated appears to be very close to 0.5. Consequently, the y-stress in the bone is greater than that within the tooth; between -61.4 and 45.8MPa as opposed to between -46.9 and 12.5MPa. The highest region of compressive stress is therefore in the cortical bone, adjacent to the root in the bottom third of the tooth.

Ignoring the elements closest to the point of application of the displacement constraint further reduced the stress range within the rest of the tooth to between -42.3MPa and 12.5MPa.

It is interesting to note that there is very little tensile stress under this load type within the tooth, outside of the region affected by the applied displacement load.

5.2.3 *Horizontal Loads*

A horizontal displacement of 0.1mm was applied to the incisal tip of the tooth. This analysis was a great deal more complicated for the NL and MLE material models, and some difficulties were experienced during the analyses. Figures are not shown for most of the analyses because they were unavailable at the time of writing this chapter.

5.2.3.1 *ANSYS LE models*

The results of the 3 LE models in ANSYS are presented in Fig. 5.2.3.1 below.

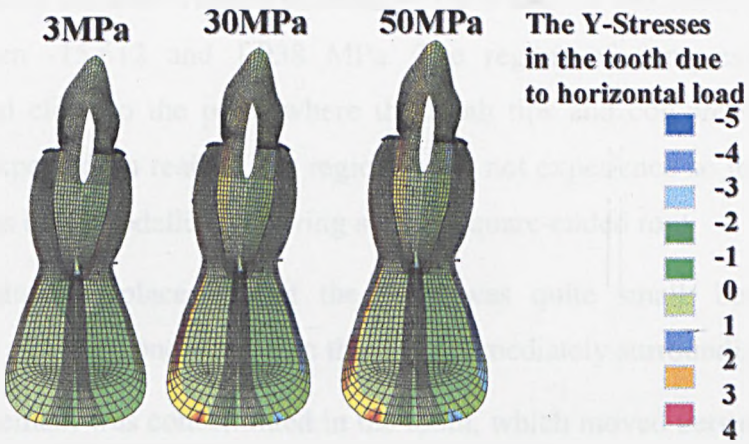

Fig. 5.2.3.1: Comparing the stress distributions for the 3 ANSYS LE models subjected to a horizontal load.

For all three models (*i.e.* E = 50MPa, 30MPa, 3MPa), the y-stress in the bone lay between -14.263 and 14.182MPa, and the x-stress was between -2.891MPa and 2.686MPa. The x-stress in the tooth was between -1.489 and 1.819MPa and the y-stress in the tooth was between -7.467 and 6.453MPa. Unselecting the tapers and the

the 8 nodes nearest to the constraint reduced the y-stress in the tooth to between -4.235 and 6.423 MPa. The maximum and minimum stresses were located in the dentine just below the crown. The stresses and displacements were identical for all of the LE cases analysed with a horizontal load.

The x-displacement of the bone in the 50 MPa model was between -0.00059 and 0.052mm; very little, and that of the tooth was between 0.00481 to 0.1mm The displacement of the tooth was the same for all 3 models. Thus, most of the displacement occurred within the tooth. For the 30 MPa model, the bone displaced horizontally between $-0.59x10^{-4}$ and 0.0524mm In the 3 MPa model, the displacement of the bone was between-0.007 and 0.02mm horizontally and between $0.38x10^{-4}$ and -0.021mm vertically.

5.2.3.2 ANSYS MLE Model.

The stresses within the bone were significantly higher for the MLE model than for the linear elastic model, although the stress range within the tooth was very similar. The y-stress in the bone ranged between -11.973 and 14.753 MPa, and the x-stress was between -15.612 and 1.938 MPa. The region of compressive stress was concentrated close to the point where the tooth tips and compresses the bone, as would be expected. In reality, this region might not experience so much stress since the tooth has been modelled as having a fairly square-ended root.

The resultant displacement of the bone was quite small; between 0 and -0.0432mm, and was concentrated in the bone immediately surrounding the tooth. The displacement was concentrated in the tooth, which moved between 0.03614 and 0.1105mm overall.

The y-stress in the tooth lay between -1.944 and 10.897 MPa; however, most of the tensile stress was due to the hotspot caused by the loading. Unselecting the nodes surrounding the displacement constraint reduced the range of stress experienced by the tooth to between -1.545 and 3.654 MPa for the y-stress, and -1.352 and 0.915 MPa for the x-stress. The lower third of the root experienced most of tensile stress.

(The tensile stress was mostly stress in the global x-direction). Including the constrained nodes had little effect upon the magnitudes of the stresses in the tooth.

5.2.3.3 LS-DYNA3D Non-Linear model

At time t = 0.000380s, the model had settled, and the stresses and displacements predicted were analysed. The x-stress was found to range between -75.52 and 75.05 MPa within the tooth. The region identified as a "hotspot" in the vertical loadcases contained stresses of between -23.86 and 16.29 MPa in this analysis, hence it is not a hotspot in this analysis. The maximum and minimum stress occurred within the enamel tapers, and hourglassing was not a problem.

The y-stress in the tooth was found to be between -67.41 and 136.90 MPa, with the maximum and minimum values again observed in the tapers. The rest of the tooth (with the tapers unselected) only experienced stress in the y-direction of between -34.67 and 43.37 MPa, and unselecting the constrained region had little further effect upon this; the stress range was only reduced to between -31.87 and 37.63 MPa.

The x-stress transferred to the bone was very small; between -0.438 and 0.525 MPa. Similarly, the y-stress in the bone was all between -0.309 and 0.867 MPa, and this was all within the cortical bone. As in the previous non-linear analyses, the bone displaces very little; between 0 and 0.00257mm overall.

The tooth displaces between -0.0707 and 0.167mm in the x-direction.

5.2.3.4 *ABAQUS models*

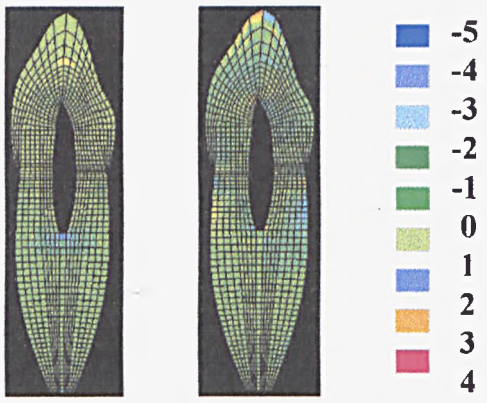

Fig. 5.2.3.4: The x-stresses due to a horizontal load in the ABAQUS models.

The distributions of x-stress for the NL and the LE models analysed using ABAQUS predict very low stress magnitudes. A stress concentration occurs at the tip of the tooth, where the load is applied. The LE model predicts that concentrations of stress will occur in the dentine, at the cemento-enamel junction (CEJ). The greatest stresses within the LE model of the PDL occur here under horizontal loads. However, the NL ABAQUS model does not predict stress concentrations in this region. Stress concentrations occur close to the pulp chamber within the NL model; however the stresses predicted by the NL model are very small.

Table 5.3.4.1: Displacement of nodes subject to a vertically applied displacement of -0.1mm.

Vertical Software	Load Type	Tip		Buccal		Lingual		Apex		Top		Middle	
		UX	UY	UX	UY	UX	UY	UX	UY	UX	UY	UX	UY
ANSYS	LE (3MPa)	3.37e-02	-0.1	2.35e-02	-0.10193	2.24e-02	-9.21e-02	-2.67e-3	-9.37E-02	2.09E-02	-1.54E-02	-3.58E-03	-1.24E-02
	LE (30MPa)	5.52e-02	-0.1	3.78e-02	-9.90e-02	3.44e-02	-8.34e-02	-7.53e-04	-8.06E-02	3.06E-02	-4.90E-02	1.11E-03	-4.01E-02
	LE (50MPa)	5.41E-02	-0.1	3.67E-02	-9.79E-02	3.30E-02	-8.27E-02	-1.01E-04	-7.85E-02	2.85E-02	-5.54E-02	2.78E-03	-4.52E-02
	MLE	4.28E-02	-0.1	2.78E-02	-9.03E-02	2.90E-02	-0.10347	-5.27E-03	-9.30E-02	1.81E-02	-1.32E-02	2.55E-04	-1.34E-02
DYNA	LE	1.39E-02	-0.1	-4.40E-04	-8.70E-02	3.84E-03	-9.32E-02	-3.88E-03	-7.79E-02	7.09E-02	-4.72E-02	-2.08E-03	-4.30E-02
	NL	1.33E-02	-0.1	2.35E-04	-9.08E-02	3.30E-03	-9.64E-02	-4.36E-03	-8.72E-02	6.52E-03	-1.58E-02	-1.28E-03	-1.66E-02
ABAQUS	LE	0.203e-2	-0.856e-1	0.868e-2	-0.892e-1	0.873e-2	-0.792e-1	-0.247e-1	-0.819e-1	-0.127	-0.461e-1	-0.19e-1	-0.841e-1
	NL	0.34	0.85e-1	0.247	0.133	0.247	0.323e-1	0.142	0.85e-1	0.116e-4	0.102e-5	0.247e-5	0.587e-6

Table 5.3.4.2: Displacements of nodes subject to a horizontally applied displacement of 0.1mm

Horizontal	Loading	Tip		Buccal		Lingual		Apex		Top		Middle	
Software	**Type**	**UX**	**UY**	**UX**	**UY**	**UX**	**UY**	**UX**	**UY**	**UX**	**UY**	**UX**	**UY**
ANSYS	LE (3MPa)	0.1	-0.10377e-2	0.72305e-1	0.14016e-1	0.72322e-1	0.14228e-1	-0.49721e-2	0.59309e-2	0.46647e-1	0.56026e-2	0.45475e-2	0.31627-2
	LE (30MPa)	0.1	-0.11580e-2	0.73649e-1	0.13174e-1	0.73642e-1	0.13099e-1	0.47750e-2	0.35223e-3	0.5137e-2	0.93286e-2	0.95607e-2	0.59954e-2
	LE (50MPa)	0.1	-0.11631e-2	0.7387e-1	0.12983e-1	0.73857e-1	0.12896e-1	0.67375e-2	0.32445e-3	0.52128e-1	0.10279e-1	0.10840e-1	0.67475e-2
	MLE	0.1	-0.69064e-3	0.69446e-1	0.15456e-1	0.69521e-1	0.14791e-1	-0.10516e-1	0.12463e-2	4.22667e-3	3.05176e-4	-6.02364e-4	-7.33733e-5
DYNA	LE	7.071069e-2	-1.649857e-3	3.61145e-2	1.4946e-2	3.643084e-2	-1.52607e-2	-1.6188e-2	3.4627e-4	1.0338e-2	4.5547e-3	-9.3667e-3	1.160800e-4
	NL	7.071069e-2	-1.585007e-3	3.568459e-2	1.557732e-2	3.588891e-2	-1.58787e-2			4.2667e-3	3.05176e-4	-6.02364e-4	-7.33733e-5
ABAQUS	LE	0.85e-1	-0.347e-4	0.826e-1	-0.117e-2	0.826e-1	0.115e-2	0.802e-1	-0.249e-4	0.818e-1	0.951e-3	0.201e-1	0.448e-2
	NL	0.85e-1	0.257e+1	0.549e-1	0.256e+1	0.595e-1	0.258e+1	0.343e-1	0.257e+1	0.277e-5	0.714e-6	0.132e-4	0.126e-5

5.3 Displacements

The results of the displacements predicted for the different material models and FEA codes used are presented in this section.

The resultant displacements of the tooth and the bone were recorded at 6 points; the incisal tip of the tooth (1), a point on the lingual surface (2), the apex of the tooth (3), and at the top (4), the middle (5) of the alveolar bone, also on the lingual surface (6). The displacements at these points are recorded in Tables 5.3.4.1 and 5.3.4.2 for vertical and horizontal loads respectively.

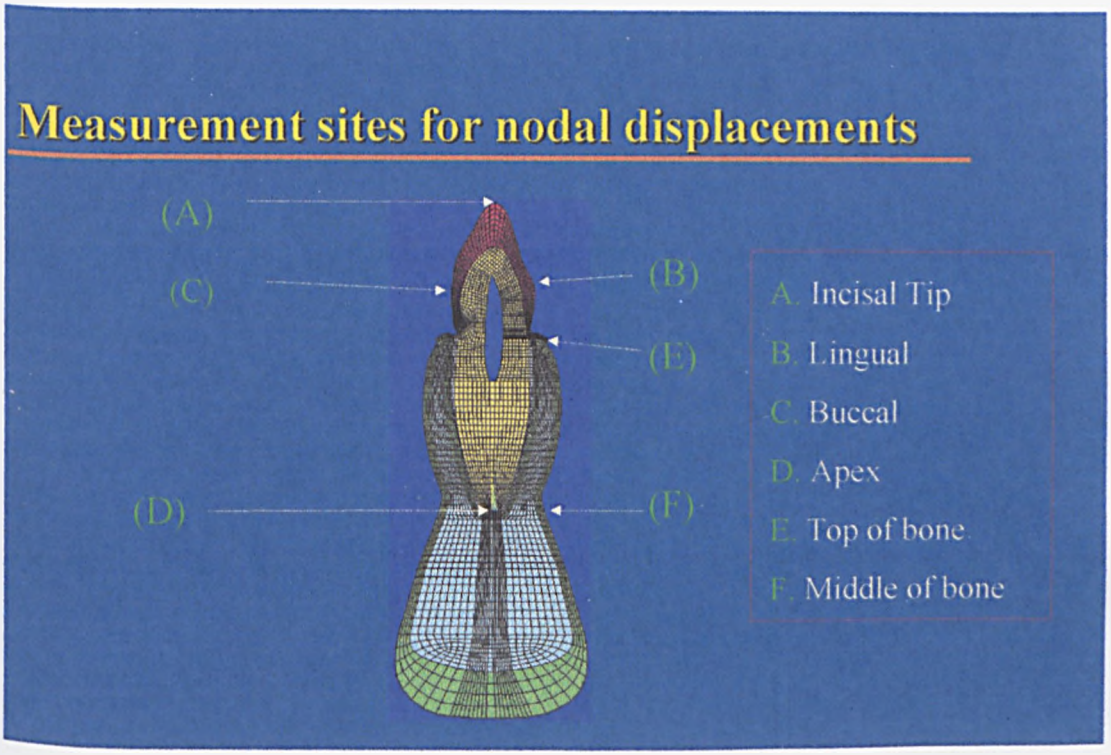

Fig. 5.3.1: The points at which the displacements were measured.

Considerable variation was shown between the magnitudes of the displacements for all software codes and material models used. However, the comparison of resultant displacements could be misleading since the resultant displacement is composed of both the horizontal and vertical components of movement. Hence, the value could be influenced by either factor.

Thus, the individual components of displacement also need to be compared. Figures 5.3.2-5.3.4 show graphs of the magnitudes of the displacements predicted at these 5 nodes.

Key relating points on Fig.'s 5.3.2 – 5.3.7 to locations on the model:

Point on graph	*Location on model (See Fig. 5.3.1)*
1, 2	A
3, 4	B
5, 6	C
7, 8	D
9, 10	E
11, 12	F

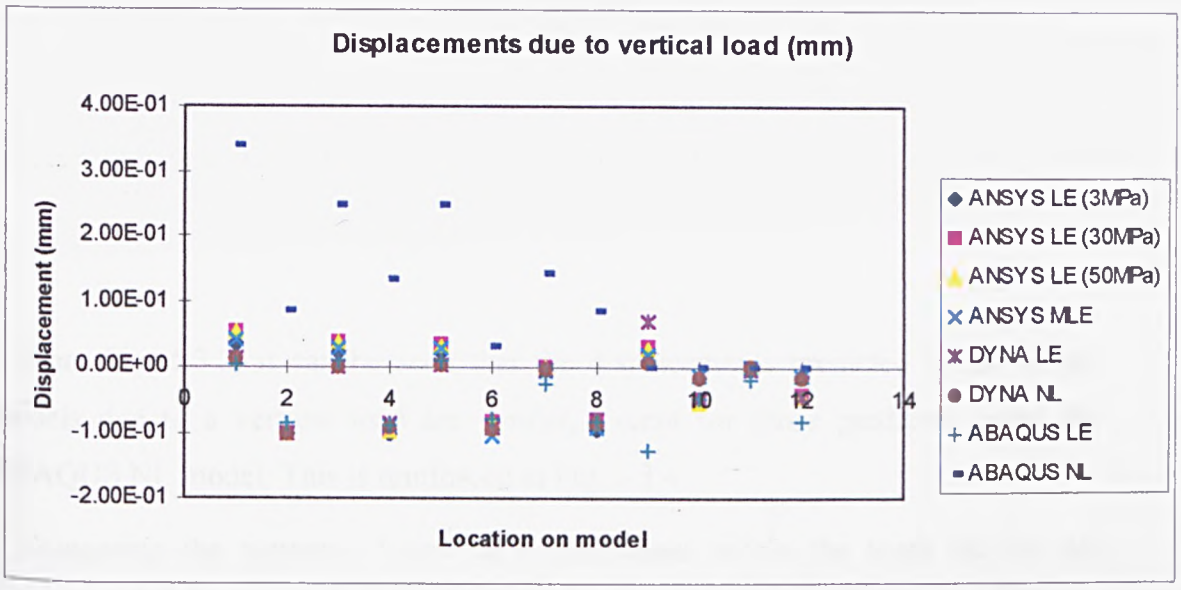

Fig. 5.3.2: Comparing the displacements of all of the models subjected to a vertical load.

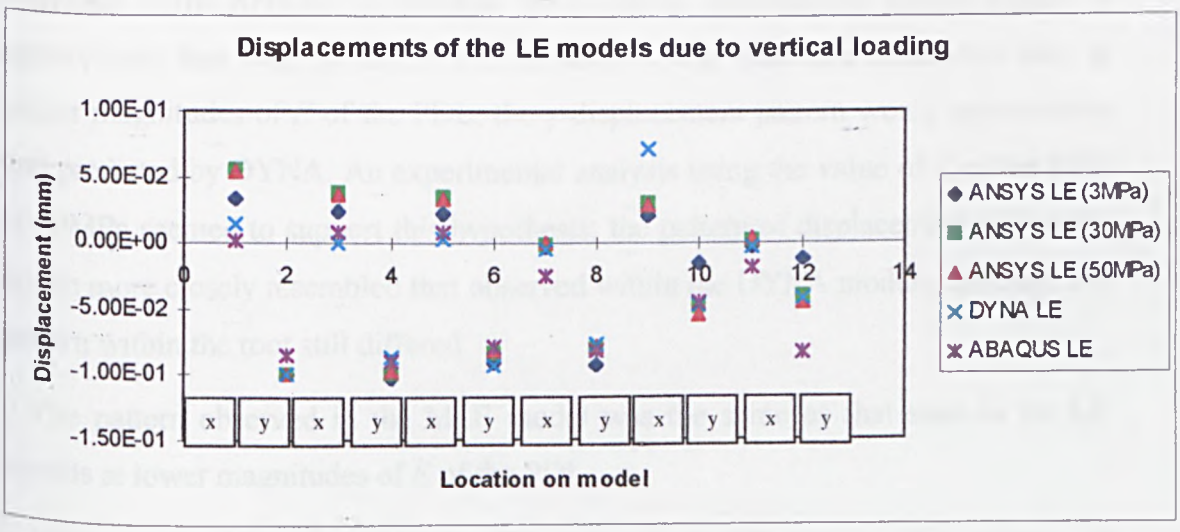

Fig. 5.3.3: Comparing the displacements of the LE models subjected to a vertical load.

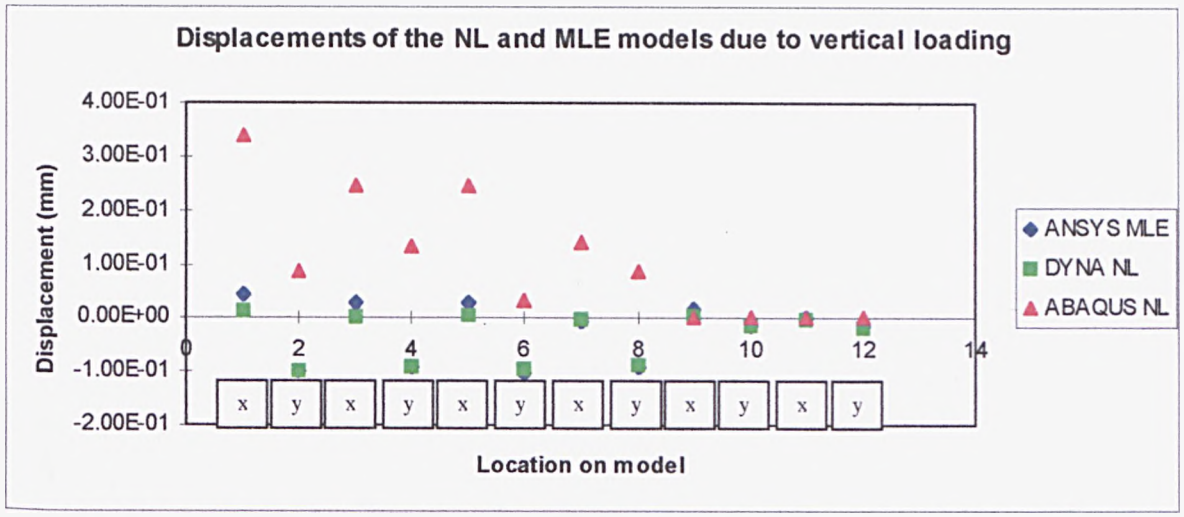

Fig. 5.3.4: Comparing the displacements of the NL and MLE models subjected to a vertical load.

From Fig. 5.3.2, it can be seen that the displacements predicted by all of the models due to a vertical load are similar, except for those predicted using the ABAQUS NL model. This is reinforced in Fig. 5.3.4.

Comparing the patterns of vertical displacement within the tooth for the LE models at 30MPa (Fig. 5.4.4.2), the DYNA model predicts significantly different patterns of displacement to the others. However, as the value of E of the PDL is increased in the ANSYS LE models, the resulting displacement pattern begins to approximate that seen in the DYNA models. It was therefore postulated that, at higher magnitudes of E of the PDL, the y-displacement pattern would approximate that predicted by DYNA. An experimental analysis using the value of E of the PDL of 80MPa seemed to support this hypothesis; the pattern of displacement within the crown more closely resembled that observed within the DYNA models, although the pattern within the root still differed.

The pattern observed in the MLE model was the same as that seen in the LE models at lower magnitudes of E of the PDL.

Interestingly, both the DYNA NL and LE model predict this pattern of displacement within the tooth for vertical loading.

The displacement pattern in the root also differed between the DYNA LE and NL models.

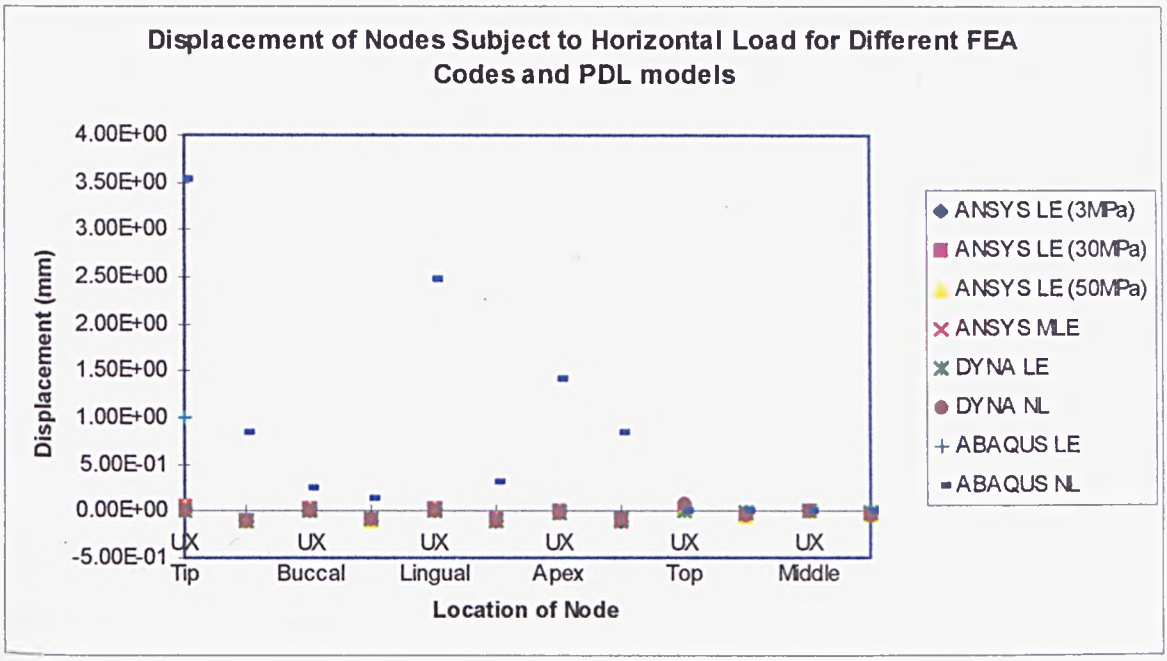

Fig. 5.3.5: The displacements predicted due to horizontal loading for all of the different material models and FEA codes used.

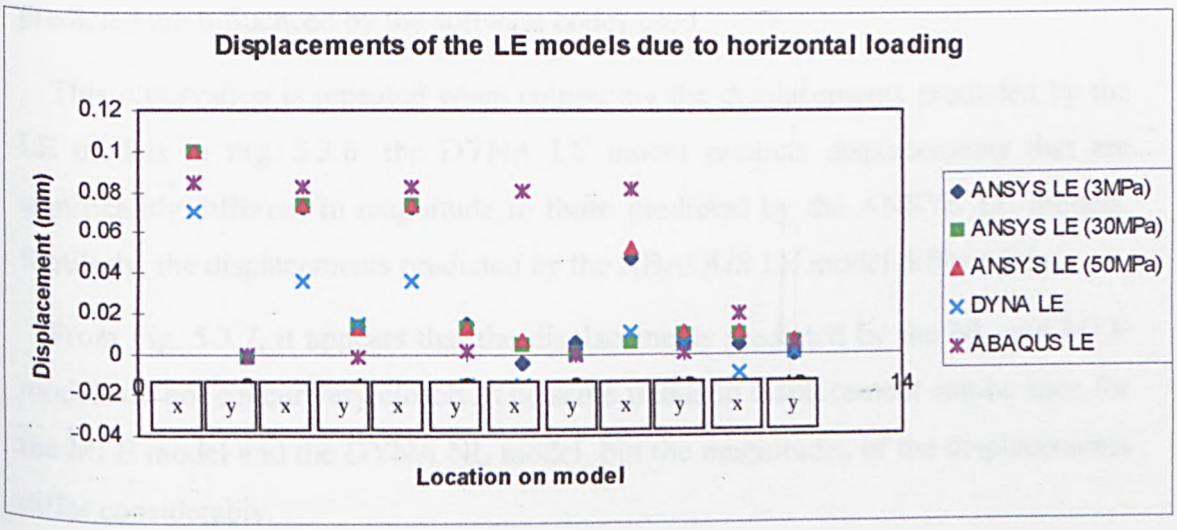

Fig. 5.3.6: Comparing the displacements predicted for all the LE models due to horizontal loading, different FEA codes.

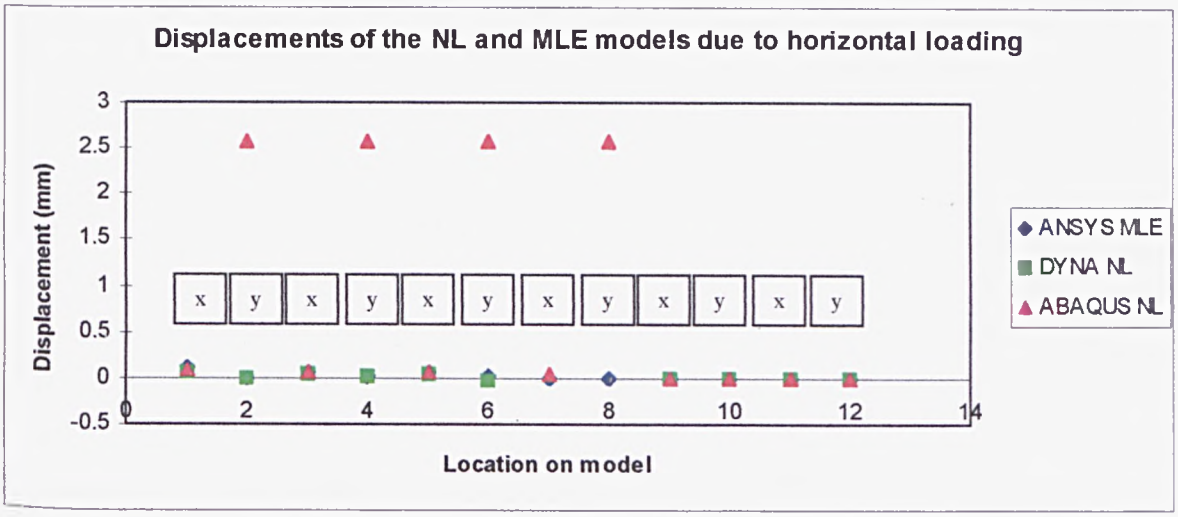

Fig.5.3.7: Comparing the displacements predicted for the NL and MLE models due to horizontal loading.

Fig.5.3.5 suggests that the displacements due to horizontal loading predicted by ANSYS all concur very well with one another; those predicted by DYNA also concur well, and those predicted by ABAQUS also show concurrence with one another. Since concurrence is observed for both NL and LE models using the same software codes, but not between software codes, this implies that the displacements predicted are influenced by the software codes used.

This observation is repeated when comparing the displacements predicted by the LE models in Fig. 5.3.6; the DYNA LE model predicts displacements that are significantly different in magnitude to those predicted by the ANSYS LE models. Similarly, the displacements predicted by the ABAQUS LE model differ again.

From Fig. 5.3.7, it appears that the displacements predicted by the NL and MLE models do not concur very closely. The same trends in displacement can be seen for the MLE model and the DYNA NL model, but the magnitudes of the displacements differ considerably.

Comparing the time-dependent load transfer patterns in DYNA, it can be seen that displacement occurs in the bone much earlier in the LE model than in the NL model, and hence more displacement of the bone occurs for the LE model over the time of the analysis (0.00056s, currently). This finding must be a result of the different PDL models; the NL model is able to absorb more of the displacement, thus less is transferred to the bone. It is likely that this observation also accounts for the

difference in y-displacement pattern observed in the root. (This simulation has been archived on video tape, c/o the Sports Engineering Research Group, University of Sheffield.)

5.4 Discussion

Considering firstly the square test cases, certain material models were found to be unsuitable. The Mooney-Rivlin hyper-elastic material model (specified using the *MOONEY command in ANSYS) was found to give very unusual results. This command requires the specification of an array of strains and engineering stresses measured experimentally. An initial gradient also needs to be specified. However, for the material model to solve, the gradient specified needed to be less than that of the initial slope of the model. This is because the typical curve shape for a Mooney-Rivlin material is as shown in Fig. 5.4.1a. However, the shape of the generic natural tissue model is approximately as illustrated in Fig. 5.4.1b, and from a comparison of the two figures, it can be seen that the initial slope for the Mooney-Rivlin model is the greatest slope, whereas for the generic, hyper-elastic tissue model, the initial slope is the least.

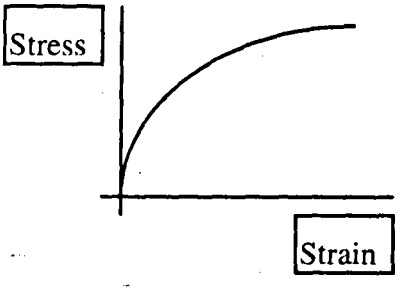

Fig. 5.4.1a: A typical Mooney-Rivlin hyperelastic material curve.

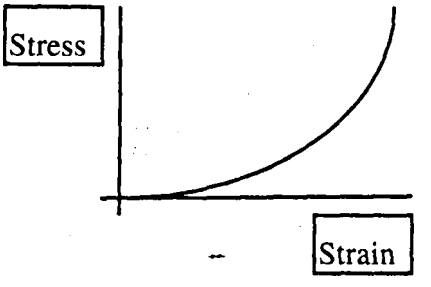

Fig. 5.4.1b: The generic hyperelastic natural tissue model.

This meant that the results of the hyper-elastic material model specified using the Mooney-Rivlin model were not close to those of the generic tissue model.

From consideration of the displacement behaviour of the different models, it would appear that, in all cases, the tooth experiences the majority of the displacement. For the linear elastic models of E = 50 MPa and 30 MPa, more displacement is directed into the bone than for low modulus linear elastic case, or for the multi-linear elastic, and non-linear models.

This might suggest that the PDL is stiffer overall than that used by the NL models. Either the LE model if the PDL is artificially stiff, thus reducing the deformation of the mandible, or the NL models used are not stiff enough. Similar displacements are predicted by the LS-DYNA3D NL analysis to those measured experimentally by Jones *et al.* (1998) and Picton (1965), which would tend to support the stiffness of the NL model. However, Rees and Jacobsen (1997) report that 50 MPa is the most appropriate value of E to represent a LE PDL to replicate the strain gauge measurements of Hood.

5.4.1 Vertical Loads

The distributions of y-stress within the tooth are found to be very similar for all cases, regardless of software used, or whether the PDL was modelled as a LE, NL or MLE material. This statement implies that the same regions of the tooth experience tension, compression or zero stress in the different models.

However, the magnitudes of the displacements vary considerably between the different models. Some of this variation can be attributed to the hot spots caused by the application of the displacement load.

The distributions of y-stress within the bone differ very markedly. The distributions of all of the LE models appear similar to one another. However, the LS-DYNA3D NL model predicts areas of tension and compression within the cortical bone adjacent to the PDL and tooth root. The ABAQUS NL model predicts different patterns of tension and compression, and the ANSYS MLE model predicts a distribution of stress similar to that of the LE models.

It is conceivable that some of the differences between the ABAQUS NL model and the DYNA NL model may be attributable to the fact that a PDL of uniform thickness of 0.33mm was used in the ABAQUS model, whereas the model of the PDL in all of the other software codes varies in thickness between 0.1mm and

0.33mm. This has been cited as a potential source of introduction of error by Cobo *et al.* (1993).

5.4.2 *Horizontal Loads*

Comparing the resultant displacements within the tooth for the DYNA NL and LE models, at t = 0.00056s, both models have the same range of displacements, but the apex of the tooth has displaced more in the NL analysis than in the LE case. Studying the resultant displacement behaviour over time, it can be seen that the crown of the tooth displaces more (relatively), earlier in the LE analysis than the NL case. This would suggest that the stiffness of 30 MPa of the PDL in the LE case makes the root of the tooth artificially stiff; a similar effect to applying constraints directly to the root of the tooth.

Comparing the distributions of y-stress over time between these 2 models, (DYNA LE and NL), both experience the same stress distributions within the tooth, but have different PDL behaviour, and stress distributions within the bone. The magnitudes of the y-stresses are slightly higher in the LE model than in the NL model.

Similarly, the distribution of x-stress over time within the tooth does not appear to differ between the NL and the LE models in DYNA. Also, the MLE and NL distributions compare well in both x- and y-stress distributions, although the magnitudes do vary, and for x and y-displacement within the tooth. However, the stress distribution in the bone is significantly different; more tension and compression is observed in the cortical bone adjacent to the PDL and root in the LE model than in the NL model. This again supports the hypothesis that the PDL absorbs more of the load. (The y-stress distribution in the bone also differs markedly between the LE and NL analyses). Comparing the DYNA NL model to the MLE model, the x-displacement of the bone differs markedly in pattern. In the MLE model, the pattern is symmetrical, whereas on side of the cortical bone experiences significantly more displacement than the other in the DYNA NL model. However, the x and y-stress distributions are comparable in both models.

The distribution of x-stress differs significantly in the bone between the ANSYS LE model and the DYNA NL and ANSYS MLE models. In the LE model, more stress is observed close to the constraints, in the base of the bone, and less is seen in the cortical bone adjacent to the tooth. The magnitudes of x-stress are much reduced for the ANSYS LE model. The DYNA and ANSYS LE models predict similar patterns of x-stress within the bone; the same trends can be observed in both cases.

The distributions of y-stresses in the ANSYS LE, DYNA LE, and NL models in the bone are all similar.

The x-displacement plots differ; the ANSYS LE plot is very similar to that of the MLE. The DYNA NL plot predicts more displacement on the lingual side of the cortical bone, and the LE model is similar to the ANSYS model except that the thinnest part of the bone displaces less than the bone just below it in the DYNA model, whereas the ANSYS model predicts the same displacement throughout. This reflects that the ANSYS model and the DYNA NL model predict less bending, and displacement in the lower portion of the bone than the DYNA model.

The y-displacement patterns appear approximately the same in the bone for all the models. The stress distributions and displacement patterns within the tooth were similar for the DYNA NL, LE and ANSYS LE models.

More stress appears to be transmitted into the bone in the MLE models than for the LE models.

5.5 Conclusions

The results indicate that, for functional loading conditions, a linear elastic model of the PDL will enable the stresses in the crown of a tooth to be studied accurately, regardless of the software package used. However, if the displacement (movement) of the tooth, or the stresses and displacements of the bone are of interest, then the type of material model used for the PDL will significantly affect the results obtained.

5.6 Evaluation of Software Used

In this chapter, various software codes have been used in the comparative analysis of material models to represent the PDL. The merits of the different codes used are discussed here, with particular respect to their use in the Bio-engineering environment. Attention is paid to the ease of use of the software codes and their applicability to stress analysis of bio-mechanical applications.

The software codes that have been used in this project are:

ANSYS

LS-DYNA3D

ABAQUS

HYPERMESH

FEMGV

TOMECH

A variety of element types were used. The main problem was that the behaviour of the PDL is very different from that of most commonly used engineering materials. FEA codes are generally designed to model the behaviour of such materials. If material behaviour such as hyper-elasticity, visco-elasticity and non-linearity are included in FEA codes, they tend to have a strong bias towards the materials that would commonly be used in engineering. Thus, the behaviour of rubbers, wires and synthetic materials can be investigated relatively easily. However, the material model proposed by Huang *et al.* (1990) and Chew *et al.* (1994) is significantly different to any of these materials, as illustrated in Fig. 4.3.1.

This difference in behaviour necessitates the investigation of the importance of this type of material model in the FEA of natural and restored teeth. The following chapter outlines the different approaches used to define material behaviour of this type in various FEA codes.

Most modern FEA programmes are divided into three parts; a pre-processor stage, when the geometry of the model is defined, the solution phase that calculates the

stresses and displacements experienced by the model, and a post processor, which enables the results to be viewed graphically.

Traditionally, FEA programmes did not use a pre-processor; the co-ordinates of the elements comprising the model, the loads and the constraints were all specified by hand, directly to a text file to be read by the solver. The pre-processor permits geometric shapes to be created easily and viewed on-screen, providing a simple an effective method of ensuring that the model represents the object that it is meant to reasonably accurately.

Pre-processors are supplied with various levels of sophistication; some permit complex shapes to be created by Boolean algebra (the process of creating shapes from addition or subtraction of other shapes), whereas others require geometry to be specified using only straight lines or arcs. The advantages of more sophisticated pre-processors are evident:

simple models can be created quickly,

less experience of 2 or 3-dimensional modelling is required to create models quickly and simply,

complex models can more easily be created by combining or intersecting standard geometrical shapes,

the resulting geometry can be viewed before meshing and analysis, enabling better meshes to be produced,

line divisions can be specified interactively and the mesh viewed, enabling the quality of the elements to be reviewed.

The solvers of the different software codes operate in a variety of ways. There are generally two types of solvers, as described in Chapter 3; implicit solvers and explicit solvers. The majority of the software codes use implicit solution algorithms. However, ABAQUS permits the use of either implicit or explicit solution algorithms, giving it a great deal of versatility.

5.6.1 Ease of use of the different software codes to define the material model

The linear elastic material models in ABAQUS and ANSYS required only the specification of simple material properties, such as E, the density and the Poisson's ratio of the material. Since LS-DYNA3D is a dynamic solver, specification of the load curve was still necessary.

The codes that already incorporate various non-linear material models as standard would at first glance appear easier to use. For example, using the *MOONEY feature in ANSYS, experimental data can be specified through a data table. The data table can incorporate as much data as is available, so long as at least 9 points are specified, and that engineering stress and strain are used. The data table provides a simple-to-use, interactive method of specifying the hyper-elasticity curve. Graphs can be plotted of the input data for verification.

Similarly, the data points defining the multi-linear elastic model were specified by means of an interactive data table.

By comparison, to specify the material model in ABAQUS using the UHYPER routine, the first, second and third derivatives of the constitutive equations of the SEDF (strain energy density function) have to be specified. These must be written to a separate file; the UHYPER routine, which is a FORTRAN sub-routine to be referenced by the solver. Evidently, this requires the calculation of the derivatives and the correct specification of the FORTRAN routine.

This is clearly not as straightforward as simply entering laboratory data. Other constants also have to be specified, such as the shear modulus, the bulk modulus and the hourglass coefficient. However, it does have the advantage of making the model very specific, and hence increases the level of control that you have.

Other hyper-elastic material models were available in ABAQUS, such as the polynomial model, the Ogden model, and also the Mooney-Rivlin and Neo-Hookean models. However, these models had already either been shown to be inappropriate by other researchers, or in previous analyses using ANSYS.

In ANSYS, the Mooney-Rivlin model was found to be inappropriate to model hyper-elastic behaviour of this type. Since the equations describing the behaviour of

the material were already specified within the software and merely used the laboratory data to evaluate the constants, there was no way round this problem in ANSYS. The only alternatives were therefore to either program an entirely new material model or to use the multi-linear elastic model as an approximation.

From this point of view, therefore, the method of specification permitted by ABAQUS was far superior to that of ANSYS, even though it was less user-friendly, and required more experience at the outset.

In LS-DYNA3D, the non-linear hyper-elastic material model has already been specified (Chew *et al.,* 1994). To specify the material model, a load curve had to be defined in the input file, and certain constants had to be amended. Specification of the load curve is required by all dynamic analysis programs, but it is a little more complicated than LE analysis using an implicit solver.

Overall, to specify a LE material model, ANSYS would be easiest to use, since all of the data can be entered interactively. ABAQUS requires the construction of an input file, which is written in FORTRAN, and although the manuals are extremely well-written, this method is not as user-friendly to a novice; particularly one who is not an engineer. The task can be made easier by defining the model in another package such as HYPERMESH or FEMGV. Files can then be exported from these programs ready to be solved by ABAQUS.

CHAPTER 6

Validation of the FEA Model

6.0 Introduction

FEA is a very useful technique for predicting the distributions of stresses, strains and displacements within a structure, but the results of the analyses are sensitive to the data supplied originally. Since the whole field of Bio-engineering is plagued by the difficulty of obtaining accurate material properties, it can be expected that the results of an analysis will only be approximately accurate. Furthermore, it is difficult to know to what extent it is possible to extrapolate the results of an FEA model to the total biological situation, although every care has been taken to ensure that the constraints applied and assumptions made are as close as possible to those experienced in the natural situation. Hence, the quality of this study would be enhanced if some experimental evidence could be provided, supporting the findings of the FEA work.

One of the problems associated with experimental stress analysis techniques is that it is difficult at the outset of a study to choose the most appropriate technique. Olden (1998) developed a formalised technique selection method, finding that most experimental techniques were selected based on the experience of the analyst, or the equipment available at the time. To test the procedure, Olden used three case studies. The selection of the most appropriate technique for a human canine tooth was the third of these case studies, and details are given in her thesis (Olden, 1998). The technique recommended was SPATE; Stress Pattern Analysis by measurement of Thermal Emission. A brief description of this technique is outlined in section 6.1, and details of the experimental procedure used are given in section 6.3.

6.1 Thermoelastic Stress Analysis

Thermoelastic stress analysis is defined as:

"The estimation of the state of stress in a structure by measurement of the thermal response resulting from the application of a load within the elastic range of the material." (Harwood and Cummings, 1991). The first observation of this effect is attributed to Weber, in 1830. He was experimenting with vibrating wires, and noted that a delay occurred between the application of a sudden increase of tension in the wire, and the corresponding change in its fundamental frequency. He proposed that

the delay was due to a temperature change in the wire, caused by the increase in stress (Rauch and Rowlands, 1993).

The theory to explain the effect was not proposed until 1853 by William Thomson, who later became Lord Kelvin. It says that a change in the sum of the principal stress in an isotropic solid will cause a proportional change in temperature. Compton and Webster confirmed the hypothesis experimentally in 1915, and Biot extended the theory for anisotropic, visco-elastic, and plastic materials in the 1950s. (Rauch and Rowlands, 1993).

6.2 SPATE

SPATE systems are produced commercially in the UK by Ometron Ltd. A SPATE system measures load correlated temperature changes at various points on the surface of a material subject to a dynamic, cyclic load. From this information, the full-field stress patterns can be estimated. The equipment that is used has to be very sensitive, since the change in temperature of a material due to a cyclic load is usually very small.

The technique of thermoelastic stress analysis was used to study stresses in human teeth by Meredith, Setchell and Swanson (1997). Unfortunately, Meredith, Setchell and Swanson (1997) was not published their findings at the time that the author was attempting to use this technique, so it was not possible to benefit from their experience at the time. In this study, molar teeth containing MOD (mesio-occluso-distal) cavities were used. The teeth were tested with the cavities cut, but not restored; with the cavities filled with amalgam; and with the amalgam removed and the cavities refilled with an enamel-etched and dentine-bonded restoration.

Prior to testing, the teeth were examined radiographically to detect caries, and were trans-illuminated to identify any cracks or evidence of extraction damage. Any teeth showing signs of this were rejected.

Meredith, Setchell and Swanson (1997) kept the cavity moist by the presence of a dampened cotton wick. Rauch and Rowlands (1993) state that the SPATE system can be used with frequencies of loading between 0.5Hz and 20kHz, but this is dependent on the material properties, since the response of the system must be

adiabatic for this technique to work. Most non-metals, therefore, have to have a loading frequency of at least 10Hz to achieve an adiabatic response.

All of the teeth used by Meredith, Setchell and Swanson (1997) were coated with R.S. matt black paint to ensure an even surface emissivity, and to make the tooth a black body radiator. This is recommended by Harwood and Cummings (1986) and is shown to increase the emissivity of certain metals greatly. However, Rauch and Rowlands (1993) state that most non-metallic materials do not require painting (except for brick and concrete).

Emissivity is a material property that varies between 0 and 1. An emissivity of 1 makes a material a black body; the ideal radiator. The value of emissivity of a material is the ratio of energy emitted by the body to that which it would emit if it were a black body (Berger, Goldberg and Lewis, 1996). (Emissivity is a function of the photon wavelength.) The emissivity of skin is stated as being between 0.97 and 0.99, regardless of pigmentation. This is very high; very close to ideal radiation. The emissivity of polished steel is 0.066, and of copper is 0.023. Glass has an emissivity of 0.94, and water of 0.95 - 0.963. (Berger, Goldberg and Lewis, 1996).

The black paint layer can act as an insulator, or can introduce a lag between the detector signal and the loading frequency. Also, the tooth needed to be kept moist throughout testing, in order to preserve the material properties, and the paint may have prevented the water from penetrating the tooth structure.

6.2.1 *Equipment*

Photographs of the test specimens and the loading situation are shown in Fig.'s 6.3.1 and 6.3.2 respectively, Section 6.3.1.

The function of the different parts is explained here.

6.2.2 *The Detector*

The detector must be capable of measuring very small changes in temperature, which in turn give the changes in stress induced in the component due to the applied

cyclic load. Original SPATE systems used a raster scanning infra-red detector to convert incident radiant energy into electrical signals, which could then be measured, providing the required stress information. However, photon detectors are more sensitive (Rauch and Rowlands, 1993), and are used in commercial SPATE systems. The output voltage from a photon detector is directly proportional to the rate of incident photons. The photon detector is cooled by liquid nitrogen (at 77K) in order to improve specific detectivity (*i.e.* the signal to noise ratio), and to minimise the effects of background radiation. (Rauch and Rowlands, 1993).

The detector head uses a system of precision mirrors to focus the photon detector on a particular part of the specimen. The quality of the scan obtained can be improved by increasing the overlap between the spots on which the detector focuses. However, this increases the time taken for each scan considerably.

6.2.3 *Lock-in Analyser*

The voltage signals from the photon detector (the response signals) are then fed to a lock-in analyser. This comprises a series-connected signal mixer and a low-pass filter. A reference signal is taken from the load cell, a strain gauge attached to the component, or from a signal generator (Harwood and Cummings, 1991). This permits the relationship between the reference and the response signals to be determined, and, by mixing this signal with the detector output at the same frequency as the applied load, the thermoelastic response can be extracted in the following way.

If two distinct signals, ω_1 and ω_2, are mixed (*e.g.* the signal transmitted from the photon detector scanning the component, and the reference signal) they produce a resulting signal with frequencies $\omega_1 + \omega_2$ and $\omega_1 - \omega_2$. The signal from the photon detector will include the thermoelastic response of the component, which will occur at the reference frequency, ω_r; the frequency of loading of the component. Therefore, if the thermoelastic response signal is mixed with the reference frequency (from the load cell, strain gauge, or signal generator), the output signal will include a dc signal of $\omega_r - \omega_r = 0$, a signal at twice the original frequency of $\omega_r + \omega_r = 2\omega_r$, and the noise. The noise is now negligible, and the low-pass filter is used to recover the

dc signal from the mixer output, by removing a proportion of the signal above a certain, specified cut-off frequency.

The filter used is a two-pole, low-pass filter, and it takes an appreciable time for the filter to settle. Hence, noise can be reduced more efficiently by using the A-D converter in the lock-in analyser rather than by a filter.

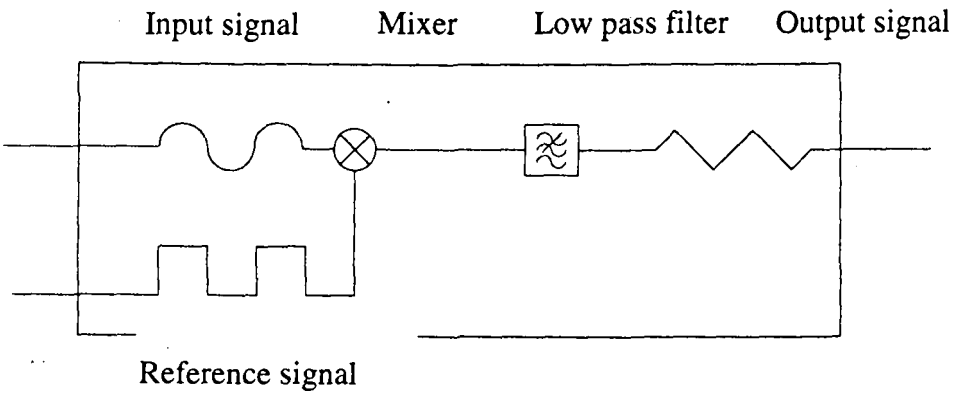

Fig.6.2.1: The signals are mixed within the analyser to eliminate background noise.

6.2.4 Calibration

The thermoelastic signal must then be calibrated by the operator in order to calculate meaningful stress data. Calibration can be achieved in a variety of ways. For linear, isotropic structures, a strain-gauge rosette placed on the test specimen will give a factor relating the principal stresses from the gauges to the thermoelastic response signal. This signal is the sum of the orthogonal stresses in the specimen, known as the first stress invariant. For anisotropic materials, the thermoelastic response of the material is influenced by the dilatational stresses along the material axes. The actual stress information can be extracted from the calibrated thermoelastic signals as described by Rauch and Rowlands (1993).

Meredith, Setchell and Swanson (1997) used the method of direct calibration, using the material properties of the specimen and the characteristics of the measurement system. Other calibration methods include using a test specimen of simple geometry (enabling the results to be compared to theoretical solutions) loaded in the same way, at the same frequency, as the specimen under examination. Strain gauges are mounted on the test specimen, in regions experiencing low stress,

and their output is compared to that calculated from the thermoelastic signals to determine a calibration factor. This is not really feasible with a human tooth.

6.3 SPATE Testing

The aim of the tests was to:

Validate of the FEA studies

Look for evidence for the theory of abfraction

Many FEA simulations of tooth under applied, compressive load have been carried out, but good quality, experimental data which can be used to validate an FEA model is rare.

6.3.1 *Materials and Methods*

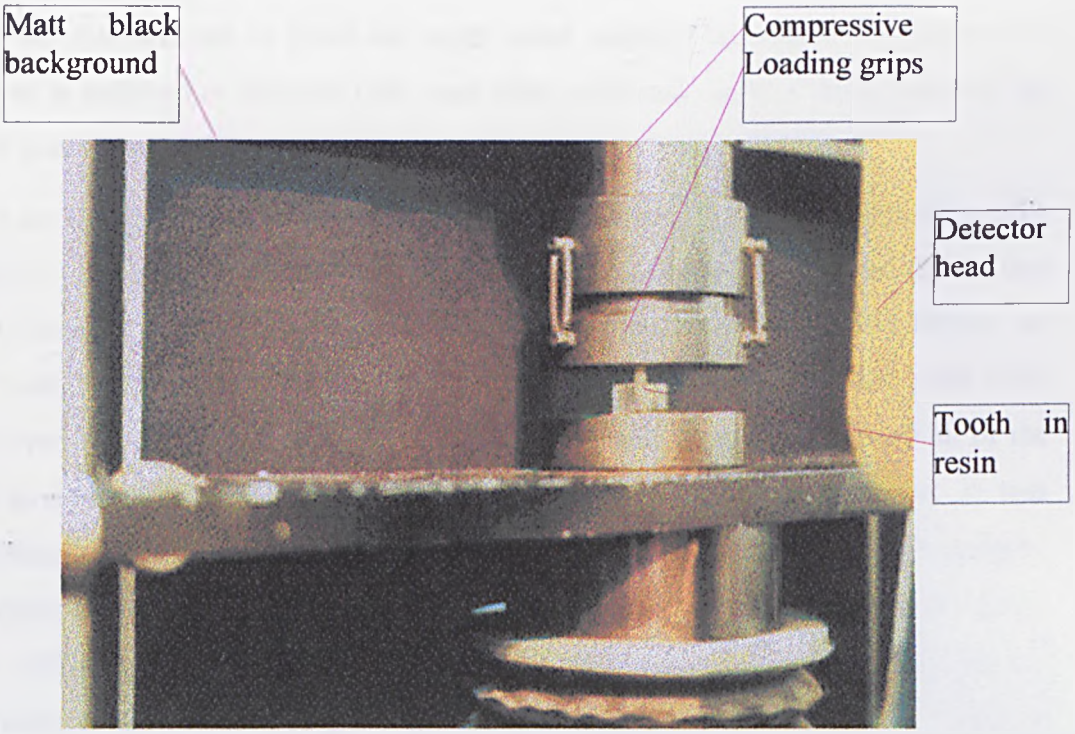

Fig. 6.3.1: Photograph of the experimental set-up used.

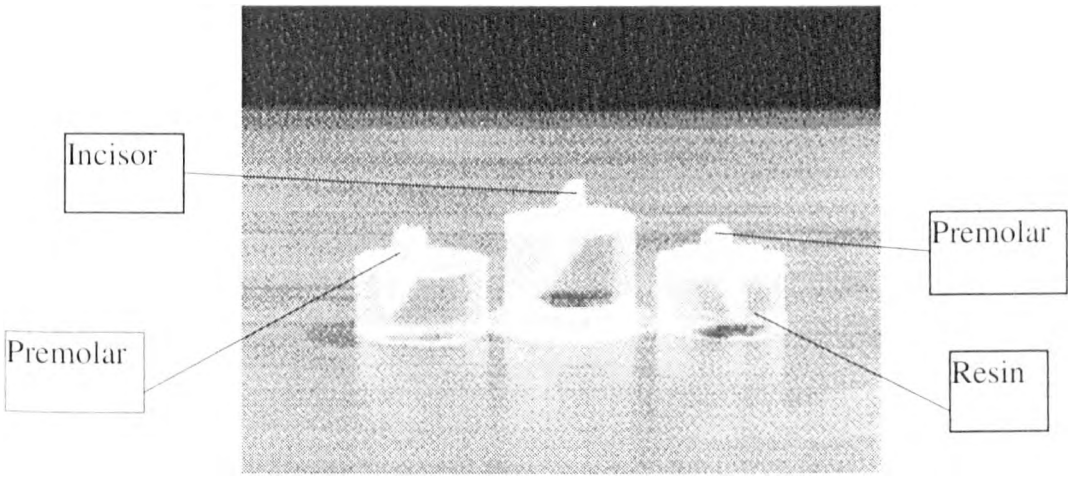

Fig. 6.3.2: The teeth mounted in polyester resin.

The MAYES cyclic loading machine was set up as shown in Fig. 6.3.1, with the tooth placed on the compressive loading plate, under 200N compressive load, cycling to zero stress. The detector head was positioned using a powerful light source and focusing the cross hairs in the centre of the spot of light on the centre of the tooth. The distance from the detector head to the tooth was measured, and the detector head focused accordingly.

It was decided not to paint the tooth black initially because the emissivity of enamel is believed to be quite high, and other problems, such as dehydration of the tooth could result from this practice.

To set the scan area, the light source was switched on, and the mirrors within the detector head were adjusted to focus the cross-hairs on the top left and the bottom right "corners" of the tooth. This was not straight-forward; if the detector focuses on the tooth, then a proportion of the tooth must be missing from the scan area. However, the backing board used was matt black and designed to absorb all of the background emissions. It was therefore matt black, which meant that it was extremely difficult to locate the cross hairs. The tooth does not have square corners, so trying to set up the scan to include the entire tooth involved some guess work. This difficulty was further exacerbated by the problems associated with the curvature of the surfaces of grips and specimens, and the fact that the specimen is further away from the detector than the resin and the grips. Fig. 6.3.3 illustrates this problem.

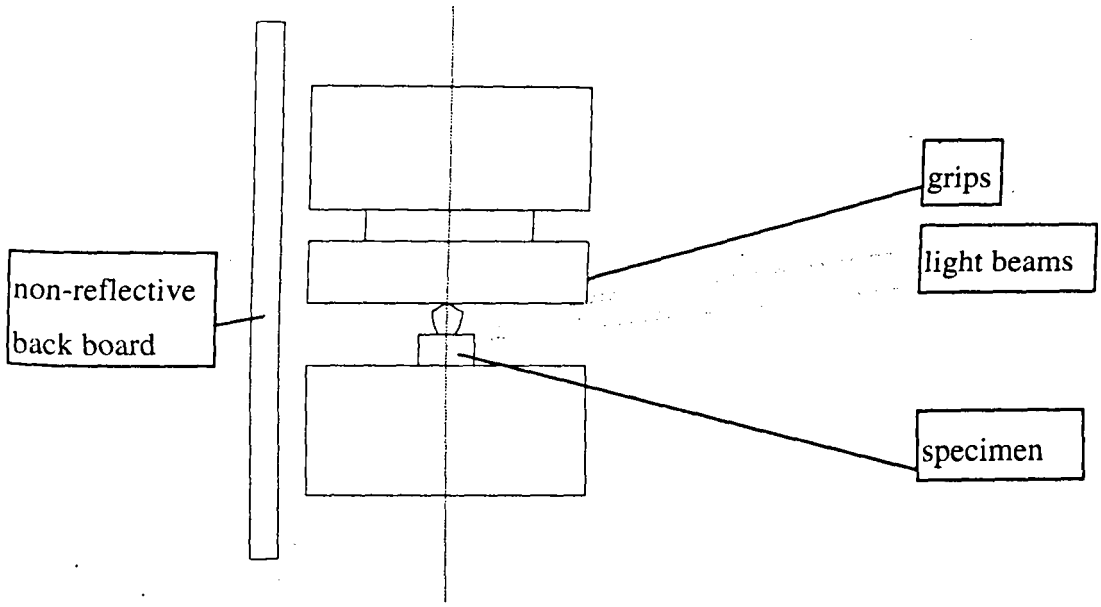

Fig. 6.3.3: Showing how the scan was set up using the light source.

As can be seen from Fig. 6.3.3, the curvature of the surfaces makes it difficult to work out exactly where the light source is in relation to the boundaries of the tooth, and unless the light source is orientated very precisely, the grips and the resin interfere with the locus of the light source.

The amplifier was built to amplify the reference signal from the loading machine into the SPATE analyser. This was because SPATE normally operates with a signal in the range of 1kN upwards, but the normal bite load on a human tooth is between 100N and 400N. Hence the amplifier multiplies the signal by a factor of 10.

Initial experiments were undertaken to determine whether this system could be a viable method of verifying the FE studies already carried out, and if SPATE could provide useful evidence in support of the anisotropy theory, and in investigation into restoration design.

A number of interesting observations resulted from these initial tests, although no useful SPATE data was gained from them.

6.3.2 *Observations*

The tooth dehydrated quite quickly during the experiments. This was partly due to the hot weather, but in normal function, a tooth is almost always in a moist environment, and it is known that the material properties alter when the tooth dehydrates. Hence a water spray of some description was necessary.

The magnitude of the load decreased slightly after initial application, causing a fall-off of load on the system during testing. Enquiries were made as to whether the mounting material absorbed some of the water that the teeth were stored in, as it was noted that the top surface of the resin went white during storage overnight, but dried out to become colourless as the day wore on. However, it appears that the top layer of the material is uncured resin, and that, although this layer absorbs water, the polymerised resin does not.

The initial results did not yield any useful data, beyond that the technique seemed feasible, and it was feared that the angle of the detector head to the specimen might permit the loading grips to interfere with the loci of the mirrors. Hence, the detector head was raised slightly on the tripod.

Difficulties were experienced in eliminating the background "noise" from the data obtained from the tooth. It was felt that this could be due to the fact that the emissivity of enamel is very high (it is believed to be between 0.95 - 0.99, based on data for water and skin, Berger, Goldsmith and Lewis (1996)), which would be similar to that of the black, cloth-covered boards used to shroud the testing set-up to reduce background interference. Hence a small piece of white paper was inserted behind the test specimen to see if this made the boundaries clearer. This seemed to have a positive effect on the results.

In order to overcome the problems of de-hydration of the tooth, it was originally decided to interrupt the scans at regular intervals to douse the tooth in water, and wipe it away from the grips, *etc.* without interfering with the scan results. However, it quickly became apparent that this process immediately preceded the system crashing. Since many promising sets of data were lost as a result of this practice, it was decided to spray the tooth with water as the detector was on the edge of the scans.

It was also noted that switching the light box on or off, either during scanning or whilst setting up the frame area apparently caused the SPATE system to crash. Similarly, there appeared to be a correlation between the change in tone of the fatigue machine (possibly due to a mains spike) and the system crashing.

In initial tests, the entire tooth was mounted in resin, up to the cemento-enamel junction, and was stored in water, and refrigerated overnight, to reduce the possibility of bacteria growing on the tooth. A correlation was noted between the range of values seen by the detector and the temperature of the specimen. When scans were attempted in the afternoon, and the tooth was warmer, the range of values predicted was much more limited. It was therefore decided to store the tooth at room temperature prior to testing.

6.3.3 *Observations from SPATE Testing*

The University acquired a more recent version of the SPATE system from Ometron Ltd. in March, 1998. This system permitted the data from scans to be saved for future analysis, and the way in which the scan area was set up was altered. A new correlator and detector head were also used. The observations from these experiments are described below.

Three extracted human teeth (2 premolars and one incisor) were slit longitudinally using a water-cooled, diamond saw. Half of each of the teeth were then mounted in colourless poly-styrene resin, which was left for 24 hours in the fume cupboard to polymerise. This was a cause of concern, since it meant that, for 24 hours, the tooth was dehydrated.

A mounted, sectioned incisor tooth was sprayed black with a single coat of R.S. matt black paint, in an attempt to improve the uniformity of the surface emissivity, following from the work of Meredith, Setchell and Swanson (1997). Ideally, more than one coat of the paint ought to have been applied, as white flecks of the tooth were visible through the paint in places. However, due to a miscalculation in the amplitude of the load, when cyclic loading commenced, the specimen fractured, and the enamel split off the tooth down one side. This could also have been due in part to dental caries in the incisor tooth, but this is more difficult to evaluate when the tooth is painted black.

Testing was continued on the broken specimen, with the view that more experimental risks could be taken, and hence more information could potentially be gained. Loading at 60 cycles per minute (1Hz) commenced with an amplitude of 6% and an initial load of 20N. No useful data was obtained. This was to be expected, since loading frequencies of less than 10Hz are not recommended for non-metals (Rauch and Rowlands, 1993).

The scan was re-aligned and repeated, and the difference between the grips, the tooth and the resin was faintly discernible. An attempt was made to reset the scan area to be "the useful part" (*i.e.* the area containing the tooth), but the new software is not as amenable to this process as the old software was. Again, the scan did not yield any quality data, but it was possible to differentiate between the resin and the tooth substance. Interestingly, the chipped surface of the tooth, whitish in colour corresponded to an area of high signal, whereas the body of the tooth, painted black, gave a high negative signal.

Increasing the amplitude of the load again (to 10%) gave better distinction between the tooth and the surroundings, but increasing the amplitude further to 15% resulted in further fracture of the tooth. It was observed after this scan had been stopped that the tooth and resin mounting had bodily displaced quite markedly during the testing. Since the tooth structure was severely crushed by this stage, some of the lateral displacement could be attributed to the energy released by fracture, an increase in the horizontal component of the load transmitted from the tooth into the resin as a result of the fracture, slipping of the specimen or it could be a problem inherent in the testing set-up.

Movement of the specimen would result in a smeared scan, or, in the case of a tooth-sized object, the detector could simply be scanning the background, and not looking at the tooth at all. If this "rigid body motion" was occurring, then it could account for the inconclusive results of previous tests.

It would have been useful to have increased the frequency of loading with an amplitude of 10%, but the specimen appeared to be too badly damaged to continue testing.

Personal communication with a representative from DeltaTherm (a competitor of Ometron Ltd.) suggested that poster paint provided a very uniform, high emissivity

surface, and was also water soluble, so should therefore be easy to remove and not affect the material properties of the tooth.

6.3.4 Results

An example of the results obtained are shown in Fig. 6.3.4.

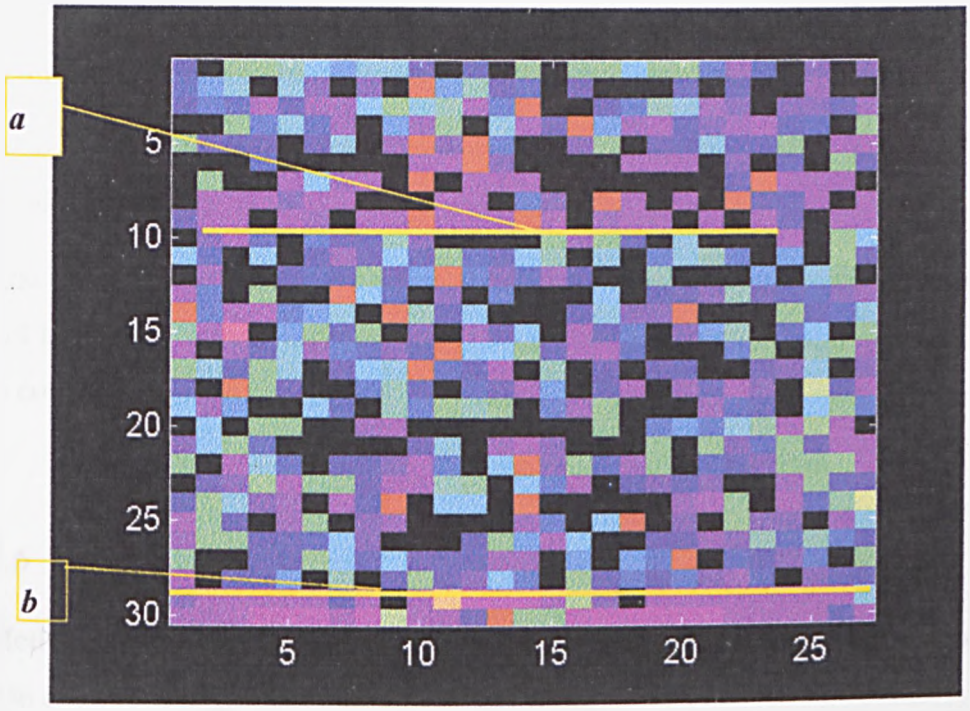

Fig. 6.3.4: An example of the results obtained from SPATE.

It is possible that the outline of the enamel can be observed in Fig. 6.3.4, shown by line ***a***, and that line ***b*** indicates the resin. However, the rest of the scan does not show any useful data.

6.3.5 Discussion

It appears that no useful data was gained from the use of SPATE to analyse the stresses induced in human canine and premolar teeth due to a cyclic, compressive load. The scans obtained did not yield any clear results; no concentrations of stress could be observed, and the tooth could not be identified clearly from the background. This could have been due to a number of factors.

The use of water to hydrate the tooth could have affected the signal detected, and the spraying of water during the experiment could also have altered the material properties of the tooth, affecting the signals obtained.

The lock-in analyser may not have phased in correctly, despite every effort being taken to ensure that it did.

The specimen could have moved whilst the experiment was underway, causing smudging of the scan. This seems very likely to have been the case, since the specimens were seen to move during tests with an increased amplitude of loading.

Also, vibrations due to the cyclic loading machine could have caused the specimen to vibrate, again causing smudging of the scan.

The detector may not have been focused correctly on the specimen; the grips could have been interfering with the locus of the detector. Using a different type of grip could potentially circumvent this.

6.3.6 *Future Work*

Methods to improve the use of SPATE to investigate the stresses induced on teeth due to cyclic loading could include the following:

Find a new way of fixing the mounted tooth in the loading machine, or use a different loading machine with a different type of grip.

Try painting a tooth with black poster paint, to at least prove whether or not SPATE can detect signals from the tooth.

Increase the amplitude slightly, and try with 600 cycles per minute (10Hz).

6.4 *Strain Gauge Techniques*

A number of researchers have carried out studies using strain gauges to attempt to evaluate the strains experienced by teeth *in vitro*. One example of this type of study is presented in a paper by Medige *et al.* (1995). Attention has been paid to the loading mechanism in this study, but the strain gauges used are linear. A linear

arrangement of gauges is likely to be inaccurate, since it can only measure strains in one direction, and should only be used in the direction of the principal strain on one surface, and when the principal strain in the other direction is zero. If the direction of the principal strain is not known, rosette strain gauges should be used (Lee, 1992). It is unlikely that the strain in the other direction was zero in this case. The authors did use another linear strain gauge in the horizontal plane elsewhere on the tooth structure, and they do recognise that the strains measured by the gauges are only representative of the strain at that point, and cannot be extrapolated to predict failure in other parts of the tooth.

An alternative technique to strain gauge analysis is the use of Linear Variable Differential Transformers (LVDTs), as used by Hood (1985). Hood compared the performance of teeth restored with amalgam, gold onlays and with dentine bonding agents and composite resin restoratives. He found that dentine bonding agents and composite restorative materials returned values of deflection of the tooth close to those measured for the natural tooth. Gold onlays increased the resistance of the tooth to an applied load to greater than that of an unrestored tooth, whereas amalgam did not provide any more resistance to motion than an unrestored tooth with a cavity prepared in it.

Following on from this work, Reeh, Douglas and Messer (1989) used strain gauges to compare the relative deformation of teeth under physiological loads, and to compare the performance of different restorative techniques *in vitro*. Their results concurred with the findings of Hood (1985), but unfortunately, no quantitative data concerning the strains measured is presented. The authors point out that extrapolation from testing of this type to the clinical situation is unrealistic, but the test situation could have been modelled using FEA to verify part of the model.

Simulation of the work of Hood (1985) was used by Rees and Jacobsen (1995) to verify the material properties of their FEA model. They found that the most suitable values of E for dentine and enamel along the direction of the prisms were 15 GPa and 80 GPa respectively. Throughout this thesis, identical values of E were used (*i.e.* 15 GPa and 80 GPa), so it would seem reasonable to assume that at least these two materials have been adequately modelled.

Similarly, a relatively simple, edentulous 3-D model of the mandible was constructed in ANSYS, modelling the cortical and cancellous bone as two separate materials of varying thickness. Identical values to those used in the 2D simulation where appropriate. The model was constrained at the condyles (hinges), and loaded with a distributed, occlusal load, to represent the clenching loads investigated by Korioth and Hannam (1994). The results compared extremely well to those predicted by Korioth and Hannam (1994). Thus the assumptions made concerning geometry and material properties for bone would also appear to be reasonable and valid.

Furthermore, since the displacement of the tooth model D *(see Chapter 4)* compares favourably to that measured clinically by Jones *et al.* (1998) for the same magnitude of applied load, one could infer that the material properties of the PDL and bone have also been adequately modelled. Verification of the stresses predicted within the FEA model would be valuable, but such data does not seem to be readily available.

CHAPTER 7

The Influence of Different Restorative Materials in a V-Shaped Cavity

7.0 Introduction

In Chapter 4, the propriety of the boundary constraints and the material model of the PDL were established. This permits the effect of varying the Young's Modulus (E) of the restorative material in a v-shaped lesion upon the shear and interfacial stresses around the tooth restoration interface to be investigated in this chapter.

7.1 Materials and Methods

A type D model (*i.e.* one incorporating the enamel, dentine, PDL and supporting bone, as described in Chapter 3) of a mandibular canine tooth was created in ANSYS53. A v-shaped, non-carious lesion was simulated in the cervical third of the buccal surface of the tooth. The lesion extended just to the cervical margin of the tooth.

ANSYS53 was chosen as the most appropriate software for this piece of work since the previous study (Chapter 5) had shown that the stress distributions within the tooth were not significantly influenced by the FEA code used (although stresses elsewhere were affected). The advantages of ANSYS53 over the other software codes for this study were:

The simulation could reasonably be regarded as a static event, therefore solution with a dynamic solver was computationally expensive and inappropriate.

ANSYS53 has its own pre-processor, with versatile select logic, enabling properties to be selected and varied quickly and easily.

Solution could be performed, and results displayed in different co-ordinate systems.

Solution with ANSYS53 is on-line at the University of Sheffield (no queuing system is involved) and is therefore extremely rapid, facilitating the faster processing of results data.

The values of E of the restorative materials analysed were: 1 GPa, 5 GPa, 10 GPa, 15 GPa, 20 GPa, 50 GPa, and 80 GPa. The lower limit was chosen as 1 GPa to represent a generic, low stiffness restorative material. This is probably less stiff than

any tooth-coloured dental restorative currently used, but was chosen to investigate the idea that a low modulus restorative material would reduce the likelihood of the failure of a restoration. However, analysis of a low-modulus restorative material is particularly of interest in light of the recommendations to use a less stiff material for the restoration of cervical lesions (Grippo, 1992). The upper limit of 80 GPa is typical of a dental ceramic, and again is probably be much stiffer than any commercial restorative material currently used clinically. Extending the range of stiffnesses of the materials investigated is useful, since it exposes trends in the behaviour of the tooth-restoration system under different types of loading, and helps to establish sensible bounds for the values of E suitable for dental restorative materials. These models were all compared to an unrestored tooth, with anisotropic enamel.

The restorative materials represented in these analyses were divided into three groups as follows:

the *low modulus group* refers to the 1 GPa and 5 GPa restorative materials.

the *high modulus group* refers to the 50 GPa and 80 GPa restorative materials.

the *mid-range group* refers to the 10, 15 and 20 GPa restorative materials.

The model was analysed under three loading conditions shown in Fig. 7.0.1. These loads were chosen as being typical of the bite loads experienced by a canine tooth, and were:

100N vertical, occlusal compressive load on the incisal tip.

100N load perpendicular to the buccal surface of the enamel representing the case of a mandibular canine experiencing a functional load.

100N load perpendicular to the lingual surface of the enamel, representing the case of the maxillary canine experiencing a functional load.

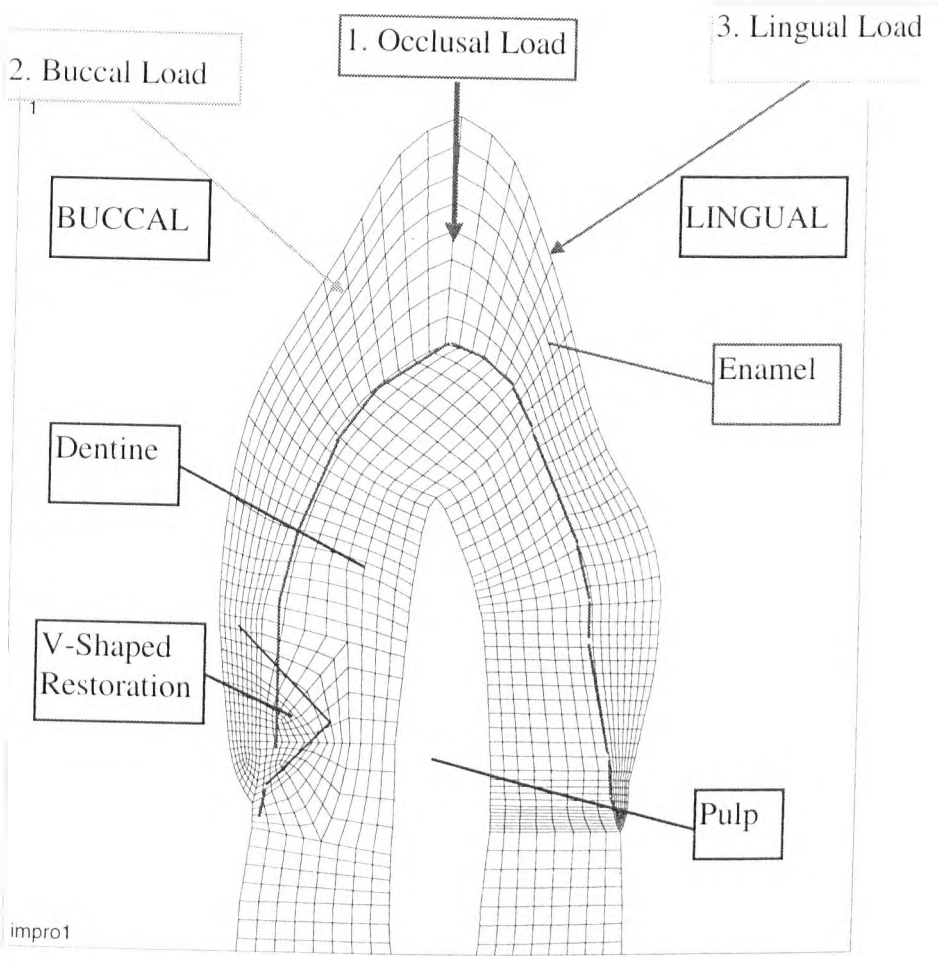

Fig. 7.1.1: Defining the materials and load cases used.

7.2 Calculation of the Interfacial Stresses

Fig. 7.2.1 defines the shear and interfacial stresses discussed in the subsequent sections of this chapter.

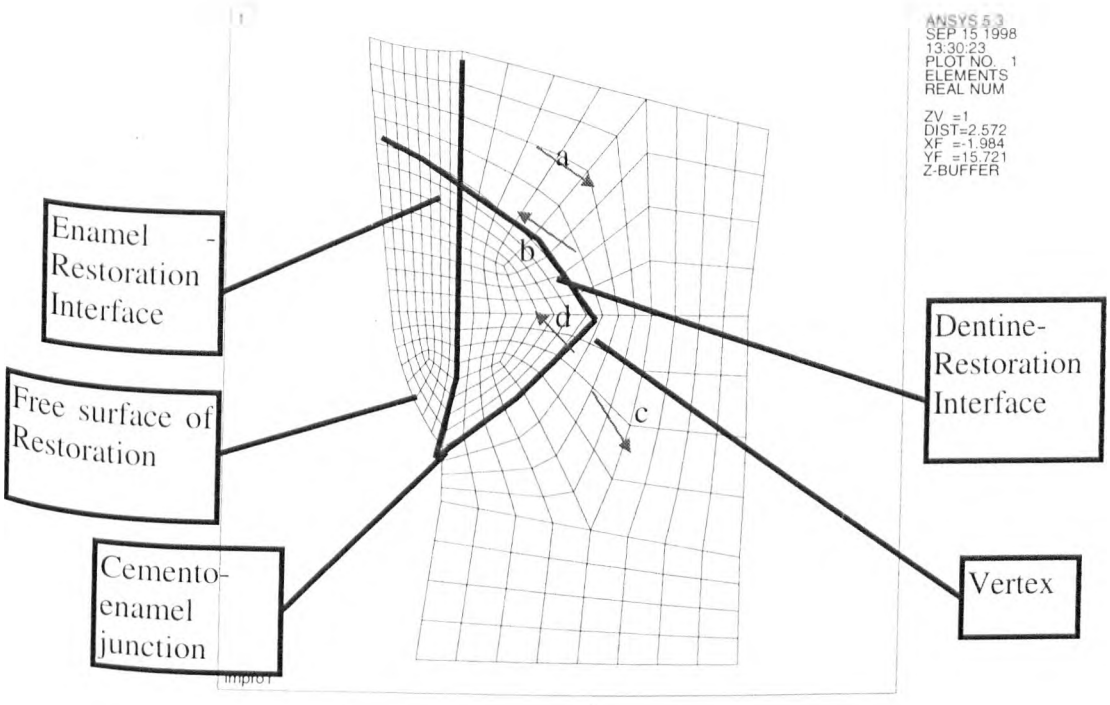

a = Positive Shear Stress

b = Negative shear stress

c = Positive interfacial stress

d = Negative interfacial stress

Fig. 7.2.1: Defining the stresses calculated and various features referenced in text.

ANSYS53 permits the use of an orthotropic, element co-ordinate system for certain element types. In this technique, the x-axis of the element co-ordinate system is set to being parallel to the i-j nodes of the element, as shown in Fig. 7.2.1. The y-

axis of the co-ordinate system is obviously perpendicular to the x-axis. This permits the stiffness in the x-direction of the element to differ from that in the y-direction. The anisotropy of the enamel was specified in this way, as described in Chapter 4.

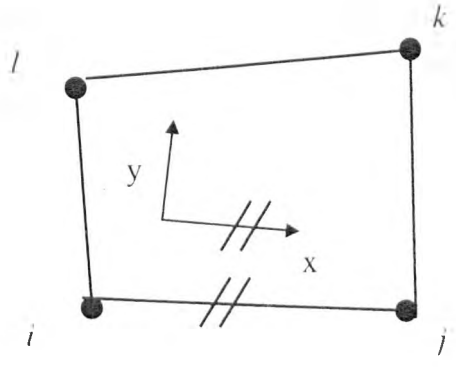

Fig. 7.2.1: Illustrating how the orthotropy is specified

Van Noort *et al.* (1988) evaluated the stresses predicted in a restored molar tooth using FEA techniques. This study was particularly concerned with the shear and interfacial stresses around a restoration, and they found that the interfacial stresses (*i.e.* the stresses perpendicular to the interface) were increased as the modulus of the restorative material was increased. Worryingly, they also found that the magnitudes of the interfacial and particularly the shear stresses predicted were in excess of the bond strengths of dental adhesives anticipated from laboratory tests. However, van Noort *et al.* (1988) examined the shear and interfacial stresses predicted by FEA with both materials selected. This can introduce errors into the estimation of the stress magnitudes.

The problem associated with evaluation of the shear and interfacial stresses using FEA techniques is that an FEA solver assumes perfect bonding between materials. That is, the materials cannot move relative to one another, regardless of the magnitude of the load applied to them. The stresses across the interface are therefore influenced by the surrounding materials. It is recommended in the ANSYS manuals that post-processing of results data where more than one material has been used, and contour displays are required, should be carried out with only one material selected at a time.

Some researchers (Peters and Poort (1983), Rees and Jacobsen, (1992)) have got around the perfect bonding problem by incorporating gap elements to their FEA simulations of restored teeth. Gap elements permit load to be transferred to a model in one direction only. These situations can be best visualised by thinking of a cable or a spar joining the two materials together.

A cable would permit tensile force to be transmitted from one material to the other across the interface (Fig. 7.2.2b), but if compression was applied to one of the materials, the cable would go slack, and no load would be transmitted (Fig.7.2.2c).

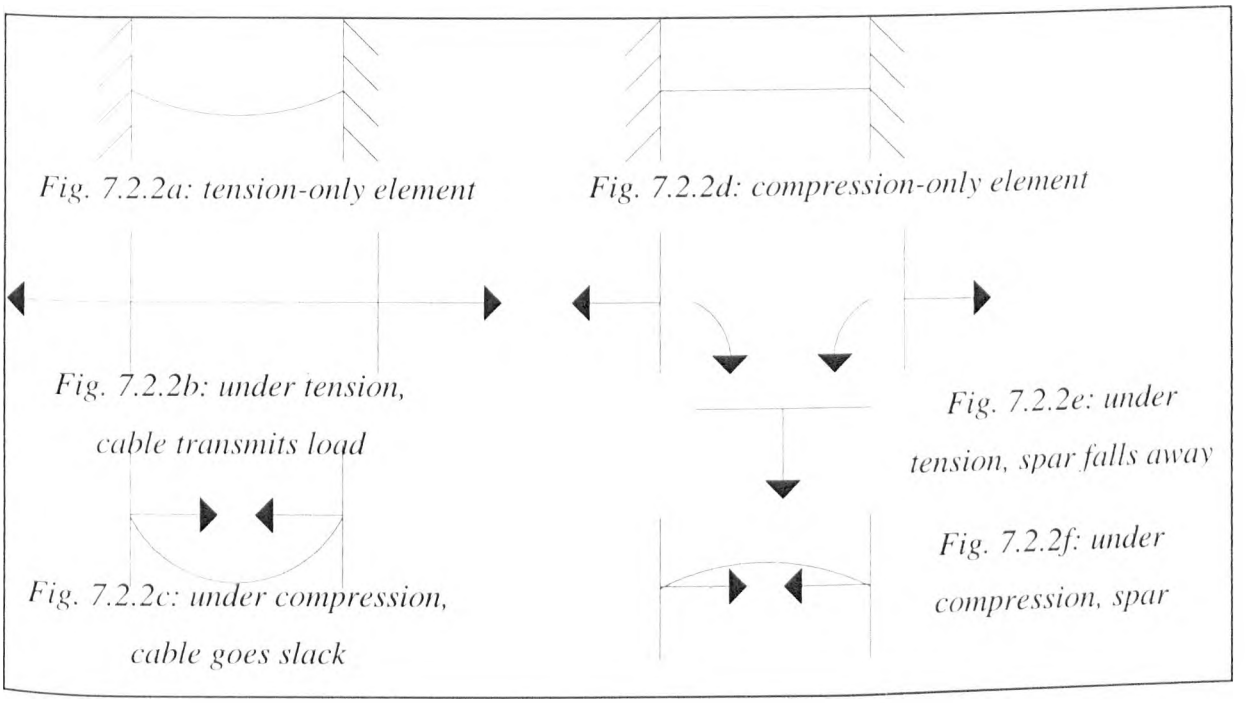

Fig. 7.2.2a: tension-only element

Fig. 7.2.2d: compression-only element

Fig. 7.2.2b: under tension, cable transmits load

Fig. 7.2.2e: under tension, spar falls away

Fig. 7.2.2c: under compression, cable goes slack

Fig. 7.2.2f: under compression, spar

A compression-only spar can be visualised as a spar wedged firmly between two surfaces, held in place by friction only. Slip is not permitted between the free surfaces and the spar. Hence, if a compressive load is applied to one of the materials, it will be transmitted to the other material. If tension is applied, however, the materials move apart, and so the spar drops out of place, transmitting no load; hence the materials move independently. This concept is illustrated in Fig. 7.2.2e.

A limiting value can also be imposed on gap elements, as used by Rees and Jacobsen, (1992) to represent the stresses across an interface due to polymerisation shrinkage. This value can effectively be thought of as the value at which the cable or the spar breaks; after this point, no more load can be transmitted from one material to the other.

Gap elements were not used in this analysis because it is only an initial analysis, to get a feel for the mechanics of the situation. Also, prescribing conditions such as tension only or compression only can be somewhat limiting; for example, this type of contact element does not permit a material to directly load another.

Using the cable analogy, if compression is applied to the material, and the materials move close enough together to induce contact, solver problems often result because the solver has not been told to expect this situation. Furthermore, the use of contact elements often means that the stress distributions cannot be analysed in the usual manner. So an analyst needs to have a clear understanding of what to expect before delving into the minefield of contact element analyses.

This analysis therefore was to gain an initial understanding of the stresses induced on the interface, while still looking at the global picture.

To obtain an initial, rough estimate of the shear and interfacial stresses that would be experienced by the tooth and restoration, the elements within the restoration were modified to posses this type of orthotropy. This meant that each element had its own co-ordinate system. However, the E in both the x- and the y-directions was identical, and hence there was no orthotropy for these materials, so, from this point of view, it did not matter which axis was which.

Ideally, the stress parallel to the interface (the shear stress) would be the x-stress in the element co-ordinate system, and the interfacial stress (the stress perpendicular to the interface) would be the y-stress in the element co-ordinate system.

If the elements are square, the y-axis would be parallel to the j-k nodes (see Fig. 7.2.1), but, since the geometry of a canine tooth is complex, it is not possible for all of the elements to be square. The tapering of the enamel in this region in the unrestored situation means that the i-j nodes are not always parallel to the tooth-restoration interface. Also, the three-sided shape of the restoration in cross-section makes it impossible to mesh without rotating the axes. In some circumstances, they are perpendicular to the interface, but inevitably, this means that for some elements, they are neither parallel nor perpendicular to the interface. However, the angle of rotation of the element co-ordinate system compared to the interface will be very small, since the elements are only small, and hence the approximation is reasonable.

The stresses at the nodes of an element are determined by interpolation from the stresses at the Gauss Points closest to this node, within the surrounding elements (see Fig. 7.2.3). If the co-ordinate system of one element is inverted in comparison to its neighbour, the x-stress within the element co-ordinate system of that element will have been calculated using the y-stress in one element co-ordinate system, and the x-stress in another.

The inherent drawback of this method is that the stresses obtained from the element co-ordinate system are calculated along axes which are not precisely aligned with the interface.

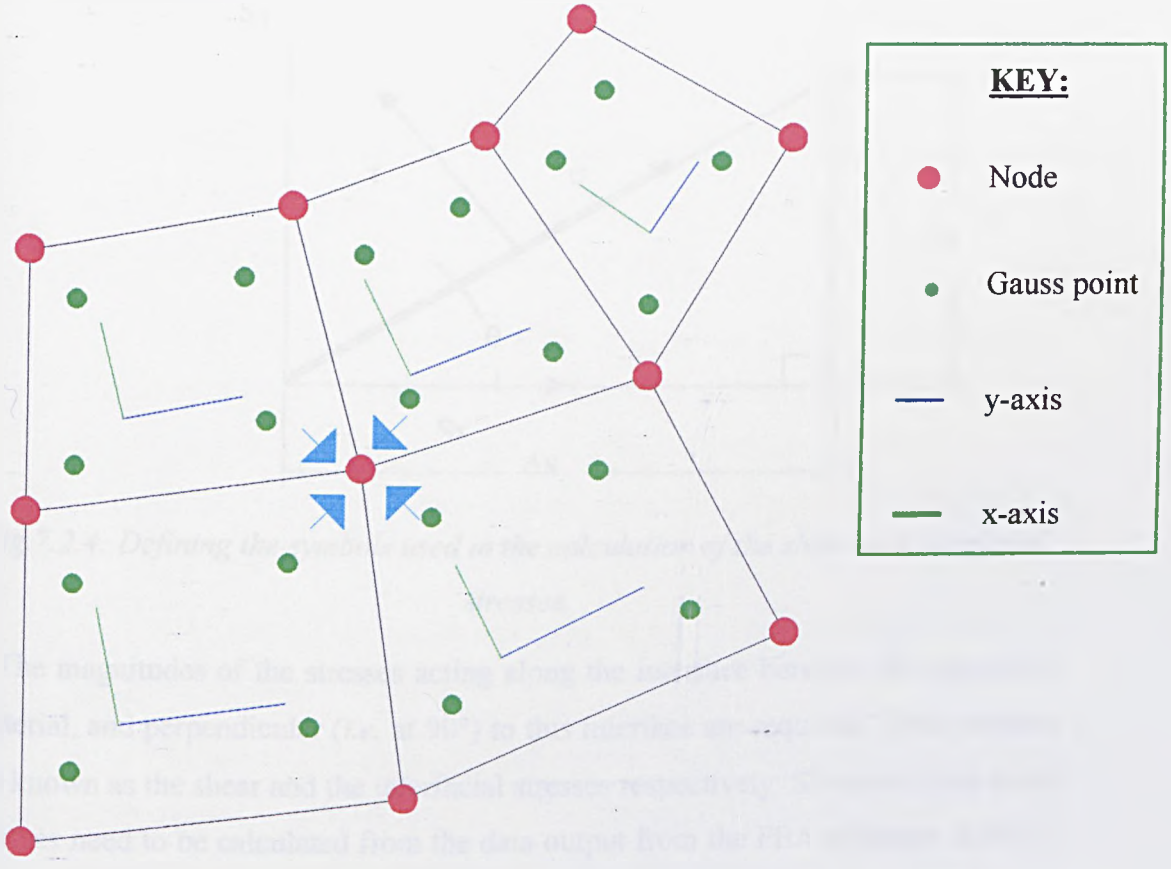

Fig. 7.2.3: Showing how an FEA solver typically evaluates the stresses in an anisotropic model.

This technique is suitable for obtaining an initial estimate of the shear and interfacial stresses, and maybe sufficiently accurate for regular geometries.

FEA codes have great difficulty dealing with a material interface; they try to average the stresses across the interface using all of the relevant material properties. Because of this, the value of *E* of the elements close to the material interface will be an amalgamation of both materials. This can therefore distort the effect that a large mismatch in material properties can have, and hence affect the shear and interfacial stress results predicted. To avoid this problem, the results were analysed for materials on either side of the interface separately.

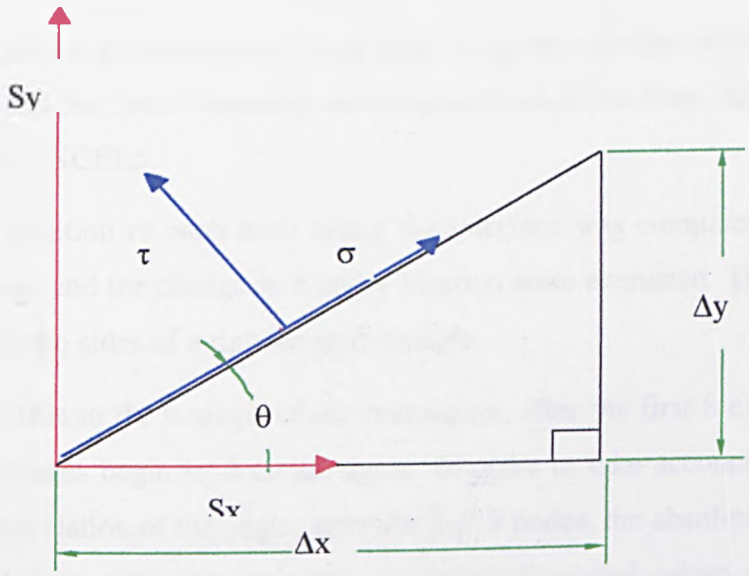

Fig.7.2.4: Defining the symbols used in the calculation of the shear and interfacial stresses.

The magnitudes of the stresses acting along the interface between the restorative material, and perpendicular (*i.e.* at 90°) to this interface are required. These stresses are known as the shear and the interfacial stresses respectively. Shear and interfacial stresses need to be calculated from the data output from the FEA software. ANSYS provides the direct stresses S_x and S_y, (see Fig. 7.2.4) and the shear stress S_{xy} at every node. The stress data is given in the global co-ordinate system. The shear stress (σ) and interfacial stress (τ) are related to the direct stresses by the angle θ (see Fig. 7.2.4).

Benham, Crawford and Armstrong (1996) define the equations to calculate the shear and interfacial stresses. The equations to determine the shear and interfacial stress in a 2-D stress system are given in Eqn.'s 7.2.1 and 7.2.2.

$$\tau = -\tfrac{1}{2}\left(S_x - S_y\right)\sin 2\theta + S_{xy}\cos 2\theta \qquad \textit{Eqn. 7.2.1}$$

$$\sigma = \tfrac{1}{2}\left(S_x + S_y\right) + \tfrac{1}{2}\left(S_x - S_y\right)\cos 2\theta + S_{xy}\sin 2\theta \qquad \textit{Eqn. 7.2.2}$$

Eqn.'s 7.2.1 and 7.2.2 are derived from the combination of the equations to determine the shear and interfacial stresses in an element subject to normal stresses and those in an element subject to shear stresses. Fig. 7.2.4 explains the symbols used. The reader is referred to this text for the full derivation of these relationships.

To improve upon the approximate method outlined previously, the following method was employed:

1. The global co-ordinates of each node along the interface between the restoration and the tooth structure were exported as a list from ANSYS53 and read into EXCEL5.

2. The position of each node along the interface was compared to the previous node, and the change in x and y location were evaluated. This gave the length of two sides of a right-angled triangle.

N.B. Due to the v-shape of the restoration, after the first 8 elements, the x co-ordinates begin to decrease again. In order to take account of this fact in the calculation of the angle, after the first 8 nodes, the absolute values of the x and y- co-ordinates was used, instead of the actual values used for the first 8 nodes.

3. The angle θ that the element edge along the interface made with these two sides was then evaluated.

4. In ANSYS53, the nodes and elements within the restoration adjacent to the interface were selected. A list of the global x- and y- stresses for these nodes were exported as a text file. This was read into EXCEL, where the data had to be sorted in to the order in which the nodes occurred along the interface.

This process was then repeated with the nodes and elements within the tooth and adjacent to the interface only selected.

7.3 Results

In this section, graphs of the shear and interfacial stresses around the restoration are presented, for the occlusal load (in Section 7.4), the buccal load (Section 7.5) and the lingual load (Section 7.6).

Section 7.7 presents the stress distributions within the tooth and the restoration for the various load cases and models considered here.

Fig.'s 7.4.1 to 7.4.4 shows graphs of the shear and interfacial stresses calculated from the FEA models as described in section 7.2. The graphs show the results for the models containing restorations of value E = 1 GPa, 15 GPa, and 80 GPa, since these models represent the extremes of the situation, and the average.

7.4 Occlusal Loading

The following figures present graphs of the shear and interfacial stresses within the tooth and the restoration for a model of type D subject to an occlusal load of 100N.

Graphs of shear stress in the restoration are shown in Fig. 7.4.1.

Graphs of interfacial stress in the restoration are shown in Fig. 7.4.2.

Graphs of shear stress in the tooth are shown in Fig. 7.4.3.

Graphs of interfacial stress in the tooth are shown in Fig. 7.4.4.

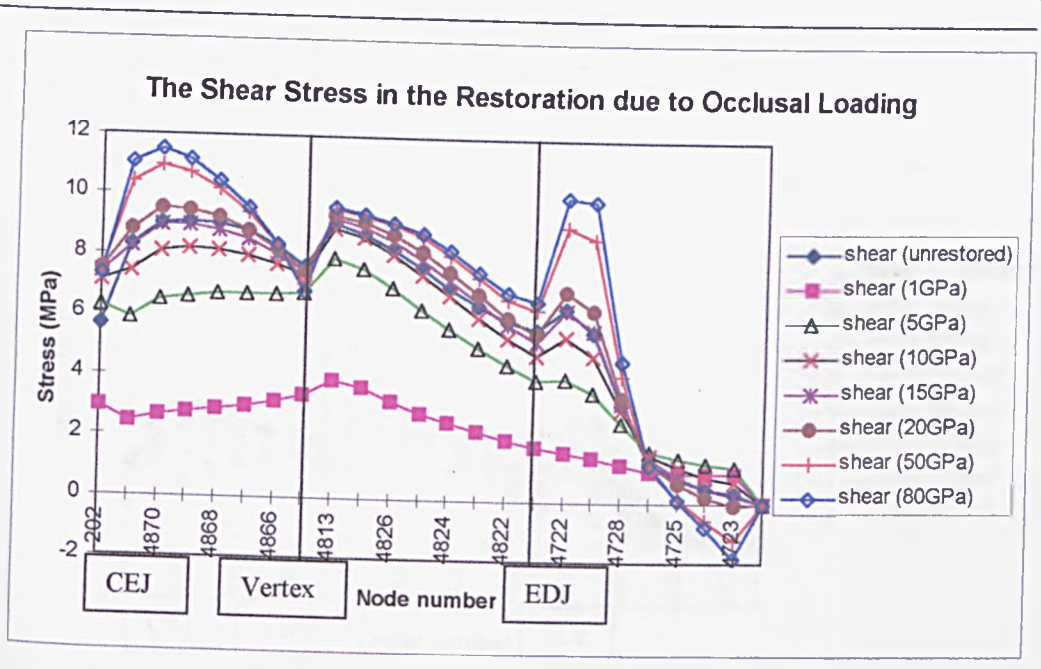

Fig. 7.4.1: The shear stresses in the restoration due to occlusal loading

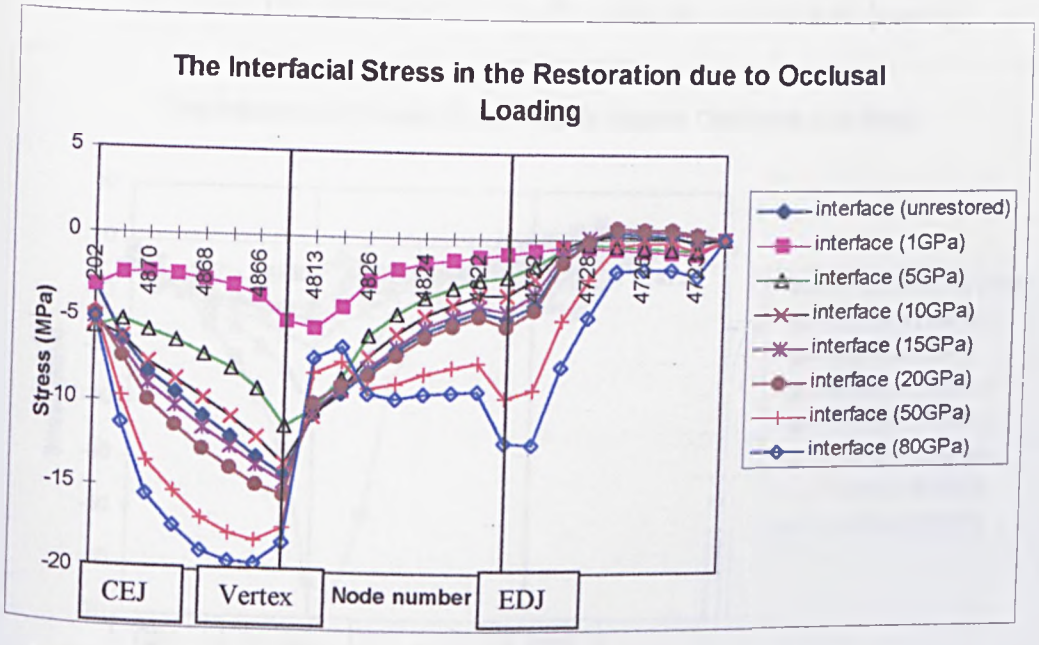

Fig. 7.4.2: The interfacial stresses in the restoration due to occlusal loading

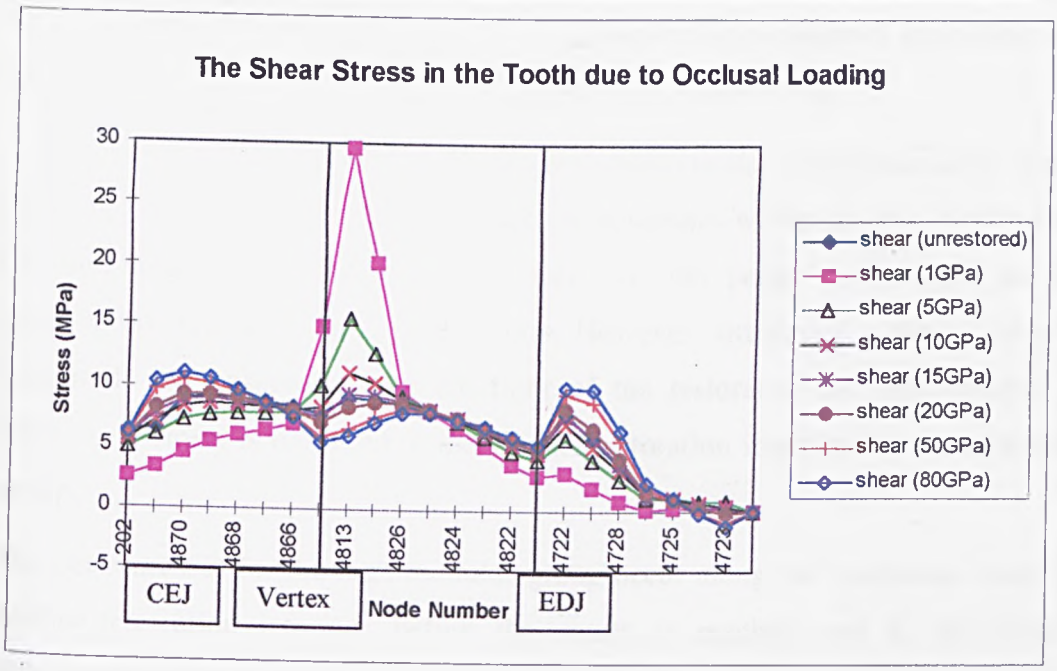

Fig. 7.4.3: The shear stresses in the tooth due to occlusal loading

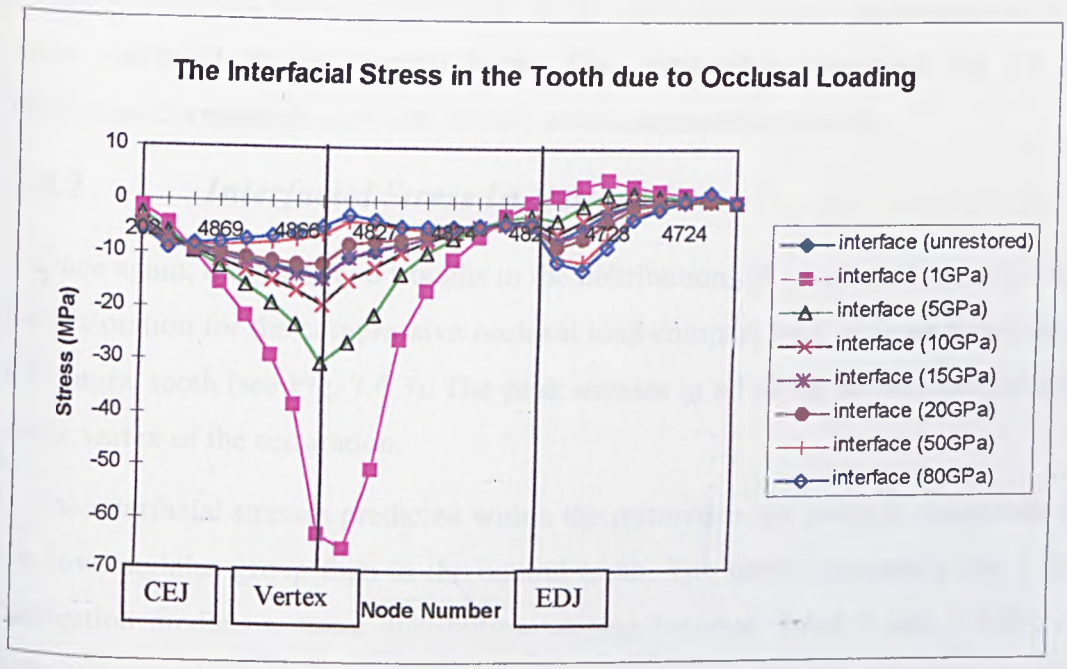

Fig. 7.4.4: The interfacial stresses in the tooth due to occlusal loading.

In the following presentation of the results, section 7.4.1 refers to Fig. 7.4.1, etc.

7.4.1 Shear Stress in Restoration

Generally, the distribution of shear stresses along the interface of the restored teeth subjected to an applied occlusal load compares well to that of the natural tooth *(see Fig. 7.4.1)*. The model containing the 1GPa restoration is notable in that the stress predicted within the restoration is markedly lower than that predicted by all

the other models. The stress in the 1 GPa restoration lies between 0 and 4 MPa; less than that predicted in the natural tooth by between 3 and 5 MPa.

The stress predicted within the 5 GPa restoration is also lower than in the natural tooth, but only by 2 - 3 MPa. The peak shear stresses within the low modulus and the mid-range group occur at the vertex, but the peaks and troughs are less pronounced than in the mid-range group. However, stresses of a similar order of magnitude are observed along the floor of the restoration for both groups. An increase in stress is observed at the enamel-restoration interface for the mid-range group.

The peak stresses for the high modulus group occur along the restoration floor; the dentine-restoration interface before the vertex is reached, and at the enamel-restoration interface.

The stresses and stress distributions for the mid-range group correspond closely to those predicted by the natural tooth. The restoration containing the 15 GPa restoration corresponds the most closely to the unrestored situation.

7.4.2 *Interfacial Stress In Restoration*

Once again, the peaks and troughs in the distributions of interfacial stresses within the restoration for the compressive occlusal load compare well to those predicted by the natural tooth (see Fig. 7.4.3). The peak stresses in all of the models are predicted at the vertex of the restoration.

The interfacial stresses predicted within the restoration are lower in magnitude for the low modulus group than in the natural tooth. The model containing the 1 GPa restoration predicts a stress distribution varying between about 0 and 5 MPa; *i.e.* between 5 and 10 MPa less than the stress distribution predicted by the natural tooth. This means that very little stress is expected in the 1 GPa model. The stress magnitudes and distributions for the model containing the 5 GPa restoration are similar to those of the mid-range group and the natural tooth. The stress magnitudes differ from those predicted by the natural tooth by approximately 2 - 3 MPa along the floor of the restoration, and 1 - 2 MPa after the vertex; before the enamel-dentine interface.

The mid-range group predict similar magnitudes and distributions of stress to those predicted by the natural tooth.

The magnitudes of the stresses predicted by the high modulus group are generally greater than those predicted by the natural tooth; of the order of 5 - 7 MPa greater along the restoration floor, and about the same around the enamel-dentine interface.

7.4.3 Shear Stress in Tooth

Generally, the distributions of the stresses for the restored teeth compare very closely to those of the natural tooth. Differences between the restored and natural models are more pronounced for the low and high modulus groups. The results deviate the most along the dentine-restoration interface, on the incisal side (after the vertex), and along the enamel-restoration interface. The stresses for all of the models are lowest along the enamel-restoration interface, towards the free edge of the restoration.

The greatest shear stresses within the tooth are observed in the low modulus group. However, the stresses along the floor of the restoration and along the enamel-restoration interface are the lowest in the 1 GPa model. The peak stresses in the low modulus group occur at the vertex. The stresses in the natural tooth do still exhibit a small peak at the vertex, but are of roughly the same magnitude along the restoration floor, and at the enamel-dentine interface. Away from the nodes around the vertex of the restoration, there is generally little difference between the stresses predicted by all of the models; the stresses along the floor of the restoration differ from those predicted by the natural tooth by around ± 2 MPa, and by about ± 4 - 5 MPa along the enamel-restoration interface. However, at the vertex, the stresses in the tooth of the model containing the 1 GPa restoration are approximately 22 MPa higher than in the natural tooth, and about 7 MPa greater in the tooth containing the 5 GPa restoration.

The stresses in the mid-range group correspond closely with those predicted by the natural tooth. The high modulus group also predict similar stresses to these, but the magnitudes are marginally higher along the restoration floor (of the order of 1 - 2 MPa) and at the enamel-dentine interface (about 2 MPa higher).

The stresses in the high modulus group are lower than those predicted by the natural tooth at the nodes around the vertex.

7.4.4 *Interfacial Stress in the Tooth*

The major differences between the natural and restored models again occur at the vertex, and the nodes immediately following this point, on the incisal surface of the dentine-restoration interface, and along the enamel-restoration interface.

The peak stresses in the low modulus group are at the vertex, but all of the restored models predict significantly higher stresses in the dentine than occurs in the natural tooth. The stresses in the 1 GPa model are approximately -10 to -50 MPa greater than in the natural tooth. The peak stresses are about -70 MPa for the 1 GPa model, and -30 MPa for the 5 GPa model, as opposed to about -15 MPa in the natural tooth. The stresses in the low modulus group become tensile along the enamel-restoration interface; they remain compressive in all of the other models.

The mid-range group have stress distributions that correspond closely with the distribution of stresses predicted by the natural tooth.

The distributions of stresses predicted by the high modulus group are very close in magnitude to one another. Less stress is predicted in the dentine for the high modulus group; the stresses are of the order of 2 to 5 MPa less than those predicted by the natural tooth. The stresses along the enamel-restoration interface are slightly greater in the high modulus group than in the natural tooth; of the order of -2 to -4 MPa greater in the high modulus group.

Overall, the stresses in the restoration are greatest in the high modulus group. The stresses in the 1 GPa restoration are significantly lower than the stresses predicted by any other model.

The stresses predicted in the tooth are significantly higher in the low modulus group than any of the others. The shear and interfacial stresses within the tooth are much greater than in the restoration for the model containing the 1 GPa restoration.

7.5 Stress Due to Buccal Loading

Graphs of shear stress in the restoration are shown in Fig. 7.5.1.

Graphs of interfacial stress in the restoration are shown in Fig. 7.5.2.

Graphs of shear stress in the tooth are shown in Fig. 7.5.3.

Graphs of interfacial stress in the tooth are shown in Fig. 7.5.4.

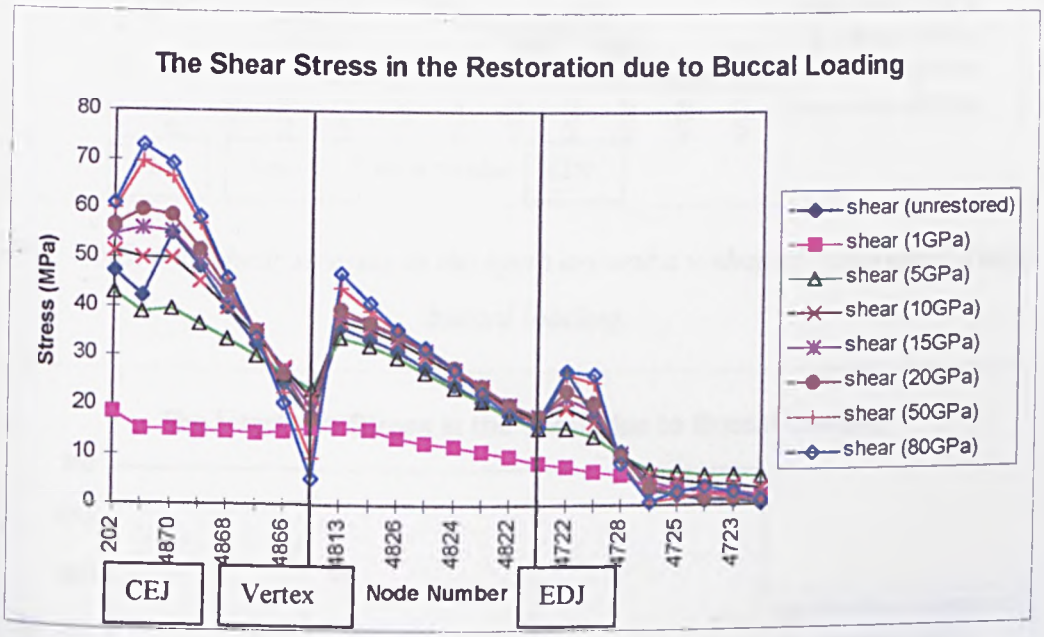

Fig. 7.5.1: The shear stresses in a v-shaped restoration due to buccal loading.

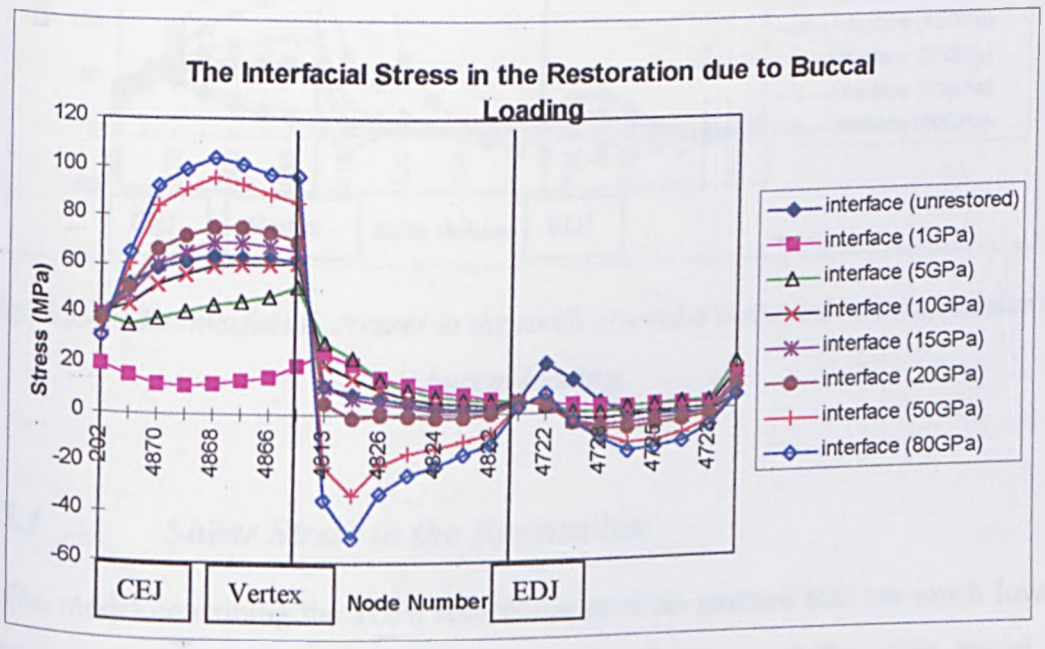

Fig. 7.5.2: The interfacial stresses in a v-shaped restoration due to buccal loading.

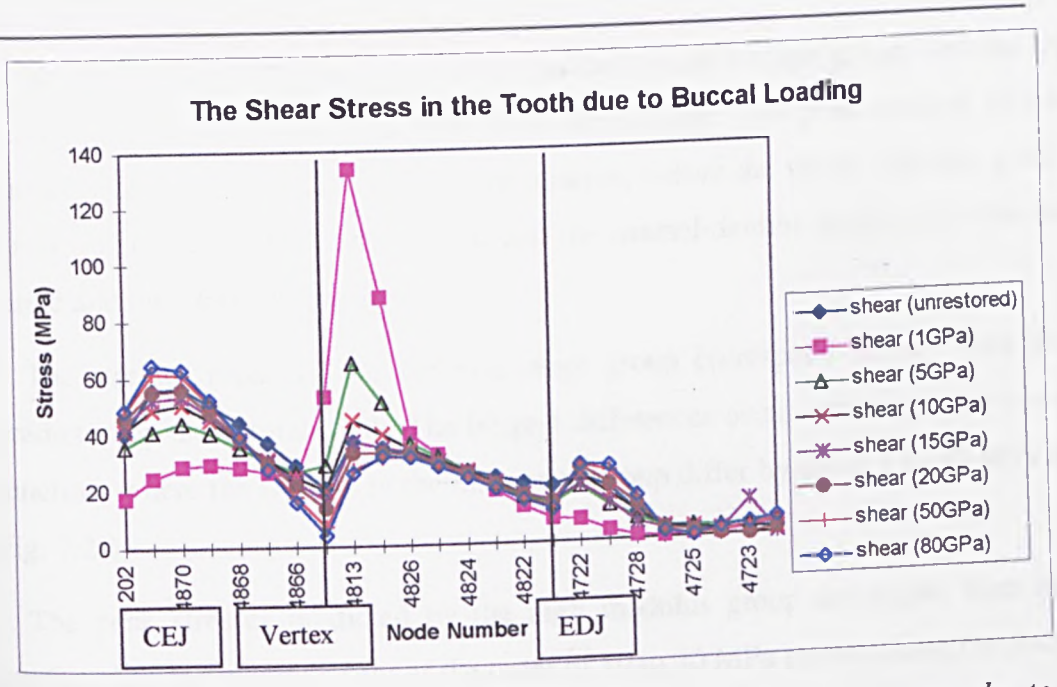

Fig. 7.5.3: The shear stresses in the tooth around a v-shaped restoration due to buccal loading.

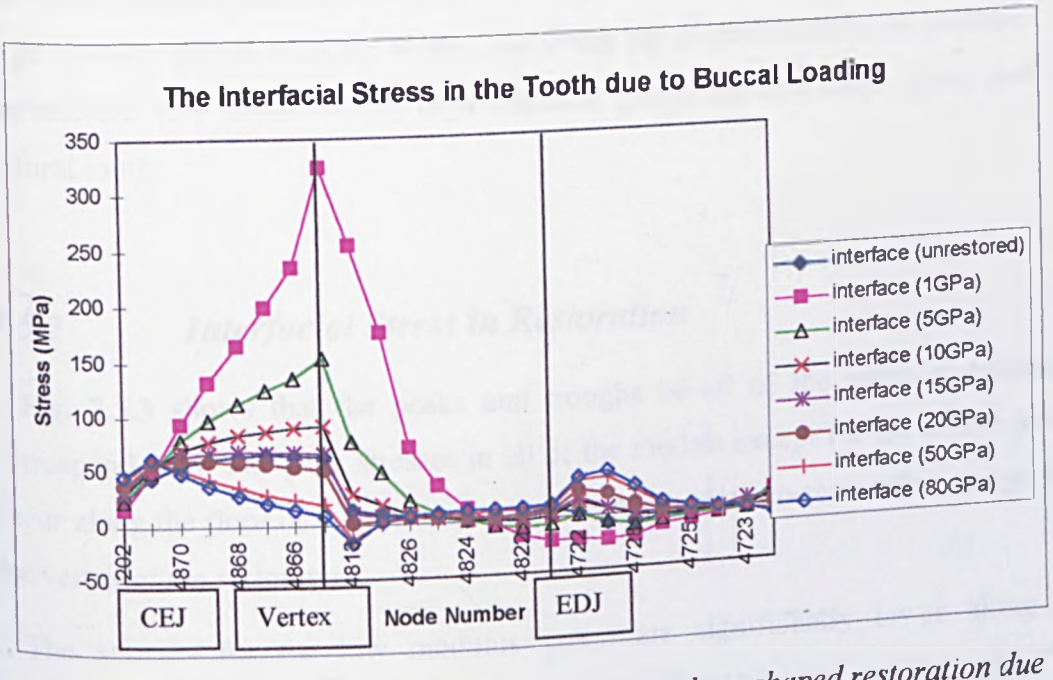

Fig. 7.5.4: The interfacial stresses in the tooth around a v-shaped restoration due to buccal loading.

7.5.1 *Shear Stress in the Restoration*

The model containing the 1GPa restoration predicts stresses that are much lower than in all of the other models. The distribution of stresses in the 1GPa model is much flatter than that observed in any of the other distributions.

The stress distributions for the 5 GPa model, the mid-range group, and the high modulus group all correspond well with one another. The peak stresses in these models occurs along the floor of the restoration, before the vertex. Another peak in stress magnitude occurs at the vertex, and the enamel-dentine interface for the mid-range and high modulus groups.

The stresses predicted for the mid-range group correspond closely with those predicted by the natural tooth. The biggest differences occur at the cemento-enamel junction, where the stresses in the mid-range group differ by about 5 to 10 MPa (see Fig. 7.2.1).

The peak stresses predicted by the high modulus group are higher than those predicted by the natural tooth; of the order of 10 to 30 MPa greater along the floor of the restoration, and 5 - 10 MPa greater at the vertex and the enamel-dentine interface. The stresses just before the vertex of the restoration are lowest of all in the high modulus group. After the vertex, and along the enamel-restoration interface, the stresses are very similar in the high modulus group, the mid-range group and the natural tooth.

7.5.2 *Interfacial Stress in Restoration*

Fig. 7.5.3 shows that the peaks and troughs of all of the stress distributions correspond well. The peak stresses in all of the models except for the 1 GPa model occur along the floor of the restoration, between the cemento-restoration margin and the vertex of the restoration.

The stresses for the low modulus group are significantly lower along the restoration floor (until the vertex) than those predicted by the natural tooth. The stresses predicted by the 1 GPa model are of the order of 15 to 20 MPa for the 1 GPa model, and 40 to 50 MPa for the 5 GPa model along the floor of the restoration. This compares to 40 - 60 MPa in the natural tooth. Similarly, the predicted stress in the high modulus group in this region lies between 40 and 100 MPa; this is significantly greater than that predicted by the natural tooth model.

At the vertex, the interfacial stress in the restoration drops down to about 10 MPa in the natural tooth. The stresses in the low modulus group are a little higher; of the

order of 20 MPa. The stresses predicted for the mid-range group, the low modulus group and the natural tooth tend towards zero after the vertex, towards the enamel-dentine interface. In the high modulus group, the interfacial stresses from the vertex towards the enamel-restoration interface are compressive; between 0 and -40 MPa for the 50 GPa model, and between 0 and -60 MPa for the 80 GPa model. The stresses along the enamel-restoration interface are close to zero in all of the models. The largest stresses are predicted in the high modulus groups; up to about -10 to -15 MPa.

The stresses at the enamel-restoration interface are all lower than those predicted in the natural tooth.

7.5.3 *Shear Stress in Tooth*

The distributions of shear stress within the tooth are similar for all of the models. The highest stress occurs in the model containing the 1 GPa restoration, at the vertex. The peak stress predicted by the 1 GPa model is about 140 MPa, as compared to a peak of about 40 MPa at the vertex of the natural tooth.

The low modulus group predict lower stresses than the natural tooth along the floor of the restoration, with a peak around the vertex of the restoration. The stresses at the enamel-restoration interface are lower again in the 1 GPa model. The 5 GPa model predicts stresses of a similar order of magnitude to those of the mid-range group, and the natural tooth.

The stresses predicted by the mid-range group correspond closely in both magnitude and distribution to those predicted by the natural tooth.

The stresses predicted by the high modulus group are slightly higher than those experienced by the natural tooth; roughly between 0 and 4 MPa greater along the first few nodes of the floor of the restoration, but falling away to being less than all of the other models towards the vertex. The stress only increases above the level predicted by the natural tooth at the enamel-dentine interface.

7.5.4 *Interfacial Stress in the Tooth*

The peak interfacial stresses for the low modulus group occurs at the vertex. The predicted peak stresses at the vertex are significantly higher in the low modulus group than those predicted by any other models and the natural tooth. The peak stress at the vertex of the natural tooth is approximately 50 - 60 MPa; as compared to about 150 MPa in the 5 GPa model, and about 330 MPa in the 1 GPa model. The stresses in the low modulus group are significantly higher along the dentine-restoration interface

7.6. Lingual Loading

Graphs of shear stress in the restoration are shown in Fig. 7.6.1.

Graphs of interfacial stress in the restoration are shown in Fig. 7.6.2.

Graphs of shear stress in the tooth are shown in Fig. 7.6.3.

Graphs of interfacial stress in the tooth are shown in Fig. 7.6.4.

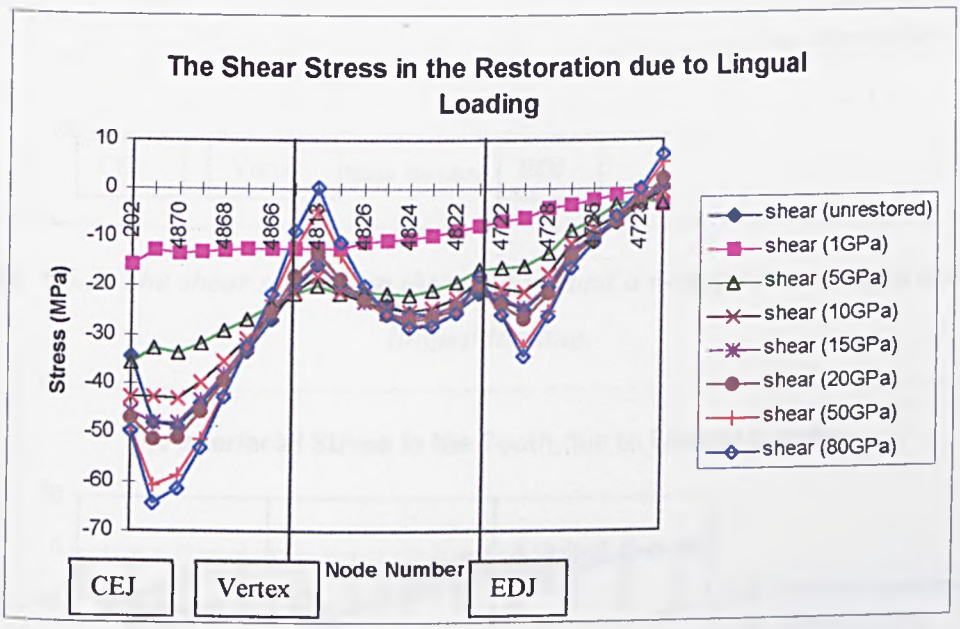

Fig. 7.6.1: The shear stresses in the v-shaped restoration due to lingual loading.

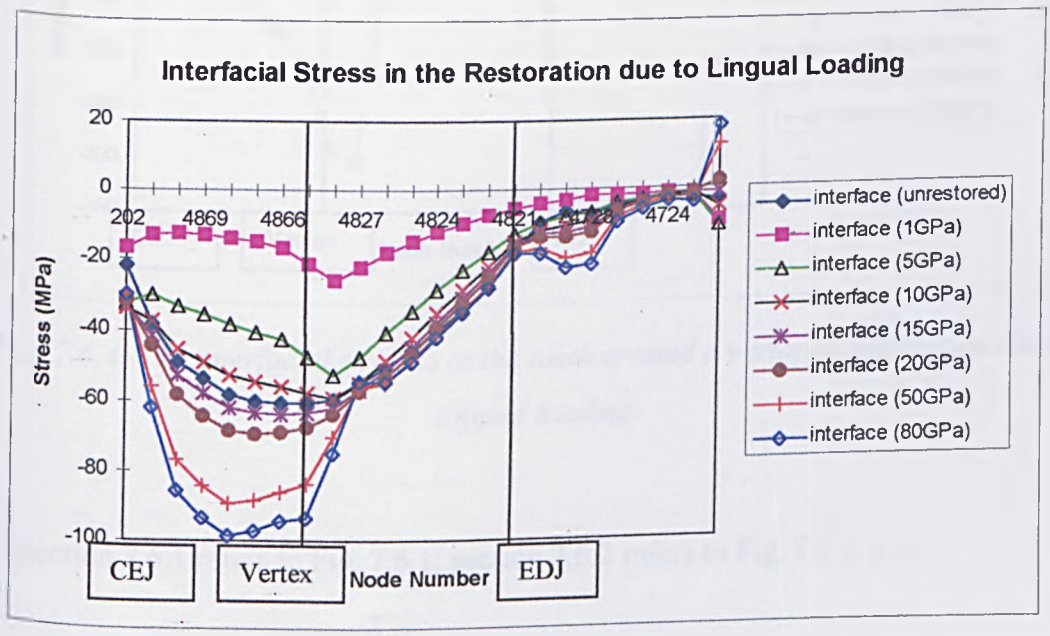

Fig. 7.6.2: The interfacial stresses in the v-shaped restoration due to lingual loading.

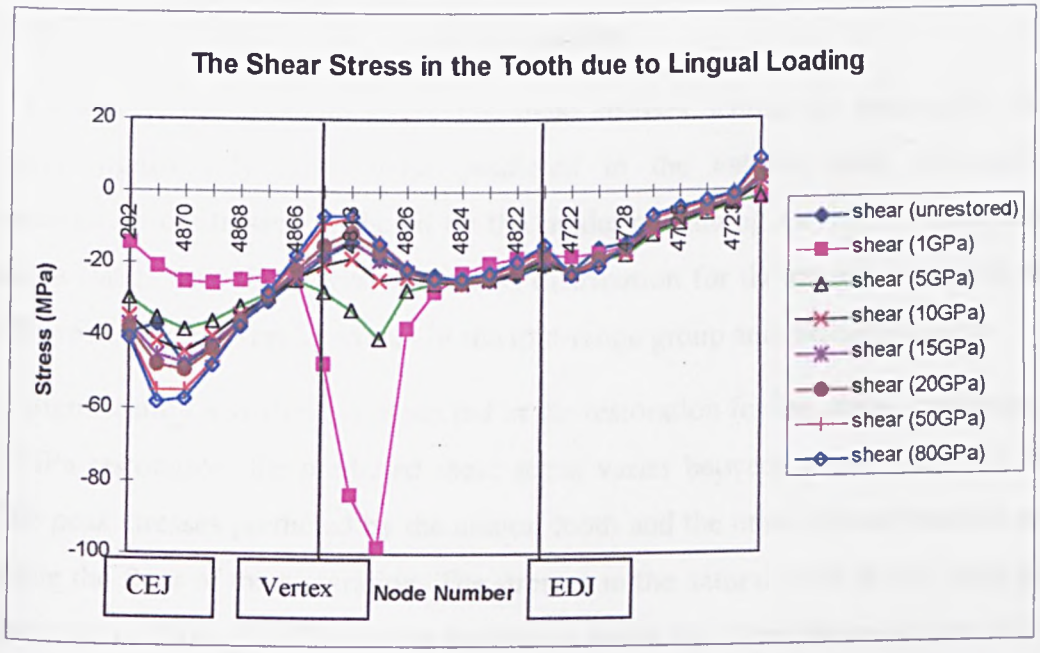

Fig. 7.6.3: The shear stresses in the tooth around a v-shaped restoration due to lingual loading.

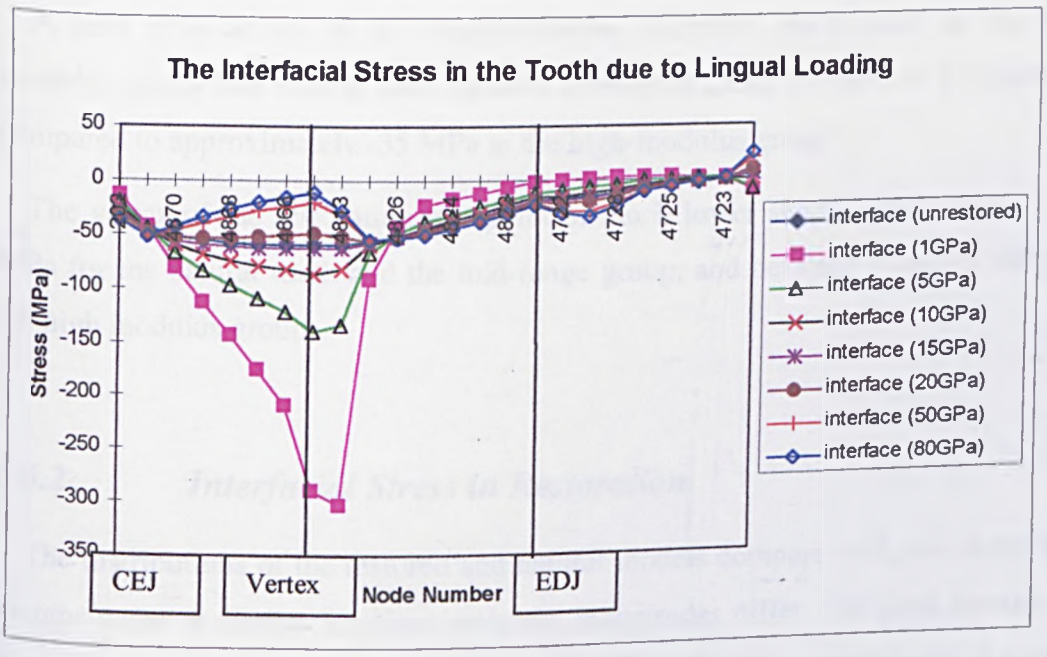

Fig. 7.6.4: The interfacial stresses in the tooth around a v-shaped restoration due to lingual loading.

Section 7.6.1 refers to Fig. 7.6.1; section 7.6.2 refers to Fig. 7.6.2, *etc.*

7.6.1 *Shear Stress in Restoration*

Generally, the distributions of the shear stresses within the restoration do not differ significantly from those predicted in the natural tooth, although the distribution of stresses predicted by the model containing the 1 GPa restoration is much flatter than the others. The stress distribution for the model containing the 5 GPa restoration is similar to that of the mid-range group and the natural tooth.

Significantly less stress is predicted in the restoration for the model containing the 1 GPa restoration; the predicted shear stress varies between about 0 and -15 MPa. The peak stresses predicted by the natural tooth and the other restored models occur along the floor of the restoration. The stresses in the natural tooth at this point are of the order of about -50 MPa; in the mid-range group they vary between about -42 and -50 MPa, whilst the high modulus group predicts stresses of the order of -60 to -65 MPa.

A peak also occurs at the enamel-dentine interface, particularly in the high modulus group. The natural tooth predicts stresses of about -27 MPa at this point, as compared to approximately -35 MPa in the high-modulus group.

The vertex of the restoration is a point of much lower stress; approximately -10 MPa for the natural tooth and the mid-range group, and between 0 and -5 MPa for the high modulus group.

7.6.2 *Interfacial Stress in Restoration*

The distributions of the restored and natural models compare well; the peaks and troughs occur at similar locations, only the magnitudes differ. The peak stresses in the low modulus group occur at the vertex, whereas for the natural tooth, the mid-range and the high modulus groups, the peak stresses occur along the cervical floor of the restoration.

Less stress is predicted in the model containing the 1 GPa restoration, and the distribution of interfacial stresses within this model is very flat. The peak stresses at the vertex are of the order of -20 MPa, as opposed to approximately -60 MPa at this point in the natural tooth. The high modulus group predicts interfacial stresses of about -70 MPa at this point.

After the vertex, the magnitudes of the stresses along the coronal side of the dentine-restoration interface are very similar in all models. At the enamel-restoration interface, the high modulus group predicts a small increase in the interfacial stress (about -20 MPa as opposed to -10 MPa for the natural tooth), but the magnitudes of the stresses predicted are similar for all of the models towards the free surface of the enamel-restoration interface.

The stresses predicted by the mid-range group compare well to those predicted for the natural tooth.

The stresses along the floor of the restoration are greatest in the high modulus group; of the order of -100 MPa, as compared to about -60 MPa in the natural tooth.

7.6.3 *Shear Stress in the Tooth*

The distribution of shear stresses within the tooth are similar for the natural tooth and all of the restored models. After the vertex, the magnitudes of the stresses predicted quickly converge to very similar values for all of the models analysed. However, the magnitudes of the stresses predicted by the 1 GPa model are significantly greater around the vertex than for any of the other models.

The stresses in the 1 GPa model are greatest around the vertex of the restoration; significantly higher than the peak stresses predicted by the natural tooth, or any of the other restored models. The stresses predicted by the 1 GPa model at the vertex are approximately -100 MPa, whereas the stresses at this point in the natural tooth are approximately -10 MPa. Peak stresses of roughly equal magnitude (approximately -40 MPa) occur in the 5 GPa model along the floor of the restoration and at the vertex.

The peak stresses for the mid-range and high modulus groups, and for the natural tooth occur along the floor of the restoration. However, the stresses predicted by the 1 GPa model are significantly lower in this region (of the order of -15 to -25 MPa as opposed to -40 to -50 MPa in the natural tooth). The magnitudes of the stresses predicted at the vertex for the mid-range and high modulus groups, and for the natural tooth are very small; of the order of -10 to -20 MPa. The stresses for the high modulus groups are greatest near to the cemento-enamel interface; greater than the

stresses predicted by all of the other models (about -60 MPa compared to -40 MPa for the natural tooth). The stresses predicted by the high modulus groups at the vertex are less than those predicted by all of the other models (-10 MPa as compared to approximately -20 MPa for the natural tooth).

7.6.4 *Interfacial Stress in Tooth*

The greatest stresses are predicted by the 1 GPa model. For the low modulus group, the peak stresses occur at the vertex. The low modulus group also predicts significantly higher stress along the floor of the restoration than is predicted in the natural tooth, and in all of the other models. The interfacial stresses in the tooth are of the order of -300 MPa at the vertex for the 1 GPa model, and -150 MPa for the 5 GPa model. Stresses at the vertex in the natural tooth are approximately -50 MPa.

The stresses predicted by the mid-range group are very similar in magnitude and distribution to those predicted by the natural tooth. After the vertex, the stresses predicted by the 1 GPa model are the lowest, but all of the models predict a very similar distribution of stresses along the coronal side of the dentine-restoration interface, and along the enamel-restoration interface.

The stresses at the vertex of the restoration are lowest in the high modulus group; of the order of between 0 and -50 MPa. The high modulus group also predict a small increase in stress at the enamel-restoration interface; of the order of about -10 MPa.

7.7 Stress Distributions within the tooth

Section 7.7 presents the stress distributions in the vicinity of the restoration for the natural and restored models.

7.7.1 *Occlusal Load*

Fig. 7.7.1 shows the patterns of direct stress in the global x and y directions for the portion of the tooth within the vicinity of the restoration, resulting from a vertical load of 100N applied on the incisal tip.

Considering firstly the plots of global y-stress in Fig.'s 7.7.1a to 7.7.1h subject to occlusal loading, a general increase in the magnitudes of both the tensile and the compressive stress can be observed with increasing value of E of the restorative material. For the models restored with the 1GPa and 5GPa materials, very little stress (both x and y-stress) occurs within the restoration. The maximum compressive stress occurs within the tooth, at the vertex of the v-shaped restoration. Since the shape of the restoration is similar to that of a notch-defect, this point has a stress concentrating effect, and it is possible that further failure of the tooth substance might be initiated at that point. It is very interesting to observe that, for the high modulus group, the x-stress at the vertex in the tooth is actually tensile, although the magnitude of the stress is much lower. For the teeth restored with the mid-range group of materials, the stress at this vertex within the tooth is close to zero.

Very little tensile stress is predicted to occur for the low modulus group. Most of the tensile stress is x-stress, and occurs within the tooth. Higher values of tensile y-stress occur in the enamel for the high modulus group, extending from the top third of the restoration into the enamel above.

An area of compressive stress exists directly beneath the restoration, at the dentine-restoration interface. Again, this increases in magnitude with the increasing E of the restorative material.

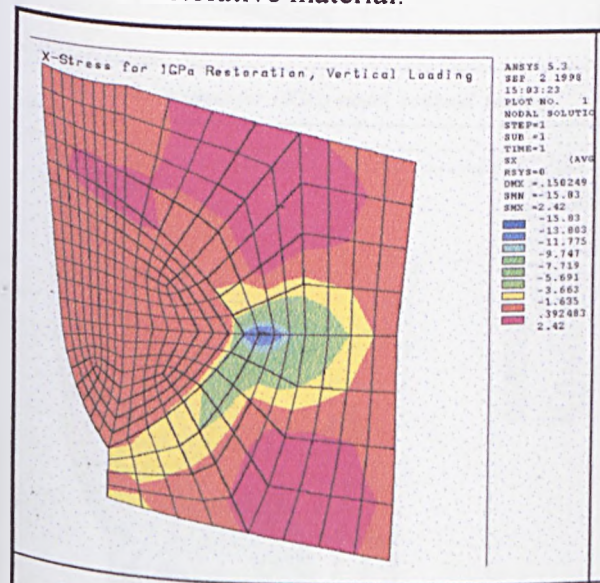

Fig. 7.7.1a: x-stress for 1GPa model, occlusal loading.

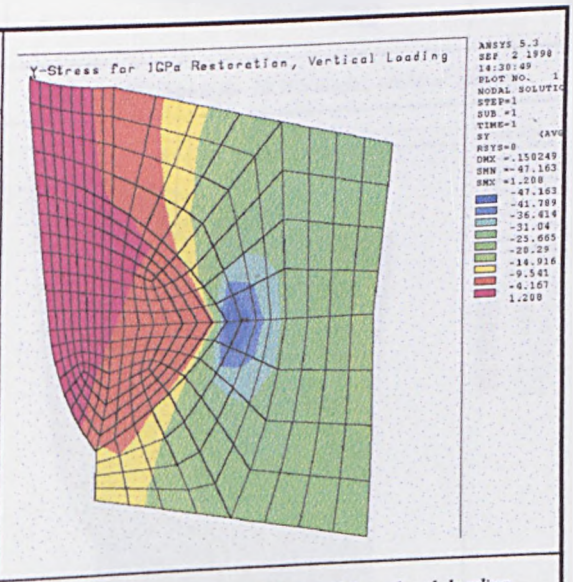

Fig. 7.7.1b: y-stress for 1GPa model, occlusal loading.

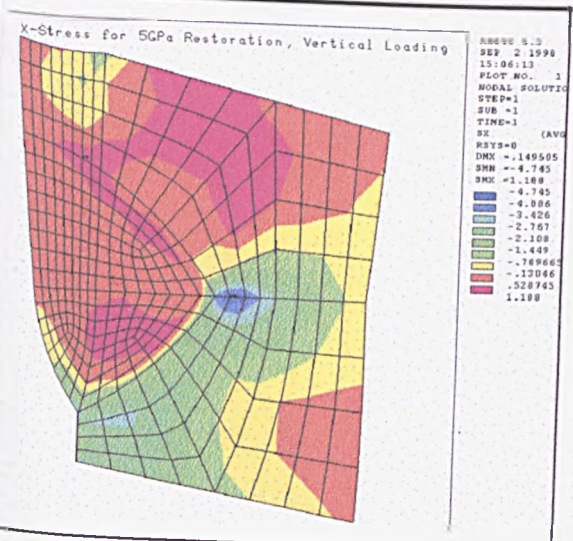

Fig. 7.7.1c: x-stress for 5GPa model, occlusal loading.

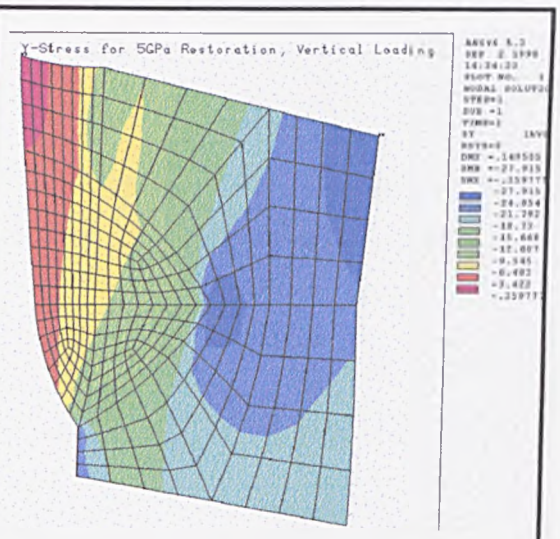

Fig. 7.7.1d: y-stress for 5GPa model, occlusal loading

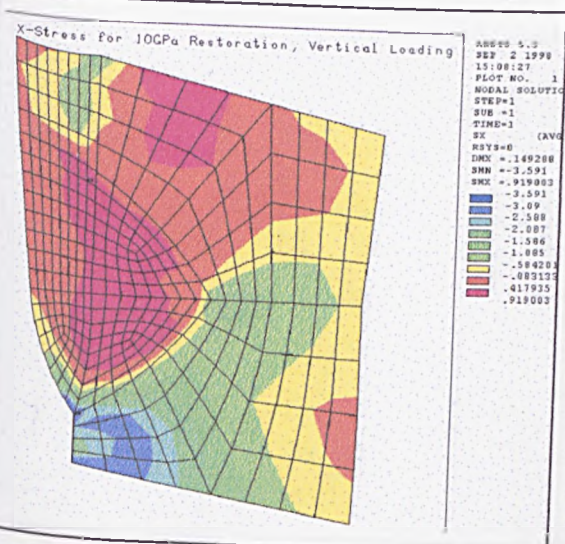

Fig. 7.7.1e: x-stress for 10GPa model, occlusal loading.

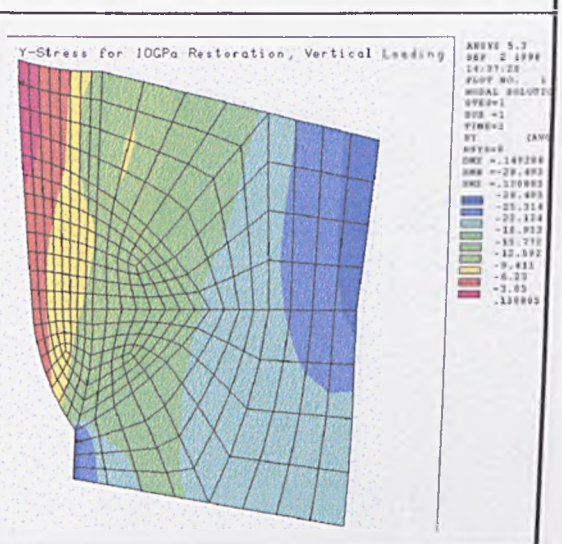

Fig. 7.7.1f: y-stress for 10GPa model, occlusal loading.

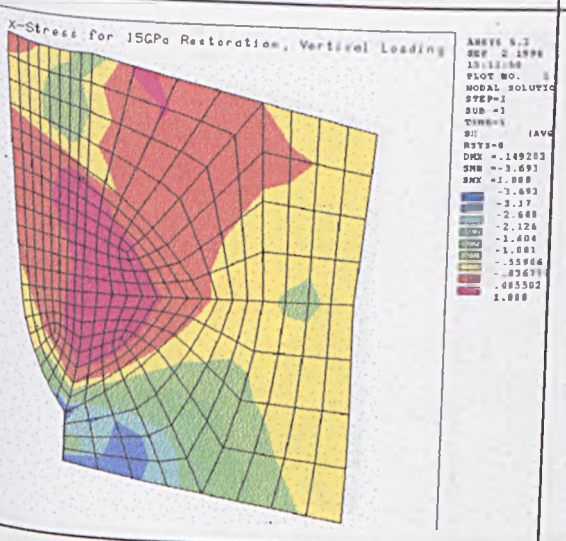

Fig. 7.7.1g: x-stress for 15GPa model, occlusal loading.

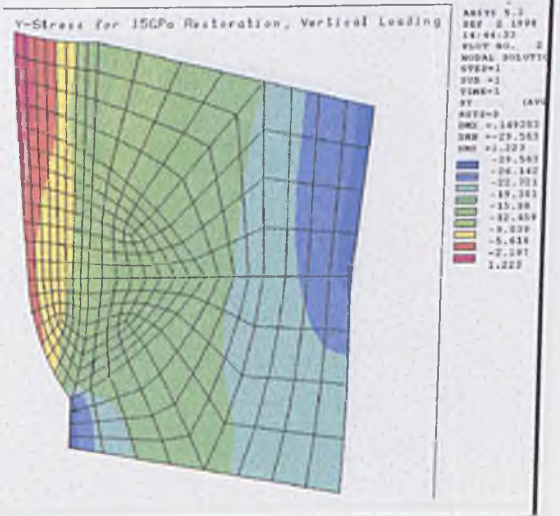

Fig. 7.7.1h: y-stress for 15GPa model, occlusal loading.

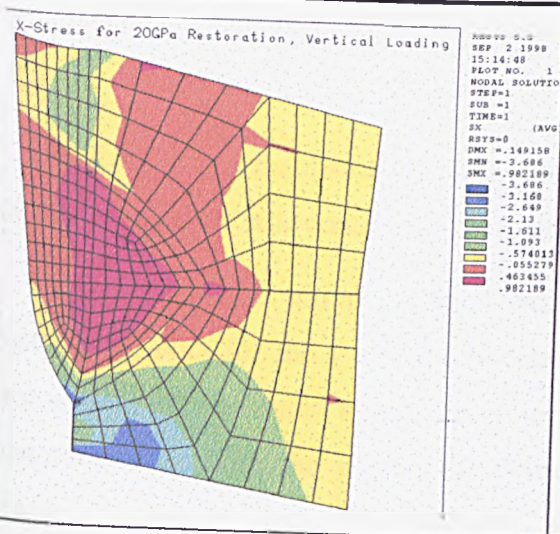

Fig. 7.7.1i: x-stress for 20GPa model, occlusal loading.

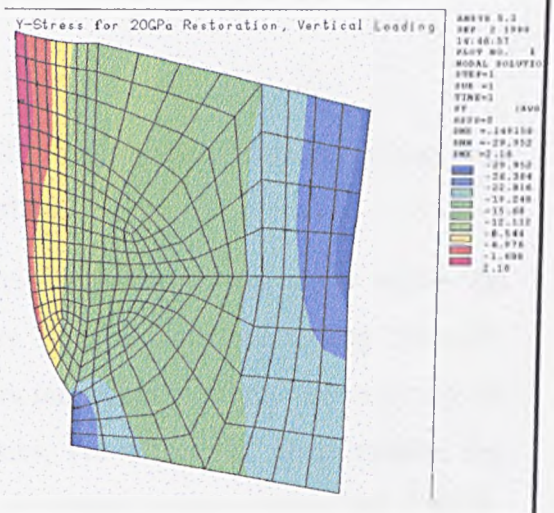

Fig. 7.7.1j: y-stress for 20GPa model, occlusal loading.

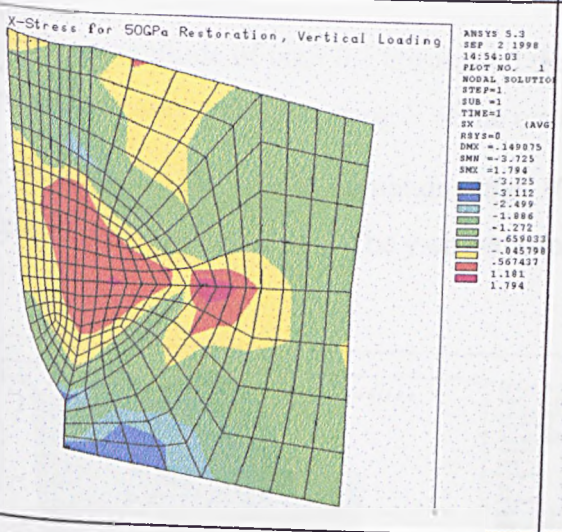

Fig. 7.7.1k: x-stress for 50GPa model, occlusal loading.

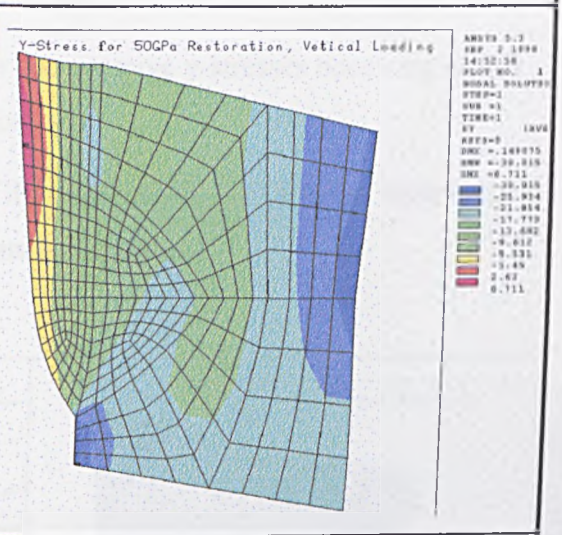

Fig. 7.7.1l: y-stress for 50GPa model, occlusal loading.

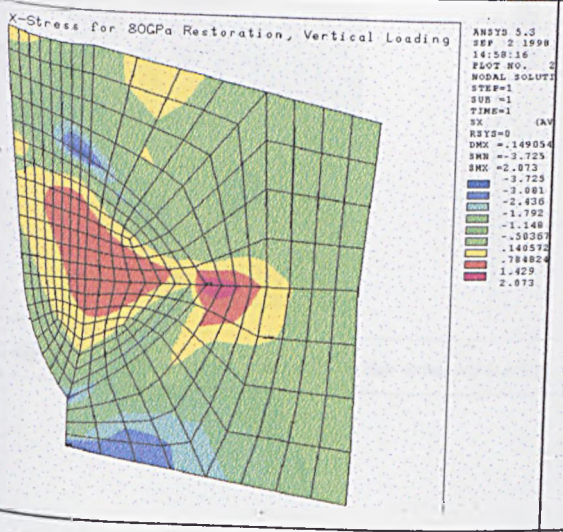

Fig. 7.7.1m: x-stress for 80GPa model, occlusal loading.

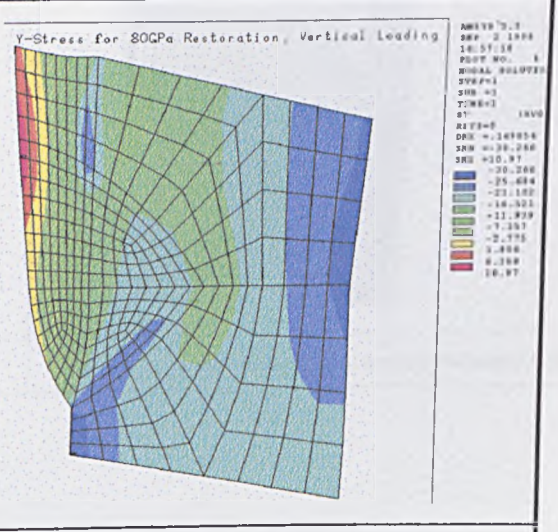

Fig. 7.7.1n: y-stress for 80GPa model, occlusal loading.

7.7.2 *Buccal Loading*

Fig. 7.7.2 shows the distributions of global x and y-stress within the cervical third of the tooth on the side containing the restoration.

The low modulus group predicts that very little stress will occur within the restoration, both for the y and the x-stresses. For the model containing the 1GPa restoration, the maximum tensile stress occurs immediately behind the vertex of the restoration, for both the x- and the y-stresses. For all of the other models, the maximum tensile stress, both global x- and y-stress occurs within the dentine, immediately below the dentine-restoration interface.

The magnitude of both the tensile and the compressive y-stresses occurring at this point increases with increasing E of the restoration.

Except for the model containing the 1GPa restoration, the x-stress within the restoration is compressive. The y-stress is tensile throughout.

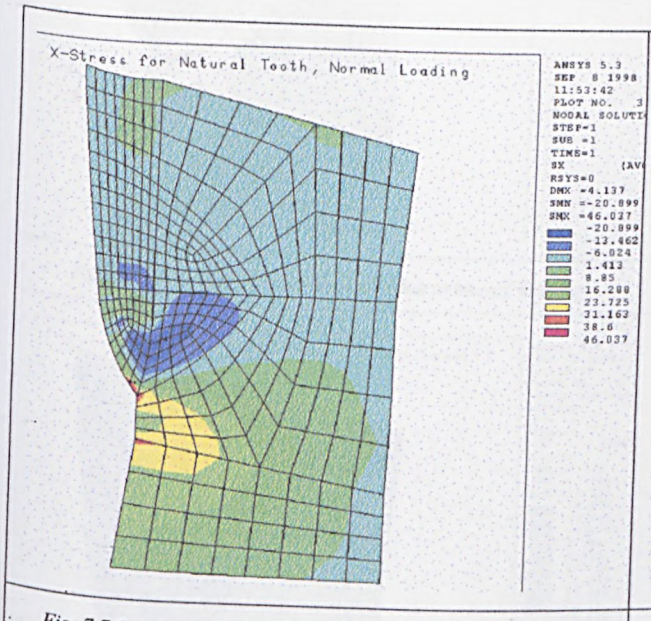

Fig. 7.7.2a: x-stress in the natural tooth due to buccal loading.

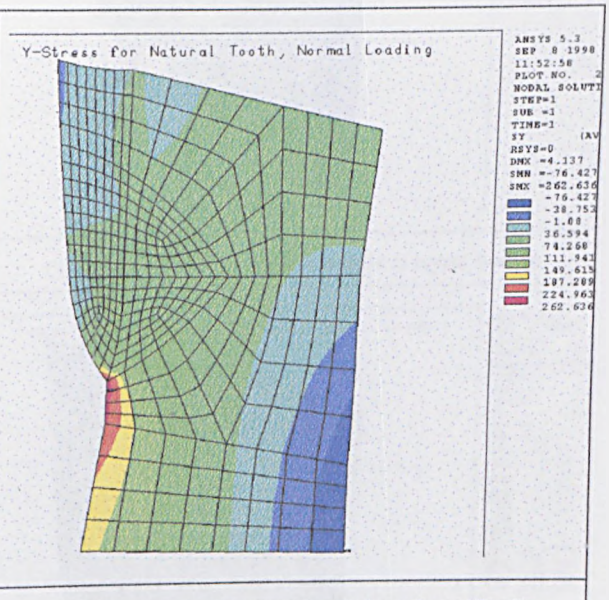

Fig. 7.7.2b: y-stress in the natural tooth due to buccal loading.

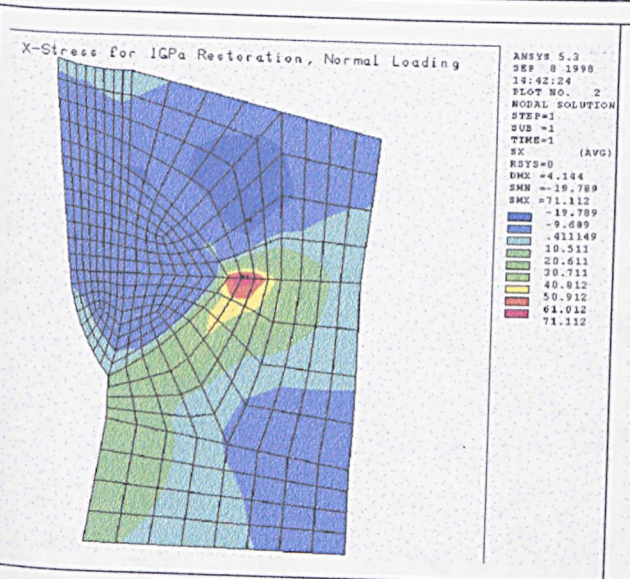

Fig. 7.7.2c: x-stress for 1GPa model due to buccal loading.

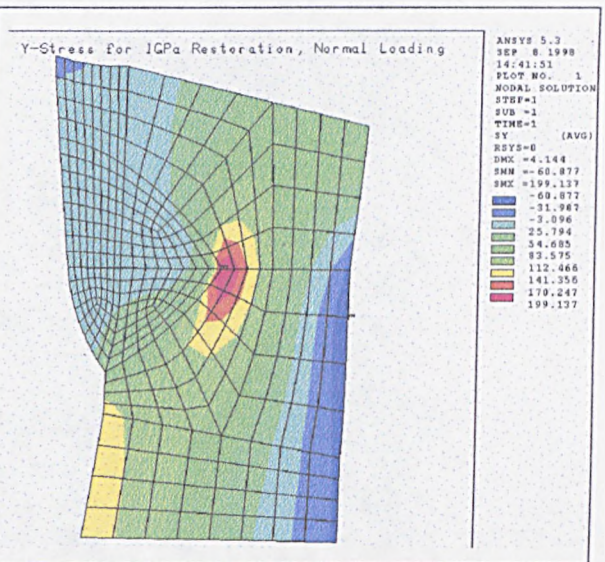

Fig. 7.7.2d: y-stress for 1GPa model due to buccal loading.

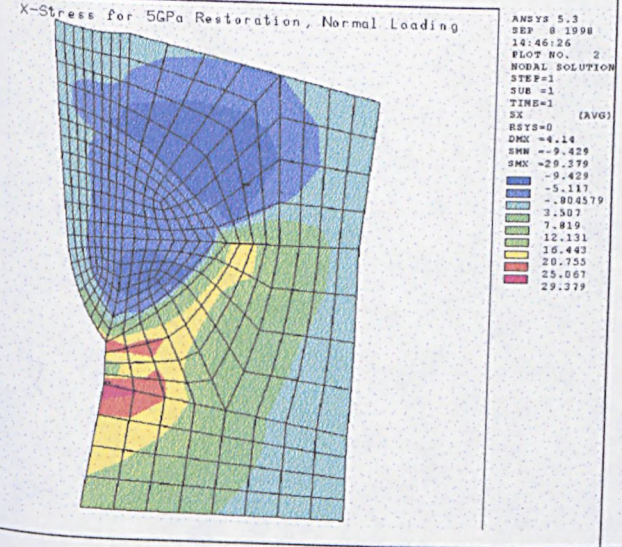

Fig. 7.7.2e: x-stress for 5GPa model due to buccal loading.

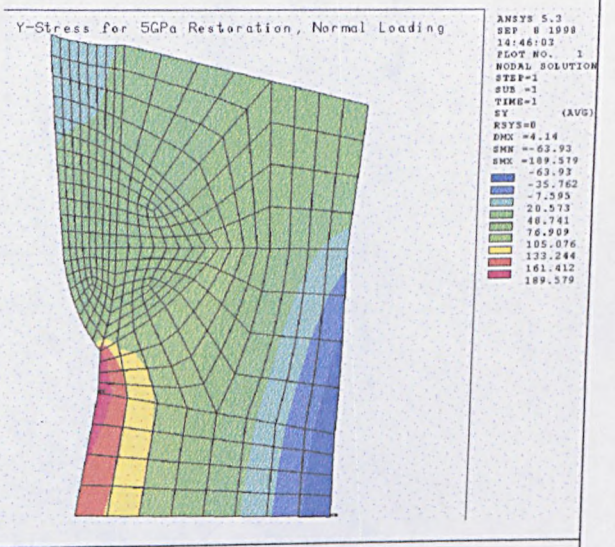

Fig. 7.7.2f: y-stress for 5GPa model due to buccal loading.

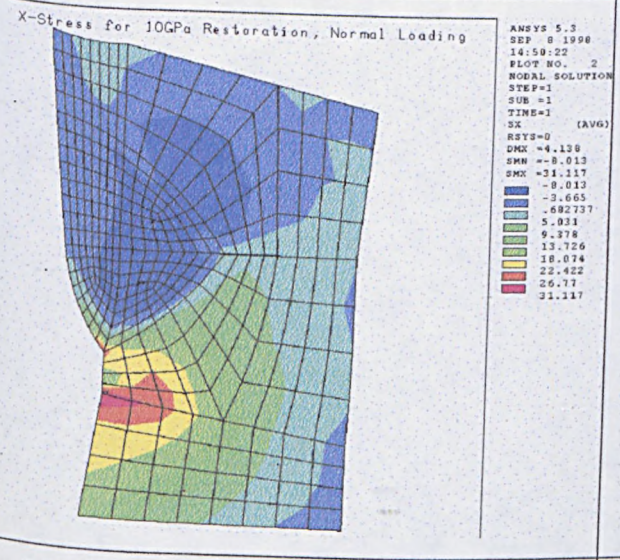

Fig. 7.7.2g: x-stress for 10GPa model due to buccal loading.

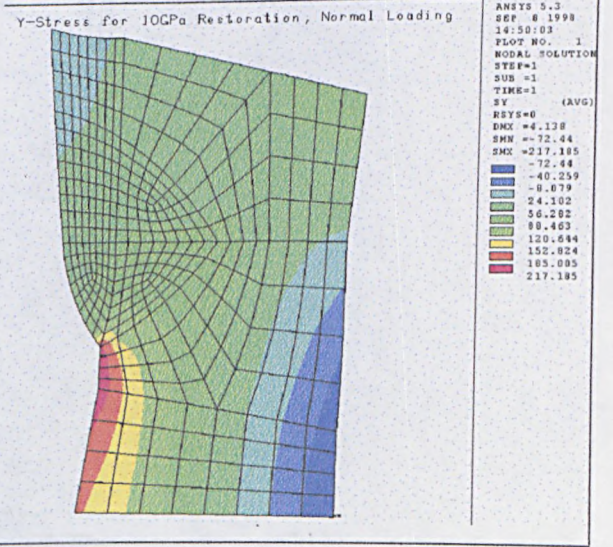

Fig. 7.7.2h: y-stress for 10GPa model due to buccal loading.

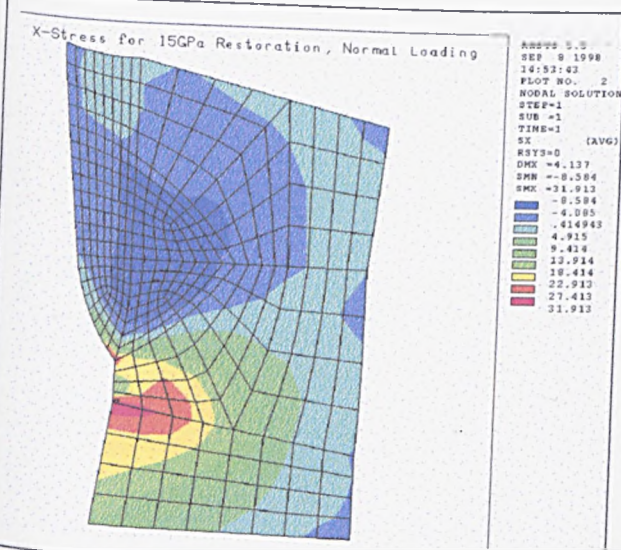

Fig. 7.7.2i: x-stress for 15GPa model due to buccal loading.

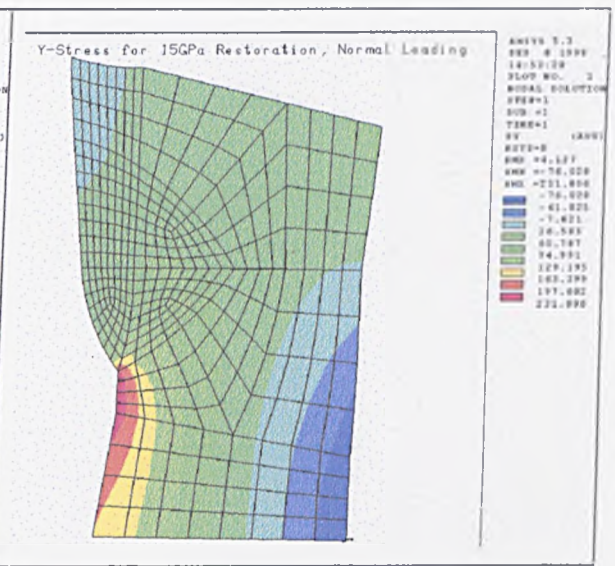

Fig. 7.7.2j: y-stress for 15GPa model due to buccal loading.

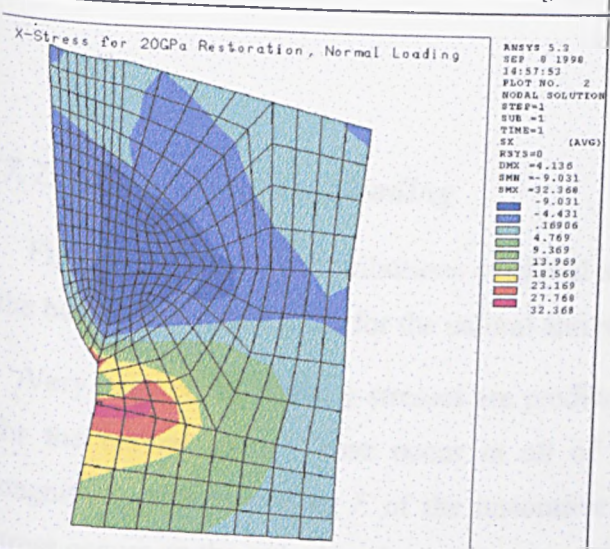

Fig. 7.7.2k: x-stress for 20GPa model due to buccal loading.

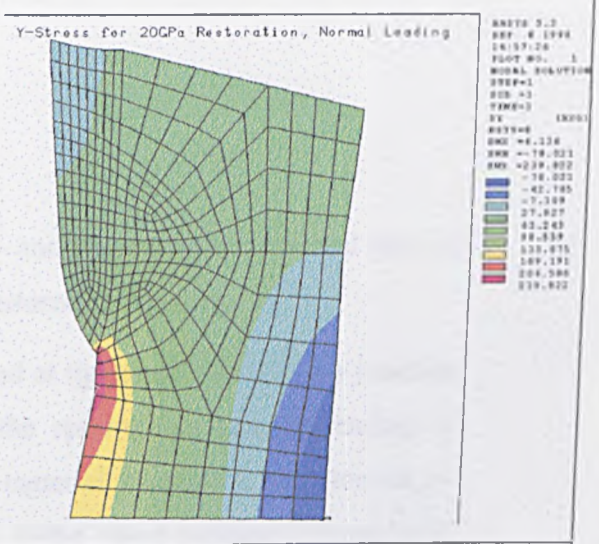

Fig. 7.7.2l: y-stress for 20GPa model due to buccal loading.

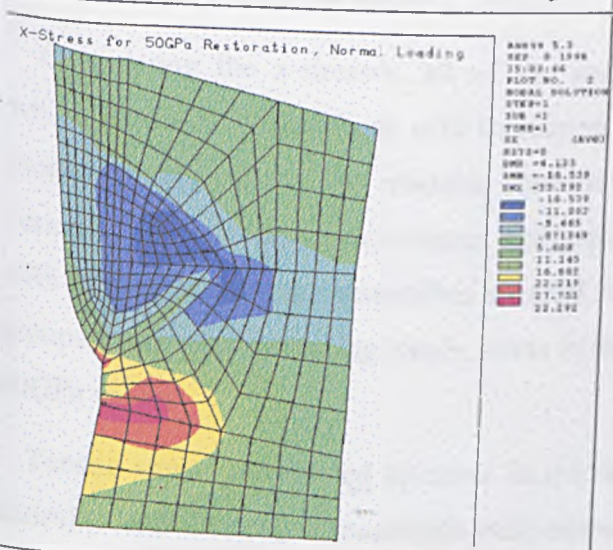

Fig. 7.7.2m: x-stress for 50GPa model due to buccal loading.

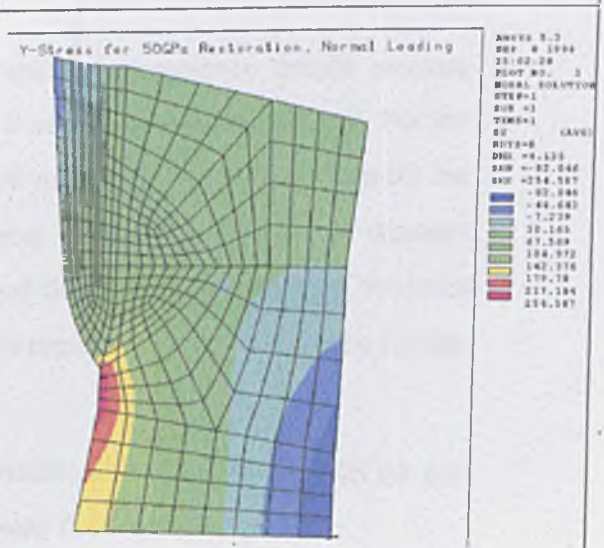

Fig. 7.7.2n: y-stress for 50GPa model due to buccal loading.

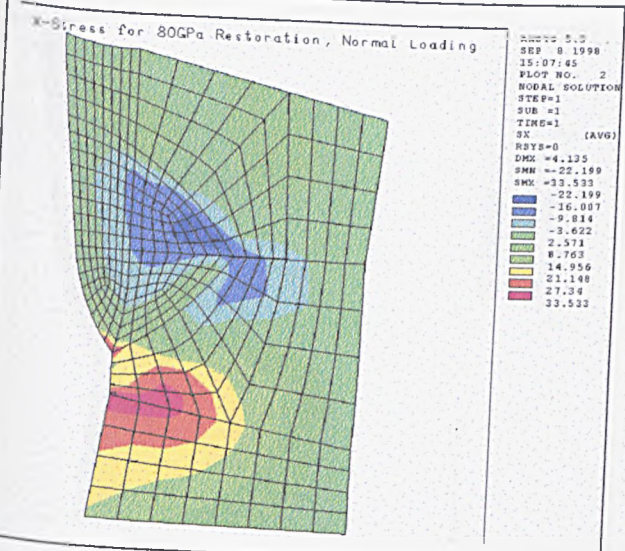

Fig. 7.7.2o: x-stress for 80GPa model due to buccal loading.

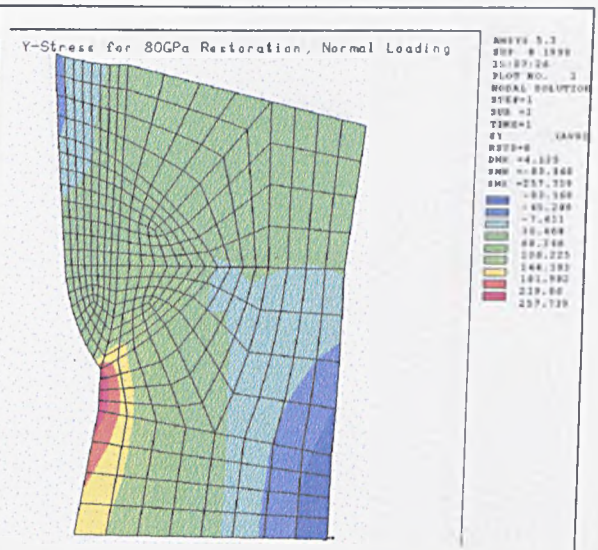

Fig. 7.7.2p: y-stress for 80GPa model due to buccal loading.

7.7.3 *Lingual Loading*

Fig. 7.7.3 shows the distributions of global x- and y-stress in the cervical third of the buccal side of the tooth for the natural and restored models.

Very large compressive y-stresses are predicted at the enamel-cementum junction for the natural tooth. These occur in all of the restored models, increasing in magnitude with increasing E of the restorative material. Similarly, high tensile y-stress occurs on the pulpal surface of the dentine. Again, these increase in magnitude as the E of the restorative material increases.

Considering the x-stresses, all of the restorations experience tensile x-stress, which increases in magnitude with increasing E of the restorative material. For the models containing the low modulus restorative materials, the dentine behind the vertex of the restoration experiences compressive x-stress. However, this changes with increasing E of the restorative material, and the mid-range and high modulus groups experience increasing tensile stress in this region; up to about 21MPa for the 80GPa model.

Tensile stress is predicted to occur in the dentine, above the restoration on the incisal side, decreasing in magnitude with increasing E of the restoration.

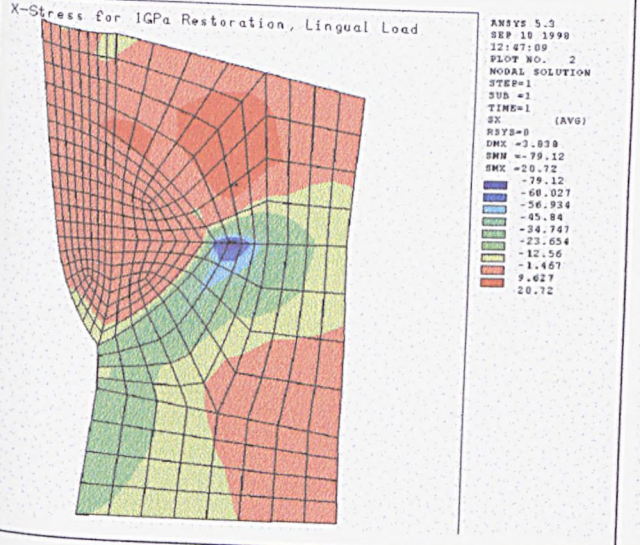

Fig. 7.7.3a: x-stresses in 1GPa model, lingual load

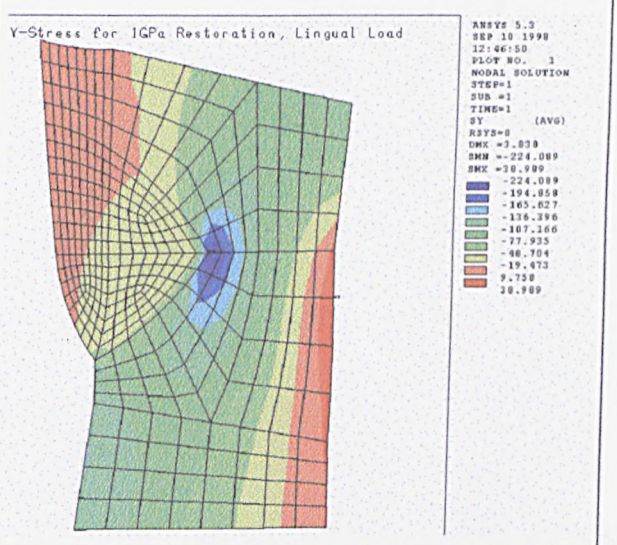

Fig. 7.7.3b: y-stresses in 1GPa model, lingual load

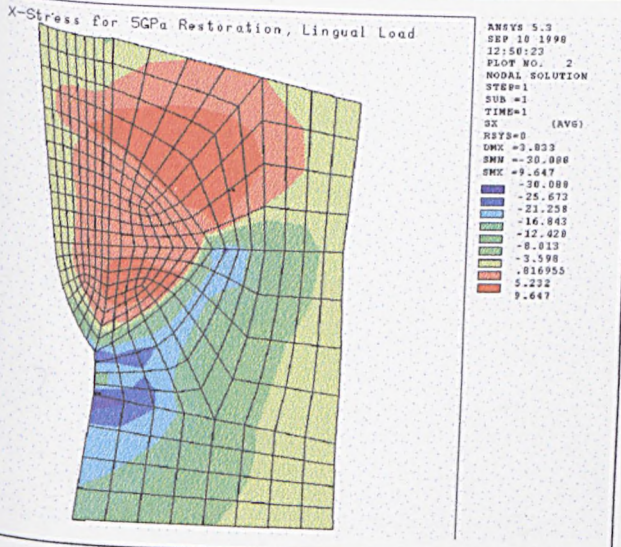

Fig. 7.7.3c: x-stresses in 5GPa model, lingual load

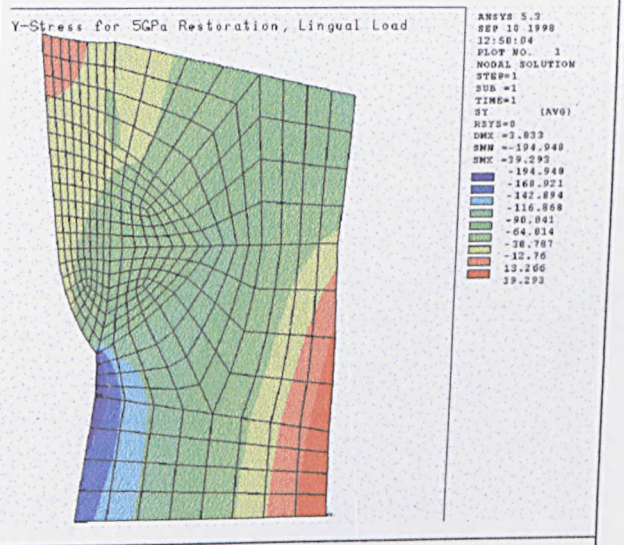

Fig. 7.7.3d: y-stresses in 5GPa model, lingual load

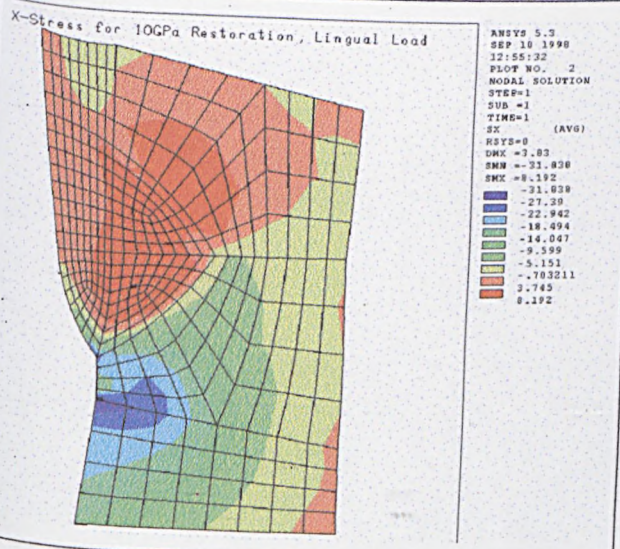

Fig. 7.7.3e: x-stresses in 10GPa model, lingual load

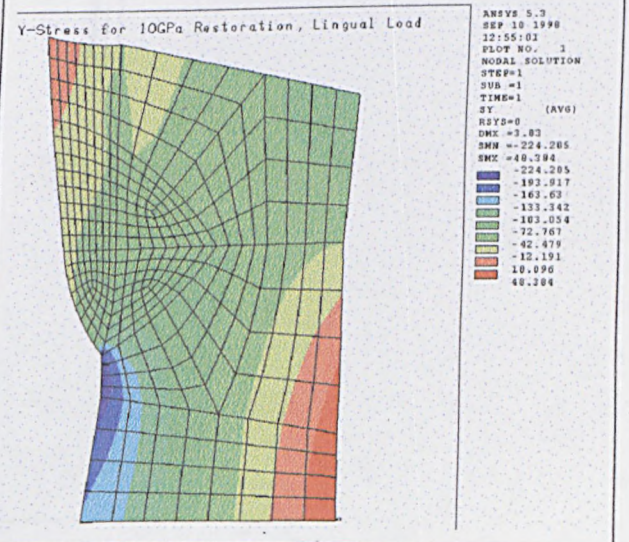

Fig. 7.7.3f: y-stresses in 10GPa model, lingual load

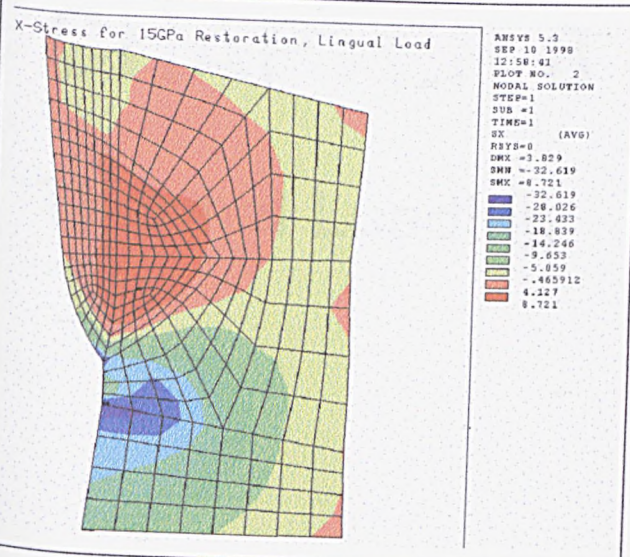

Fig. 7.7.3g: x-stresses in 15GPa model, lingual load

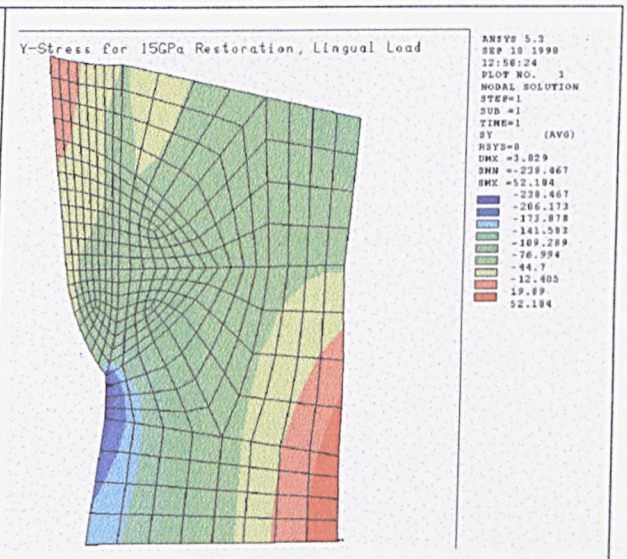

Fig. 7.7.3h: y-stresses in 15GPa model, lingual load

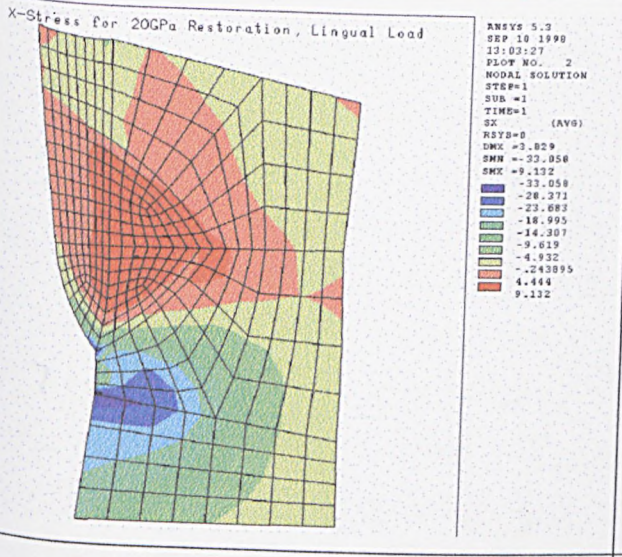

Fig. 7.7.3i: x-stresses in 20GPa model, lingual load

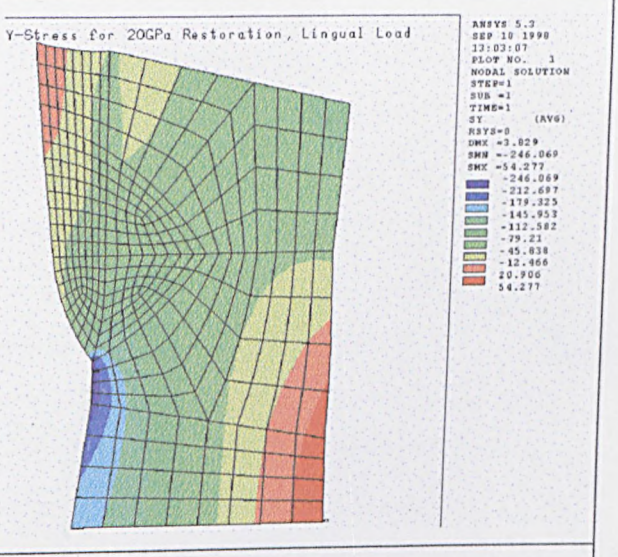

Fig. 7.7.3j: y-stresses in 20GPa model, lingual load

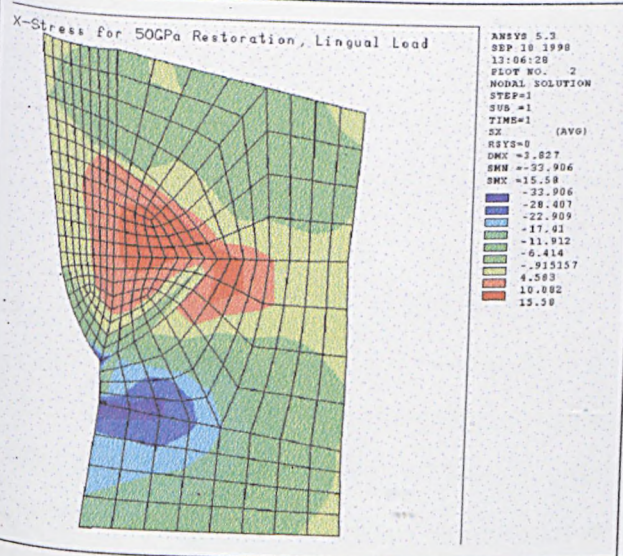

Fig. 7.7.3k: x-stresses in 50GPa model, lingual load

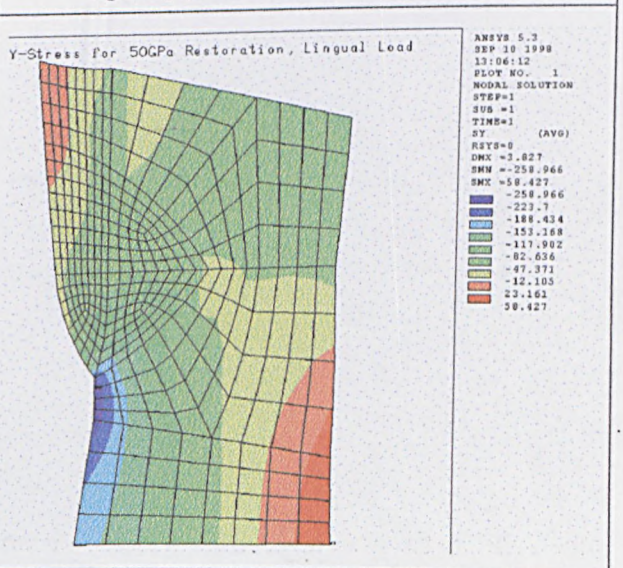

Fig. 7.7.3l: y-stresses in 50GPa model, lingual load

CHAPTER 8

Thermal Loading

8.0 Introduction

In this chapter, the effects of thermal loading and different cavity shapes on the stress distributions surrounding a restored cervical lesion are explored, and compared to the stresses in the same region for a natural tooth. The objective of this thesis has been to evaluate the major factors that affect restoration design, using a hierarchy of models. This permits each factor to be considered, both individually and in the context of the other factors that affected the design. The philosophy behind this approach is that a design that appears to be benign under one loading condition may not be under others, and for a restoration design to be pronounced truly benign, it is important that as many factors as possible are considered.

It has been stated that the analysis of human teeth subject to thermal loads has not been reported frequently (Spierings *et al.*, 1984a). However, it is known that sensitivity to thermal stimuli is a common problem following restorative dental treatment; up to 50% of patients reported hypersensitivity to cold, and 19% to hot stimuli, within 24 hours after restorative treatment (Spierings *et al.*, 1984a). Temporary post-operative hypersensitivity affects many patients, and is believed to be due to the thermal properties of the materials as well as operative procedures (Spierings *et al.*, 1986). It would seem reasonable that the mismatch in thermal properties between the natural tooth and the restorative materials used would cause a concentration of stress to result in the tooth. Whilst this is likely to be more of an issue with a metallic material such as amalgam, as considered in many of the earlier papers concerning the analysis of teeth subjected to thermal loads (Wright and Yettram (1978), Spierings *et al.*, (1984), (1986)) the effect of the so-called aesthetic restorative materials subjected to functional thermal loading is also worthy of consideration.

Wright and Yettram (1978) examined stresses due to thermal loading, and concluded that the stresses produced by thermal loading were similar in magnitude to those induced in the teeth under normal mastication. This implies that thermal analysis of natural and restored teeth is significant. Given this information, and the problems associated with marginal leakage and post-operative sensitivity of patients

with Class V restorations, it seems unusual that more work has not been carried out in this field.

The magnitudes of the thermal loads experienced by human teeth are generally reported to be within the range of 0°C to 60°C (Wright and Yettram (1978), Spierings *et al.* (1984)). However, some researchers use a technique known as thermal cycling for artificially ageing restored teeth to investigate the onset of micro-leakage. Typical values used in such analyses range from between 5°C and 55°C, though some use the range 30°C to 45°C; a much smaller amplitude of loads than the range used in thermal shock analyses.

Barclay, at a presentation at the IADR meeting in Nice, June 1998, reported a study which investigated the extents of the range of thermal loads that teeth experience. They were concerned with the validity of the technique of thermocycling in microleakage studies. For this process, the magnitudes of the thermal loads applied tend to lie between 30°C and 45°C, and the presenter questioned whether the thermocycling process actually did simulate ageing of the teeth, and whether this range of loads was realistic.

The researchers placed thermistors at various locations in the mouth, and bravely measured the greatest and lowest thermal loads that could be experienced without sustaining damage to the soft tissues of the mouth. They found that the highest load was 63°C, induced by drinking very hot coffee, depending on the exact location of the tooth in the mouth, and the lowest was of the order of 1°C, induced by eating ice cubes. Anterior teeth experienced a greater range of loads than posterior teeth.

It is known that a fluctuating thermal load, or a severe thermal shock can damage the pulp tissues (Spierings *et al.*, 1984b). Wright and Yettram (1978) considered the effect upon a tooth of expansion due to setting of an amalgam restoration, and further expansion due to a fluctuating thermal load. Although the model was an axi-symmetric, 2-D, type A model, meshed with triangles, as discussed in Chapter 3, the loading conditions studied are valid for an initial investigation into the effects of thermal loading on normal and restored teeth. Wright and Yettram (1978) state that the normal mouth temperature is close to 37°C, and that the teeth and restorations within the mouth are subject to loads between 0 and 60°C. However, for most of the time, the temperature in the mouth remains close to

37°C; excursions to these extreme temperatures are short-lived. These extreme temperatures represent the peaks of the fluctuations in temperature.

To apply thermal loads to their model, Wright and Yettram (1978) applied a temperature of 57°C (20°C above the datum) to the occlusal surface of the Class I restoration, whilst they constrained the pulpal surface of the restoration at 37°C. They state that this situation is unlikely to be experienced *in vivo*, but that it is a reasonable assumption to make for an initial analysis. However, to assume that the entire temperature graduation should occur within the restoration is somewhat unreasonable, and could have a significant influence on the distribution and the magnitude of the stresses predicted.

Heat transfer occurs by one of three processes; conduction, convection or radiation. **Conduction** is the simplest process, involving the transfer of heat from a hot object to a cold one through direct contact. An example of this would be that heat is transferred from the enamel to the dentine by conduction, since the two materials are in direct contact with one another. The quantity of heat transferred from the enamel to the dentine is determined by the thermal conductivity (k) of the materials.

Convection occurs if a fluid in motion transfers heat from a hot body to a cold one. This is the process that occurs here; hot food or drink is taken into the mouth and comes into contact with the oral fluids that coat the teeth. Heat is transferred from the hot substance to this fluid, and then from the fluid to the enamel of the tooth. The material property that determines the quantity of heat transferred from the fluid to the cold body is the film coefficient. The film coefficient can be thought of as a measure of how much of the heat that has been transmitted from the hot food or liquid to the oral fluids will be transmitted to the surface of the tooth.

Radiation is the third process of heat transfer; and this involves transfer of heat from a hot object even if no intervening matter is present.

The mechanisms for transmitting heat from the tooth surface to the pulp are not fully known or understood. Spierings *et al.* (1984a) investigated the change in temperature distribution in human teeth restored with various materials. They state that the analysis of human teeth subjected to thermal loads has not been reported frequently. This is perhaps because the magnitudes of the thermal loads experienced

in functional behaviour are very small, and so it has been reasoned that the stresses resulting from these loads would therefore be less significant than bite loads. However, the effect of thermal loading on anterior teeth may in itself be significant in terms of inducing stress upon normal and restored teeth in their functional roles. Previous FEA studies have reported the temperature distributions that resulted from a thermal analysis of human natural and restored teeth (Spierings *et al.*, 1984a, 1986). In this study, the temperature distribution was evaluated and was then used to predict the stresses due to thermal loading within the tooth. Hence, the stress magnitudes and distributions associated with the application of thermal loads were investigated, and are presented in this chapter.

8.2 Materials and Methods

The thermal analyses were undertaken in 2 stages: analysis of the temperatures induced in the tooth structure, and analysis of the stresses that result from this.

The model D, designed to permit restoration of a non-carious, v-shaped lesion, was used initially in this work. A diagram of this model is shown in Fig. 8.2.1. To permit the application of thermal loads, the elements used in ANSYS had to be modified from *plane42* to *plane55*. *Plane42* elements are 4 noded, 2-dimensional structural solid elements, as stated in Chapter 4. *Plane55* elements are the thermal equivalent of these elements, and thus also permit the specification of orthotropic element properties for the enamel. However, *plane55* elements only predict the temperatures experienced at each node and element; no stress or strain information is available. Similarly, *plane42* elements do not permit the evaluation of temperatures.

In order to obtain the stresses induced in the tooth and supporting tissues due to the application of thermal loads, a short program, entitled *fer3* was written that could be run as a macro within ANSYS. This programme read the temperature predicted at each node, and wrote them to a file in the same directory called *tlist*. The programmes *fer3* and *tlist* are listed in Appendix 2. A format statement was used to specify the nodal temperatures as boundary conditions in *tlist*. This meant that when

an identical model meshed with structural elements was loaded in ANSYS, the nodal temperatures could be prescribed at each node by reading in the file *tlist* as a macro.

To analyse the stresses that would be induced within the model due to the thermal loads, the model was remeshed with *plane42* elements. In /PREP7, the ANSYS pre-processor, the file *tlist* was read in, constraining every node in the model at the temperature that was experienced during the thermal simulation. No other loads were applied, and a structural, static analysis was performed.

The stresses induced could then be studied in the usual way.

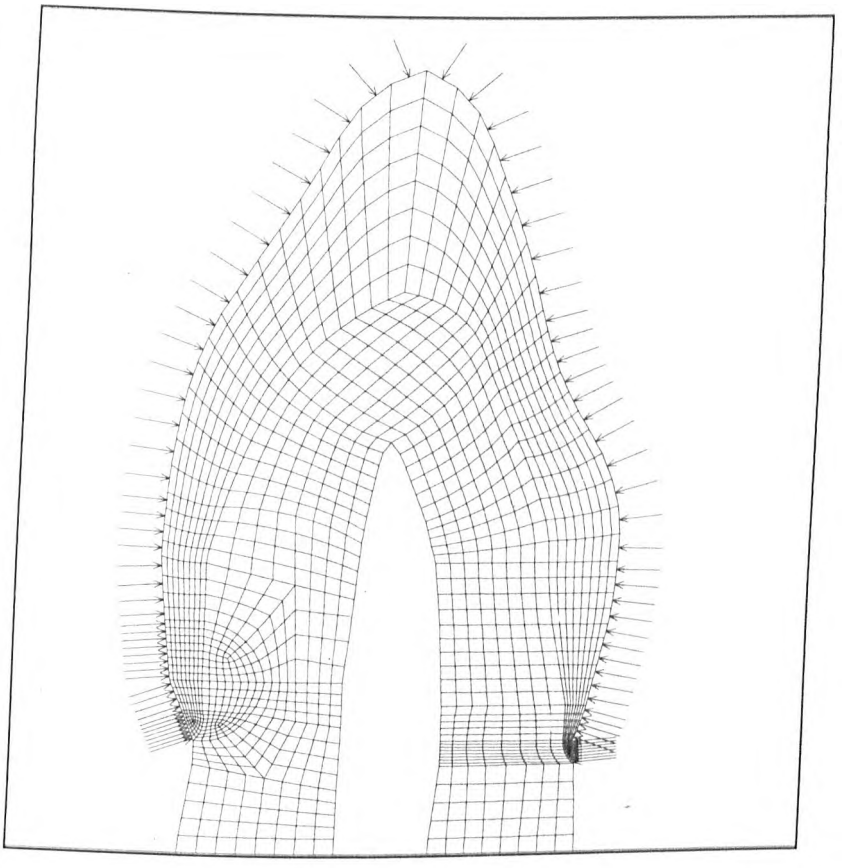

Fig. 8.2.1: The convection loads applied (rounded restoration model).

Based upon this information, loads of 60°C and 4°C were used in this study. These values compare well to the values used by Spierings *et al.* (1984), and Wright and Yettram (1978).

8.2.2 *Material Properties*

Table 8.2.2.1 defines the material properties used in this study.

Table 8.2.2.1: The Material Properties used.

Material	E *(MPa)*	ν_{xy}	ρ (kg/m^3)	k (W/mm^3)	α ($^\circ C^{-1}$)
Enamel	E_x =80 000 E_y =15 000	0.3	2.8×10^{-6}	$0.653\times10^{-3(b)}$	$12\times10^{-6(a)}$
Dentine	15 000	0.3	1.96×10^{-6}	$08.\times10^{-3(b)}$	$14\times10^{-6(a)}$
Restoration	1 000 - 80 000	0.3		0.18×10^{-3}	$35\times10^{-6(a)}$
PDL	30	0.45	1000×10^{-6}	0.85×10^{-3}	10×10^{-6}
Cortical Bone	13 700	0.3		$1.0\times10^{-3(b)}$	14×10^{-6}
Cancellous Bone	689	0.3		$1.0\times10^{-3(b)}$	14×10^{-6}
Gum	30	0.3		0.85×10^{-3}	10×10^{-6}

(a) R. van Noort, *Introduction to Dental Materials*, Mosby 1994 (pg. 53).

(b) S. A. Berger, W. Goldsmith, E. R. Lewis, *Introduction to Bioengineering*, Oxford University Press, 1996 (pg.s 206 and 212).

Using the material properties specified in Table 8.2.2.1, and the *plane55* elements, a transient thermal analysis was performed in ANSYS.

Based upon these experiments a thermal load of magnitude 60°C was applied to the tooth as a convection load placed upon the lines that define the outer surface of the enamel. A value of 1.0×10^{-6} was specified as the film coefficient. This value was a generic value obtained from consideration of the film coefficients of materials with similar properties to enamel. The load curve used is shown in Fig. 8.2.2.1.

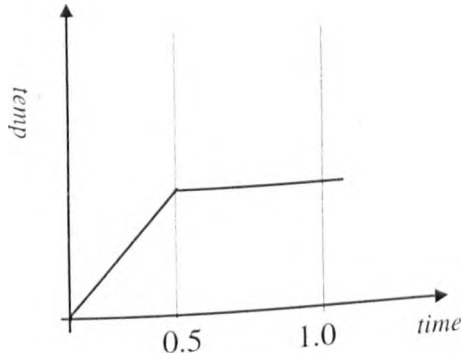

Fig. 8.2.2.1: The load curve used for thermal analyses.

The stresses were evaluated after 0.5 seconds.

8.3 Results

The stresses induced in the natural tooth due to thermal loading are presented in Fig. 8.3.1.

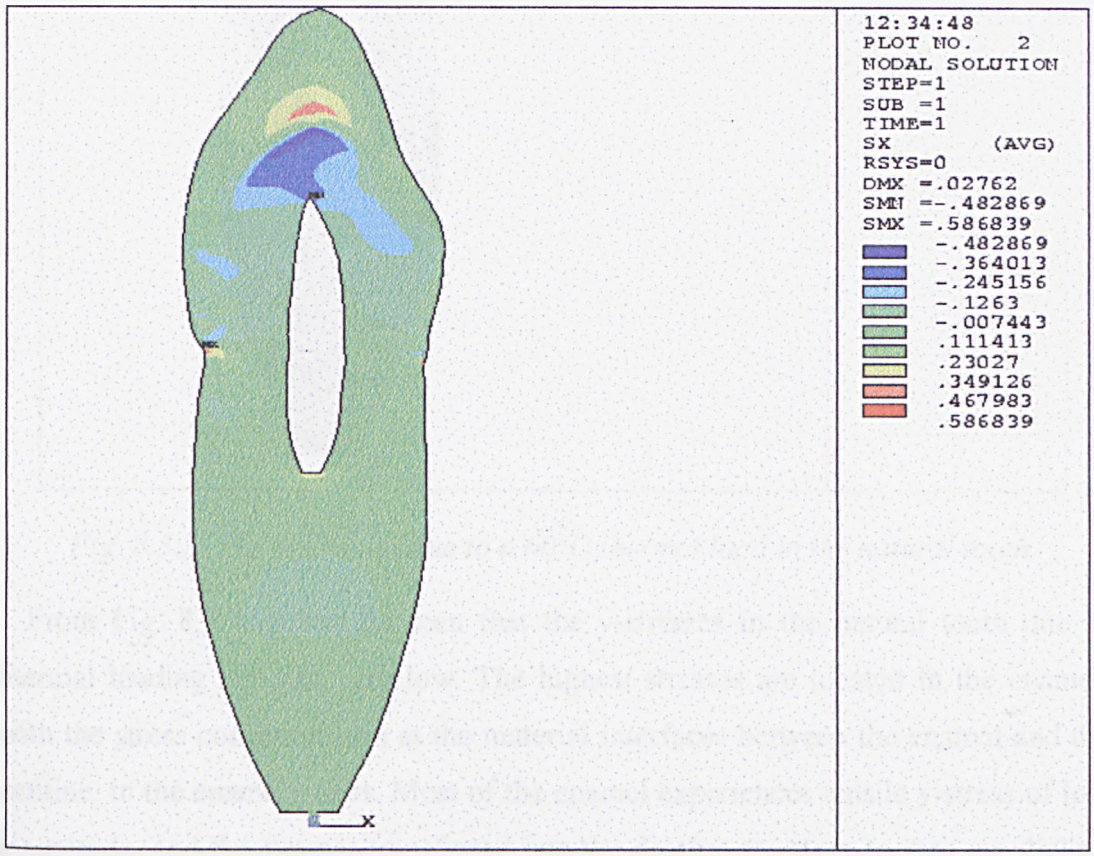

Fig. 8.3.1: The x-stresses due to a 60°C thermal load in the natural tooth.

From Fig.8.3.1, it can be seen that the magnitudes of the x-stresses induced in the tooth due to a thermal load of 60°C, with the material properties specified, are very small. Areas of higher tensile x-stress exist in the enamel, at the EDJ, close to the tip of the tooth. A corresponding area of compressive stress exists in the dentine below this region.

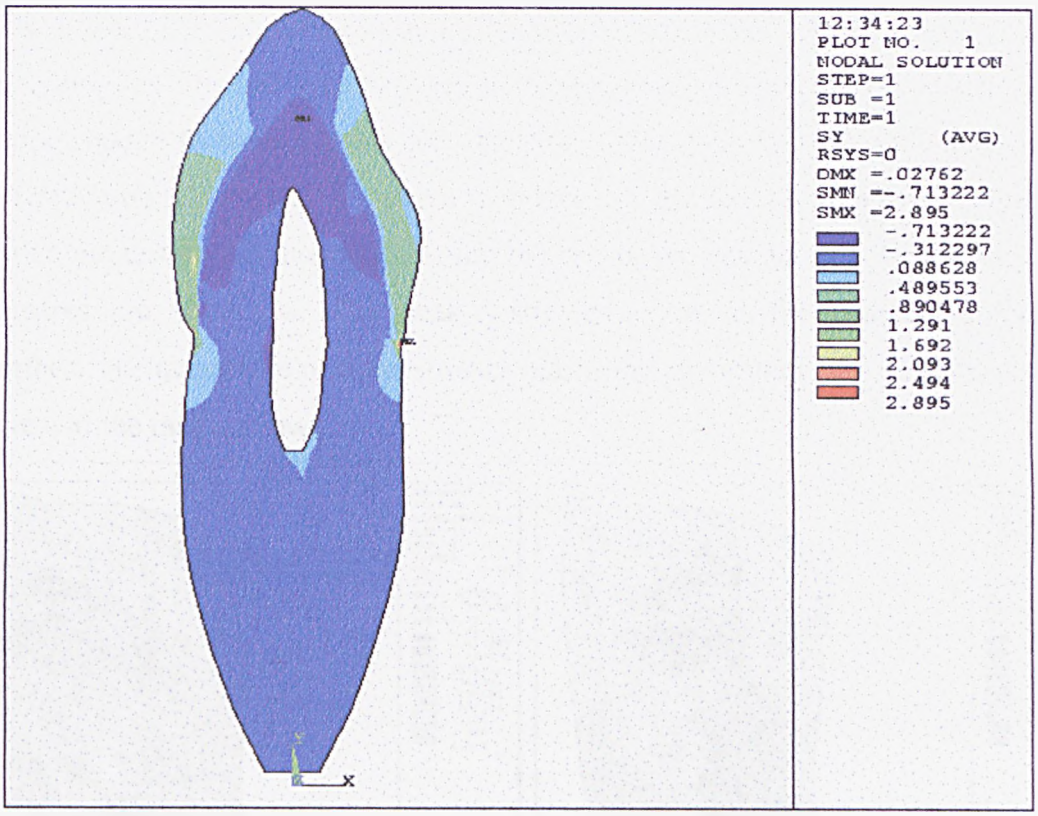

Fig. 8.3.2: The y-stresses due to a 60°C thermal load in the natural tooth.

From Fig. 8.3.2, it can be seen that the y-stresses in the natural tooth due to thermal loading are also very low. The highest stresses are located in the enamel, with the stress concentrations at the material interfaces between the enamel and the dentine, in the enamel tapers. Most of the enamel experiences tensile y-stress of low magnitude, and the stresses transferred into the dentine are close to zero, or slightly compressive.

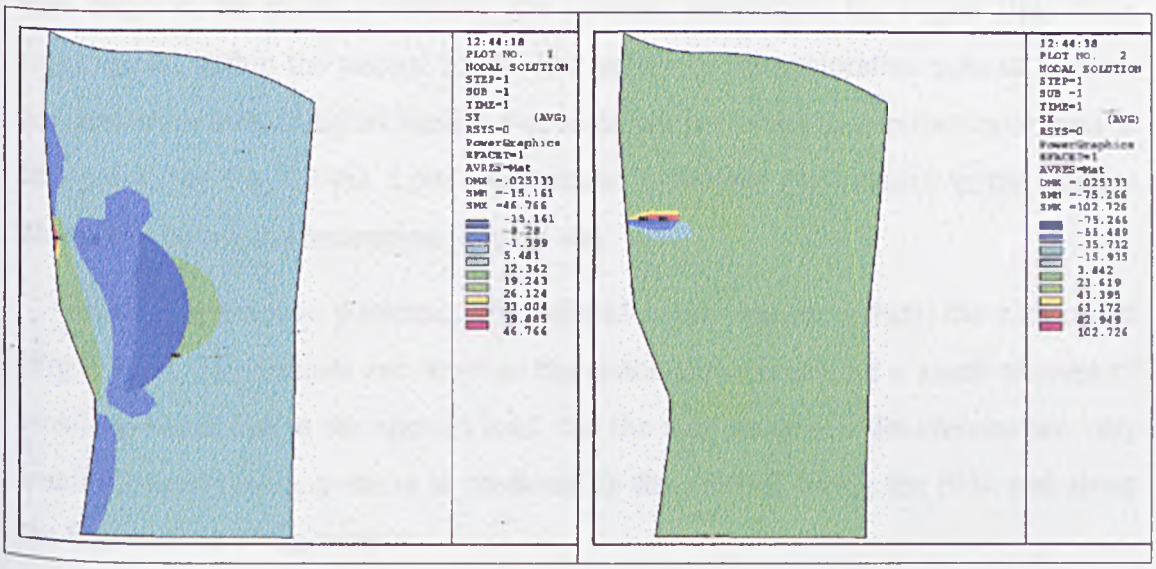

Fig. 8.3.3a and b: The stresses around the rounded restoration due to a 60°C thermal load.

The majority of the stresses due to thermal loading were induced in and around the restoration. The interface between the restorative materials and the enamel and dentine appears to cause a stress concentration, particularly between the enamel and the restoration. Compressive x-stress is induced in the restorative material close to the dentine-restoration interface. Within the rest of the enamel and the dentine, the x-stresses are very low. The peak y-stresses occur at the enamel-restoration interface. The magnitude of these stresses masks the distribution of y-stresses within the rest of the model shown.

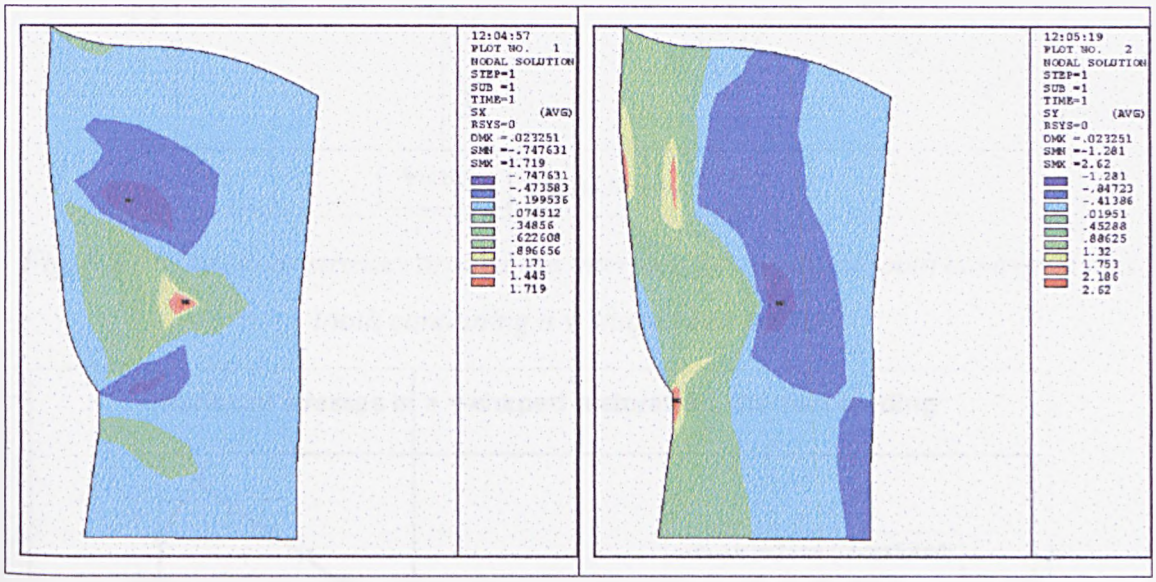

Fig. 8.3.4a and b: The x and y-stresses due to a 60°C thermal load around a v-shaped restoration.

The stresses predicted in the model containing the v-shaped restoration are lower than those in the model containing the rounded restoration, but higher than those experienced within the natural tooth. The vertex of the restoration acts as a stress concentration factor; higher tensile x-stresses are predicted within the restoration at this point (see Fig.8.3.4a). Low compressive x-stresses are induced in the dentine above and below the restoration (Fig.8.3.4a).

Small compressive y-stresses are induced in the dentine behind the restoration (Fig.8.3.4b). The enamel and most of the restoration experience a small amount of tensile y-stress due to the applied load, but the magnitudes of the stresses are very small. Greater tensile y-stress is predicted in the enamel, along the EDJ and along the free surface of the enamel.

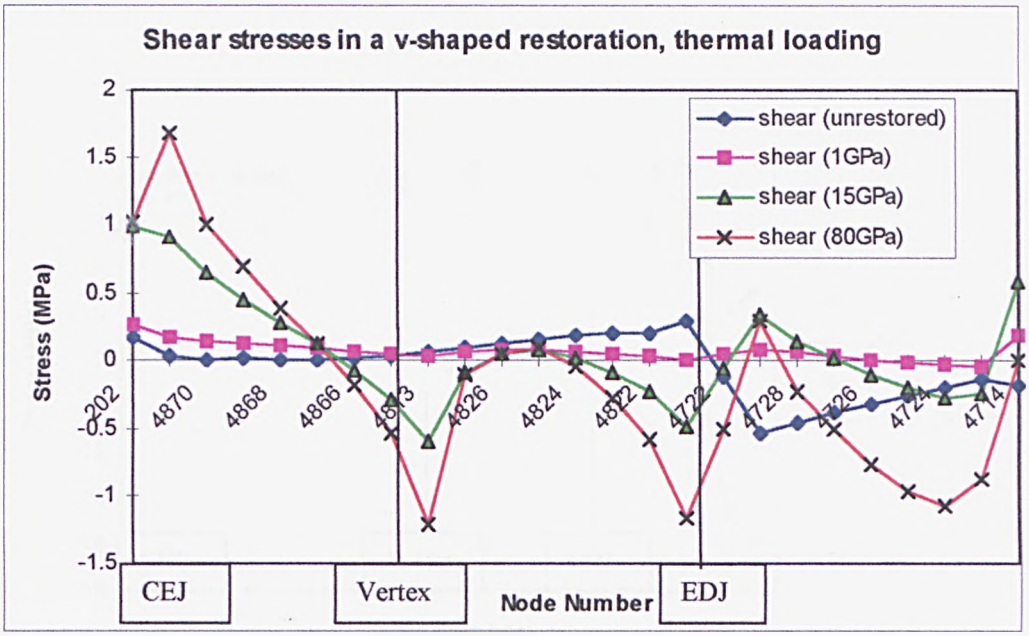

Fig. 8.3.5: The shear stresses around the interface for a natural tooth compared to a tooth containing a v-shaped restoration.

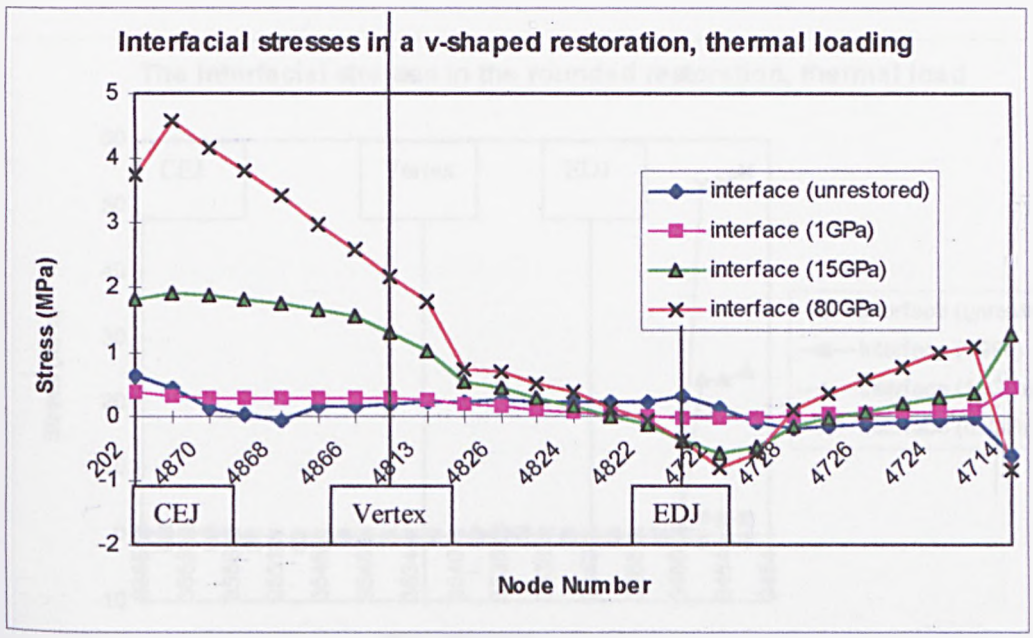

Fig. 8.3.6: The interfacial stresses around the interface for a natural tooth compared to a tooth containing a v-shaped restoration.

The shear and interfacial stresses were evaluated using the technique described in Chapter 7. Fig.'s 8.3.5 and 8.3.6 show that both the shear and interfacial stresses within the restoration are greatest for the 80GPa model. However, the magnitudes of the stresses predicted are very small. In both cases, the 15GPa model predicts very similar stresses to those predicted by the natural tooth.

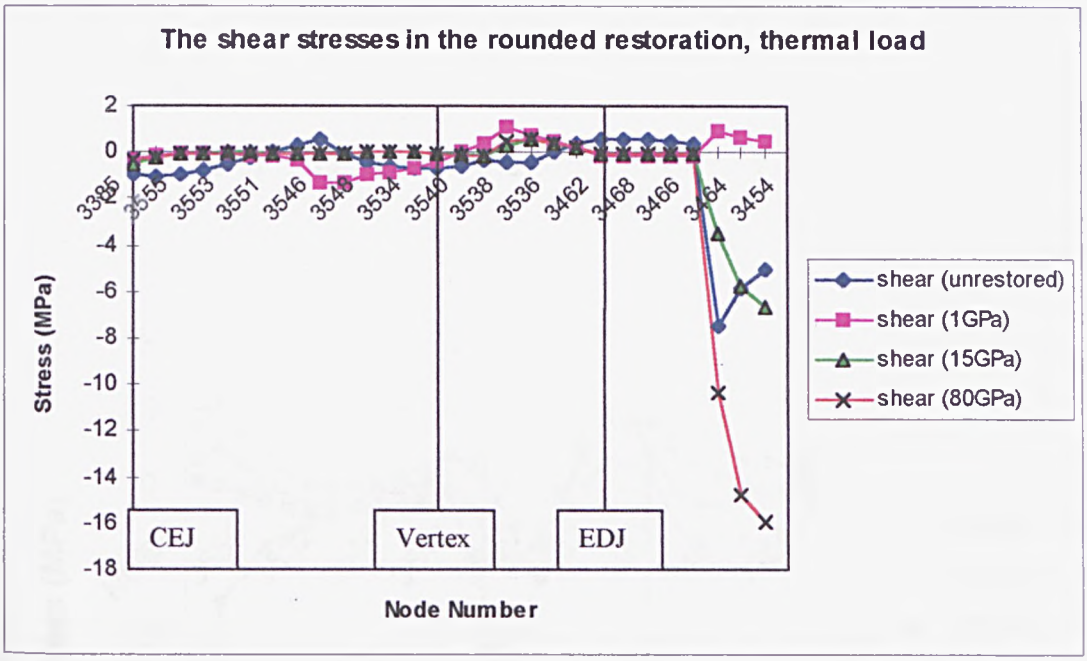

Fig. 8.3.7: The shear stresses in the rounded restoration due to a 60℃ thermal load.

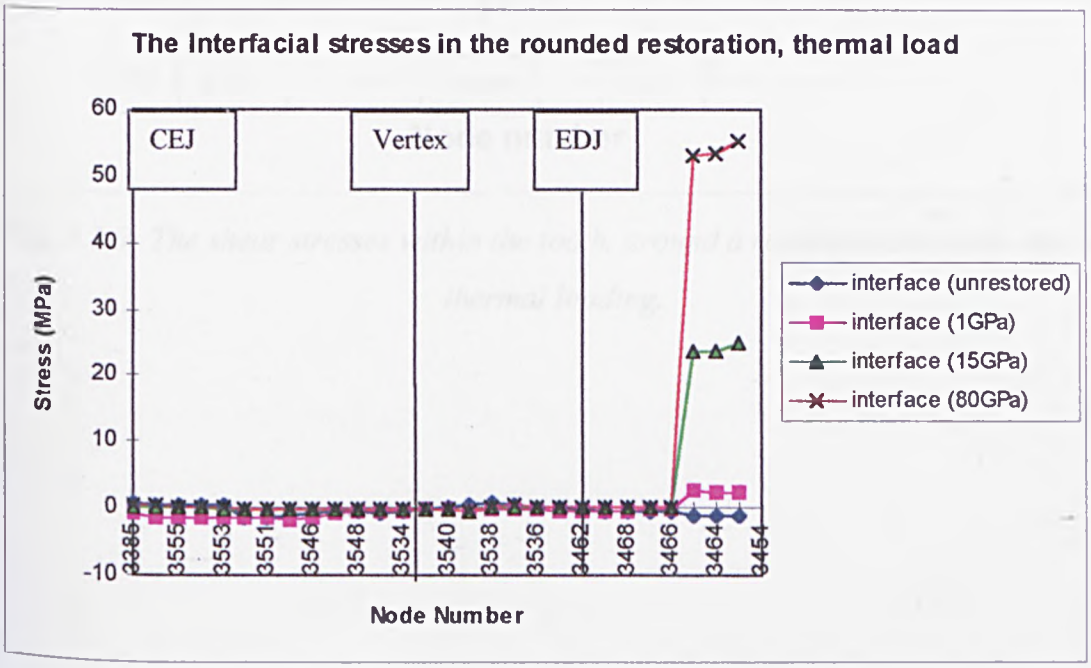

Fig. 8.3.8: The interfacial stresses in the rounded restoration due to a 60℃ thermal load.

Fig.'s 8.3.7 to 8.3.10 shows the stresses induced in the restoration due to a 60°C thermal load around a rounded restoration. It can be seen from Fig.'s 8.3.7 and 8.3.8 that the stresses along the enamel-restoration interface are very large for the models

containing the rounded restoration. This is particularly the case for the mid-range and high modulus groups. The stresses along the dentine-restoration interface are relatively small.

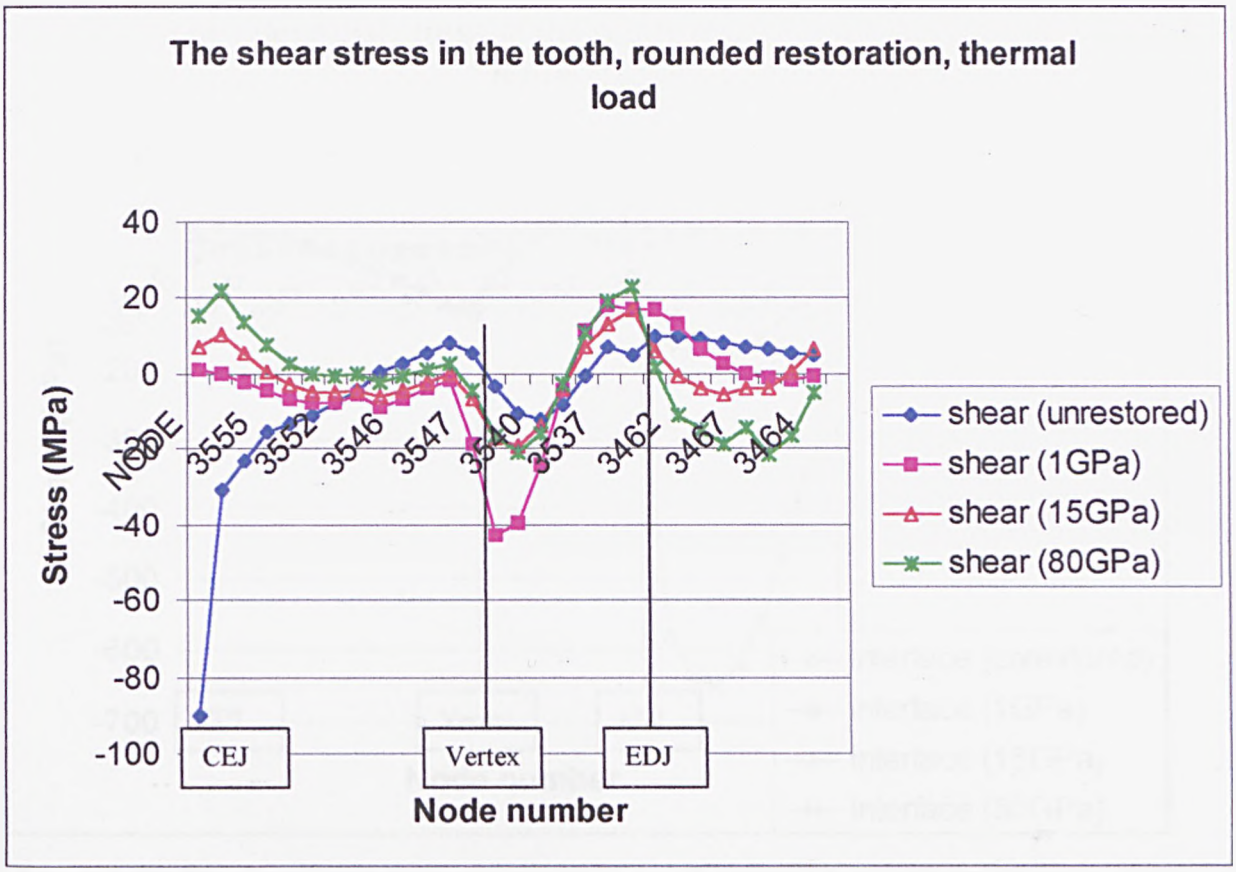

Fig. 8.3.9: The shear stresses within the tooth, around a rounded restoration due to thermal loading.

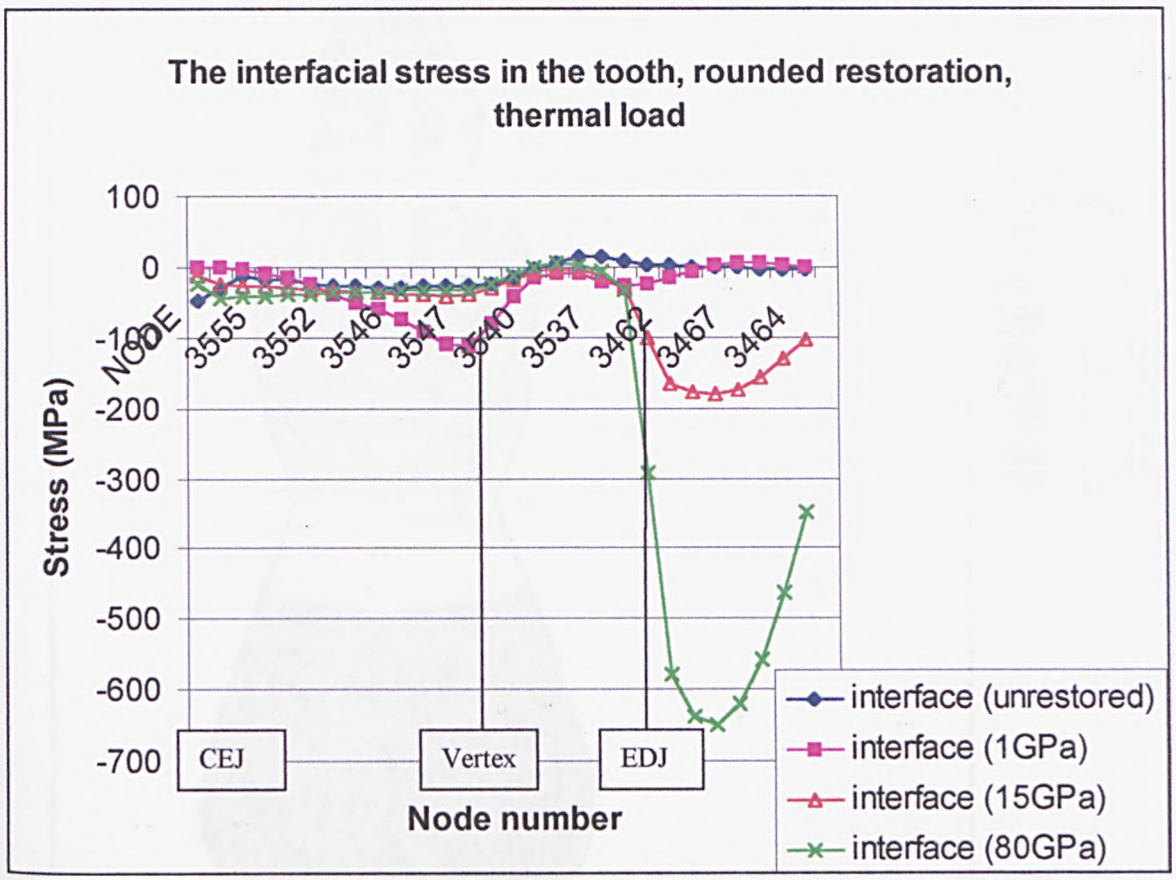

Fig. 8.3.10: The interfacial stresses within the tooth, around a rounded restoration due to thermal loading.

Both the shear and interfacial stress distributions are very smooth for the natural tooth.

8.4 *Stresses due to a 4°C Thermal Load*

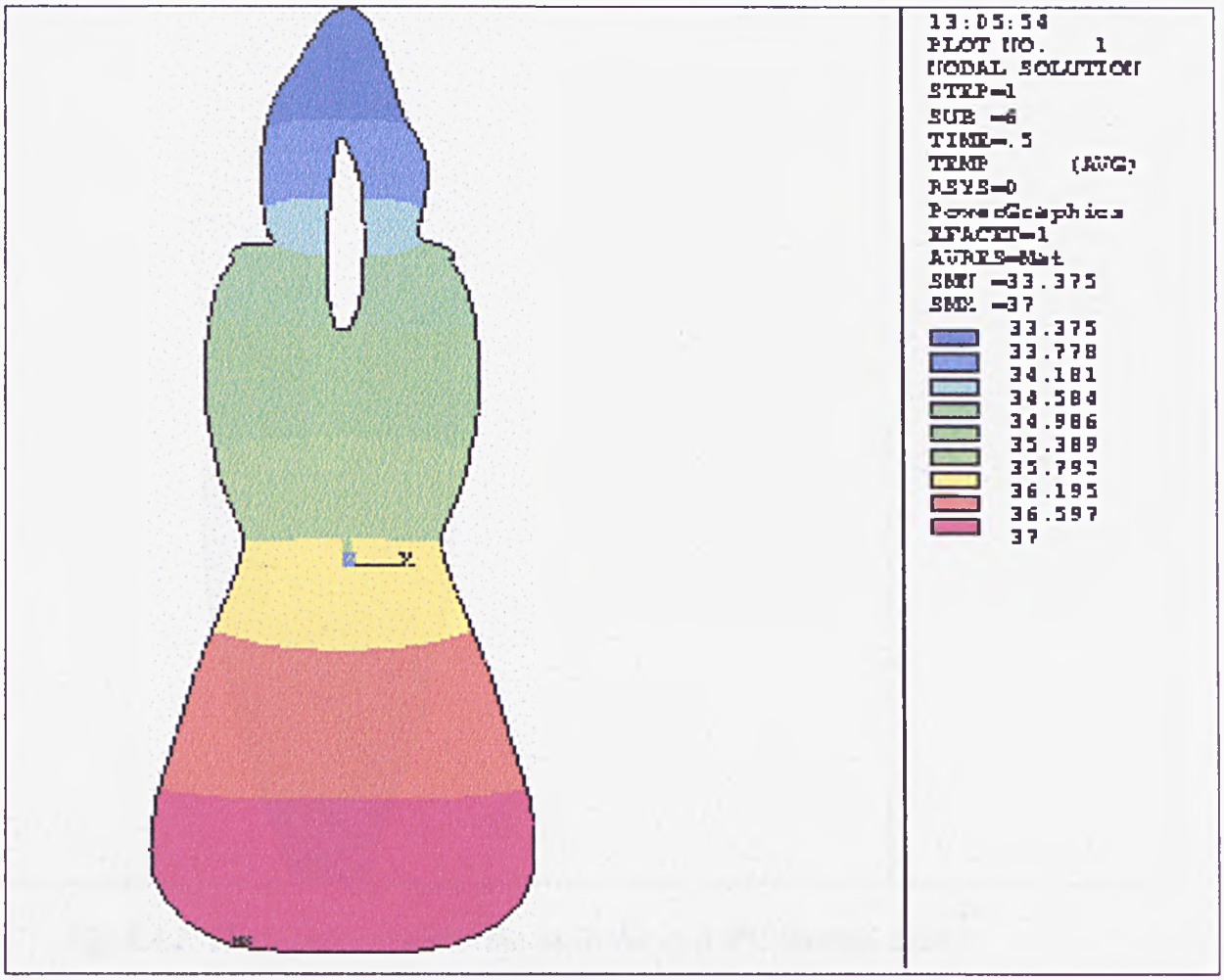

Fig. 8.4.1: The temperatures induced due to a 4°C thermal load.

Fig. 8.4.1 shows the distribution of temperatures resulting from a 4°C thermal load. The enamel and the dentine close to the pulp experience a temperature change approaching 3°C. This would cause a considerable fall in temperature of the pulp.

The thermal properties of enamel have been assumed to be isotropic, in the absence of more detailed information. It seems reasonable that the cold thermal load should induce greater stresses than the 60°C load since the change in temperature is greater. However, a cold thermal load should not endanger the pulp like a hot one does.

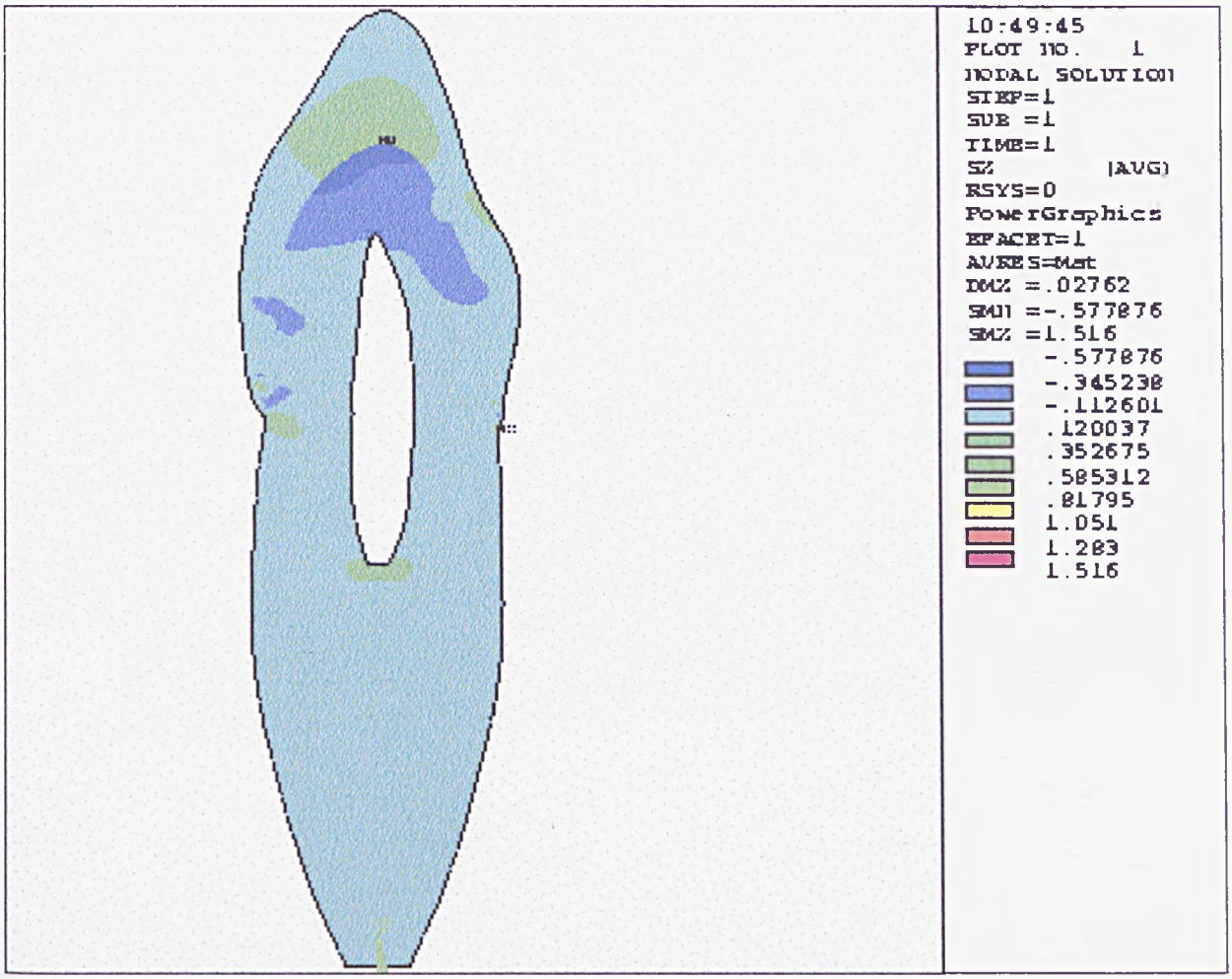

Fig. 8.4.2: The x-stresses within the tooth due to a 4°C thermal load.

The magnitudes of the x-stresses induced in the tooth due to a thermal load of 4°C are very small (Fig. 8.4.2). Most of the tooth experiences very little x-stress; however, what stress there is predicted is concentrated at the enamel-dentine interface below the cusp tip.

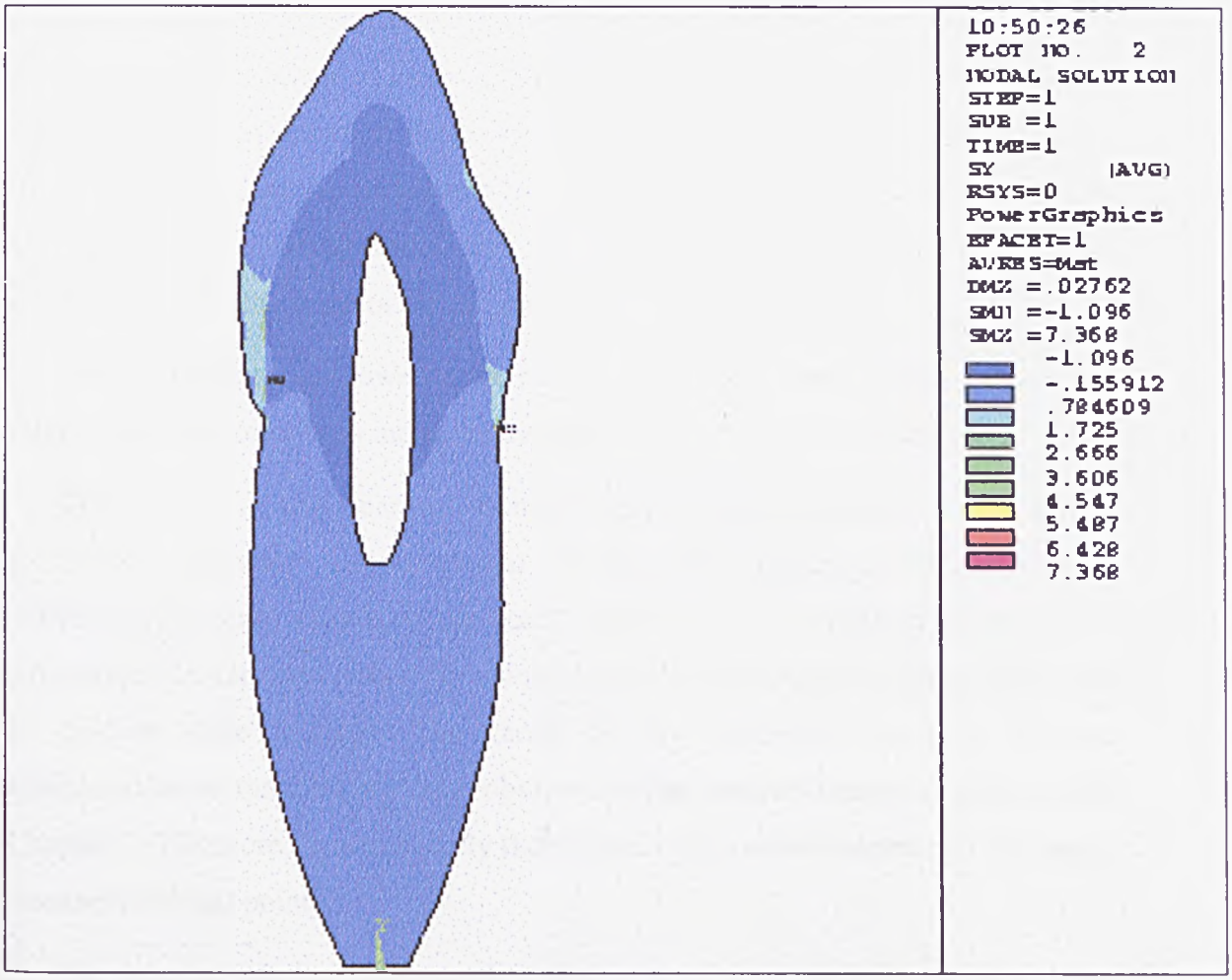

Fig. 8.4.2: The y-stresses within the tooth due to a 4°C thermal load.

Fig. 8.4.2 shows the y-stresses within the tooth. The magnitudes of the y-stresses are slightly greater than the x-stresses. The greatest stresses occur within the enamel, and the cervical region of the tooth. The magnitudes of the y-stresses predicted for the 4°C load are slightly larger than those predicted by the 60°C analysis; of the order of about 7MPa instead of about 3MPa. The majority of the tooth experiences very little stress due to the thermal load of 4°C.

8.4 Discussion

The thermal properties of enamel have been assumed to be isotropic, in the absence of more detailed information. It seems reasonable that the cold thermal load should induce greater stresses than the 60°C load since the change in temperature is greater. However, a cold thermal load should not endanger the pulp like a hot load does.

The location of the maximum thermal stresses within the cervical region of the tooth is significant when considering the idea of abfraction; low cyclic loads cause fatigue failure of materials. If the cervical enamel experiences the greatest stress due to a thermal load, this region is more likely to fail due to fatigue. This finding could also imply that thermal loads are more significant than structural loads in consideration of abfraction or the fatigue failure of teeth.

Since the stresses are lower in the natural tooth than in the restored teeth, it can inferred that the restoration increases the thermal stresses within the tooth.

The presence of a non-carious, v-shaped restoration in the tooth does not appear to increase the shear and interfacial stresses predicted around the restoration sufficiently to cause failure of the bond. However, it is recommended that these simulations are repeated with other values of the thermal material properties in order to confirm these findings. The vertex of the restoration acted as a stress concentration factor. This was also observed in the structural analyses presented in Chapter 7. Therefore, it seems likely that failure of the tooth-restoration bond could commence at this point.

The material interface between the enamel, the dentine, and the restoration also caused a concentration of stress in the outer surface of the enamel and at this interface. *(see Fig. 8.3.3b).*

Compressive x-stress was induced in the restorative material close to the dentine restoration interface within the rounded restoration (as shown in Fig. 8.3.3a). This would tend to indicate that the restorative material is being pulled away from dentine, and that the restoration is contracting in this region, and trying to pull the restoration away from the dentine. The restorative material close to the surface is experiencing tensile stress due to the applied thermal load, so the restoration as a whole experiences considerable stress in opposing directions.

The tooth containing the rounded restoration experienced significantly higher stresses than both the natural tooth and the tooth containing the v-shaped restoration. High stress in the global y-direction was predicted along the dentine-restoration interface, greater than the reported values of dentine bond strength. This is thought to be due in part to the slightly larger size of the rounded restoration, and partly because of the cavity shape. The shape of the cavity is significant because the

rounded restoration modelled has a flat interface adjacent to the stiffer direction of the enamel prisms. This would cause a greater component of the load to be channelled directly along the interface. Obviously, this would put the integrity of the interfacial bond in jeopardy.

This is a significant finding, and implies that the stresses induced in a restored tooth due to thermal loads ought to be considered in the stress analysis of dental restorations.

The interface between the enamel and the restoration also appeared to be a stress concentration, for the case of the rounded restoration. This applied to stresses in both the global x and y-directions. This is attributed to the difference between the anisotropic nature of the enamel and the isotropic restorative material, and the action of transferring a higher component of the load along this material interface, as described above.

It is possible that the stress concentration in this region may not be as large as predicted here. Potential reasons for this are that the load is applied directly to the outer surface of the enamel *(see Fig. 8.2.1),* the close proximity of the load, and the interface of 3 different materials at one node, are highly likely to influence the results of an FEA simulation.

Also, as explained in Chapter 5, FEA has difficulty in interpolating stresses across material interfaces, so some of the stress concentration effects observed can be attributed to the material mismatches.

Efforts were made to reduce the effects of these factors by incorporating more elements through the thickness of the enamel (as described in Chapter 4), and by applying the load on the model by convection instead of directly to the elements. However, with all of these factors involved in such a small area, it is probable that the stress concentration shown reflects these limiting features of the modelling process. Consideration was obviously given to these features throughout this analysis, but the material interfaces do exist on such a scale as is modelled here, and the load would be applied at such close proximity to these features. Hence, the stress concentration effects observed here are due at least in part to real geometrical features and not just the limitations of the FEA model.

Unfortunately, it is very difficult to further refine the model whilst still maintaining all of the other geometrical features. It is recommended that the technique of cut-boundary interpolation modelling, or sub-modelling should be pursued to address these issues in more detail in the future.

Experimental validation of the effects of thermal loading on natural and restored tooth would also be an extremely valuable aspect of future work.

8.5 Conclusions

A natural tooth subjected to a thermal load of 60°C did not experience significant levels of thermal stress.

A tooth containing a non-carious, v-shaped restoration experienced greater stresses than the natural tooth, but these were not felt to be high enough to cause significant damage.

The vertex of the v-shaped restoration acted as a stress concentration factor. Since this region was also found to be a stress concentration factor in the structural analyses, it is recommended that the two cases are combined in order to better assess the impact of these two load cases on benign restoration design.

The tooth containing the rounded restoration experienced significantly higher levels of stress than the natural tooth and the tooth containing the non-carious restoration. This was attributed to the cavity geometry modelled, permitting a greater component of the load to be channelled along the interface. It is recommended that other designs of rounded cavities are analysed, and that the effect of bevelling the margins is considered.

The material interface between enamel, dentine and the restoration was also shown to be a stress concentration factor, in both the rounded and the non-carious cases. This observation was attributed partly to the load channelling effect of the anisotropic enamel, and partly to the presence of a restoration. Magnitudes of the stresses predicted may be higher than those measured experimentally because of the difficulties associated with applying FEA to material interfaces.

Chapter 9

Polymerisation Shrinkage

9.0 Introduction

The design requirements of a dental restorative material are that its viscosity must initially be low enough to permit the material to be worked into the prepared cavity, and high enough to prevent the material from running away. The material then needs to be cured in order to attain similar material properties (*i.e.* hardness and stiffness) to that of the tooth structure that it replaces. As discussed in Chapter 2, curing of the restorative can be initiated in a variety of ways.

All resin-based restorations exhibit volumetric contraction upon curing (or polymerisation) of the resin (Labella *et al.*, 1998). This shrinkage is a result of the changes that occur in the atomic bonding of the constituents of the restorative material as it sets; *e.g.* as double bonds (C=C) break, and single bonds (C-C) reform. Chapter 2 has addressed some of the problems associated with this, such as the rupture of the tooth-restoration bonds due to the large stresses caused by this contraction. However, if the bonds survive this initial contraction, a residual stress field results. Residual stress is defined as *"that stress which would exist in an elastic solid body if all external load (forces, couples and applied stresses), acceleration and gravitation were removed."* (Heindlhofer, 1948.) Residual stress exists both if no other load is present, but also when an external load is applied. The residual stress can therefore be added to the stress resulting from other applied loads, by the principle of super-position.

It is important to consider the effects of an existing residual stress field in this hierarchy of design criteria. Sakaguchi *et al.* (1992) state that the tooth-restoration complex is pre-stressed even before occlusal forces cause further coronal deformation. A structure containing a residual stress field will respond in a different manner to an applied load than one with no existing residual stress.

To model the effects of polymerisation shrinkage, other researchers have used the analogy of thermal stress. This technique was first employed by Hickman (1991) and is also well documented by Winkler, Katona and Paydar (1996). The restorative material is assigned an arbitrary, non-zero coefficient of thermal expansion. By applying a temperature fall of 1°C to the restorative material, this causes the restoration to shrink in a manner similar to that which would result from contraction

due to polymerisation. Since the degree of volumetric shrinkage is generally reported to be between 1 and 3%, the contraction resulting from this thermal load is then used to scale the stresses predicted by this thermal analysis to those which would result if a 1% volumetric contraction had occurred, for example. Feilzer (1989) measured the curing contraction that occurred in 24 hours for 26 commercial composite resins, and 2 glass ionomer cements. He reported that the volumetric contraction of the composite resins was between 2.9% and 7.1%, and between 3.8% and 4.8% for the glass ionomer cements.

In further studies, Feilzer investigated the influence of polymerisation contraction upon adhesion to enamel and dentine, and concluded that the shape of the cavity (often described as the C-factor) significantly influences the survival of this adhesion. For this reason, it was deemed important to investigate the effect of polymerisation shrinkage using FEA techniques applied to a model of a restored tooth.

9.1 Method

In this study, a simulated 1°C temperature fall was applied to the boundaries of the restoration by applying convection loads on the lines. The thermal conductivity and coefficients of thermal expansion of the materials were specified, and were the same as those used in Chapter 8. Convection was used to apply the thermal load so that the material would shrink as a result of the contraction calculated from the thermal properties rather than by prescribed conditions.

9.2 Results

By this method, the overall temperature fall within the tooth was less than 1°C. The resulting stress in the tooth was between -17.59 MPa and 8.21 MPa, with the extremes occurring in the enamel, adjacent to the restoration. Most of the enamel and the dentine experienced very little direct stress; the stress was concentrated at the interface. The stress distributions are shown in Fig. 9.2.1.

The tensile y-stress in the dentine was concentrated at the v-shaped notch. This region experienced compressive x-stress. The greatest tensile x-stress occurred at the

majority of the displacement was vertical, and that the resin did not appear to shrink away from the free surface.

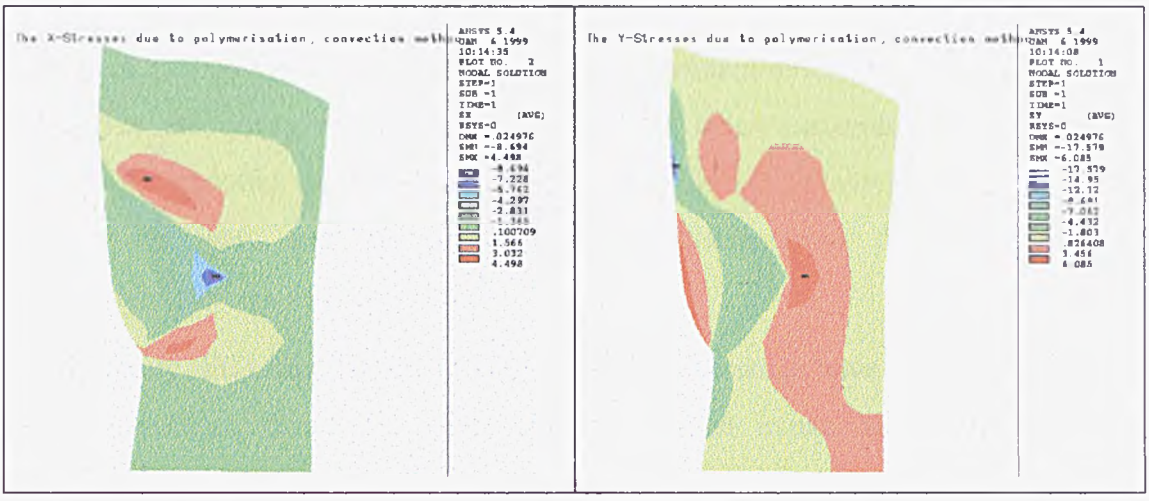

Fig. 9.2.1: The stresses due to polymerisation shrinkage, convection method.

However, further investigation of the displacements of the tooth and restorative material showed that most of the deformation of the restoration was vertical, and that the displacement in the horizontal direction was to the left (negative). This is the opposite of what would be expected; one would intuitively predict that the restoration would contract away from the free surface. This effect is believed to be due to the constraints of FEA and the other material properties defined; by allowing the material to shrink in a non-prescribed way, the horizontal deformation reflects the larger vertical shape change, so as the material shrinks vertically, the restoration grows horizontally.

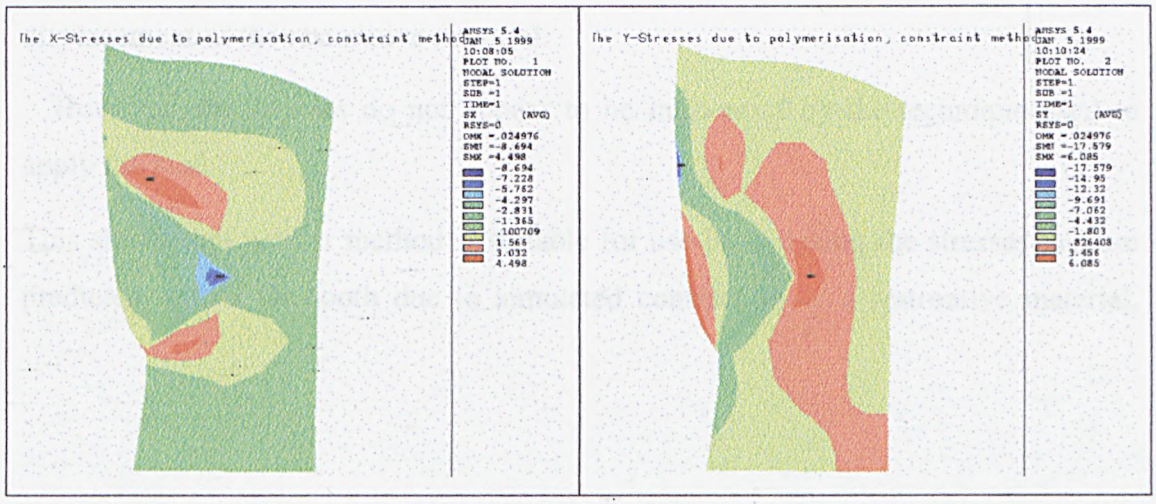

Fig. 9.2.2: The stresses around the restoration due to polymerisation shrinkage, constraint method.

9.3 Discussion

This technique has generally been employed to model using FEA the *in vitro* simulation of polymerisation shrinkage. An experiment described by Feilzer (1989) modelled the cavity *in vitro* as a cylinder of brass suspended by wires. The restorative material under investigation was put into the cavity, and cured in the appropriate way, and the displacements resulting from the polymerisation contraction stresses were measured.

Generally, FEA simulations of polymerisation shrinkage have sought to replicate this experiment. Since the coefficient of thermal expansion assigned in the simulations is arbitrary, it makes sense to model an *in vitro* situation for which the results are accurately known. In this way, a suitable value for the coefficient can be determined, enabling laboratory data to be accurately replicated.

Since this technique has been employed with some success, an attempt was made to simulate what the effect of polymerisation shrinkage on a restored tooth would be; *i.e.* modelling an *in vivo* situation. By applying the temperature change by means of convection, it was hoped that this would permit the restorative material to shrink in a more natural manner. Most FEA simulations to date have applied the temperature change directly to the nodes or elements required. In order to verify whether this method influenced the shrinkage of the cavity, a 1°C temperature fall was also applied to every node in the cavity. The same result occurred as regards horizontal displacement of the restorative material.

However, the stresses do not appear to be influenced by the technique used to apply the load.

This shows that neither method is suitable for use in analysing the stresses that are predicted within the tooth due to simulated contraction of a restorative material.

CHAPTER 10

Benign Design for Dental Restorations

10.0 General Discussion

The studies detailed in the previous chapters of this thesis have all been concerned with comparing the behaviour of natural and restored teeth. The purpose of this work is to further our understanding of how the performance of a restored tooth will differ from that of a natural tooth, and to investigate what factors associated with the form and material properties of a Class V restoration will adversely influence their behaviour. An attempt has been made throughout this work to construct a hierarchy of FEA models. Each one examines a different aspect of the loads experienced by a human canine tooth in functional behaviour, building up in complexity from basic engineering principles to ensure that the answers obtained are relevant to the situation under simulation. A philosophy of design to be employed when restoring cervical lesions can then be conceived.

The work described in Chapter 4 has shown that the assumptions made when analysing a FEA model of a tooth are fundamental to the results obtained. In particular, the supporting structures of the tooth are shown to play an important part in the reaction of applied loads.

Chapter 5 investigated the importance of the material model used to simulate the behaviour of the PDL in studies of impact loads (*i.e.* not time-dependent loads). Here, it was shown that the material model used to represent the PDL did not significantly influence the stresses within the area of interest; *i.e.* the tooth. However, the stress distributions within the bone were affected by the material model used to represent the PDL. Future studies concerned with the stresses within the bone should therefore give consideration to the model of the PDL used.

The influence of different FEA codes on simulations of impact loading of a tooth was also investigated. This showed that the FEA code used did affect the results obtained (due to the different ways in which the material was modelled), and a discussion concerning the propriety of each of the codes for this type of analysis is included in Chapter 5.

Chapter 6 addressed the issues of validation of the FEA models used, and employed the experimental technique of thermo-elastic stress analysis using SPATE (Ometron Ltd.) to investigate the stresses induced in an extracted human tooth. The results of the thermo-elastic analyses using SPATE were inconclusive, probably due to problems with the experimental setup. Hence, validation by this method was not possible.

Experimental use of strain gauges to measure the stresses induced in a natural tooth were reviewed, but generally, either there was insufficient data given to be able to reproduce the experiments using FEA, or the experiments involved extracted teeth, and Rees and Jacobsen (1997) have verified the material properties for enamel and dentine in this way. The values of E used in this study compared very well to those found by Rees and Jacobsen (1997), and hence these materials can be assumed to be verified.

Benefiting from the findings of the earlier chapters, Chapter 7 compared the shear and interfacial stresses surrounding a class V restoration to those at identical locations in an intact tooth. The Young's modulus (E) of the restorative material was varied from 1 GPa to 80 GPa. The effect of cavity geometry was also investigated to a moderate extent, comparing the v-shaped and rounded forms typical of a non-carious and a carious lesion respectively. From these studies, it was shown that a low modulus restorative would transfer too much stress into the remaining tooth structure, causing stress concentrations at sites from which cracks are likely to propagate within the restored structure. This situation is clearly far from benign.

Chapter 8 investigated the influence of thermal stresses upon the series of cavity designs that were used in Chapter 7. Thermal loads predict lower stresses than those predicted by the bite load analyses detailed in previous chapters. However, the stress distribution that results from a thermal load is notably different to that of the bite load case, hence the investigation was of interest. Also, it was shown that the presence of a restoration in the tooth significantly altered the distribution of the stresses predicted due to thermal loading, and that the form of the restoration further influenced the locations of stress concentrations within the restored tooth. Although

the magnitudes of the thermal loads are smaller than bite loads, it is felt that that the effects of low cycle fatigue may be significant. The effect of combining these different load cases is considered in this chapter.

The effects of polymerisation shrinkage are considered in Chapter 9. However, the approach used to simulate the contraction due to polymerisation was not suitable; hence the only conclusions that can be drawn from this study are that future researchers should adopt a different approach to modelling this phenomenon.

The results of the each of the simulations in this hierarchy of models are now compared to produce a design philosophy for benign dental restorations. The Design Council (1998) have produced a book based upon the work of Pahl and Beitz (1976). They recommend that a design methodology must incorporate the following features:

It must encourage a problem-directed approach.

Inventiveness and understanding are needed to obtain optimum solutions.

It must be compatible with the findings of other disciplines, and the concepts and methods used within these.

It must not rely on chance.

The application of existing solutions to related tasks should be facilitated.

It should be compatible with current electronic data processing technology.

It must be easy to learn and teach.

It should reduce the workload, save time, prevent human error and help to maintain active interest.

Applying each of these recommendations in turn to the design of dental restorations, the following issues might be raised.

A problem-directed approach is fundamental to research. If research and design are not driven by attempting to solve the problems associated with the product or

issue, they become meaningless. A problem-directed approach entails consideration of the aims of the product, the way in which it will be used, and the installation process. Pahl and Beitz recommend clarification of the task as the initial step in the design process.

In the case of dental restorations, the task can be defined as the need to restore tooth structure lost either through decay or other causes in order to limit further damage to the tooth structure and to restore the tooth as nearly as possible to its original strength and functionality. Further considerations are that the material must be bio-compatible, and that the dental surgeon should be able to place the restoration as quickly and easily as possible. A restorative material must be able to adapt to the form of the cavity left or cut in the tooth, which will be different in every case.

Restorative materials currently used to fill Class V lesions are discussed in Chapter 2, and the problems associated with them are discussed in detail there. To recapitulate here, they are that the preferred, "aesthetic" restorative materials currently used are bonded to the remaining tooth structure, and that the bond is weak, particularly to dentine. For the dentist to place the restoration easily and quickly, and to accommodate the variation in cavity shapes, a material that is initially fluid, but that sets hard is required. Unfortunately, the aesthetic materials currently used all contract upon setting, causing stress to be inflicted upon the bonds. Experimental evidence indicates that this stress exceeds the bond strength, causing failure along part of the interface; in particular at the CEJ. This can lead to marginal discolouration, secondary caries, and potential loss of the restoration. Materials scientists are developing materials that fulfil the above criteria, but which might not contract upon setting, and primers and adhesives are improving.

In Chapter 7, the design of dental restorative materials was considered. Simulations of models containing restorative materials of very low, moderate, and very high elastic modulus (E) were compared to a natural tooth under functional loading, and it was found that the low E group was unsuitable for this application. The research that has led to the production of materials of very low E was problem-directed in that several researchers have proposed that such a material would flex with the tooth, thereby reducing the stresses exerted on the tooth-restoration bond.

However, the analysis presented in Chapter 7 indicates that this would result in a transfer of stress into the tooth. This is a worse situation, since further damage would then be more likely to be inflicted upon the sound tooth structure, instead of being limited to replacement of the restoration. Hence, the materials with a medium or high value of E are more benign for bite-loading conditions.

The thermal analyses indicated that the mismatch of material properties caused a concentration of stress within the restored structure and that restored teeth experienced greater levels of stress than natural teeth. Hence, the restored cases were less benign. Moreover, the tooth containing the simulated rounded restoration exhibited higher stresses in the region of the restoration than the non-carious, v-shaped restoration. It is believed that this is due partly to the larger size of the rounded restoration, and partly because of the shape of the cavity. The vertex of the v-shaped cavity acted as a stress concentration factor, but the stresses predicted were not sufficiently large enough to rupture the tooth-restoration bonds. However, in the rounded restoration, high stresses were experienced around the dentine-restoration interface, which would exceed the predicted bond strength of the dental adhesives.

Also, the mismatch between the anisotropic enamel and the restorative material was notably more significant for the case of the rounded restoration. This suggests that the geometry of the cavity is important to the resulting stress distribution within the tooth, and that thermal loading is more significant than previous research may have suggested.

Despite the systematic, hierarchical approach to modelling that has been adopted throughout this work, the magnitudes of the stresses predicted can only be as accurate as the material properties specified. Data for biological tissues is scarce, and not terribly reliable due to the difficulties associated with obtaining it. Hence, the magnitudes of the stresses predicted throughout this thesis ought not to be regarded in any way as absolute. However, they do indicate the trends that are likely to be observed, and as more accurate data becomes available in the future, it is straightforward to either scale up or down the results according to the changes, or to re-run the analyses if the assumptions made in modelling are sound.

FEA simulations do not cope well with material interfaces, and the stresses and stress distributions predicted at the interfaces of materials should be interpreted with

a good deal of caution. A material interface could concentrate stress, and the stress concentrations shown are not necessarily "wrong". However, the magnitudes of the stresses predicted are likely to be much higher than would be experienced in practice. This is partly due to the way in which FEA codes calculate the stresses (see Chapter 5), and also partly due to the fact that biological tissues in particular do not have uniform material properties throughout their thickness. Enamel is often more mineralised at the surface than at the EDJ, the porosity and the composition of dentine varies through the thickness, and the properties of the PDL are believed to vary with location.

It is possible that this issue may be resolved in future revisions of FEA codes. Researchers in automotive and aeronautical fields are also increasingly concerned with the strength of adhesives and the behaviour of material interfaces, and FEA is routinely used in these industries. If a sufficient demand exists for this technology, then it is likely to become available. Hence, it may be appropriate to return to some of these issues in the future. On the other hand, there is little point in running increasingly complex analyses if sufficiently sensitive material property data does not exist.

The manner in which the tooth is loaded also causes stress concentrations, which again are likely to be much higher than those experienced in reality. These magnitudes should be ignored.

10.1 Conclusions

Summarising the discussion in Chapter 10.0, the conclusions from this thesis are as follows:

The boundary constraints used in the FEA of human teeth are significant.

It is necessary to include the PDL to obtain a realistic stress distribution within the tooth.

If the displacements of the tooth are of interest, then the bone should also be incorporated into the EA model.

The material model used to represent the PDL does not appear to influence the stress distributions within the tooth under functional loads.

However, the stress distribution within the bone is affected by the material model used. Hence, studies concerned with the stress distribution within the bone need to consider carefully the material model used to represent the PDL.

The FEA code used to study the effect of Linear Elastic (LE), Non-Linear (NL) and Multi-Linear Elastic (MLE) models of the PDL is also shown to affect the stress distribution within the bone.

Considering the LE models of the PDL used, the E of the material was shown to affect the magnitudes of the stresses induced in the tooth, but the distributions of stress within the tooth remain unaffected.

The effect of varying the E of the restorative materials used to restore a rounded and a v-shaped cervical lesion were investigated. The materials used could be divided into 3 groups; a low-modulus group (E = 1 GPa and 5 GPa), a mid-range group (E = 10, 15 or 20 GPa), and a high modulus group (E = 50 or 80 GPa). The results predicted by the mid-range group corresponded most closely with those predicted by the natural tooth, and are therefore most benign.

The low-modulus groups reduce stress in the restoration but increase stress in the tooth when compared to the natural tooth model.

The high-modulus group increase stress in the restoration, but reduce stress within the tooth compared to the natural tooth model.

The v-shaped restoration causes a stress concentration in the tooth, behind the vertex of the restoration.

Using a more rounded form of restoration reduces this stress concentration; however, the stress along the enamel-restoration interface is significantly increased for the rounded restoration. It is thought that this is due to the angle at which the interface intersects the enamel.

Stresses induced due to thermal loading are smaller than those induced by bite loads; however, they are thought to be significant when considering the fatigue loading of teeth.

Teeth containing a v-shaped restoration experienced greater stress than natural teeth.

Teeth containing a rounded restoration experienced much greater stresses than natural teeth.

10.2 Future Work

In the author's opinion, future research could usefully be directed into the following areas:

10.2.1 Validation

Further validation of the FEA simulations described in the previous chapters is clearly required. Meredith, Setchell and Swanson (1997) have shown that SPATE is a valid technique for experimentally measuring the stresses on the surface of a molar tooth, and, with a better loading rig, in all probability, this technique will work for an anterior tooth also. Other companies manufacture equipment capable of measuring the thermoelastic effect. One such company is Deltatherm, and their scanner is supposed to be much faster and easier to use, so future researchers may be advised to consider this alternative.

Continuation of the work using the SPATE system is also recommended, but it is suggested that modification is made to the method of securing the test tooth in the rig, and possibly also to the method of application of the load to the tooth, in order to apply the load more precisely, and to facilitate positioning of the detector head prior to scanning.

10.2.2 Cavity Geometry

The cavity designs investigated in this report are very limited, due to the attention and time given to ensuring that all of the other modelling criteria (such as boundary constraints, the material model used to represent the PDL, *etc.*) were satisfied. It would be useful to compare simulations of models containing more typical cavity shapes in order to study benign restoration design further. Also, it would be interesting to expand the study to increase the number of load cases analysed.

Further investigation of the effect of Young's modulus (E) or the restoration in models subjected to thermal loads is advocated.

10.2.3 Polymerisation Shrinkage

The analogy of thermal stress was shown to be unsuitable to attempt to simulate polymerisation shrinkage in a model of a human tooth and supporting structures. If the entire tooth model had been constrained and only the restorative material

permitted to shrink, then perhaps valid displacement patterns might have been predicted. However, this would have been at the expense of useful information as to the stress distribution within the tooth due to the contraction stress, and so is not recommended.

It is the opinion of the author that the technique for simulating the behaviour of polymerisation contraction is inappropriate, since a realistic pattern of displacement due to contraction cannot be replicated on a tooth model. LS-DYNA3D might be more appropriate for the study of time-dependent loads of this type. Also, LS-DYNA3D, MARC Autoforge, and Pro-Mechanica have been adapted to study the flow of cast materials. These FEA codes may facilitate the modelling of contraction stresses during cooling, and the introduction of fluid-solid interaction in LS-DYNA3D may also prove to be advantageous in these studies in the future.

10.2.4 Modelling the PDL

Representation of the material model of the PDL is an area that presents itself for further study. In the case of impact loading, it was shown that the tooth was not particularly sensitive to the material model used. However, if future researchers were concerned with the time-dependent behaviour of a tooth, *e.g.* in attempting to simulate polymerisation shrinkage, or in the study of tooth movement, then this issue would require further attention.

It was also found that it was very difficult to produce a non-linear model of the PDL that was able to model all types of loading and concurrence of results among FEA codes was difficult to obtain.

10.2.5 Thermal Stress Analysis

Very little research seems to have been directed into the study of natural and restored teeth subjected to thermal loads. The basic analyses outlined in Chapter 8 have suggested that this is an important issue for certain cavity designs, and an issue which should certainly not be overlooked because the stresses induced in the natural tooth due to a thermal load are very small. Further study should explore the effects

of thermal loads upon a variety of typical cavity shapes, and consider the different thermal properties of commercial restorative materials.

References

Andersen, K.I., Pedersen, E.H., Melsen, B., *Material parameters and stress profiles within the PDL,* American Journal of Orthodontics and Dentofacial Orthopaedics, **99,** 1991, 427-44

Annusavice, K.J., Glasspoole, E.A., *Introduction to invited papers at the 1994 ADM,* Southampton, Bermuda, Dental Materials, **11,** (3), 1995, 102

Aydin, A.K., Tekkaya, A.E., *Stresses induced by different loadings around weak abutments,* Journal of Prosthetic Dentistry, **68,** (6), 1992, 879-884

Baguley, D., Hose, R., *Back to basics: idealisation and geometry,* Benchmark, **10,** 1996, 3-7

Baguley, D., Hose, R., *Back to basics: understanding finite element jargon,* Benchmark, **1,** 1996, 4-7

Baguley, D., Hose, R., *What designers should know about design analysis in integrated systems,* Benchmark, **7,** 1998, 6-9

Baguley, D., Hose, R., *Back to basics: why do finite element analysis?,* Benchmark, **1,** 1995, 8-10

Barone, S., Patterson, E.A., *Full-field separation of principal stresses by combined thermo & photoelastic stress analysis,* Experimental Mechanics, **36,** (4), 1996, 318-324

Barclay, Presentation, IADR meeting, Nice, 1998

Benham, P.P, Crawford, R.J., Armstrong, C.G., *Mechanics of Engineering Materials,* Longman Group Ltd., 2nd edition, 1996

Berger, S.A., Goldsmith, W., Lewis, E.R., *Introduction to Bio-engineering,* Oxford University Press, 1996

Berkovitz, B.K., Moxham, B.J., Newman, H.N., *The periodontal ligament in health and disease,* Mosby-Wolfe, 2nd edition, 1995

Bitter, N.C., *Class ionomer microfill technique for restoring cervical lesions,* Journal of Prosthetic Dentistry, **56,** (6), 1986, 661-662

Braem, M. , *Stress induced cervical lesions,* Fenestra, **4,** (2)7, 1995

Brunski, J.B., *Biomechanics of oral implants: Future research directions,* **52,** (12), 1988, 775-787
Chew, G.G., Howard, I.C., Patterson, E.A., *Non-linear modelling of porcine bioprosthetic heart valves,* Engineering Failure Analysis, **1,** 1994, 231-242

Clift, S.E., Fisher, J., Watson, C.J., *Finite element stress and strain analysis of the bone surrounding a dental implant: effect of variations in bone modulus,* Proceedings of the Institution of Mechanical Engineers, Part H - Journal of Engineering in Medicine, **206,** (4), 1992, 233-41

Cobo, J., Sicilia, A., Arguelles, J., Suarez, D., Vijande, M., *Initial stress induced in periodontal tissue with diverse degrees of bone loss by an orthodontic force: tridimensional analysis by means of the finite element method,* American Journal of Orthodontics & Dentofacial Orthopedics, **104,** (5), 1993, 448-54

Andersen, K.I., Pedersen, E.H., Melsen, B., *Material parameters and stress profiles within the PDL,* American Journal of Orthodontics and Dentofacial Orthopaedics, **99,** 1991, 427-44

Annusavice, K.J., Glasspoole, E.A., *Introduction to invited papers at the 1994 ADM,* Southampton, Bermuda, Dental Materials, **11,** (3), 1995, 102

Aydin, A.K., Tekkaya, A.E., *Stresses induced by different loadings around weak abutments,* Journal of Prosthetic Dentistry, **68,** (6), 1992, 879-884

Baguley, D., Hose, R., *Back to basics: idealisation and geometry,* Benchmark, **10,** 1996, 3-7

Baguley, D., Hose, R., *Back to basics: understanding finite element jargon,* Benchmark, **1,** 1996, 4-7

Baguley, D., Hose, R., *What designers should know about design analysis in integrated systems,* Benchmark, **7,** 1998, 6-9

Baguley, D., Hose, R., *Back to basics: why do finite element analysis?,* Benchmark, **1,** 1995, 8-10

Barone, S., Patterson, E.A., *Full-field separation of principal stresses by combined thermo & photoelastic stress analysis,* Experimental Mechanics, **36,** (4), 1996, 318-324

Barclay, Presentation, IADR meeting, Nice, 1998

Benham, P.P, Crawford, R.J., Armstrong, C.G., *Mechanics of Engineering Materials,* Longman Group Ltd., 2nd edition, 1996

Berger, S.A., Goldsmith, W., Lewis, E.R., *Introduction to Bio-engineering,* Oxford University Press, 1996

Berkovitz, B.K., Moxham, B.J., Newman, H.N., *The periodontal ligament in health and disease,* Mosby-Wolfe, 2nd edition, 1995

Bitter, N.C., *Class ionomer microfill technique for restoring cervical lesions,* Journal of Prosthetic Dentistry, **56,** (6), 1986, 661-662

Braem, M. , *Stress induced cervical lesions,* Fenestra, **4,** (2)7, 1995

Brunski, J.B., *Biomechanics of oral implants: Future research directions,* **52,** (12), 1988, 775-787
Chew, G.G., Howard, I.C., Patterson, E.A., *Non-linear modelling of porcine bioprosthetic heart valves,* Engineering Failure Analysis, **1,** 1994, 231-242

Clift, S.E., Fisher, J., Watson, C.J., *Finite element stress and strain analysis of the bone surrounding a dental implant: effect of variations in bone modulus,* Proceedings of the Institution of Mechanical Engineers, Part H - Journal of Engineering in Medicine, **206,** (4), 1992, 233-41

Cobo, J., Sicilia, A., Arguelles, J., Suarez, D., Vijande, M., *Initial stress induced in periodontal tissue with diverse degrees of bone loss by an orthodontic force: tridimensional analysis by means of the finite element method,* American Journal of Orthodontics & Dentofacial Orthopedics, **104,** (5), 1993, 448-54

Coffey, J.P., Anusavice, K.J., deHoff, P.H., Lee, R.B., Hojjatie, B., *Influence of contraction mismatch and cooling rate on flexural failure of PFM systems,* Journal of Dental Research, **67,** (1), 1988, 61-65

Combe, E. C., *Notes on dental materials,* Churchill Livingstone, 6th Edition, 1990

Cook, S.D., Weinstein, A.M., Klawitter, J.J., A 3-D finite element analysis of a porous-rooted Co-Cr-Mo alloy implant, Journal of Dental Research, **61,** 1982, 25-29

Darendeliler, S., Darendeliler, H., Kinoglu, T., Analysis of a central maxilliary incisor using a 3D finite element method, Journal Oral Rehabillitation, **19,** 1992, 371-383

Della Bona, A., Bond strength techniques & effectiveness of ceramic repair techniques, M.Med.Sci. thesis, 1993

Digby, F.N., *Back to basics 9: dimensions in finite elements,* Benchmark, **9,** 1994, 36

Ganong, W.F., *Review of Medical Physiology,* 17th edition, Prentice-Hall, 1995

Grippo, J.O., *Abfraction: A New Classification of Hard Tissue Lesions,* Decker Periodicals Publishing Inc., 1991

Grippo, J.O. , *Non-Carious Cervical Lesions: The Decision to Ignore or Restore,* Decker Periodicals Publishing Inc., 1992

Gere, S., Timoshenko, *Mechanics of Solids,* Chapman and Hall, 3rd Edition, 1991,

Gordon, J.E., *Structures, or why things don't fall down,* Penguin, 1991

Gray, H., *Anatomy descriptive and surgical,* Parragon Book Service Ltd., 1995

Hargreaves, A.S., *The effects of cyclic stress on PMMA ;. thermal and environmental fluctuation,* Journal of Oral Rehabillitation, **10,** (1), 1993, 75-85

Hargreaves, A.S., *The effects of cyclic stress on dental PMMA II; Flexural Fatigue,* Journal of Oral Rehabillitation, **10,** (2) 1983, 137-151

Harwood, N., Cummings, W.M., *Thermoelastic Stress Analysis,* IOP Publishing Ltd, 1991

Hojjatie, B., Annusavice, K.J., *3-D finite element analysis of glass ceramic dental crowns,* Journal of Biomechanics, **23,** (11), 1990, 1157-166

Hood, J.A.A., *Biomechanics of the intact, prepared & restored tooth; some clinical implications,* International Dental Journal, **41,** 1991, 23-32

Jones, M.L., *Computer methods in bio-mechanics and bio-engineering* Vol. 2, 1998

Jones, R.R.H., Cleaton-Jones, P., *Depth and area of dental erosions and dental caries in bulimic women,* Journal of Dental Research, **68,** (8), 1989, 1275-279

Kardos, T.B., Simpson, L.O., *A new periodontal membrane biology based upon thixotropic concepts,* American Journal of Orthodontics, **77,** (5), 1980, 508-515

Katona, T.R., Moore, B.K., *Effects of load misalignment on tensile load testing of direct bonded orthodontic,* American Journal of Orthodontics and Dentofacial Orthopaedics, **105,** 1994, 543-51

Katona, T.R., Moore, B.K., *Effects of load location & misalignment on shear/peal testing of direct bon,* AmJOrthod & Dentofacial Orthop, **106,** 1994, 395-402

Kelly, J.R., Perspectives on strength (Bermuda 1994 ADM), Dental Materials, **11,** (3), 1995, 102

Kelly, J.R., Tesk, J.A., Sorensen, J.A., Failure of all-ceramic fixed partial dentures in vitro & in vivo:, Journal of Restorative Dentistry, **74,** (6), 1995, 253.25

Korioth, T.W.P., Hannam, A.G., *Deformation of the Human Mandible During Simulated Tooth Clenching,* Journal of Dental Research, **73,** (1), 1994, 56-66

Krejci, I., Hausler, T., Sagesser, D., Lutz, F., *New adhesives in class V restorations under combined load & simulated dentinal fluid,* Dental Materials, **10,** (9), 1994, 331-335

Kurowski, P.M., *Problems with CAD-FEA interface,* Benchmark, **4,** 1995, 10-11

Labella, R., Davy, KW., Lambrechts, P., Van Meerbeek, B., Vanherle, G., *Monomethacrylate co-monomers for dental resins,* European Journal of Oral Sciences, **106,** (3), 1998, 816-24

Lavelle, C.L.B., *Applied Oral Physiology,* 2nd Edition, Butterworth & Co, 1988

Lee, W.C., Eakle, W.S., *The possible role of tensile stress in etiology of cervical erosive lesions,* Journal of Prosthetic Dentistry, **52,** (3), 1984, 374-38

Lin, C.P., Douglas, W.H., *Failure mechanisms at dentine-resin interfacef; a fracture mechanics approach,* Journal of Biomechanics, **27,** (8), 1994, 1037-47

Mair, L.H., *Wear in dentistry - current terminology,* Journal of Dentistry, **20,** 1992, 140-144

McCabe, J.F., Carrick, T.E., *A statistical approach to the mechanical testing of dental materials,* Dental Materials, **2,** 1986, 139-142

McCabe, J.F., Rusby S., *Dentine bonding agents - characteristic bond strength as a function of dentine depth,* Journal of Dental Research, **20,** (4), 1992, 225

McCrory, P.V., Piddock, V., Combe, E.C., Tinston, S., Arnell, R.D., Weglicici, Evaluation of a potential dental application of vapour deposition technique, Journal of Science of Materials in Medicine Part C, **5,** (8), 1995, 507-568

McGuinness, N., Wilson, A.N., Jones, M.L., Middleton, J., A stress analysis of the PDL under various orthodontic loads, European Journal of Orthodontics, **13,** 1991, 231-242

Mecholsky Jr., J.J., *Fracture mechanics principles (Bermuda 1994 ADM),* Dental Materials, **11,** (3), 1995, 111-112

Mecholsky Jr., J.J., *Fractography: determining sites of fracture initiation* (Bermuda 1994 ADM), Dental Materials, **11,** (3), 1995, 113-116

Medige, J., Deng, Y., Yu, X., Davies, E., Joynt, R., *Effect of restorative materials on cuspal flexure,* Quintessence International, **26,** (8), 1995, 571-58

Meredith, N., Setchell, D.J., Swanson, S.A.V., *The application of thermoelastic analysis to study stresses in human teeth,* Journal of Oral Rehabillitation, **24,** 1997, 813-822,

Momoi, Iwase, Nakano, Kohno, Asanuma, Yanagisawa, *Gradual increases in marginal leakage of resin composite with thermal stress,* Journal of Dental Research, **69,** (10), 1990, 1659-664

Muhlemann, H.R., *Clinical implications of tooth mobility measurements,* A Symposium, Oxford, 6-8 July, 1965

Nikaido, T., Burrow, M.F., Tagami, J., Takutsu, T., *Effect of pulpal pressure on adhesion of resin composites to dentine: Bovine,* Quintessence International, **26,** 1995, 221-226

Nimni, M.E., *Collagen: its structure & function in normal & pathological connective tissues,* Seminars in Arthritis and Rheumatism, **4,** (2), 1974, 95-150

O'Grady, J., Sheriff, M., Likeman, P., *A finite element analysis of a mandibular canine as a denture abutment,* European Journal of Prosthodontics and Restorative Dentistry, **4,** (3), 1996, 117-121

Olden, E.J., PhD thesis, 1998

Parfitt, G.J., *The physical analysis of the tooth supporting structures, A Symposium,* Oxford, 6-8 July, 1965

Pashley, D., Sano, H., Ciucchi, B., Yoshiyama, M., *Adhesion testing of dentine bonding agents: a review* (Bermuda 1994 ADM), Dental Materials, **11,** (3), 1995, 117-125

Picton, D.C.A., *Extrusive mobility of teeth in adult monkeys,* Archives of Oral Biology, **31,** (6), 1986, 369-372

Picton, D.C.A., *On the part played by the socket in tooth support,* Archives of Oral Biology, **10,** 1965, 945-955

Picton, D.C.A., *Viscoelastic properties of the periodontal ligament and mucous membrane,* Journal of Prosthetic Dentistry, **40,** (3), 1978, 263-272

Picton, D.C.A., Davies, W.I.R., *Distortion of the socket with normal tooth mobility,* A Symposium, Oxford, 6-8 July, 1965

Pidaparti, R.M.V., Beatty, M.W., *Fracture toughness determination of dental materials by lab test & FE model,* Journal of Biomedical Materials Research, **29,** (3), 1995, 309-315

Rabinowitz, S., Beardmore, P., *Cyclic deformation and fracture of polymers,* Journal Material Science, **9,** (2), 1974, 81-99

Ralph, W.J., *Tensile behaviour of the periodontal ligament,* Journal of Periodontal Research, **17,** (4), 1982, 423-426

Ramsay, A., *Comparison of hex and tet meshes,* Benchmark, **6,** 1994, 11-13

Rasmussen, S.T., Patchin, R., Scott, D.B., Heuer, A.H., *Fracture properties of human enamel and dentine,* Journal of Dental Research, **55,** 1976, 154-164

Rauch, B.J., Rowlands, R.E., *Handbook on experimental mechanics, Chapter 14, Thermoelastic stress analysis,* **book**

Rees, J.S., Jacobsen, P.H., *Stresses generated by luting resin during cementation of composite & ceramics,* Journal of Oral Rehabillitation, **19,** 1992, 115-122

Rees, J.S., Jacobsen, P.H. , *Modelling the effects of enamel anisotropy with the finite element method,* Journal of Oral Rehabillitation, **22,** 1995, 451-454

Rees, J.S., Jacobsen, P.H., *Elastic modulus of the periodontal ligament,* Biomaterials, **18,** (14), 1997, 995-999

Rees, J.S., Jacobsen, P.H., Hickman, J., *The elastic modulus of dentine determined by static & dynamic methods,* Clinical Materials, **17,** (1), 1994

Remizov, S.M., Prujansky, L.Y., Matveevsky, R.M., *Wear resistance and microhardness of human teeth,* Proceedings of the Institution of Mechanical Engineers Part H - Journal of Engineering in Medicine, **205,** (3), 1991, 201-2

Sahay, K.B., *Choice of strain energy function for mechanical consideration of soft biological tissues,* Engineering in Medicine, 1984, 11-14

Saunders, W.P., *Effect of fatigue upon interfacial bond strength of repaired composite resins,* Journal of Dentistry, **18,** (3), 1990, 158-162

Scott, J.H., Symmonds, N.B.B., *Introduction to dental anatomy,* 9th Edition, Churchill Livingstone, Edinburgh, 1982

Sicher, H., *Oral anatomy,* Mosby, 5th edition, 1970

Spears, I.R., Crompton, R.H., Van Noort, R., Howard, I.C., Cardew, G.E., *The effects of enamel anisotropy on distribution of stress in a tooth,* Journal of Dental Research, **72,** 1993, 1526-531

Spierings, T.A., Peters, M.C., Plasschaert A.J., *Surface temperature of oral tissues. A review,* Journal de Biologie Buccale, **12,** (2), 1984 Jun, 91-9 (a)

Spierings, T.A., de Vree, J.H., Peters, M.C., Plasschaert, A.J., *The influence of restorative dental materials on heat transmission in human teeth,* Journal of Dental Research, **63,** (8), 1984 Aug, 1096-100 (b)

Spierings, T.A., Peters, M.C., Bosman, F., Plasschaert, A.J., *The influence of cavity geometry on heat transmission in restored teeth. Journal of Dentistry,* **14,** (2), 1986, 47-51

Spranger, H., *Investigation into genesis of angular lesions at cervical region of teeth,* Quintessence International, **26,** (2), 1995

Stevens, H., M.Eng Thesis, 1999

Swift, E.J., Perdigao, J., Heymann, H., *Bonding to enamel and dentine; A brief history & state of the art,* 1995, Quintessence International, **26,** (2), 1995

Tanne, K., Lu, Y.C.L., Tanaka, E., Sakuda, M., *Biomechanical changes of mandible from orthopaedic chin cup forces using 3D FEA,* European Journal of Orthodontics, **15,** 1993, 527-533

The Design Council, 1998

Thornton, M., PhD Thesis, 1997

Thresher, R.W., Saito, G.E., *The stress analysis of human teeth,* Journal of Biomechanics, **6,** (5), 1973, 443-439

Thubrikar, M., *The Aortic Valve,* CRC Press, 1991

Trowbridge, E.A., Black, M.M., Daniel, C.M., *Mechanical response of gluteraldehyde-fixed bovine pericardium, to uniaxial loading,* Journal of Materials Science, **20,** 1985, 114.14

Tyas, M.J., *The class V lesion - aetiology and restoration,* Australian Dental Journal, **40,** (3), 1995, 167-170

Versluis, A., *Origin & development of internal stresses during polymerisation of composite resins,* PhD thesis, 1994

Vinson, S. Irving, S., *Can I use an auto-tet mesh?,* Benchmark, **6,** 1994, 15-19

Walker, T.W., *A model of the periodontal vasculature in tooth support,* Journal of Biomechanics, **13,** 1980, 149-157

Wills, D.J., Picton, D.C.A., Davies, W.I.R., *An investigation of the viscoelastic properties of periodontium in monkeys,* Journal of Periodontal Research, **7,** 1972, 42-51

Wilson, A., Middleton, J., Jones, M.L., McGuinness, P., The FEA of the stress in the PDL when subject to vertical orthodontic forces, British Journal of Orthodontics, **211,** 1994, 161-167

Winkler, M.M., Katona, T.R., Paydar, N.H., *Finite Element stress analysis of 3 filling techniques for class V light-cured composite restorations,* Journal of Dental Research, **75,** (7), 1996, 1477-483

Woelfel, J.B., *Dental anatomy: It's relevance to dentistry,* Lea & Ferbinger, 4th edition, 1990,

Huang, X., Black, M.M., Howard, I.C., Patterson, E.A., *A 2-D finite element analysis of a bioprosthetic heart valve,* Journal of Biomechanics, **23,** (8), 1990, 753-762

Yettram, A.Y., Wright, K.H.W., Pickard, H.M., *Finite element stress analysis of the crowns of normal and restored teeth,* Journal of Dental Research, **55,** 1976, 1004-11

Yoshikawa, D.K., *Biomechanical principles of tooth movement,* Dental Clinics of North America, **25,** (1), 1981, 19-26

Zero, D.T., *Etiology of dental erosion - extrinsic factors,* European Journal of Oral Science, **104,** (2), 1996, 162-177

Zienkiewicz, O.C., *The finite element method,* McGraw-Hill, 3rd edition, 1977

de Vree, J.H., Peters, M.C., Plasschaert, A.J., *The influence of modification of cavity design on distribution of stresses in a restored molar*, Journal of Dental Research, **63,** (10), 1984, 1217-12

deLange, C., Kortland, P.J., Luxwolda, R.J., Swijnenburg, J.T., *Restoration of non-carious cervical erosion lesions: 2 year clinical report,* Fenestra 3M Research Forum, **1,** (2), 1996

van Noort, R., *Introduction to dental materials,* Mosby, 1994

van Noort, R., Cardew, G., Howard, I.C. , *A study of the interfacial, shear and tensile stresses in a restored molar tooth,* Journal of Dentistry, **16,** 1988, 286 - 293

van Noort, R., Noroozi, S., Howard, I.C., Cardew, G., *A critique of bond strength measurements,* Journal of Dentistry, **17,** 1989, 61-67

van Noort, R., Brown, D., Causton B.E., Combe, E.C., Fletcher, A.M., Lloyd, C.H., Hatton, P.V., McCabe, J.F., Sherriff, M., Strang, R., Waters, N.E., Watts, D.C., *Dental Materials: 1998 literature review,* Journal of Dentistry, **18,** 1990, 5-23

Appendix 1

The following figures are all taken from Maxillofacial Imaging (1990), and were used to construct a model of the alveolar bone. The page numbers and figure numbers from the book are stated.

Measurements taken are indicated by the white lines on the figures.

Fig. 1 from page 44, and Fig. 2 from page 44, Maxillofacial Imaging (1990).

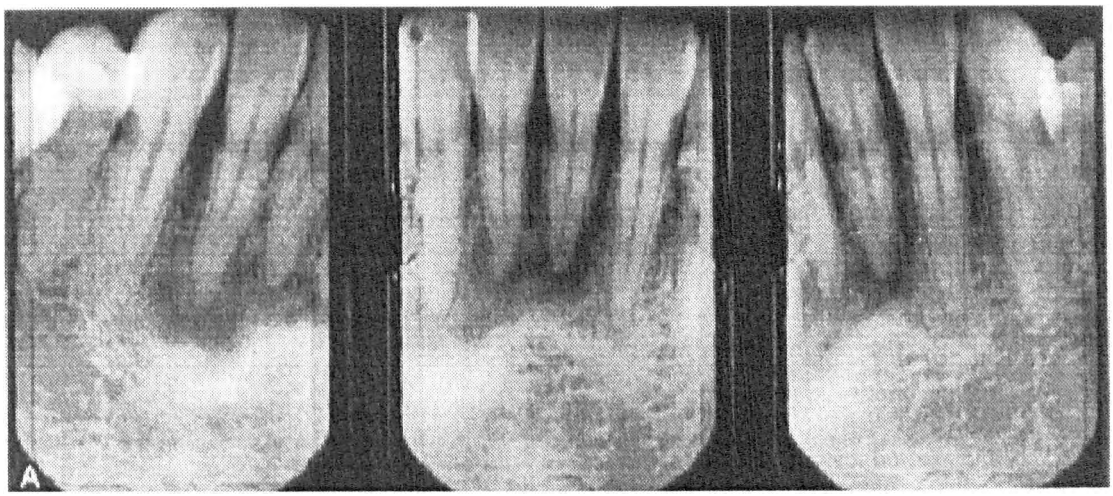

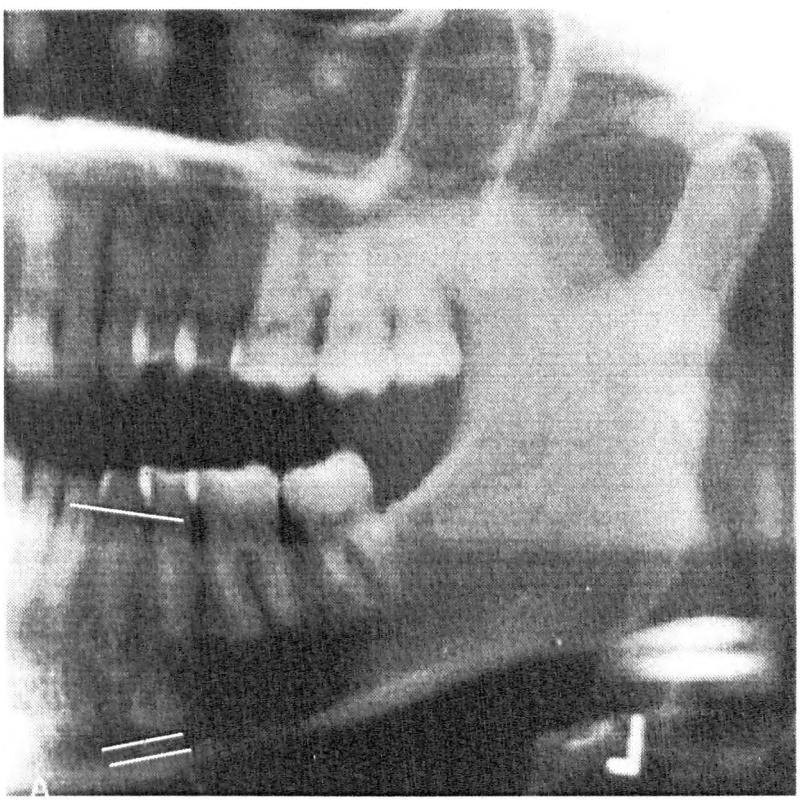

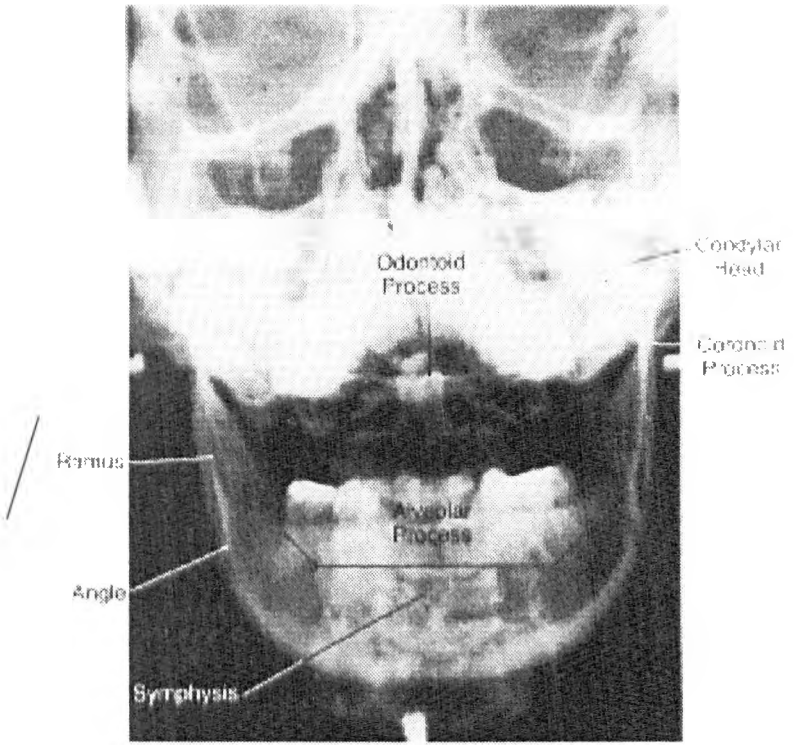

Fig. 4 from page 115, Maxillofacial Imaging (1990).

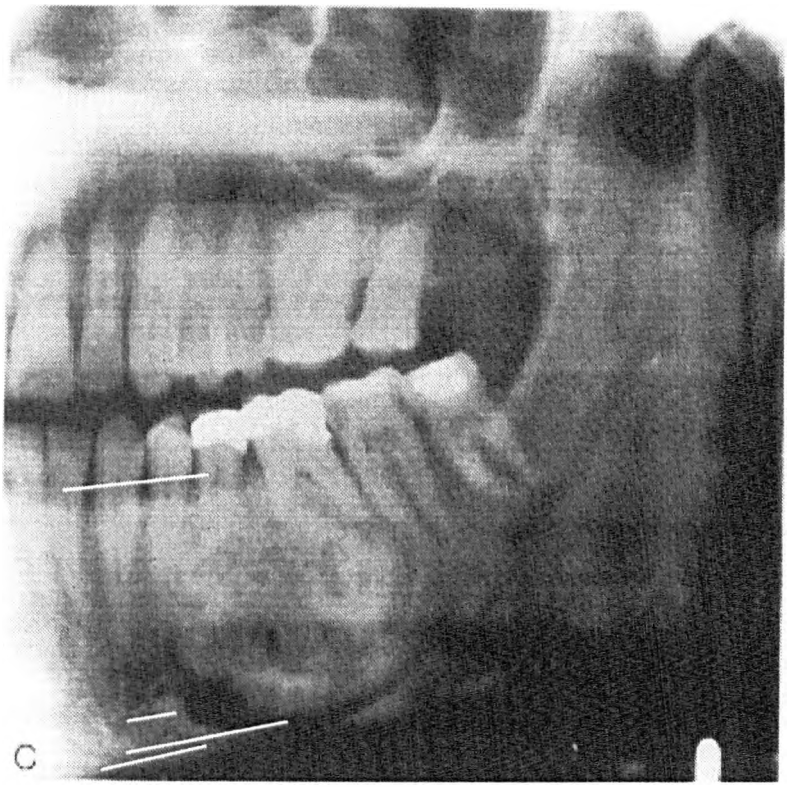

Fig.s 5and 7 from page 349, Maxillofacial Imaging (1990).

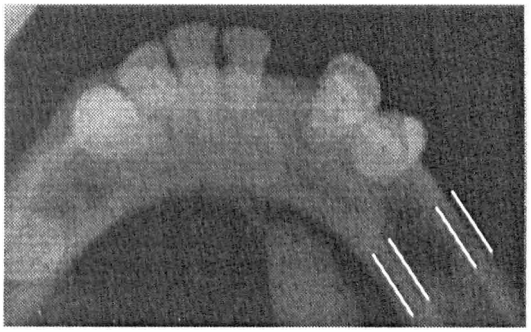

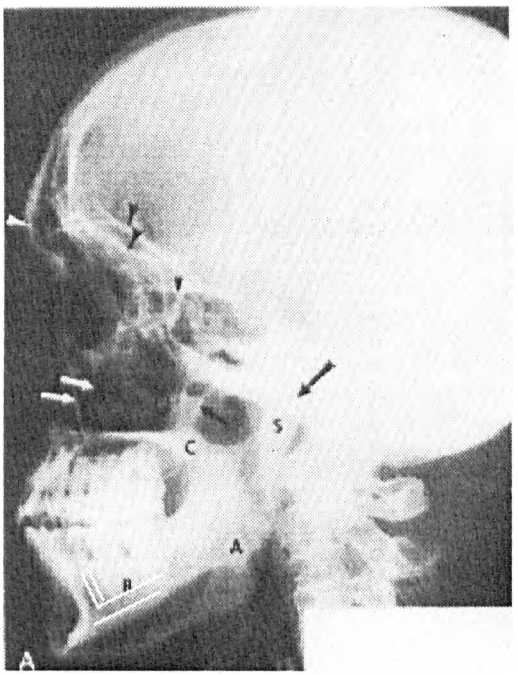

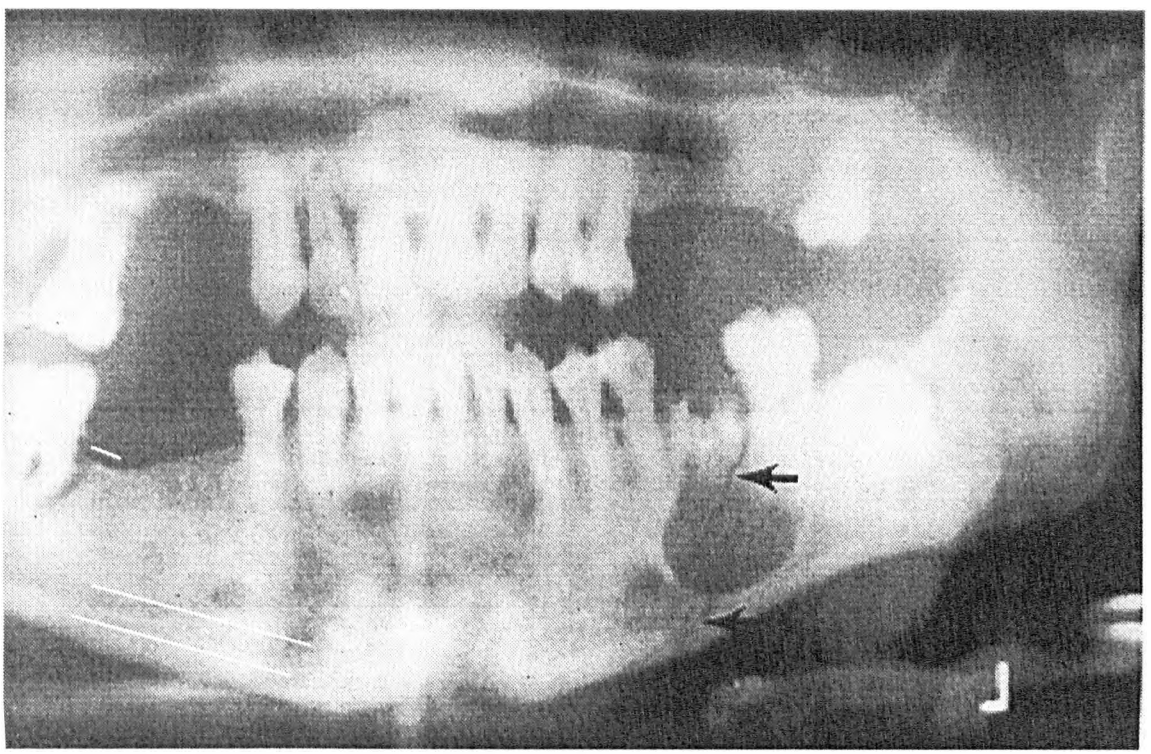

Fig. 8 from page 112, Maxillofacial Imaging (1990). NB fracture indicated in mandible.

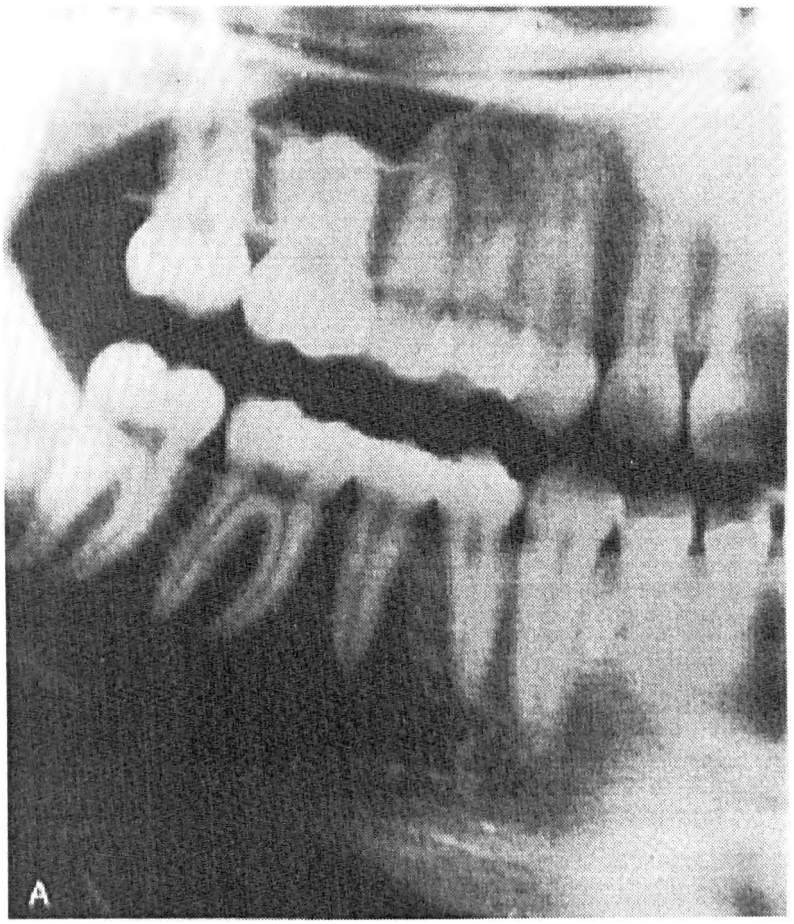
A

APPENDIX 2

FORTRAN Routines Used

This Appendix contains the text of the FORTRAN77 programmes and ANSYS macros used in this report.

1. FER3 is run from within ANSYS to obtain the temperature at every node predicted during the thermal analysis to apply as boundray constraints to the structural model.

FER3

```
ntemp(1)=
*get,totaln,node,,count
*dim,ids,,totaln,1
*dim,ntemp,,totaln,1
*cfopen,tlist
zip = 0
*do,i,1,totaln
*get,fred,node,zip,nxth
ids(i)=fred
zip= fred
*get,ntemp(i),node,ids(i),temp
*cfwrite,d,ids(i),temp,ntemp(i)
*enddo
*cfclose
```

2. Subroutine hyp.f defining the material model used in ABAQUS5.6 to model the hyperelastic material. Details of the UHYPER subroutine are given in the ABAQUS manuals.

```
  SUBROUTINE UHYPER(bi1,bi2,aj,u,ui1,ui2,ui3,temp,noel,cmname)
C
C Defines the user subroutine for the Huang et al SEDF natural tissue model
C where: W = c1*exp((c2*I1**2)+(c3*I2)+(c4*I3))
C and constants are: c1= 2800, c2= 50, c3= -70, c4= -40
C
  INCLUDE 'ABA_PARAM.INC'
C
  CHARACTER*8 cmname
  DIMENSION ui1(6),ui2(6),ui3(6)
C
C W defines the Huang et al Strain energy density function for natural tissue
C The material is assumed to be isotropic
C
  c1= 0.0028
  c2=  30
  c3= -80
  c4= -40
C
  u = c1*exp((c2*bi1**2)+(c3*bi2)+(c4*aj))
  ui1(1)= (2*c2*c1*bi1)*exp((c2*bi1**2)+(c3*bi2)+(c4*aj))
  ui1(2)= (c3*c1)*exp((c2*bi1**2)+(c3*bi2)+(c4*aj))
  ui1(3)= (c4*c1)*exp((c2*bi1**2)+(c3*bi2)+(c4*aj))
C  ui1(3)= 0
C
  ui2(1)= (2*c1*c2)*exp((c2*bi1**2)+(c3*bi2)+(c4*aj))+
```

```
     1(4*bi1**2*c1*c2**2)*exp((c2*bi1**2)+(c3*bi2)+(c4*aj))
     ui2(2)= (c3**2*c1)*exp((c2*bi1**2)+(c3*bi2)+(c4*aj))
     ui2(3)= (c4**2*c1)*exp((c2*bi1**2)+(c3*bi2)+(c4*aj))
C    ui2(3)= 0
     ui2(4)= (2*c3*c2*c1*bi1)*exp((c2*bi1**2)+(c3*bi2)+(c4*aj))
     ui2(5)= (2*c4*c2*c1*bi1)*exp((c2*bi1**2)+(c3*bi2)+(c4*aj))
     ui2(6)= (c4*c3*c1)*exp((c2*bi1**2)+(c3*bi2)+(c4*aj))
C    ui2(5)= 0
C    ui2(6)= 0
C
C    ui3(1)= 0
C    ui3(2)= 0
C    ui3(3)= 0
C    ui3(4)= 0
C    ui3(5)= 0
C    ui3(6)= 0
     ui3(1)= (2*c1*c2*c4*exp((c2*bi1**2)+(c3*bi2)+(c4*aj))+
     1(4*c1*c2**2*bi1**2*c4)*exp((c2*bi1**2)+(c3*bi2)+c4*aj))
     ui3(2)= (c1*c3**2*c4)*exp((c2*bi1**2)+(c3*bi2)+(c4*aj))
     ui3(3)= (2*bi1*c1*c2*c3*c4)*exp((c2*bi1**2)+(c3*bi2)+(c4*aj))
     ui3(4)= (2*c1*c2*c4**2*bi1)*exp((c2*bi1**2)+(c3*bi2)+(c4*aj))
     ui3(5)= (c1*c3*c4**2)*exp((c2*bi1**2)+(c3*bi2)+(c4*aj))
     ui3(6)= (c1*c4**3)*exp((c2*bi1**2)+(c3*bi2)+(c4*aj))
C
     RETURN
     END
```